Hybrid Ferrocene-Based Systems

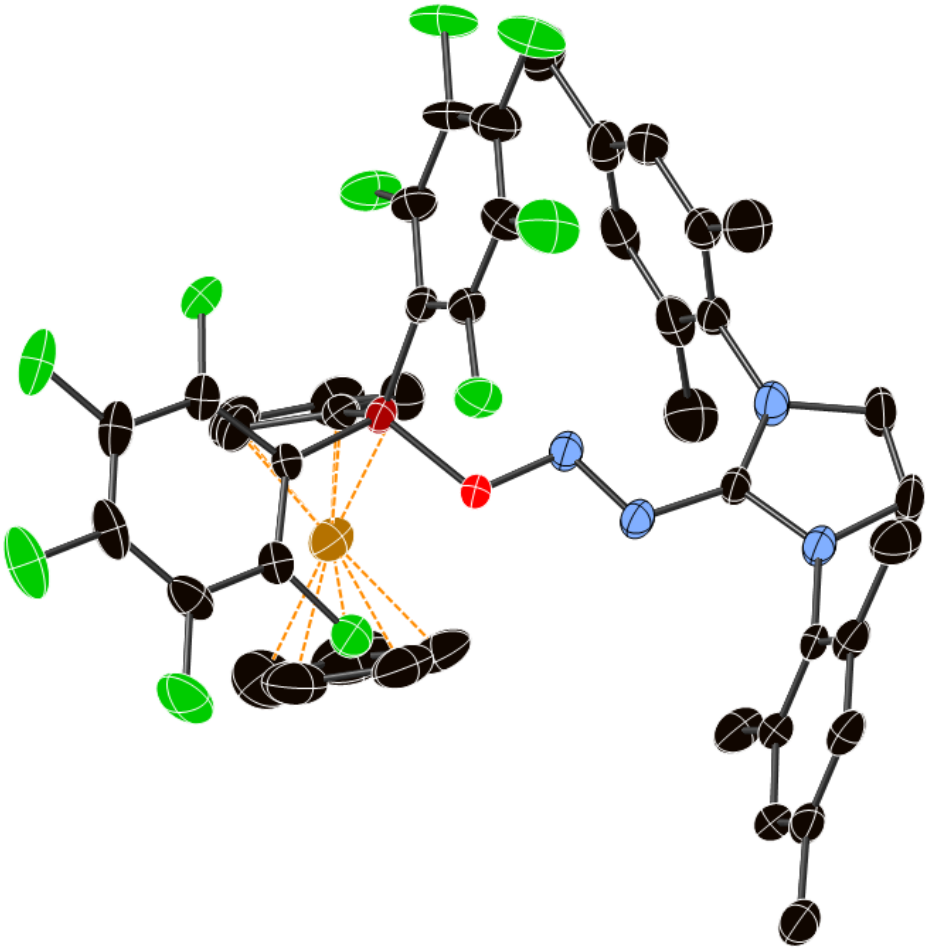

Michael Jon Kelly
The Queen's College
Oxford

October 2014

A Thesis submitted in partial fulfilment of the requirements for the degree of Doctor of Philosophy

DOCTOR OF PHILOSOPHY OF CHEMISTRY

DECLARATION OF AUTHORSHIP

Name (in capitals): MICHAEL JON KELLY **Candidate number:**

College (in capitals): QUEEN'S **[Supervisor/Adviser:] PROF. SIMON ALDRIDGE**

Title of [thesis/extended essay] (in capitals): Hybrid Ferrocene-Based Systems

Word count: ~67,000

Please tick to confirm the following:

I have read and understood the University's disciplinary regulations concerning conduct in examinations and, in particular, the regulations on plagiarism (*Essential Information for Students. The Proctors' and Assessor's Memorandum*, Section 9.6; also available at www.admin.ox.ac.uk/proctors/info/pam/section9.shtml). ☑

I have read and understood the Education Committee's information and guidance on academic good practice and plagiarism at www.admin.ox.ac.uk/edc/goodpractice. ☑

The thesis I am submitting is entirely my own work except where otherwise indicated. ☑

It has not been submitted, either partially or in full, for another Honour School or qualification of this University (except where the Special Regulations for the subject permit this), or for a qualification at any other institution. ☑

I have clearly indicated the presence of all material I have quoted from other sources, including any diagrams, charts, tables or graphs. ☑

I have clearly indicated the presence of all paraphrased material with appropriate references. ☑

I have acknowledged appropriately any assistance I have received in addition to that provided by my [tutor/supervisor/adviser]. ☑

I have not copied from the work of any other candidate. ☑

I have not used the services of any agency providing specimen, model or ghostwritten work in the preparation of this thesis/dissertation/extended essay/assignment/project/other submitted work. (See also section 2.4 of Statute XI on University Discipline under which members of the University are prohibited from providing material of this nature for candidates in examinations at this University or elsewhere: http://www.admin.ox.ac.uk/statutes/352-051a.shtml#_Toc28142348.) ☑

I agree to retain an electronic copy of this work until the publication of my final examination result, except where submission in hand-written format is permitted. ☑

I agree to make any such electronic copy available to the examiners should it be necessary to confirm my word count or to check for plagiarism. ☑

Note: The NMR calculations used to derive the data for table 3.8 were carried out by Dr. Nick Rees. The data obtained and represented in Figures 3.28 and 3.29 were obtained by Jessica Smart and Dr. Nick Rees.

Candidate's signature: Date: ……..
……

Acknowledgements

First and foremost, I would like to extend my deepest gratitude and thanks to my supervisor Simon Aldridge for the countless hours he has devoted to mentoring me and supporting my research. He has provided sage advice, boundless enthusiasm and great humour throughout my time in Oxford, which have made this an unforgettable experience.

I would like to extend my thanks to all the members of the research group, both past and present, for making these past few years enjoyable and for their help. In particular I would like to acknowledge the friendship and guidance of Dr. Inke Siewert, Dr. Jochen Niemeyer, Dr. Josh Baites Dr. Ian Riddlestone, Dr. Alexander Broomsgrove, Dr. Nicholas Phillips and Dr. Juan Urbano Baena. It has been a great pleasure to work along-side the Part II's who have always posed interesting questions and shared useful insights into this work: Philip Fitzpatrick, Jessica Smart, James Branch, Stuart Cornes and Jessica Gilbert.

Many thanks go out to Dr. Amber Thompson, Dr. Drasko Vidovic, Dr. Cristina Tang, Dr. Nick White and Mr. Remi Tirfoin for their help with crystallography. I would also like to thank Dr. Nick Rees for his modelling of complex NMR data and countless help with all things NMR. I would like to thank Prof. Stephen Kelly, Dr. Stephen Tuffnell, Dr. Ann Bergin, Dr. Hasna Zaher, Dr. Mark Irwin, Dr. Andrew Ashley, Dr. Thomas Sorensen and Dr. Ian Ingram for their invaluable insights and advice.

I would like to thank the EPSRC (Doctoral Training Account) for my funding over the past years. I would also like to thank Alan, Jude and the rest of the workshop for their endless patience and an occasional laugh (and a free cylinder of N_2O).

I cannot express how thankful I am for the unconditional love and support of my family: Mum, Dad, Dominic and Dick.

Abstract

This thesis explores the capacity of sterically and electronically unsaturated boranes to bind substrates of biological and environmental interest, and transduce such binding events into a photo-physical and/or electrochemical response, hence reporting the presence of these substrates.

Chapter three details the synthesis of a range of novel ferrocenyl boranes featuring either a proximal hydrogen-bond donor or a second Lewis acidic centre. These novel boranes were shown to be competent at binding both cyanide and fluoride anions, with the role played by a proximal hydrogen-bond donor or a second Lewis acidic centre in anion binding investigated by both NMR and crystallographic studies.

Chapter four reports the synthesis of novel pyridinyl and related boronic esters, as well as unexpected mixed alkenyl/aryl boranes. The capacity of both types of system to bind fluoride or cyanide anions in solution was investigated by UV-Vis and NMR studies. The photo-physical responses to these anions were also probed, leading to the establishment of both switch-on and switch-off fluorescent responses.

Chapter five extends the knowledge derived from selective anion receptor design and combines this with recent developments in the field of frustrated Lewis pairs (FLPs) to activate, bind and report the presence of nitrous oxide (N_2O) molecule. Thus, the syntheses of novel, highly Lewis acidic ferrocenyl boranes that incorporate a high degree of steric loading around the boron centre are reported. The electrochemical and photo-physical response of an FLP system to the presence of N_2O was investigated leading to the development of a novel N_2O reporting system.

Abbreviations

The following abbreviations will be used throughout this report:

Ar – aryl

Ar’ – aryl different from Ar

br – broad

calc. - calculated

Cy – cyclohexyl

d – doublet

DCM – dichloromethane

Dipp – 2,5-diisopropylphenyl

EI – electron impact

ESI – electrospray ionisation

g - gram

h – hours

^{i}Pr – isopropyl

J – coupling constant

m – multiplet

Me – methyl

Meas. Measured

Mes – 2,4,6-trimethylphenyl

mg - milligram

mL – millilitre

mmol - millimole

NHC – *N*-heterocyclic carbene

nm – nanometres

NMR – nuclear magnetic resonance

obs. – observed

Ph – phenyl

ppm – parts per million

q – quartet

reflns - reflections

s – singlet

sept – septet

t – triplet

THF – tetrahydrofuran

UV-Vis – Ultraviolet/Visible light spectroscopy

VT-NMR – variable temperature NMR

δ – NMR chemical shift cf. $SiMe_4$

ε – molar absorptivity

λ – wavelength (in nm)

λ_{max} – wavelength corresponding to maximum observed absorbance

μmol – micromole

Chapter One: Introduction

1. Introduction

Within the broader research area of supramolecular chemistry, the selective detection and reporting of anions in solution has grown to be a rich area of scientific investigation. Anion receptors were initially investigated by Park and Simmons during their work on halide complexation. Of particular note was the synthesis of a macrobicyclic host that was capable of binding chloride anions which represented the first man-made, inorganic anion receptor.[1] Subsequent to this early report of the anion binding affinities of such systems, early research focussed mostly on the *cation* binding capacity of related macrocyclic systems.

Anionic species typically exhibit high enthalpies of solvation, especially in polar and protic solvents. Therefore, anion receptors must out-compete the solvent for anion binding, a factor which represents a significant challenge for fluoride anion detection in aqueous media ($\Delta H_{solvation}$ (F^-/H_2O) = -504 kJ mol^{-1}).[2] Additionally, the sensitivity of anions toward pH can impose limits on receptor design. For instance phosphate anions are protonated at low pH reducing their negative charge, and thereby imposing a constraint on receptor design in terms of the pK_a of functional groups which can be included. Anions can also adopt a range of geometries and sizes, for example halide anions are spherical, cyanide anions are linear and phosphate and sulphate anions are tetrahedral; the receptor must be designed to accommodate these features. The combination of these factors therefore constitutes a challenge when it comes to receptor design.

The selective detection of F^- and CN^-, as well as their conjugate acids HF and HCN, pose significant challenges from both an applied perspective (industrial, medicinal and

defence-related), as well as from the viewpoint of supramolecular chemistry.[3] The nucleophilic cyanide anion exhibits toxicity with low lethal doses for humans (0.5 to 3.5 mg/kg body weight).[4] Due to its widespread use (~1.4 million tons of HCN produced annually, of which ~13% is used for gold extraction) and its ready availability, its release into the environment (whether accidental, malicious or negligent) is a major cause for concern.[5] The concentration of cyanide in drinking water may not exceed 1.9 μM according to the US Environmental Protection Agency (EPA).[6] With this in mind, a comprehensive review of the human-health aspects of cyanide, detection methodologies and their drawbacks has been produced by the World Health Organization.[7]

Aqueous detection of fluoride is also of interest due to its widespread presence in drinking water and toothpaste, as well as being administered during the treatment of osteoporosis.[7,8] Despite the generally positive effects of these water treatment procedures, excessive fluoride anion consumption can lead to dental or skeletal fluorosis.[9,10] Fluoride and cyanide anion sensors can also be envisaged to be of use in the detection of phosphorofluoridate and phosphorocyanate nerve agents in the case of terrorist attack or non-conventional warfare.[3,11]

1.1. Approaches to Anion Recognition excluding Boranes

1.1.1. Exploiting Electrostatic Interactions

The simplest conceptual anion receptor design exploits the fundamental characteristic of anions, namely the bearing of one or more atomic units of negative charge. Designs seeking to exploit this characteristic feature anion hosts bearing a positive charge and rely on the Coulombic forces between two charged species (Equation 1).[12-14]

Designs of receptors for anions typically try to maximise the interaction between host and guest, therefore hosts typically feature high charges, and try to minimise the distance between the charges of the host and the anionic guest.[14-16]

$$F = k_e \frac{|q_1 q_2|}{r^2}$$

Equation 1: Coulombs law. The force of attraction between two oppositely charged particles (F) is proportional to the magnitude of the product of the charges of the two particles and inversely proportional to the square of the distance between the two particles.[12,13]

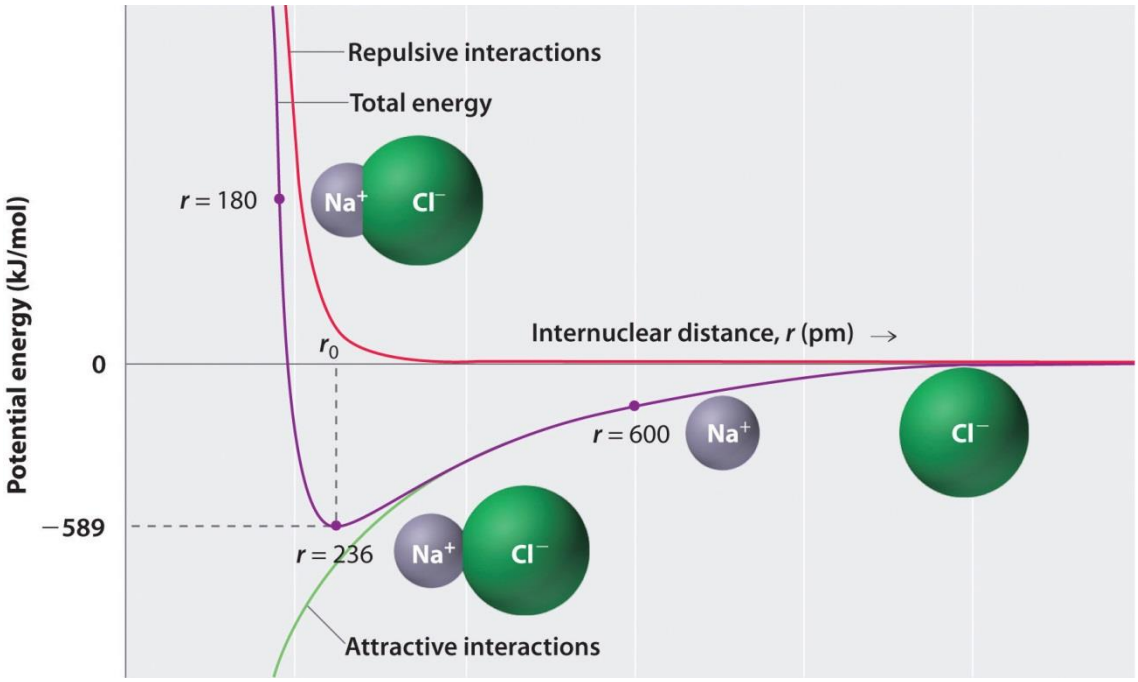

Figure 1.1. A pictorial representation of the potential energy of the interaction of a sodium cation with a chlorine anion (reproduced from the work of Averill and Eldredge).[17]

The minimisation of distance between the charges of host and guest is limited by steric repulsion (Figure 1.1). All other factors concerning the interaction between host and guest being equal, positively charged hosts will interact more strongly with smaller, more highly charged anions than with larger, less highly charged anions (Figure 1.2). However, a problem inherent in the sole exploitation of Coulombic forces in *selective* anion

receptors is that this force is non-directional, with the differences in association energy between similarly sized/charges species being too low to allow facile discrimination. Early work sought to overcome this limitation by imposing spatial (and hence directional) constraints, on the host/guest interaction.[18-21] This imposition of spatial constraints on the anionic guest was achieved by positioning positive charges on the host in a semi-rigid manner around a cavity in which anionic guests could bind (Figure 1.3).[18-21] A pictorial representation of the effect of having two cationic centres within the host on the binding energy profiles of two different anions is depicted in Figure 1.4. This inclusion of multiple cationic centres around a cavity (**1** and **2**) allows for the selective binding of larger anions (Br^- and I^-) over smaller anions (Cl^-) despite the smaller anions being capable of interacting more strongly with a single cationic centre (Figure 1.3).[18-20] Hosts designed to include cation surrounded cavities can also achieve anion binding *selectivity* through size as very large anions cannot accommodate the steric imposition of residing in the cavity. Thus host molecules **1** and **2** were shown to exhibit size selectivity by Schmidtbauer, where **1** features an exceptionally high dissociation constant and a small cavity, whereas **2** features an exceptionally low dissociation constant and a larger cavity for the chloride anion.[20] Comparable systems synthesised by Hossain *et al.* have been exploited in the encapsulation of chloride anions.[22] The cobaltocenium system **3** synthesised by Beer *et al.* is also posited to bind anions such as hydroxide, chloride and hexafluorophosphate through electrostatic interactions alone.[23]

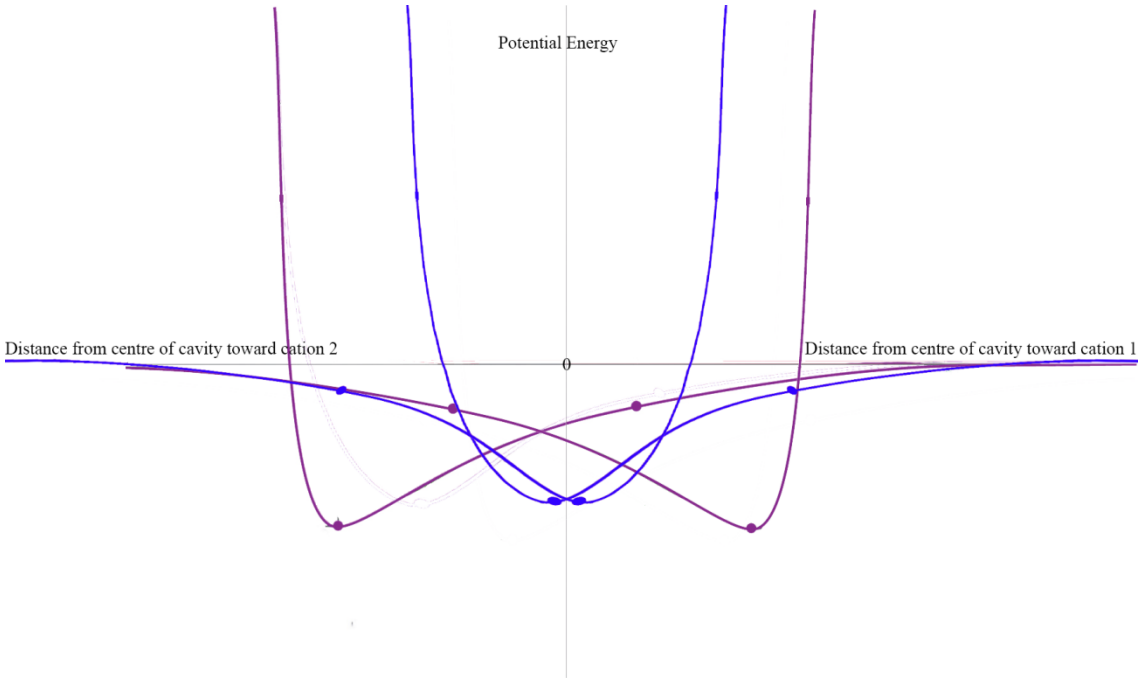

Figure 1.2. A pictorial representation of the two components of the potential energy of an anion on a line between two charged cations with 0 denoting the centre of the line (or a cavity in a host). The purple line represents a smaller anion bearing a single charge, the blue line a larger anion bearing a single charge. In this example the host offers optimal binding to the larger anion, as there is a location within the cavity where the sum of the two potential energy profiles is greater than the sum possible for the smaller anion at any point in the cavity, despite a greater magnitude of potential energy to a single point charge.

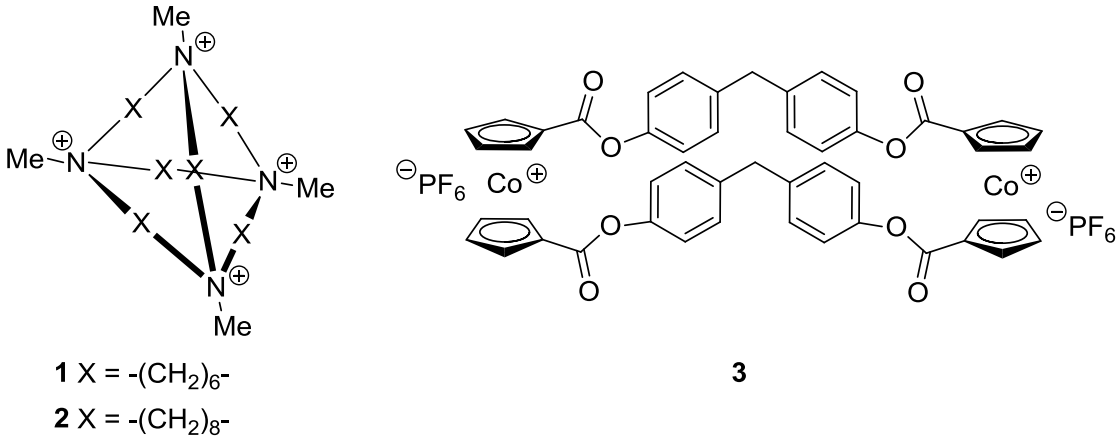

Figure 1.3. A macrocyclic quaternary ammonium host **1** and **2** reported by Schmidtchen *et al* (left) and a macrocyclic *bis*cobaltocenium receptor **3** reported by Beer *et al* (right).[18-21,23]

A limitation in synthesising host molecules bearing positive charge is that they must be synthesised with counter anions as prescribed by the principle of electro-neutrality, and as such there exists competition between the counter-ion present in the starting material and the target anion. This difficulty was overcome by Worm and co-workers with the synthesis of zwitterionic host molecules bearing cationic sites in proximity to a central cavity, and more remote negative charges on the outside of the host molecules **4** and **5** (Figure 1.4).[24,25] These systems were shown to form adducts with a variety of anions (CN^-, Cl^-, Br^-, I^- and PF_6^-) by ^1H NMR titration. As such, complex **4** was found to possess a higher halide anion affinity than the related system **1**.

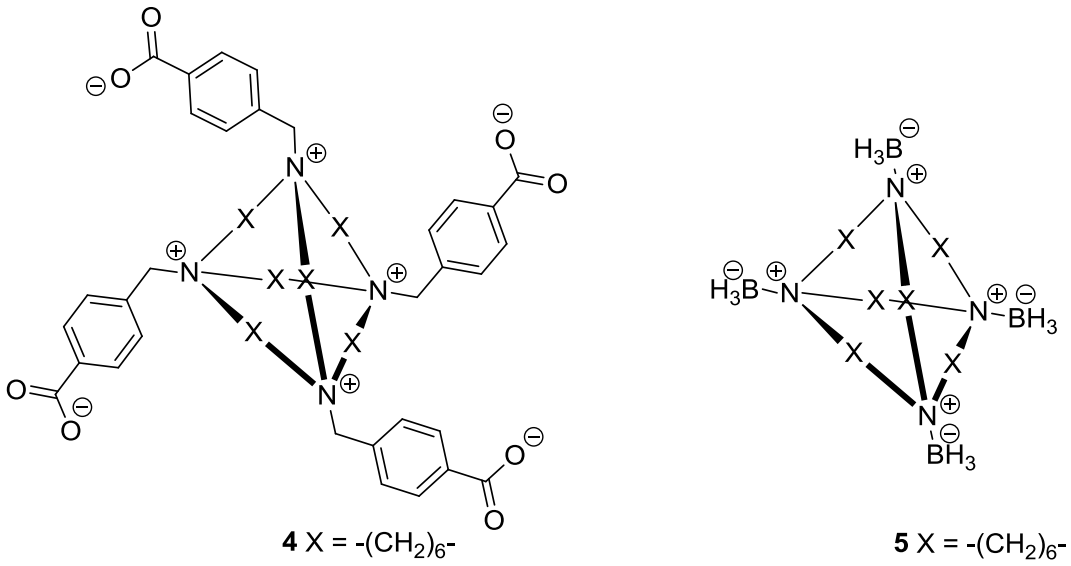

Figure 1.4. The zwitterionic complexes **4** and **5**.[24,25]

1.1.2. Binding Anions using Hydrogen Bonds

Anions can be conceived of as electron pair donors and, as such, are capable of donating an electron pair to a sufficiently strong Lewis acid. Hydrogen bonds are a specific sub-set of these interactions where the Lewis acid is comprised of a hydrogen atom bound to a relatively electronegative atom (such as O-H or N-H functions). The formal definition of a hydrogen bond is "a form of association between an electronegative atom and a hydrogen atom attached to a second, relatively electronegative atom. It is best considered as an electrostatic interaction, heightened by the small size of hydrogen, which permits proximity of the interacting dipoles or charges".[26] The association energies for hydrogen bonds in the gas phase have been shown to range from zero to extremely strong (161.5 kJ mol^{-1} for FH_2^+),[27,28] although most commonly encountered interactions (N-H···N/O-H···O) correspond to intermediate values (20 - 25 kJ mol^{-1}).[26] The nomenclature adopted in discussions of hydrogen bonding use "hydrogen bond donor" to refer to the hydrogen atom directly bound to the second electrostatic atom and "hydrogen bond acceptor" to refer to the electronegative atom to which the bond is made.[27]

As with Coulombic interactions between ions of opposite charge, the strength of hydrogen bonding varies with the distance between the hydrogen bond donor and acceptor, however the energy profiles vary with the strength of the hydrogen bond established (Figure 1.5).[27] Furthermore, the strength of the interaction between hydrogen bond donor and acceptor is dependent on the angle described by the nuclei of the three atoms involved in the hydrogen bond.[27,29,30] For instance, Dreyfus and Pullman calculated that the angle θ(C-O···H) adopted by the hydrogen bond in the formamide dimer $(H_2NCO_2H)_2$ is 120º, and calculated that a change of θ to 180º would come at an energetic cost of 6.3 kJ mol^{-1}.[30] The exploitation of hydrogen bonding in the field of selective anion

detection is therefore somewhat more complicated than the exploitation of point charges alone, as the hydrogen bonding interactions are typically of lower energy than Coulombic forces whilst imposing greater geometric demands on host-guest complementarity due to the directionality of the bonding.

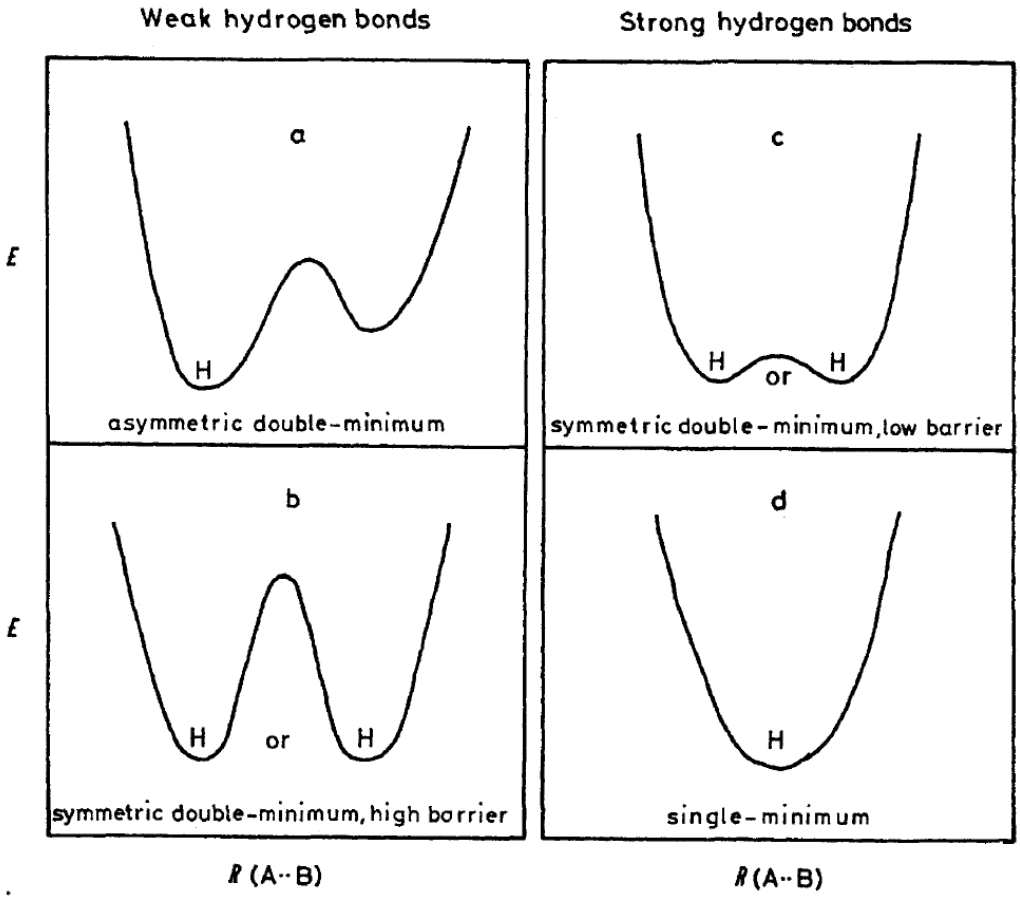

Figure 1.5. Pictorial representation of hydrogen bond energy profiles *viz.* distance between hydrogen bond acceptor and donor, reproduced from the work of Emsley.[27]

The concept of host/guest complementarity due to the spatial and geometric demands of a hydrogen bonding motif is perhaps best illustrated by the pairing of "base pairs" in DNA (Figure 1.6.). The geometries of the base pairs make hydrogen bonding between both the thymine and adenine pair and the cytosine and guanine pair more

energetically favourable than any other pairing allowing for selective pairing of these two pairs.

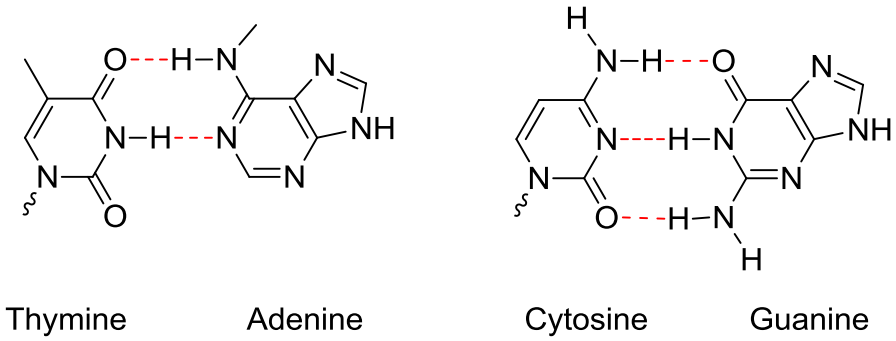

Figure 1.6. The hydrogen bonding (shown in red) between thymine and adenine (left) and between cytosine and guanine (right).

The spatial and geometric constrains of hydrogen bonding, as well as the typically low association energies, have led to anion receptors being designed featuring multiple hydrogen bond donors in a quasi-rigid framework. The first example of an anion receptor that solely exploits hydrogen bonding was reported by Spergel and co-workers (**6**, Figure 1.7).[31] This macrocyclic receptor was shown to bind fluoride anions by titration followed by ^{1}H and ^{19}F NMR spectroscopy.

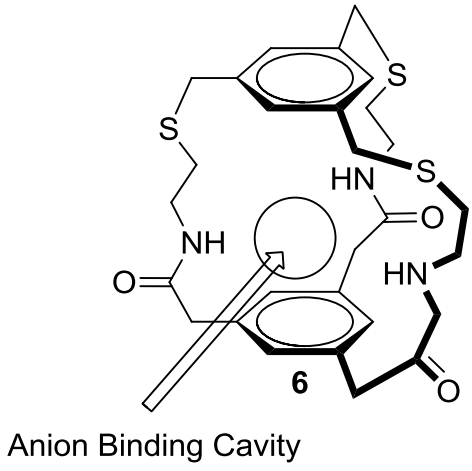

Figure 1.7. The fluoride anion binding receptor **6** reported by Spergel and co-workers.[31]

That some degree of flexibility is preferable in receptor design is illustrated by the work of Sessler and co-workers in their synthesis of the calix[4]pyrrole **7** (Figure 1.8).[32] The free receptor **7** was crystallised by slow evaporation and the crystal structure shown to exhibit a 1,3-alternate conformation in which adjacent rings are orientated toward opposite faces of the molecule (Figure 1.8).[32] This receptor was shown to interact with a fluoride anion guest by ^{1}H NMR titration experiments.[32] The crystal structure obtained clearly shows hydrogen bonding of the fluoride anion to each of the four pyrrole units, all of which now face in the same direction (Figure 1.8).[32]

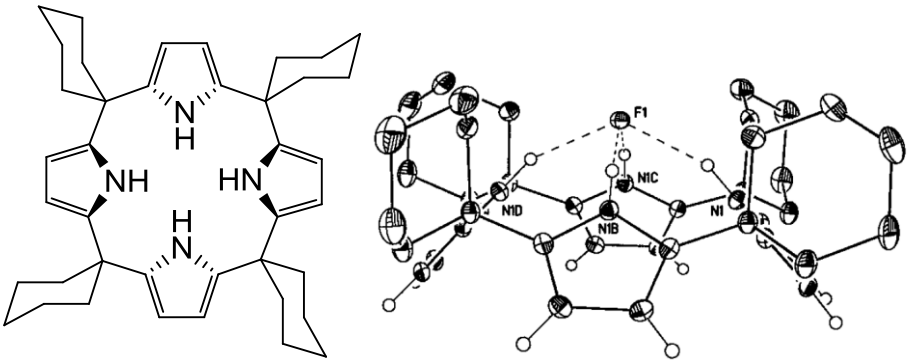

Figure 1.8. The structure of the fluoride anion receptor **7** (left) and the partial crystal structure of [**7**·F]$^{-}$ (right) with thermal ellipsoids drawn at the 30% probability level (reproduced from the original paper of Sessler).[32]

This calix[4]pyrrole type receptor was further exploited by Sessler and co-workers in a displacement assay, by synthesising the (colourless) hydrogen bonded adduct of the 4-nitrophenolate anion, [**8**·($C_6H_4NO_3$)]$^{-}$ (Figure 1.8).[33] When this adduct was treated with a source of fluoride, the 4-nitrophenolate anion was displaced, resulting in a colour change to yellow due to the presence of the free 4-nitrophenolate anion in solution (Figure 1.8).[33] This work was subsequently extended to 'super extended cavities' by Gale and co-workers.[34]

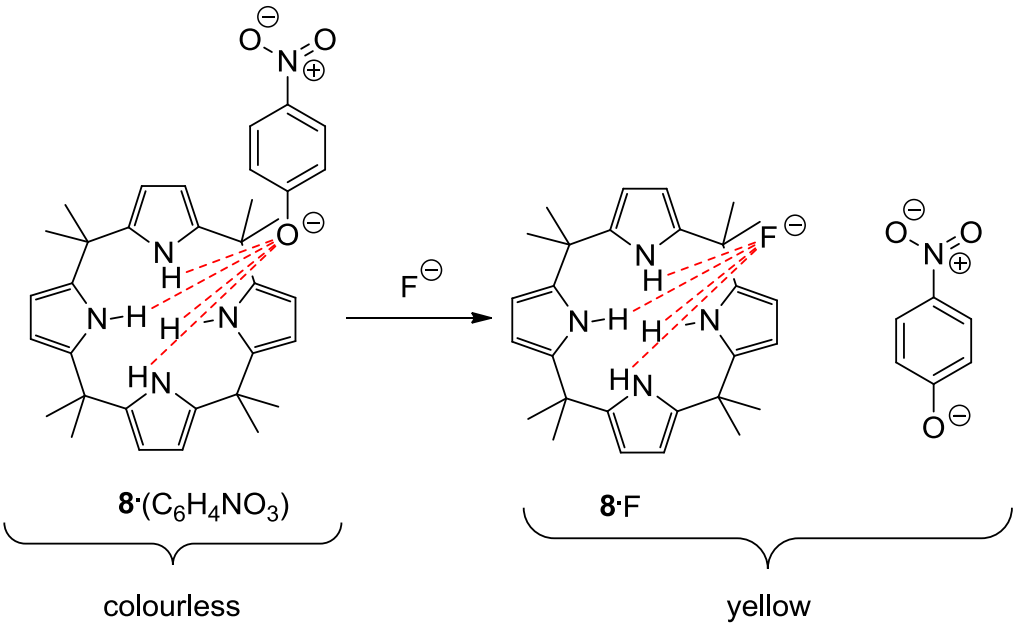

Figure 1.9. The colorimetric detector for fluoride anions described by Sessler and co-workers.[33]

A more synergic approach to anion binding incorporates both Coulombic interactions - with their high interaction energies - and a hydrogen bonding motif within a semi-rigid framework - to provide greater selectivity. Early examples include the work of Graf and Lehn with their protonated cryptand **9** (Figure 1.10).[35] This system was shown to encapsulate fluoride, chloride and bromide anions by ^{13}C NMR titration.[35]

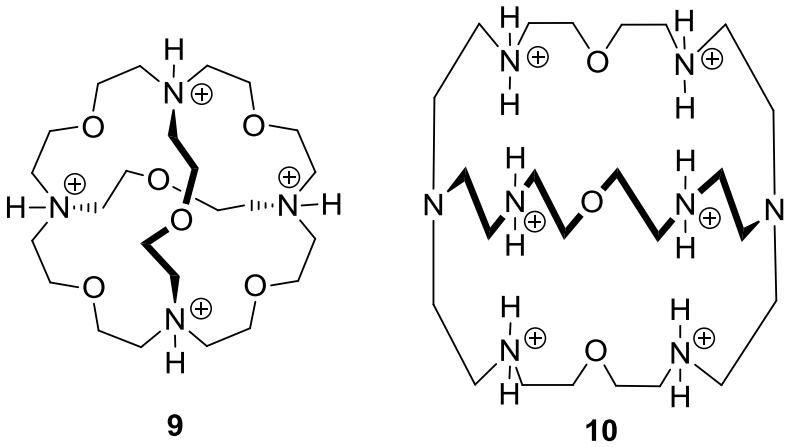

Figure 1.10. Protonated cryptands **9** and **10**.

Cryptand **10** was designed by Lehn *et al.* as a selective host for the linear azide anion, featuring an ellipsoidal cavity with the capacity to form hydrogen bonds at the termini of the azide guest.[36] The azide molecule was shown to bind *via* two sets of three hydrogen bonds each arranged to yield an overall tetrahedral geometry at nitrogen. The size of the cavity is thought to preclude strong binding events with larger anions on steric grounds. **10** was, however, found to bind smaller, spherical anions such as fluoride, chloride and bromide. The latter two anions were found to form six hydrogen bonds in an octahedral arrangement, whereas the fluoride anion was found to form only four hydrogen bonds in a tetrahedral arrangement.[36] This highlights a key limitation of the use of hydrogen bonding in designing selective anion receptors, in that the host usually incorporates flexibility to maximise the strength of hydrogen bonding to the anion at the cost of selectivity. Further approaches that have been employed to maximise both anion selectivity and anion binding strength can be found in the review of Gale and Beer.[14]

1.1.3. Lewis Acids in Anion Recognition

By the Lewis definition, acids are electron-pair acceptors and bases are electron-pair donors. Conventionally, the two form a dative covalent bond when mixed together to give an acid-base adduct, thereby quenching the reactivity of both acid and base.[37] Anions, by definition molecules possessing more electrons than protons, typically possess a lone pair of electrons that can form a dative covalent bond to a Lewis acid of sufficient strength. In contrast to hydrogen bonding, which can be conceived of as a primarily electrostatic interaction, containing a minor covalent binding component, dative covalent bonds are best considered as primarily covalent interactions with minor electrostatic components.[37-40] Following the Pearson (Hard –Soft) acid base theory, in which hard acids interact more strongly with hard bases (enthalpically driven) and soft acids interact

preferentially with soft bases (solvation sphere driven), selectivity for anions can be envisioned through the appropriate selection of hosts acid hardness[41-44] Hard bases include cyanide, hydroxide, fluoride and chloride anions and typical hard acids include Si(IV) and BMe_3.[41-44]A typical feature of hard Lewis acids is that they possess a lowest unoccupied molecular orbital (LUMO) of high energy, whereas hard Lewis bases possess a highest-occupied molecular orbital (HOMO) of low energy.[45] A range of anion receptors have been designed that exploit the complementarity of chemical hardness as defined by Pearson.[14,44,46,47]

1.1.3.1. Late *d*-Block Metals in Anion Recognition

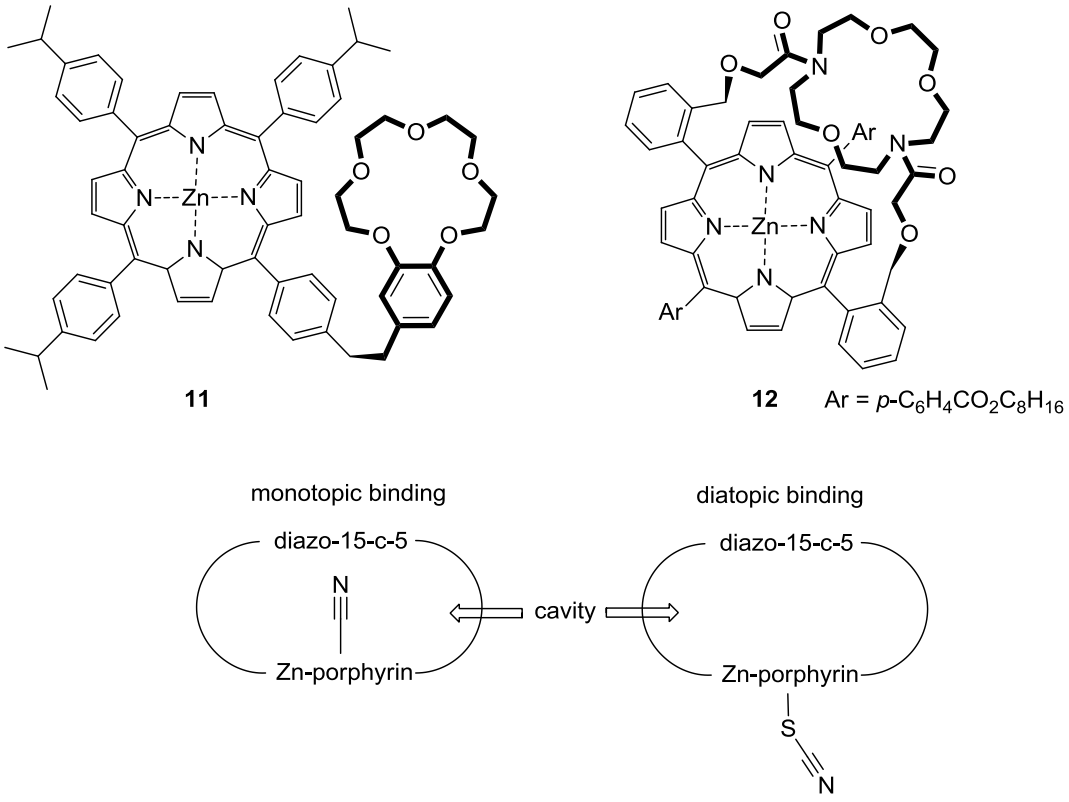

Figure 1.11. Two zinc porphyrin anion receptors.

A class of zinc-containing porphyrins capable of ion pair recognition were reported by Hong *et al.* that feature both an anion and cation binding site (Figure 1.11).[48] Receptor **11** (Figure 1.11) was shown by ^{1}H and ^{13}C NMR spectroscopy to respond to the presence of the sodium salts of F^-, Cl^-, Br^-, I^-, SCN^- and $H_2PO_4^-$, due to complexation of the sodium cation within the crown ether component.[48] The interaction of **11** with NaCN resulted in a broadening of resonances in the ^{1}H NMR spectrum and a colour change from red to green that was not observed for the other sodium salts, consistent with the cyanide ion binding at the zinc centre.[48,49] A similar response to sodium cyanide was observed with receptor **12** (Figure 1.11), as reported by Liu *et al.*, with an accompanying colour change from purple to green.[50] Moreover, **12** exhibits a marked difference in binding affinity for sodium cyanide (7.4×10^5 M^{-1} in methanol) over that of sodium thiocyanate (1.1×10^3 M^{-1} in methanol), which the authors ascribe to the smaller cyanide ion being able to bind monotopically (between the diazo-crown ether and the porphyrin), whereas the larger thiocyanate can only bind ditopically (Figure 1.11).[50] Both of these receptors illustrate that metal centred Lewis acids can bind anions, with steric effects imposing constraints on the stereochemistry of anion binding.

The Lewis acidity of ligated copper has also been exploited for the selective recognition of cyanide, for instance in systems **13** and **14** reported by Ahlers *et al.* (Figure 1.12).[51] Both **13** and **14** change colour on treatment with one equivalent of cyanide in 1:1 acetonitrile-methanol solution (from blue to purple for **13·CN**, and blue-green for 1**4·CN** respectively; Figure 1.12).[51] Moreover, it was shown that receptor **14** exhibits stronger binding of cyanide than receptor **13** (approximately 100 fold), which the authors explain by reference to dinuclear macrocyclic copper (II) complexes having higher affinities for bridging anions of appropriate size than related mononuclear

complexes.[51-53] Cyanide receptor **14** can therefore be thought of as exploiting Lewis acidity in concert with size and geometric selectivity for the cyanide anion.

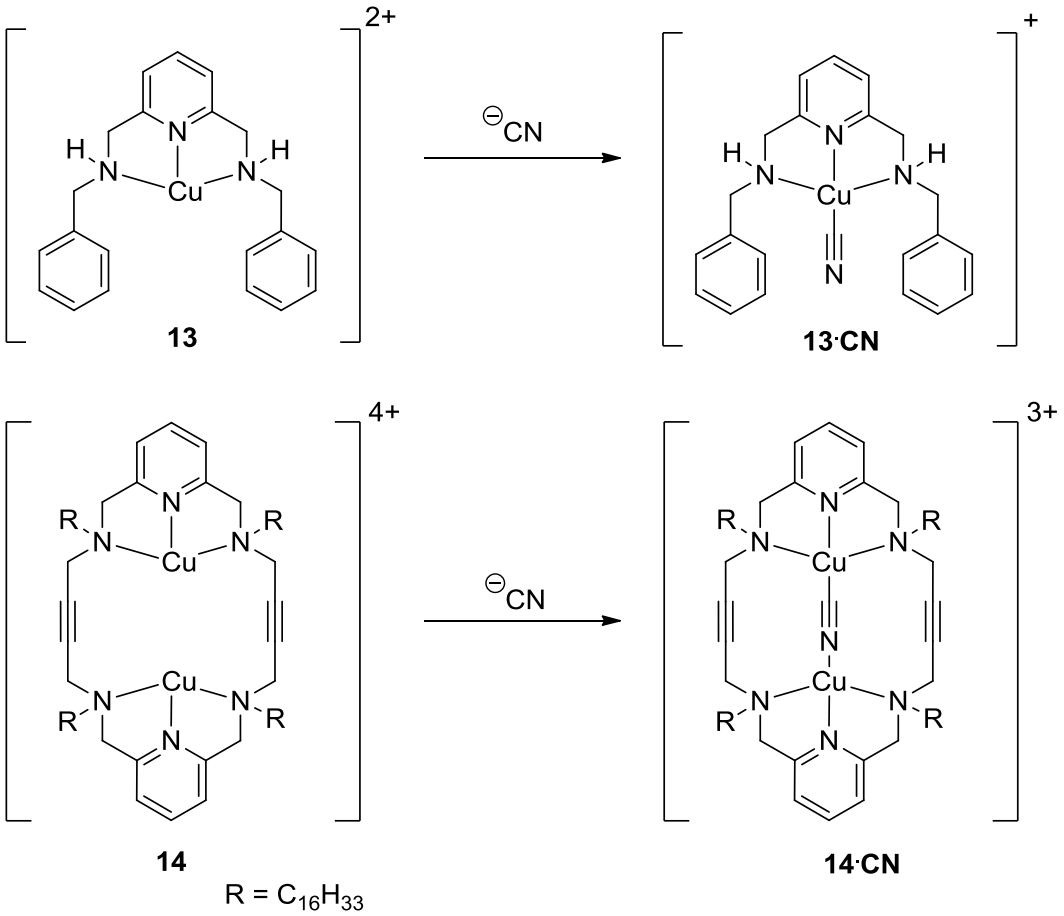

Figure 1.12. Cyanide complexation by ligated copper.[51]

The Lewis acidic nature of mercury (II) systems has also been exploited in concert with chelation to create selective receptors for halides, for instance as part of the systems described by Wüst *et al.* (**15**) and Shur *et al.* (**16** and **17**) (Figure 1.13).[54,55] Receptor **15** was shown by ^{199}Hg NMR spectroscopy to bind to chloride, bromide and iodide anions, with an X-ray diffraction study of crystals of the 2:1 host:chloride complex showing that the anion was bound in a chelating fashion.[54] The 1,2-*bis*-mercuriated phenylene framework has been further exploited by Shur *et al*., with complexes **16** and **17** exhibiting

anion association with chloride, bromide and iodide anions in acetonitrile solution by NMR spectroscopy.[55] Crystals of the 1:1 complex of receptor **17** with bromide show that the anion forms six short contacts with the three mercury atoms of two host molecules, thereby forming infinite chains in the crystalline state.[55]

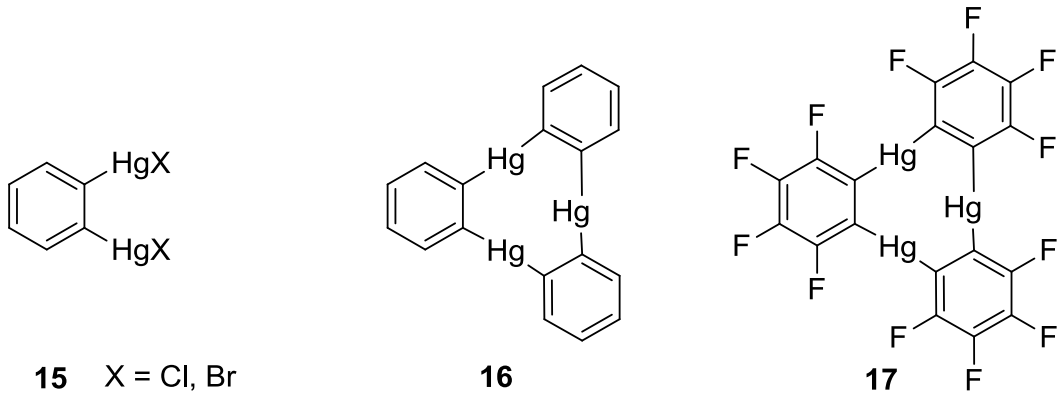

Figure 1.13. Mercury (II) receptors for halides.[54,55]

1.1.3.2. "Hypervalency": *p*-Block Lewis Acids in Anion Recognition

Compounds containing the lighter *p*-block elements normally obey the "octet-rule", in that the Main Group element forms bonds so that it formally possesses eight valence electrons.[56-58] Exceptions to the "octet-rule" for groups 14-18 are well known, typically referred to as "hypervalent," and include compounds such as PCl_5, SF_6, IF_7 and XeF_2.[58] These "hypervalent" compounds are often described using the N-X-L notation, where N denotes the number of valence electrons at the main group element, X is the chemical symbol and L is denotes the number of ligands bound to the central atom (i.e. XeF_2 would be 10-Xe-2).[59] The early theoretical consideration of "hypervalency" by Musher suggested the involvement of higher energy d-orbitals.[60] This was disputed by Magnusson, who stated that little evidence existed for the contribution of *d*-orbitals in the

bonding of "hypervalent" molecules.[61] Controversy over the use/misuse of the terms "octet-rule" and "hypervalent" have also been raised by Gillespie *et al.*[62]

The capacity of Main Group elements to act as Lewis acids by exceeding the classical octet rule, and thereby bind anions, was exploited Azuma *et al*. and Newcomb *et al*. in the design of the Lewis acidic tin macrocycles **18**, **19** and **20** (Figure 1.14).[63-65] Each was shown to bind anions (such as F^-, Cl^- and Br^-) by NMR spectroscopic studies. Of particular note, is the fact that macrocycles of type **18** were shown to sequentially form both 1:1 and 1:2 host:guest complexes with chloride anions in acetonitrile solution, with binding constants K_1 = 814 (n = 8), 684 (n = 10) $Mol^{-1}$and K_2 = 863 (n = 8), 556 (n = 10) Mol^{-1}.[65]

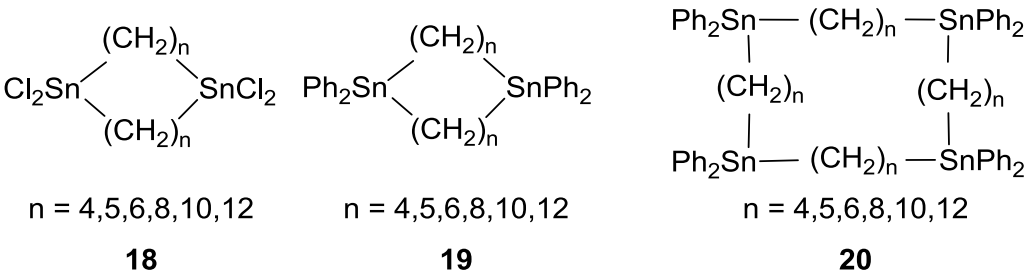

Figure 1.14. Tin-containing macrocyclic anion receptors.[63-65]

Further work on tin-containing macrocycles by Newcomb *et al.* concentrated on the related systems **21** and **22** (Figure 1.15).[66-69] Macrocyclic receptors of type **21** were found to bind chloride anions, although with slower binding kinetics than the related macrocycles **18**. Anions were found to bind increasingly slowly as the chain length, *n*, decreased, and only 1:1 host:guest complexes were formed.[66] ^{119}Sn NMR spectroscopic studies on the reactions of systems of type **21** revealed that fluoride was bound approximately five times more strongly than chloride when n = 2, which the authors ascribe to cavity size effects.[67] Analysis of the ^{119}Sn NMR spectroscopy studies of

receptor **21** (n = 6) showed that the receptor binds only one equivalent of either fluoride or chloride anions in chloroform solution, with ^{119}Sn VT-NMR spectroscopy studies suggesting that the fluoride anion is chelated, whereas the chloride anion is more closely bound to one of the two tin sites, but rapidly switches binding site on the NMR timescale at room temperature.[68] This would suggest that the rigidity of the host imposes a geometric constraint on the binding modes of fluoride and chloride anions, where the energetically optimal binding site for the fluoride anion is located approximately half-way between the two tin centres. In contrast, the chloride anion can access two energetically optimal sites, each one sited closer to one tin centre than the other, with a small energetic barrier between the two sites (calculated as 22.2 kJ mol^{-1}) as compared to the available thermal energy of the system at room temperature.[68] The chelation of the fluoride anion in the solid state was confirmed by X-ray diffraction studies, as was the increased proximity of the bound chloride anion to one of the tin centres in preference to the other.[68,69]

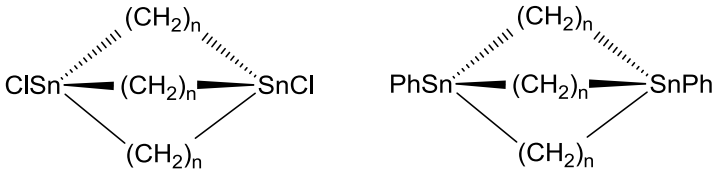

Figure 1.15. Tin-containing macrocyclic anion receptors capable of chelation.[66-69]

Tamao and co-workers reported the synthesis of receptors **23**-**25** (Figure 1.16) based around Lewis acidic Si(IV) centres that are capable of recognising the fluoride anion (and again exceeding the classical "octet" of *p*-block elements).[70,71] Receptor **23** was shown to form the adduct [**23**·F]$^-$ on addition of one equivalent of KF/18-crown-6.[70] The fluoride anion is bound in a chelating fashion in the solid state, forming bonds to both silicon centres.[70] In solution at room temperature, the ^{19}F NMR spectrum exhibits only

one broad resonance at -117.3 ppm, which implies that the silicon bound fluorine atoms interchange rapidly on the NMR timescale.[70] This is further supported by the ^{29}Si NMR spectrum, which features a sextet centred at -90.0 ppm.[70] Later studies by Tamao and co-workers showed that the relative fluoride anion affinities fall in the order **24** < **23** < **25**, suggesting that a lowering in energy of a LUMO bearing a large σ*(Si-F) contribution is key to the Lewis acid/base interaction.[71] The conflicting effects of additional stabilisation from chelation *vs* increased steric burden was probed by ^{1}H NMR spectroscopy in a competition experiment between [^{n}Bu$_4$N][PhMeSiF$_3$] and **23** (Figure 1.16); the equilibrium was found to lie in favour of the chelate effect (K = 3.3 x 10^2) Mol^{-1}.[71]

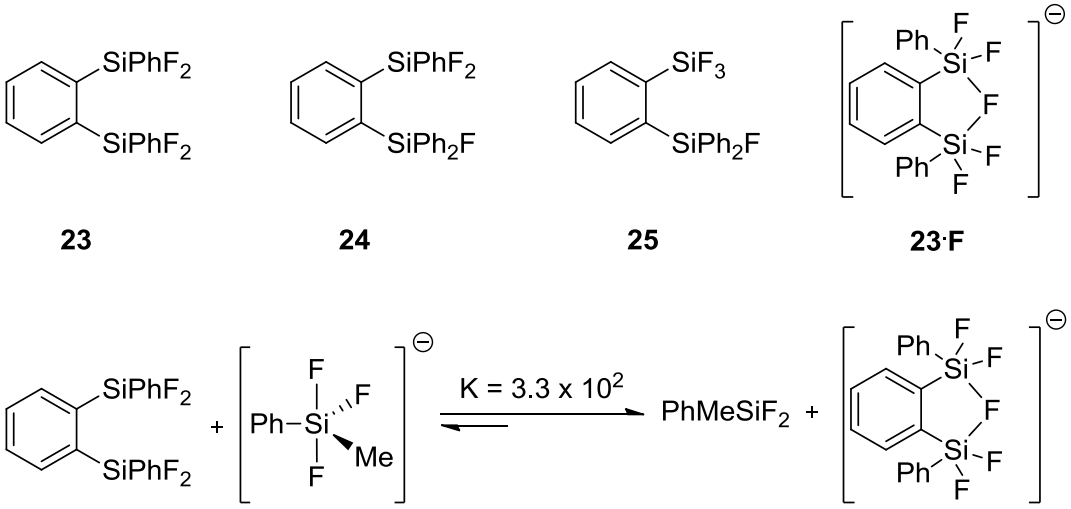

Figure 1.16. Silicon-containing fluoride anion receptors (**23**–**25**), a fluoride adduct (**23**·F) and the equilibrium between a chelating and a non-chelating fluoride anion receptor.[70,71]

The use of Lewis acidic *p*-block elements that formally have a full octet to bind anions is not limited to tin and silicon. Thus, for instance germanium has been exploited in the macrocycles of Takeuchi *et al.* for the selective binding of chloride anions.[72,73] Further examples of the exploitation of Main Group elements other than boron can be

found in the work of Gabbaï and co-workers, including the use of antimony in receptors **26** and **27** for the detection of fluoride (Figure 1.17).[74,75]

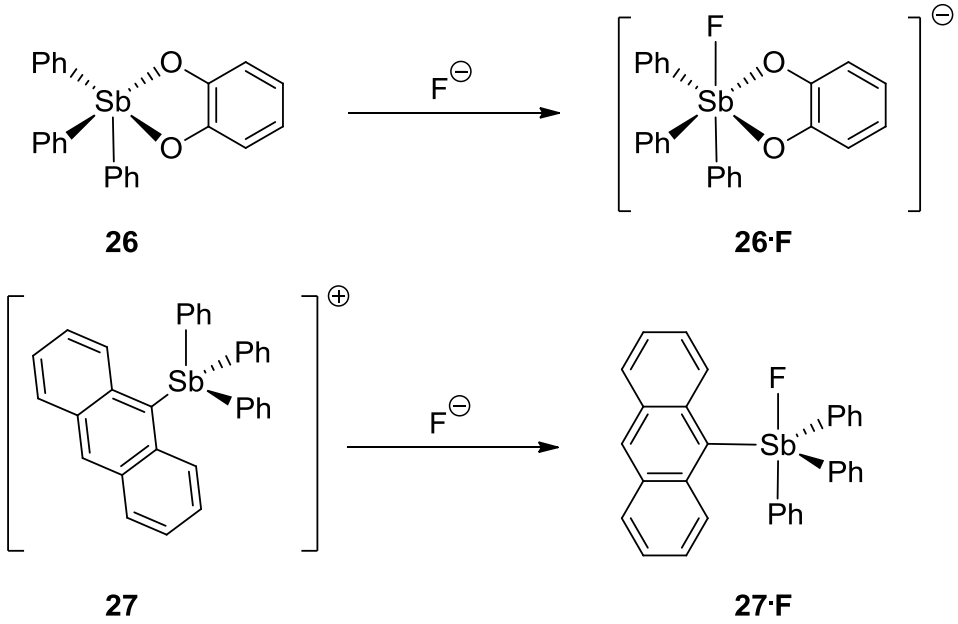

Figure 1.17. The detection of fluoride anions by antimony-containing systems.[74,76]

1.2. Anion Recognition by Lewis Acidic Boranes

Early research into this area of research was conducted by Shriver and Biallas, whose use of chelating *bis*-boranes in binding methoxide anions, and was continued by Katz, leading to the creation of the archetypal "hydride sponge".[77-79] More recent work involving boranes in binding fluoride and cyanide anions will be discussed in detail in Sections 1.2.1. through 1.3.4.[2,74,75,80-119]

In its most familiar compounds, boron adopts the oxidation state III, including its oxides, sulfates, nitrides and halides.[120] Over a hundred borate minerals are known, with the boron atom adopting both tetrahedral and planar geometries depending on the other components of the mineral.[120] The boron halide complex BF_3 adopts a trigonal planar geometry (D_{3h}). The boron forms a two-centre-two-electron σ-bond to each of the three

fluorine atoms, as well as π-back-bonding to all the three fluorine atoms. This compound, BF_3, is formally an exception to the "octet rule" as the boron formally possesses only 6 valence electrons and could be considered to be "sub-valent". As such, it would be predicted that BF_3 can act as a Lewis acid in accepting an electron pair from a Lewis base into its formally vacant p_z orbital to form a dative covalent complex (as was shown by Brown *et al.* in the reaction of BF_3 with 2,6-dimethyl pyridine).[121] Boranes of the type BR_3, such as BMe_3, are described as hard acids by Pearson *et al*,[41-43] and would therefore be expected to form stronger bonds to hard bases such as fluoride anions, than to weaker bases such as the chloride anion. Moreover, 6-valence electron boranes would be expected to form stronger bonds to hard bases such as fluoride than would softer 8-valence electron silicon or tin compounds.

1.2.1. Boronic Esters for Fluoride and Cyanide Anion Binding

Boronic esters have been exploited in fluoride anion sensing. Thus, for instance, ferrocene appended boronic acid, $FcB(OH)_2$, was shown by Shinkai *et al.* to electrochemically sense fluoride anions in mixed methanol/water solutions bearing electrolytes, through the change in the half-cell reduction potential brought about by the complexation of fluoride at the boron centre.[122] Further development by Shinkai *et al*. on these systems led to the development of related saccharide esters, $FcB(O_2C_6H_8(OH)_4)$, which were chemically more robust to B-O bond rupture whilst still affording an electrochemical shift to the presence of fluoride anions.[123] When these boronic esters were coupled to redox active dyes (that were complementary to the shift in the ferrocenyl half-wave reduction brought about by fluoride anion complexation) the binding event could be transduced into a colorimetric response.[123]

Further examples of the use of esters include compound **31** (Figure 1.20) that was shown by Bresner *et al*. to reversibly bind and electrochemically indicate the presence of fluoride anions in chloroform solution.[74] Selectivity for hard anions can be rationalised by the high enthalpic cost of pyramidalisation, due (in part) to the disruption of stabilising B-O π-interactions, with this loss only being compensated for by the binding of anions forming strong bonds to boron (e.g. F^-). Binding of fluoride to boron was evidenced by a shift of the resonance corresponding to the central boron in the ^{11}B NMR spectrum from a singlet at 34 ppm to a doublet at 8 ppm.[84] Further work on related calixarene boronic esters showed that these systems were susceptible to B-O bond cleavage, reflecting the weaker B-O bonding in B-O-Ar systems as compared to the analogous alkyl B-OR systems.[74,124,125]

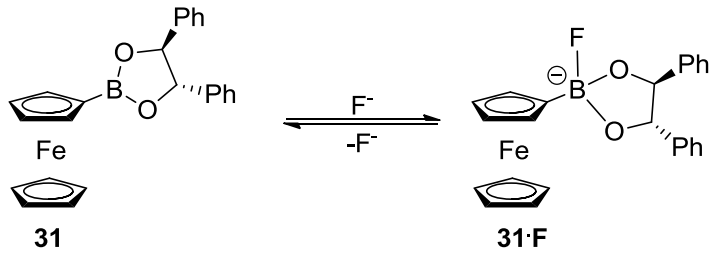

31 **31·F**

Figure 1.20. The reversible binding of fluoride anions by the boronic ester **31** in chloroform solution.[74]

1.2.2. The Use of Triarylboranes in Selective Anion Recognition

Given that three-coordinate, 6-valence electron boranes are typically strong Lewis acids, facile coordination of anions can be achieved. Complexation of anions to boranes of this type results in significant pyramidalisation and corresponding re-hybridisation of the orbitals around boron. By increasing the size of the groups attached to the boron atom, the enthalpic cost of coordination of a Lewis base to the central boron atom can be increased

such that coordination is not observed, as was demonstrated by Brown *et al.* through the differing affinities of BF_3 and BMe_3 for 2,6-dimethyl pyridine (Figure 1.18).[121] If the groups bound to the central boron atom are aromatic,[126-129] then three-coordinate, 6-valence electron compounds of the type BAr_3 can feature stabilising π-interactions between the aromatic groups and the formally vacant *p*-orbital of boron.[130-132] Loss of these stabilising π-interactions can also provide an additional enthalpic cost to complexation. Anion binding selectivity can therefore be achieved through incorporating sufficient steric bulk and conjugation to provide a high enthalpic cost to anion complexation, which can only be overcome by anions that from strong bonds to the borane (i.e. hard bases such as F^- or OH^-).

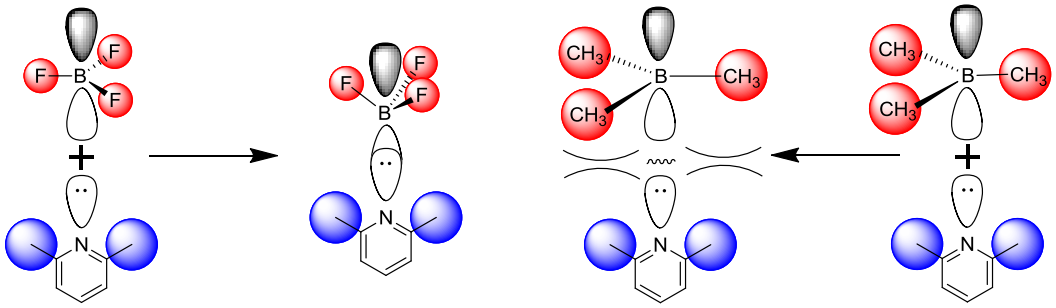

Figure 1.18. A pictorial representation of the Lewis adduct formation of 2,6-dimethyl pyridine and BF_3 (left) and the sterically frustrated Lewis pair, 2,6-dimethyl pyridine and $(CH_3)_3B$ that do not form a Lewis adduct due to steric strain (right).

The simplest example of fluoride anion binding by a triarylborane is that of Ph_3B to give $[Ph_3BF]^-$, reported first by Veltheer *et al.*[130] Theoretical studies of this reaction by Krossing *et al.* and Timoshkin *et al.* report that the gas-phase enthalpy of reaction is highly exothermic (ΔH = -342 or -345 kJ mol^{-1} respectively, depending on the level of theory used).[131,132] Timoshkin *et al.* also calculated the gas-phase enthalpies for the reaction of Ph_3B with H_2O (ΔH = -10.1 kJ mol^{-1}) and PH_3 (ΔH = 0.1 kJ mol^{-1}), thereby correlating with the expectations of Pearsons HSAB theory.[41-43,131]

That increased steric bulk of the aromatic substituents of systems of the type Ar_3B lowers the enthalpy of reaction with fluoride anions in the gas-phase was calculated by Gabbaï and co-workers, with their calculations showing a lower enthalpy of reaction for Mes_2BPh (ΔH = -254 kJ mol^{-1}) than that calculated for Ph_3B.[116,131,132] The fluoride binding constants in THF solution for three related systems Mes_2BPh (**28**), Mes_3B (**29**) and Ant_3B (**30**) were determined by Aldridge, Gabbaï, Tamao and their respective co-workers by UV-Vis titration experiments (Figure 1.19).[92,119,133] The trend of decreasing fluoride binding constant on increasing steric bulk is as expected (K_F (**28**, THF) = 5 x 10^6, K_F (**29**, THF) = 3.3 x 10^5 and K_F (**30**, THF) = 2.8 x 10^5). **28** was shown to bind cyanide anions irreversibly by Aldridge and co-workers.[92]

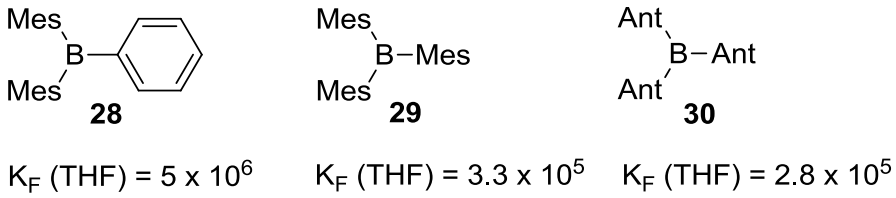

Figure 1.19. The Lewis acids Mes_2BPh (**28**), Mes_3B (**29**) and Ant_3B (**30**) and their fluoride binding constants (K_F in units of Mol^{-1}) determined by titration followed by UV-Vis spectroscopy in THF solution.

1.2.3. Effect of Electron-Withdrawing Substituents

The strength of the interaction between a triarylborane BAr_3 and anions such as fluoride and cyanide can be increased by incorporating electron-withdrawing substituents in the aromatic groups.[131] For instance, $B(C_6F_5)_3$ is calculated to have a gas-phase enthalpy of reaction with the fluoride anion of -454 kJ mol^{-1} compared to that of -345 kJ mol^{-1} for BPh_3.[131] This high fluoride binding enthalpy of $B(C_6F_5)_3$ has been exploited to abstract fluoride from Ph_3CF in solution to form $[Ph_3C][(C_6F_5)_3BF]$, with the ^{19}F NMR spectrum exhibiting a broad resonance at -187 ppm corresponding to the boron-bound

fluorine.[134] A crystal structure containing an intact $[(C_6F_5)_3BF]^-$ fragment was obtained by Taube *et al.*, which exhibits a B-F bond distance of 1.428(6) Å that is notably shorter than that exhibited by the $[Mes_2PhBF]^-$ fragment, for which a B-F bond distance of 1.481(2) Å was reported by Bresner *et al*.[74,135] This shortening of the B-F bond distance is illustrative of the greater strength of bonding between the more electron-deficient boron centre and the fluoride anion, and is in full agreement with the B-F distance of 1.43 Å predicted by Krossing *et al*.[132]

Further substantiation of the effect of electron-withdrawing groups on the fluoride ion affinity of Ar_3B systems is provided by the work of Gabbaï and co-workers.[100] Their theoretical calculations show that both $B(C_6F_5)_3$ ($\Delta H_{B\text{-}F}$ = -413 kJ mol^{-1}) and $B(C_6Cl_5)_3$ ($\Delta H_{B\text{-}F}$ = -366 kJ mol^{-1}) possess higher enthalpies of fluoride anion binding than BPh_3 ($\Delta H_{B\text{-}F}$ = -284 kJ mol^{-1} using their method).[100] A natural limitation of these highly electron-withdrawing systems is encountered in designing a *selective* receptor for small hard anions, as this greater enthalpy of interaction can be sufficient to overcome the steric cost of coordination by larger, weaker anions. This was quantified by Gabbaï and co-workers, who showed that $B(C_6Cl_5)_3$ formed adducts not only with fluoride ($K_F > 10^7$ M^{-1} in dichloromethane) and cyanide anions ($K_{CN} > 10^7$ M^{-1} in dichloromethane), but also chloride anions (K_{Cl} = 600(50) M^{-1} in dichloromethane), with equilibrium binding constants determined by titration, followed by UV-Vis spectroscopy.[100]

1.2.4. Extended π-Conjugation

An alternative strategy employed to increase anion binding strength at boron in triarylboranes is to extend the conjugation of the aromatic groups bound to boron.[136] Miyaska *et al*. suggested that a greater the degree of conjugation results in a lower energy

LUMO of the triarylborane, which was found to correlate with enhanced Lewis acidity.[136] This is exemplified by the less conjugated triarylborane **31** having a lower fluoride ion affinity (K_F = 2.3 x 10^6 M^{-1} in dichloromethane) than the more conjugated triarylborane **32** (K_F = 6.2 x 10^7 M^{-1} in dichloromethane) (Figure 1.20).[136]

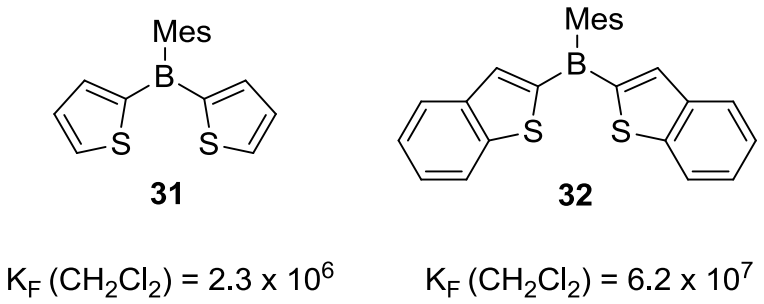

Figure 1.20. The fluoride anion receptors **31** and **32**.[136]

1.2.5. Proximal Cationic Centres: The Return of Coulombic Forces

As with hydrogen bonding, a proximal cationic site can be incorporated into triarylborane anion receptors to increase the anion binding affinity. This is most clearly demonstrated in the work of Gabbaï, with the neutral triarylborane **33** exhibiting no change in the ^{11}B NMR spectrum on addition of fluoride in chloroform solution, while the cationic triarylborane **34·**OTf exhibits a fluoride binding constant of 5.0 x 10^6 M^{-1} in 75:25 (v:v) THF/MeOH solution (Figure 1.21).[115] The receptor **34·**OTf was also shown to bind cyanide (K_{CN} = 8.0(0.5) x 10^5 M^{-1} in THF), although far more weakly than fluoride (K_F > 10^7 M^{-1} in THF), a phenomenon postulated to be due to intra-molecular hydrogen bonding.[111]

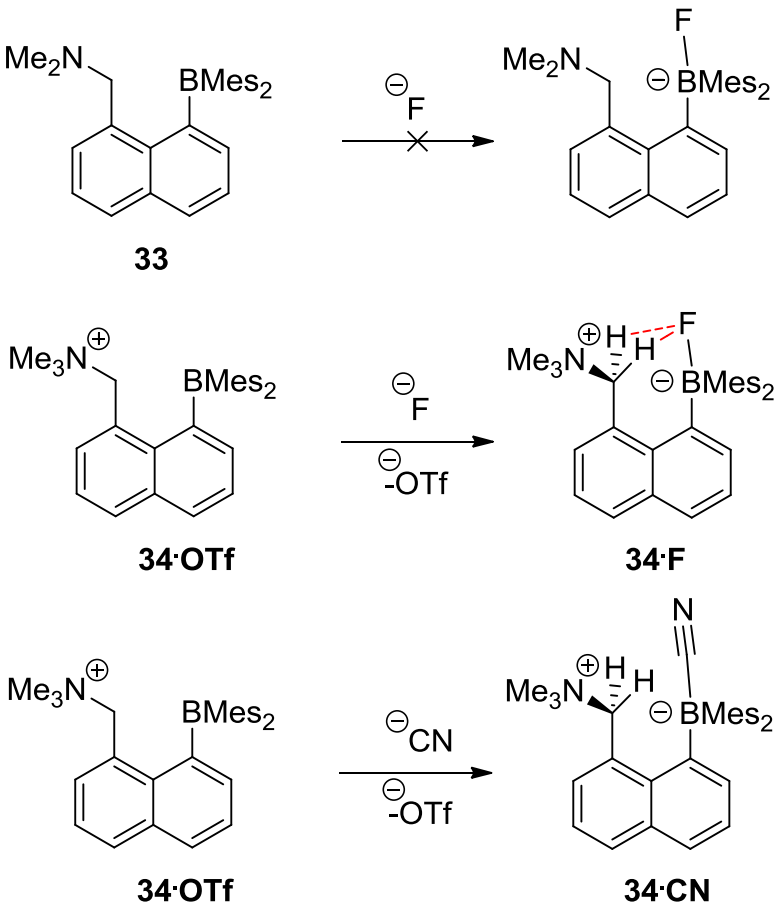

Figure 1.21. The reaction of fluoride and cyanide anions with triarylboranes **33** and **34**, presumed hydrogen bonding illustrated in red dotted lines.[115]

The extent of extra stabilisation afforded to fluoride anion adducts by proximal cationic sites was further explored by Gabbaï and co-workers with the synthesis of receptors **35-37** (Figure 1.22).[109] The reversible reduction waves for $BMes_3$, **35** and **36** measured by cyclic voltammetry come at -2.57, -2.33 and -2.09 mV (vs. FcH/FcH^+), a trend which is consistent with increasing Lewis acidity at the boron centre on increasing the number of pendant cationic functions.[109] **37** exhibits an irreversible reduction event at approximately -1.86 mV.[109] Consistent with this trend in Lewis acidity, only **37** binds cyanide anions in aqueous solution.[109]

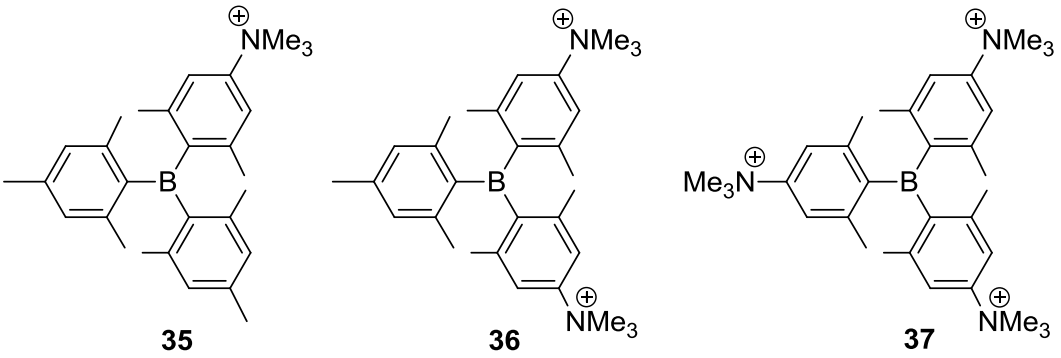

Figure 1.22. The cationic receptors **35**-**37**.[109]

Metal-centred cations have also been exploited in concert with three-coordinate, 6-valence electron boranes, an example being iridium complex **38** (Figure 1.23).[137] The free ligand is capable of binding fluoride (K_F = 4.7 x 10^4 M^{-1} in MeCN), whereas the cationic complex **38** was found to bind fluoride anions much more strongly (K_F = 1.29 x 10^6 M^{-1} in MeCN).[137]

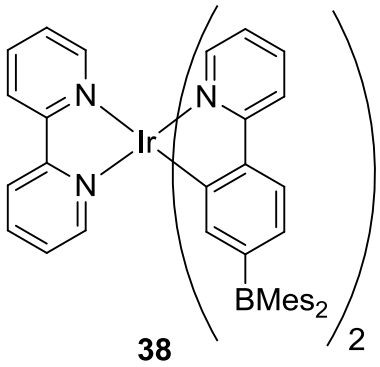

Figure 1.22. The cationic iridium complex **38**.[137]

Following the work of Beer *et al.* on the use of metallocenium derivatives todetect or recognize anions in non-aqueous media by electrochemical means,[138-140] Shinkai and co-workers sought to exploit both the Lewis acidity of boron and the electrochemical potential of ferroceneboronic acid **39** (Figure 1.23) for anion binding.[122] Addition of fluoride anions to a solution of **39** in an aqueous electrolyte led to a shift in $E_{1/2}$ of

approximately 200 mV. Moreover, oxidation of **39** to **40** led to a marked increase in the fluoride binding constant, where $K_2 > K_1 \times 10^3$ (Figure 1.23). Fluoride anions were found to bind to the receptor ($K_2 = K_F$ (H_2O electrolyte) = 700(50) M^{-1}), exhibiting a marked preference over potentially competing anions (Cl^-, Br^-, SCN^-, SO_4^{2-} or $H_2PO_4^-$) that had binding constants ranging from 2 through 20 M^{-1}. Combining compound **39** with a redox-active dye, such as methylene blue 2, allows for the transduction of the electrochemical response to the complexation of a fluoride anion to a colorimetric response *viz* the loss of blue colour from solution.[123]

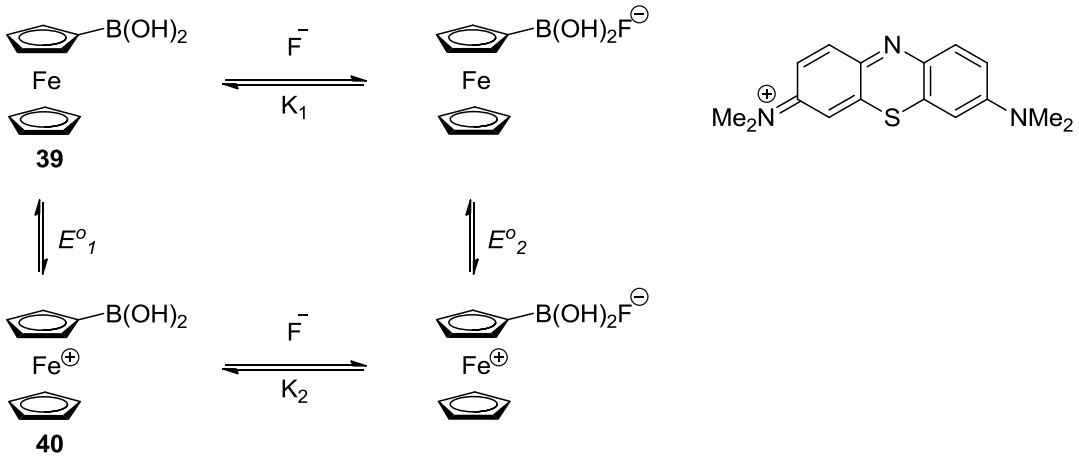

Figure 1.23. The binding of fluoride anions by ferrocene boronic acid **39** versus the binding of fluoride anions by ferrrocenium boronic acid **40**.

1.2.6. Bidentate Boranes

The chelate effect can be exploited in the binding of anions through the use of two proximal boranes, as for example shown in the early work of Shriver *et al*. on the bidentate *bis*-borane system **41** (Figure 1.24).[141] Another notable example is the "hydride sponge" of Katz (**42**) which was shown to chelate hydride, as well as fluoride and

hydroxide anions.[78,79] The chelating 1,8-*bis*(dimethylboryl)napthalene **42** was shown to be capable of extracting halide anions already bound at a mono-functional receptor.[79]

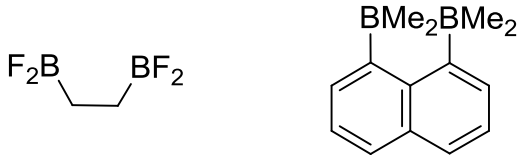

41 **42**

Figure 1.24. The anion chelating 1,2-*bis*(difluoroboryl)ethane receptor, **41**, of Shriver et al. and the anion chelating 1,8-*bis*(dimethylboryl)naphthalene, **42**, of Katz.[78,79,141]

As with other types of bonding that exploit multiple binding sites, the degree of pre-organisation, the distance between binding sites and relative positioning of the binding sites are variables that can be exploited to enhance either binding strength or anion binding selectivity. An early example of varying the inter B-B distance (*vs.* **42**) involves the chelating anion receptor **43** reported by Piers *et al.*, which was shown to be capable of extracting fluoride from BF_4^- (Figure 1.25).[142,143] The design of this highly Lewis acidic *bis*-borane exploits the capacity for chelation as well as the highly electron-deficient nature of the groups bound to the borane centres, so as to bind fluoride anions strongly, with calculated fluoride binding affinities of -510 kJ mol^{-1}(cf. -444 kJ mol^{-1} for $B(C_6F_5)_3$).[132,142,143] Again, the highly Lewis acidic nature of the borane decreases the selectivity of the borane for fluoride; **43** was also shown to also bind hydroxide anions.[142,143]

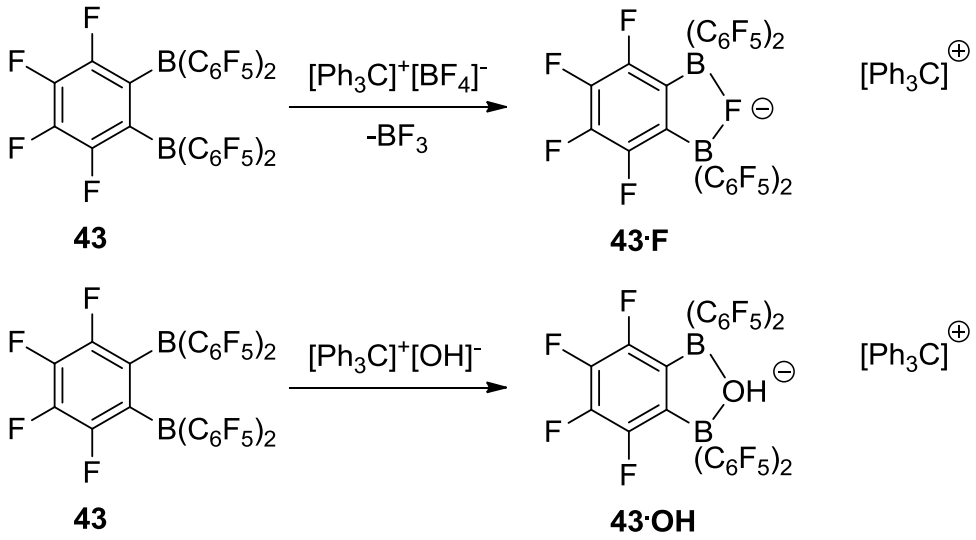

Figure 1.25. The chelation of fluoride and hydroxide anions by the *bis*-borane of Piers *et al.*[142,143]

Another example of a *bis*-borylated system capable of binding anions is the *bis*(boryl)cobaltocene, **44**, of Herberich *et al.* (Figure 1.26).[144] Receptor **44** can be oxidised by $Cu(OH)_2$, and product shown by X-ray crystallography to be the chelating hydroxide species [**44**·OH]$^-$.[144] The analogous fluoride chelate could be afforded by treating the oxidized receptor **44**$^+$ (obtained by treating **44** with $[FeCp_2][PF_6]$) with one equivalent of $[NMe_4]F$ (Figure 1.26).[145] Both **44** and **44**$^+$, were noted to exhibit a marked preference for binding hydroxide in preference to fluoride. This preference is also reflected in the higher barrier for dynamic processes involving B-X cleavage (X = F$^-$/OH$^-$), demonstrated for the hydroxide complex [**44**·OH]$^-$ than the fluoride complex [**44**·F]$^-$ by ^{1}H and ^{11}B VT-NMR spectroscopy .[145]

Studies by Gabbaï *et al.* on the 1,8-*bis*-boryl napthalene systems **45** and **46** showed that appropriate 1,8-*bis*-boryl functionalised napthalenes are capable of *selectively* binding fluoride in preference to Cl$^-$, Br$^-$, I$^-$, AcO$^-$ or NO_3^- anions (Figure 1.26).[116,119] The fluoride anion adducts of **45** and **46** were shown to feature chelating fluoride in the solid state by X-ray crystallography, and B-F bond lengths in the range 1.585-1.636 Å, [**45**:

1.636(6)/1.635(5) Å, **46**: 1.585(5)/1.633(5) Å], *i.e.* significantly longer than those typically observed for fluoride anions bound to one boron centre alone (1.47-1.49 Å).[116,119] The selectivity of these two receptors, **45** and **46**, is explained by the authors as due to the size of the cavity between the two boron centres.[116,119] The binding affinity (K_F) of **46** was reported as being too great to determine by direct UV-Vis titration, so competition experiments with $BMes_3$ were performed,[119] yielding a relative binding constant of 3.3 x 10^5 M^{-1} in THF. Treating the fluoride adduct of **46** with water does not lead to observable displacement of the fluoride anion, as is typically observed for related adducts featuring a single borane centre.[119] A limitation of the 1,8-*bis*-borylnaphthlenes **45** and **46** for the selective detection of fluoride anions, however, is their propensity to degrade in the presence of water.[116,119]

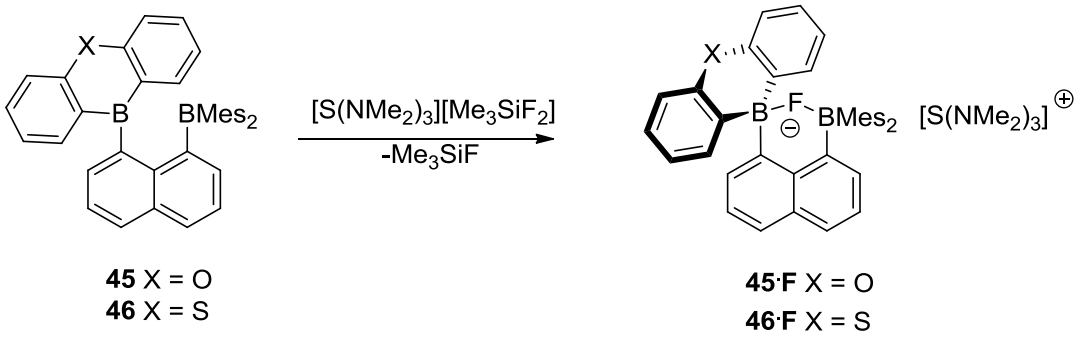

Figure 1.26. The chelating 1,8-*bis*-boryl napthalenes **45** and **46**, and their reaction with a source of fluoride anions to give the fluoride anion chelating adducts [**45**·F]$^-$ and [**46**·F]$^-$.[116,119]

1.2.7. Borane Anion Receptors featuring Auxiliary Lewis Acidic Centres

Given the propensity of 1,8-*bis*-borylnapthalene systems, such as **45** and **46**, to suffer B-C_{aryl} bond cleavage in the presence of water, alternative receptors that benefit

from the high B-F bond strength as well as the chelate effect are of interest. If one adopts the nomenclature of "primary binding site" and "secondary binding site" to denote the presumed centre to which the anions forms the strongest bond and second strongest bond to respectively, it is possible to design a receptor bearing a primary borane binding site and a proximal Main Group secondary binding site. As with the receptors based on two boranes, the geometric and steric constraints of the ligand framework are imposed on the binding site. The major advantage of including a softer Lewis acid for the proximal binding site is that the softer interaction is energetically less distance dependent, thereby reducing the degree of spatial constraint imposed by the framework on anion binding.

Examples of these mixed *bis*-Lewis-acidic receptors based on the same naphthalene ligand framework as the 1,8-*bis*-boryl naphthalenes **45** and **46** include the water-stable receptors **47** and **48** reported by Gabbaï *et al.* (Figure 1.27).[113,118] These receptors exhibit a similar separation between the Lewis acidic centres (3.3-3.5 Å) compared to the *bis*-boryl receptors **45** and **46** (3.2-3.4 Å), as shown by X-ray crystallography.[2] As expected, both **47** and **48** were shown to bind fluoride anions in mixed THF/water solution (9:1 v/v), with ^{199}Hg NMR spectroscopy of the adduct in each case being diagnostic of bonding between the mercury centre and fluoride ($^{1}J_{\text{Hg-F}}$([**47**·F]$^-$) = 135.2 Hz, $^{1}J_{\text{Hg-F}}$([**48**·F]$^-$) = 109.8 Hz).[113,118] The chelating mode of anion binding in the solid state is confirmed by X-ray crystallography, with a B-F distance of 1.483(3) Å and a Hg-F bond distance of 2.589(2) Å [cf. Σ(Van der Waals radii of Hg and F) = 3.02 Å].[113,118]

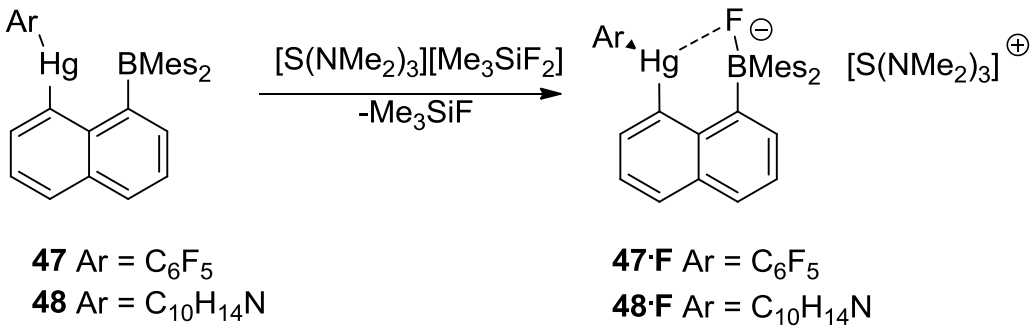

Figure 1.27. The chelating 1,8-*bis*-boryl napthalenes **47** and **48**, and their reaction with a source of fluoride anions to give the fluoride chelating adducts [**47**·F]$^-$ and [**48**·F]$^-$ in a 9:1 mixture of THF and water.[113,118]

Further work conducted by Gabbaï *et al.* on the 1,8-naphthalene framework incorporated a sulfonium group (SMe_2^+) as the secondary Lewis acid in the receptor **49** (Figure 1.28).[107] The cationic sulfonium function is Lewis acidic in the sense that its low lying σ* orbitals can accept electron density from an anion. A related receptor, **50**, based on a 1,2-functionalised phenylene framework was also synthesised (Figure 1.28).[107] The S-B distance in receptor **49** was shown by X-ray crystallography to be 3.07 Å, whereas that of **50** was shown to be 3.12 Å.[107] Neither shows any evidence by UV-Vis titration of the binding of Cl^-, Br^-, I^-, NO_3^- or HSO_4^- anions in mixed water/methanol solution (95:5 v/v), presumably due to size exclusion.[107] Moreover, receptor **49** was shown not to interact with either fluoride or cyanide anions under similar conditions, presumably due to the high solvation enthalpies of these anions in polar protic solvents.[107] By contrast, receptor **50**, with its slightly closer arrangement of the proximal sulfonium and borane functions, was found to bind cyanide under identical conditions.[107] DFT studies suggest that the cyanide adduct of **50** should exhibit significant interaction between one filled π-orbital of cyanide and the empty, low lying σ*-orbital of the sulfonium group.[107]

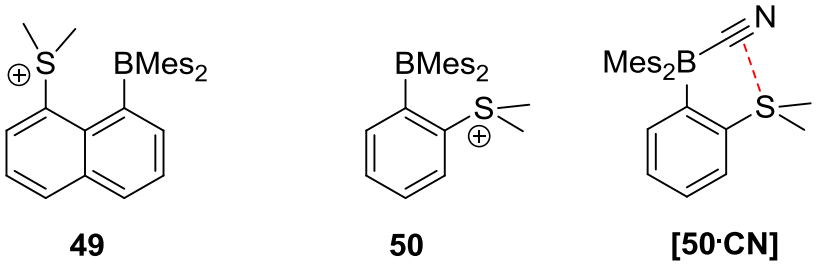

Figure 1.28. The receptors **49** and **50**.[107]

Chelation utilising both a three-coordinate borane and a proximal silane on a naphthalene framework has been explored by Katz *et al.* in 1-dimethylboryl-8-trimethylsilylnaphthalene **51** (Figure 1.29).[146] The receptor **51** was shown to undergo a shift in the ^{11}B NMR spectrum from 74.6 to 5 ppm on addition of one equivalent of fluoride, consistent with the formation of a boron-fluorine bond.[146] Moreover, ^{29}Si NMR monitoring of the reaction revealed a shift from -3.5 to -9.9 ppm, with coupling to fluorine in the product being indicative of a Si-F interaction ($^{1}J_{\text{Si-F}}$ = 13.2 Hz).[146] An X-ray crystallographic study of [**51**·F]$^{-}$ reveals a B-F bond length of 1.475(6) Å and a Si-F bond length of 2.714(7) Å, the latter being significantly shorter than the sum of the respective Van Der Waals radii (3.4 Å).[146]

An analogous receptor, 1-dimethylboryl-8-fluorodimethylsilynaphthalene, **52**, was also synthesised and its fluoride anion binding probed by Katz (Figure 1.29).[146] It would be expected that the receptor **52** would bind fluoride anions more strongly than **51** as the silane should be more electron-deficient. Although it was not possible to demonstrate this explicitly by NMR spectroscopy (as the ^{29}Si resonances were very broad) or by X-ray crystallography, receptor **52** was shown by ^{1}H and ^{11}B NMR spectroscopy to irreversibly abstract fluoride anions from [**51**·F]$^{-}$.[146]

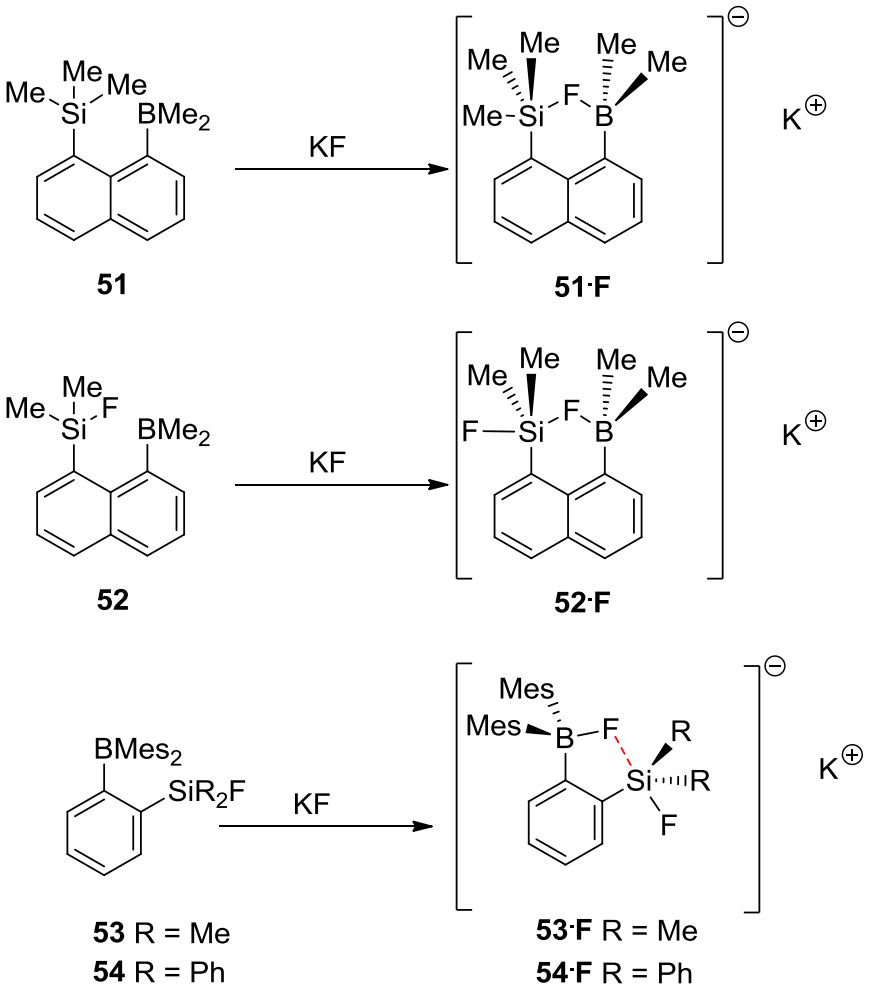

Figure 1.29. The receptors **50**, **51** and **50** and their reaction with potassium fluoride.

The propensity of four-coordinate silanes to act as an ancillary Lewis acid toward a fluoride anion bound principally at boron was further explored by Kawachi *et al.* through their 1,2-functionalised phenylene systems **53** and **54** (Figure 1.29).[147] They showed that both **53** and **54** will capture a fluoride from KF in toluene in the presence of either [2.2.2]cryptand or 18-crown-6, to give colourless crystals of the μ-fluoro-bridged adducts [**53**·F]$^-$ and [**54**·F]$^-$ respectively. The mode of binding in the solid state was elucidated by X-ray crystallography, with the geometry around silicon being pseudo penta-coordinate. The boron-fluorine bond distances of [K(18-crown-6)][**53**·F] and [K(18-crown-6)][**54**·F] were found to be 1.492(4) and 1.514(3) Å respectively, both slightly

elongated than those typically exhibited when fluorine binds only to a three-coordinate borane (ca. 1.47 Å), consistent with an ancillary interaction to a second Lewis acid.[147] The distances between the silicon and the bridging fluorine of [K(18-crown-6)][**53**·F] and [K(18-crown-6)] [**54**·F] were found to be 2.439(2) and 2.248(1) Å, respectively. These Si-F distances are shorter than the minimal non-bonded approach between silicon and fluorine of 2.63 Å.[148] Moreover, the fluorine-silicon-fluorine geometry is almost linear (175-176º), which would be expected if the bridging μ-fluorine was donating electron density into the lowest energy σ* orbital available at silicon.[147]

Evidence for retention of this chelating interaction in solution is provided by ^{1}H, ^{11}B, ^{19}F and ^{29}Si NMR spectroscopic studies of [K(18-crown-6)][**53**·F] and [K(18-crown-6)][**54**·F] in d_8-THF solution.[147] The ^{11}B NMR spectra exhibit resonances at 6 and 7 ppm respectively, typical of tetra-coordinate boranes.[147] The ^{19}F NMR spectra exhibit broad resonances for the bridging μ-fluorine [δ = -152 ppm (**53**·F) and -148 ppm (**54**·F)] and sharper resonances for the fluorine bound to silicon alone [δ = -147 ppm (**53**·F) and -145 ppm (**54**·F)].[147] The fluorine bound to silicon alone exhibits coupling in the ^{19}F NMR spectrum to the bridging fluorine ($^{2}J_{F\text{-}F}$ = 9 Hz (**53**·F) and 18 Hz (**54**·F)).[147] The ^{29}Si NMR spectra also provide evidence that the fluoride remains chelated in solution, due to the upfield shift of the silicon centres of [**53**·F]$^-$ (δ = 6.3 ppm) and [**54**·F]$^-$ (δ = -32.6 ppm) relative to receptors **53** (δ = 21.5 ppm) and **54 (**δ = -3.4 ppm).[147] Both the crystallographic data and the NMR spectra of the adducts [**53**·F]$^-$ and [**54**·F]$^-$ suggest that the more Lewis acidic silane in **54** binds the chelating fluoride anion more strongly than the silane centre in **53**.

1.3. From Borane Anion Receptors to Anion Reporters

A range of physical and photo-physical changes can be enabled upon the addition of fluoride or cyanide anions to a solution of a suitable receptor. Among the most widely used approaches in anion reporting utilising triarylboranes are colorimetric, electrochemical, phosphorescent and fluorescent responses. There are several examples where more than one of these responses are elicited from one receptor by the presence of the target anion. These will be discussed in greater detail in the following sections.

1.3.1. Colorimetric Responses

The lower energy range of the UV/Vis absorption spectrum of triarylboranes is typically dominated by transitions from filled molecular orbitals to the LUMO orbital that bears a large orbital contribution from the formally vacant *p*-orbital of boron.[133] Since co-ordination of an anion to the boron fills the formerly vacant *p*-orbital with an electron pair, transitions from the filled molecular orbitals to an orbital bearing a large orbital contribution form the *p*-orbital of boron are no longer possible. This typically results in a greatly diminished absorption band at the low-energy-range of the UV/Vis absorption spectrum.[119,133,149] By extending the conjugation of the aryl rings, the energy of the transitions from filled molecular orbitals to the LUMO can be lowered, and transitions moved from the UV into the visible range (higher wavelength, lower energy). An example where this extended conjugation (cf. the colourless $BMes_3$) has been exploited to give a colorimetric response (orange to colourless) to the presence of fluoride anions in solution is receptor **55** reported by Yamaguchi *et al*. (Figure 1.30).[133] Colorimetric responses, where colour is lost on addition of the guest anion, are often referred to as "switch off" responses.

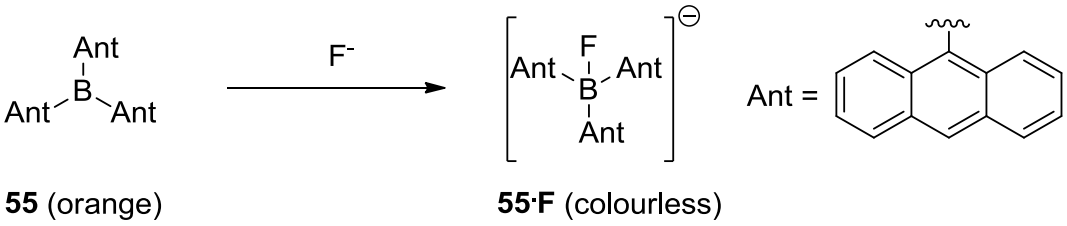

55 (orange) **55·F** (colourless)

Figure 1.30. The receptor **55** and its colorimetric reaction with fluoride anions.[133]

An alternative approach to the "switch off" colorimetric response of a receptor to the presence of a target anion is that of the "switch on" response, where a change of colour is observed in response to the presence of the target anions in solution. An example of a triarylborane-containing complex that exhibits a "switch on" response is that of Lam *et al*. who report fluoride anion receptor **56** (Figure 1.31).[150] The binding of fluoride at the boron centre changes the nature of the boron-containing ligand toward the rhenium metal centre, making it more electron donating and hence red-shifting the metal ligand charge transfer (MLCT) processes, resulting in a colour change from yellow to red on binding fluoride.[150]

Another approach commonly encountered in the use of triarylboranes for the colorimetric reporting of anions is to add redox active dye that is triggered by the change in electrochemistry of the receptor on binding the target anion, most notably in the work of Shinkai and co-workers.[123] As mentioned in Section 1.2.5, an electrochemical response of a ferrocene appended borane to the binding of fluoride anions resulted in the activation of methylene blue dye through a redox reaction.

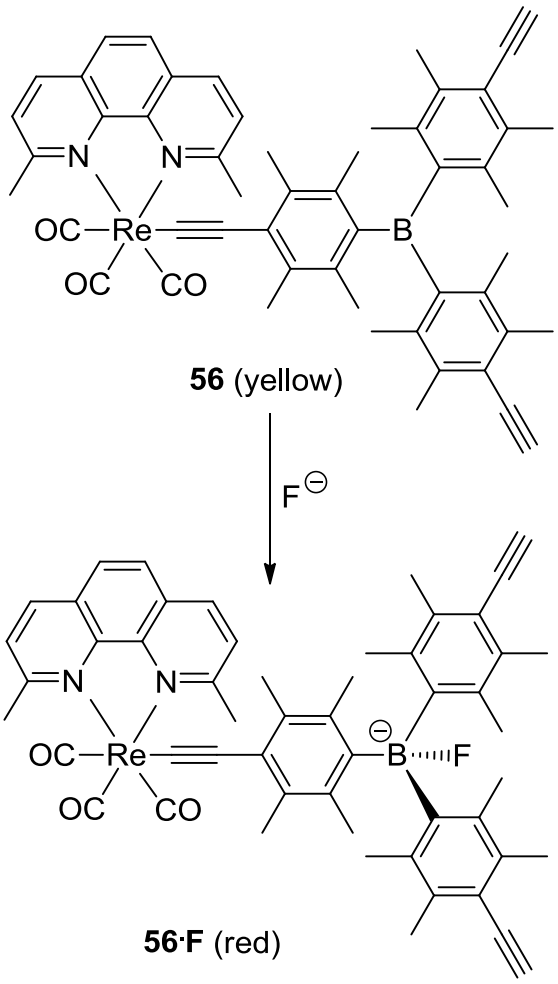

Figure 1.31. The receptor **56** and its colorimetric reaction with fluoride anions.

1.3.2. Fluorescence Responses

Triarylboranes, such as **57** and **58**, reported by Gabbaï and co-workers, exhibit intense fluorescence, with theoretical calculations suggesting that this arises from a "ligand-to-element" charge transfer (CT) from the mesityl moiety to an empty molecular orbital featuring the boron-centred formally vacant *p* orbital (Figure 1.32).[112,114] On binding fluoride, the boron centre no longer possesses an empty *p*-orbital, and so fluorescence ceases.[112,114] This "switch off" of fluorescence on reaction with fluoride is visible to the naked eye in the case of **58.**[114]

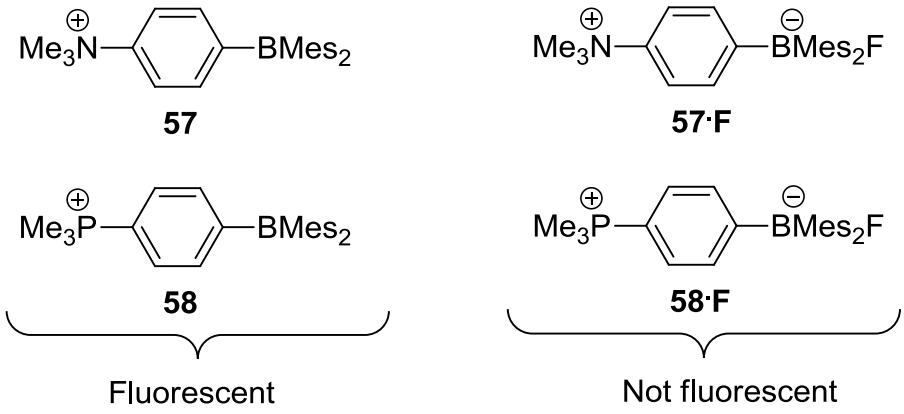

Figure 1.32. The fluorescent fluoride anion receptors **57** and **58** and their non-fluorescing fluoride anion adducts.[112,114]

Coordination of anions to the boron centre of a triarylborane interferes with CT-processes to the boron atom and hence interferes with fluorescence arising from these transitions. However in the presence of a second chromophore within the receptor, a shift in fluorescence can be observed, as in the case of the borafluorene **59** (Figure 1.33).[151] On coordination of fluoride at boron, the emission band centred at 550 nm is quenched and an intense new band centred at 417 nm is observed.[151]

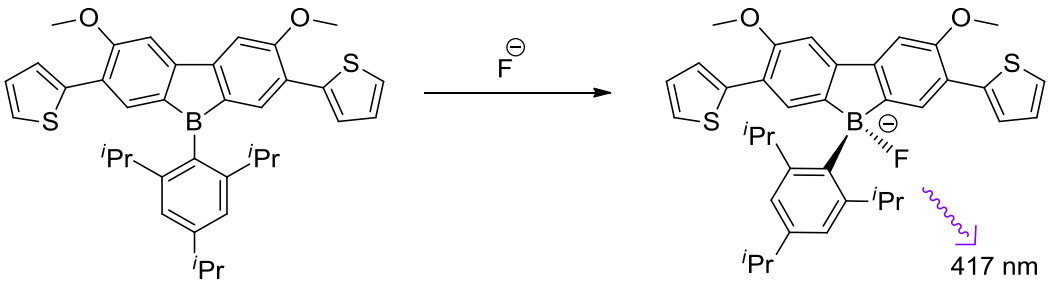

Figure 1.33. A fluorescence based reporter **59** for the detection of fluoride anions.[151]

"Switch-on" fluorescence is also possible, for instance with the fluoride anion receptor **60** reported by Wang and co-workers (Figure 1.33).[152] The free receptor **60**

fluoresces primarily due CT-transmissions, resulting in the emission spectrum of **60** being dominated by a band centred at 500 nm (with a minor emission centred at 428 nm arising from π-π* transitions of the triarylamine).[152] The CT-transitions are quenched on binding a fluoride anion, whereas the π-π* emissions increase in intensity, resulting in an overall "switch-on/switch-off" response.[152]

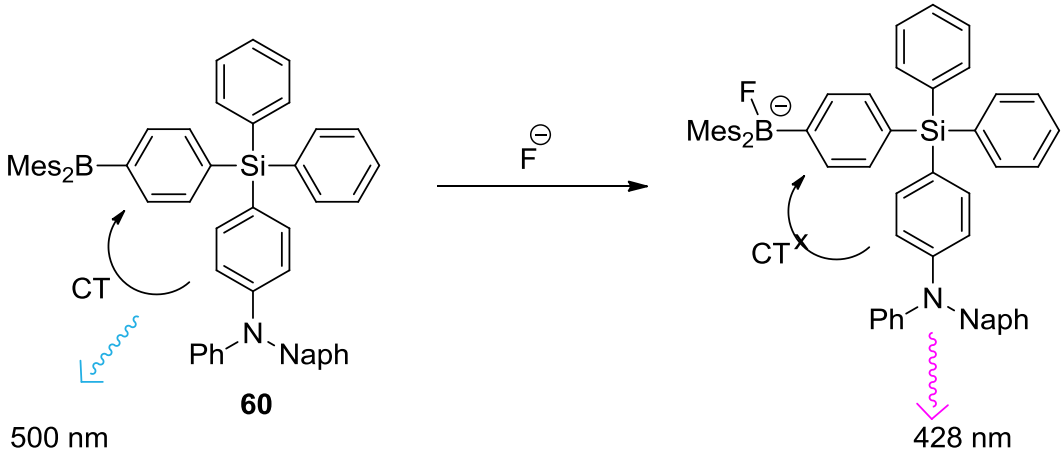

Figure 1.33. A fluorescence based reporter **60** for the detection of fluoride anions.

1.3.3. Phosphorescence Responses

Unlike fluorescence, phosphorescence is formally forbidden by the quantum mechanical selection rule $\Delta S = 0$. This rule, can however, be relaxed by spin orbit coupling to heavy atoms and phosphorescence can be exhibited by a range of compounds containing iridium, platinum, and mercury. Since many of these compounds feature phosphorescence involving ligand-centred excited states, incorporation of a ligand bearing a triarylborane can make the phosphorescence dependent on complexation of anions at boron. One of the earliest examples is the anion chelating complex **47** (Figure 1.27), which is a naturally phosphorescent (531 nm, red) compound, due to spin-orbit

perturbation provided by the mercury atom.[118] On complexing fluoride, the naphthalene and mesityl moieties are no longer conjugated, resulting in the excited state residing on the naphthalene moiety alone, thereby causing a shift in the phosphorescence to 480 nm, and hence a colour change from red to orange.[118]

Phosphorescence can also be quenched on addition of fluoride anions, as in the platinum based receptor **61** reported by Sakuda *et al.* (Figure 1.34).[153] The phosphorescence of this receptor **61** is thought to arise from MLCT that is relayed by a CT-process to the empty orbital primarily composed of the boron *p*-orbital.[153] After complexation of fluoride at the boron centre, this CT-process in no longer possible, and the phosphorescence is observed to be completely quenched.[153]

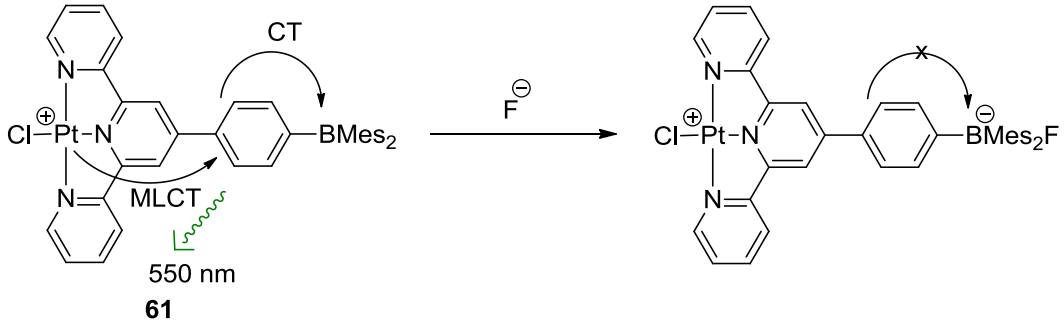

Figure 1.34. A fluorescence based reporter **61** for the detection of fluoride anions.[153]

1.3.4. Electrochemical Responses

Neutral triarylboranes can often undergo reversible one-electron reductions that are observable by cyclic voltammetry.[116,154-160] As such, the binding of an anion at the boron centre should inhibit these redox processes and such systems can therefore be exploited as electrochemical anion sensors.[116,154,161] This has been shown in the work of Melaïmi *et al*. in which the *bis*-boryl receptor **45** (Figure 1.26) experiences a synchronous disappearance of both reduction waves at $E_{1/2}$ = -2.25 and –2.62 V on reacting with one

equivalent of fluoride anions.[116] More commonly, a redox active moiety is attached to three co-ordinate boranes such that binding events at the boron centre are reflected in changes in the half cell potential ($E_{1/2}$) of the redox active moiety.[80,81,85,86,90,93,95,116,122,123] These changes in the $E_{1/2}$ can be exploited to indicate the presence of anions and the absolute shift in $E_{1/2}$ can be used to distinguish between different anions.[85] A particularly relevant example is provided by the work of Broomsgrove *et al*. involving ferrocene derivatised receptor **62** (Figure 1.35).[85] The Lewis acid **62** is reversibly oxidised at a potential E^o_1 of +181 mV (*vs*. FcH/FcH$^+$), which shifts by -550 mV on the addition of fluoride anions (E^o_2 = -369 cf. FcH/FcH$^+$).[85] **57** also exhibits a shift of -564 mV on the addition of cyanide anions (E^o_3 = -383 mV cf. FcH/FcH$^+$).[85]

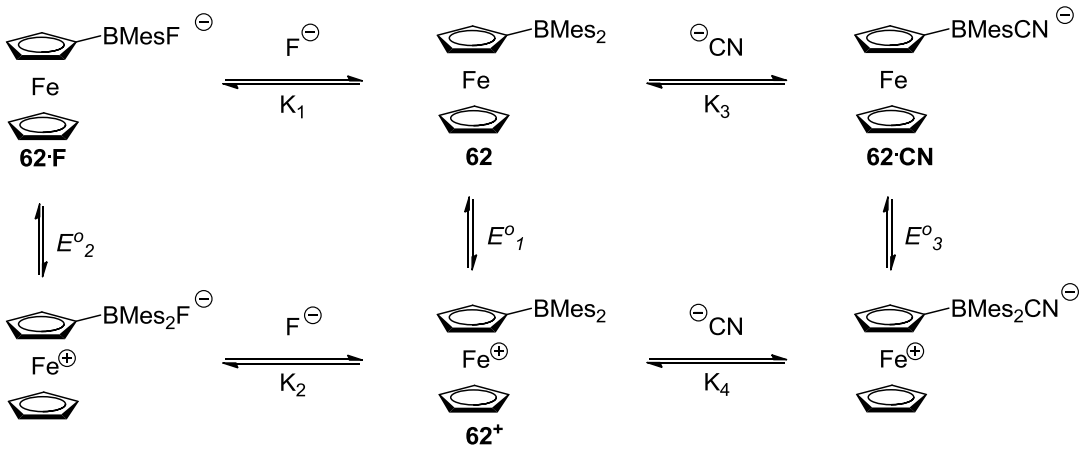

Figure 1.35. The anion receptor **62** and its interaction with fluoride and cyanide anions.

A limitation of this approach in anion sensing is that with a sufficiently Lewis acidic borane, neutral Lewis bases can also coordinate at the boron and cause a shift in the half-cell potential, for instance the Lewis acid **63** was reported by Piers *et al*. to complex PMe_3, resulting in a shift in the electrochemistry from $E_{1/2}$ = +450 mV (cf. FcH/FcH$^+$) to $E_{1/2}$ = -100 mV (cf. FcH/FcH$^+$) (Figure 1.36).[162]

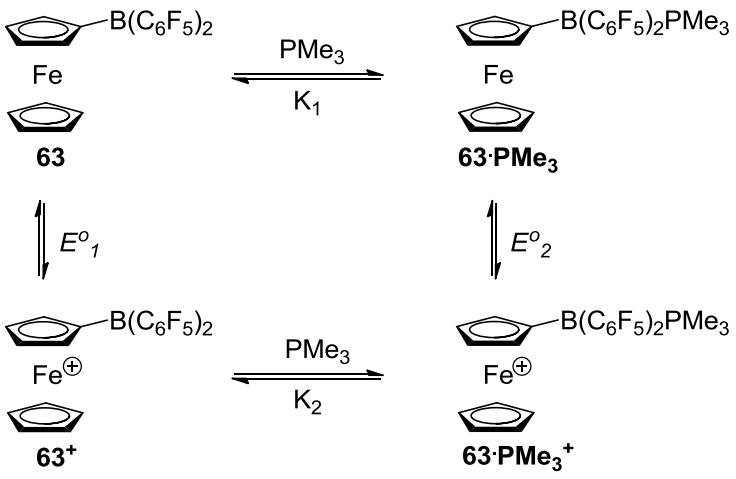

Figure 1.36. The anion receptor **63** and its interaction with fluoride and cyanide anions.

1.4. Research Proposal

When the work reported in this Thesis commenced, it was of considerable interest to design a molecule that could not only report the presence of cyanide and fluoride anions, but to distinguish between them and give a markedly differing response. Given that the chemically robust bis(aryl) mono(ferrocenyl) boranes, $FcBAr_2$, had been shown to be capable of binding, as well as colorimetrically and electrochemically reporting, the presence of both cyanide and fluoride anions in a range of solvents, this was taken as the core moeity around which our reporter molecules would be designed. It was hypothesized that it may be possible to discriminate between these two anions by exploiting auxiliary binding motifs. Early interest focussed on the inclusion of poly(amine) groups proximal to the primary binding site capable of affording hydrogen bonds to a bound fluoride anion. Later work sought to exploit the chelate effect of locating a secondary Main Group Lewis acid proximal to the borane binding site as a way to discriminate between fluoride anions (capable of chelating) and cyanide anions (thought to be incapable of this). The role of

proximal charged groups on the binding of anions by these ferrocenyl boranes was also to be investigated.

The longer-term "blue-sky" objective of this work was to probe the possibility for broadening the scope of these ferrocenyl boranes to bind and report not only small, hard anions but also softer, neutral substrates, such as the generally intractable N_2O. It was thought that this would require highly electron deficient and yet sterically protected ferrocenyl boranes, so synthetic routes to these boranes were to be investigated. An approach (akin to FLP chemistry) was envisioned where a base that was sufficiently bulky not to form an adduct with the Lewis acid could activate the substrate of interest, which in turn would bind to the borane and give rise to a colorimetric and/or electrochemical response.

1.5. References

(1) Park, C. H.; Simmons, H. E. *Journal of the American Chemical Society* **1968**, *90*, 2431.

(2) Wade, C. R.; Broomsgrove, A. E. J.; Aldridge, S.; Gabbaï, F. P. *Chemical Reviews* **2010**, *110*, 3958.

(3) Yang, Y. C.; Baker, J. A.; Ward, J. R. *Chem. Rev.* **1992**, *92*, 1729.

(4) Muir, G. *Hazards in the chemical laboratory*; the Royal Chemical Society: London, UK, 1997.

(5) Koenig, R. *Science* **2000**, *287*, 1737.

(6) Baud, F. J. *Human & Experimental Toxicology* **2007**, *26*, 191.

(7) WHO *Guidelines for drinking-water quality, fourth edition*; 4th ed., 2011.

(8) Simeonova, F. P. F., Lawrence *Hydrogen cyanide and cyanides : human health aspects*; World Health Organization: Geneva, 2004.

(9) Carton, R. J. *Fluoride* **2006**, *39*, 163.

(10) Aaseth, J.; Shimshi, M.; Gabrilove, J. L.; Birketvedt, G. S. *The Journal of Trace Elements in Experimental Medicine* **2004**, *17*, 83.

(11) Sohn, H.; Létant, S.; Sailor, M. J.; Trogler, W. C. *Journal of the American Chemical Society* **2000**, *122*, 5399.

(12) Coulomb, C. A. *Histoire de l'Académie Royale des Sciences, Imprimerie Royale* **1788**, 8.

(13) Coulomb, C. A. *Histoire de l'Académie Royale des Sciences. Imprimerie Royale* **1788**, 578.

(14) Beer, P. D.; Gale, P. A. *Angewandte Chemie International Edition* **2001**, *40*, 486.

(15) Beer, P. D. *Accounts of Chemical Research* **1998**, *31*, 71.

(16) Beer, P. D.; Hayes, E. J. *Coordination Chemistry Reviews* **2003**, *240*, 167.

(17) Averill, B. E., Patricia Flat World Knowledge: 2011; Vol. 1, p 1740.

(18) Schmidtchen, F. P. *Angewandte Chemie International Edition in English* **1977**, *16*, 720.

(19) Schmidtchen, F. P. *Chemische Berichte* **1980**, *113*, 864.

(20) Schmidtchen, F. P. *Chemische Berichte* **1981**, *114*, 597.

(21) Schmidtchen, F. P.; Muller, G. *Journal of the Chemical Society, Chemical Communications* **1984**, 1115.

(22) Ichikawa, K.; Yamamoto, A.; Hossain, M. D. A. *Chemistry Letters* **1993**, *22*, 2175.

(23) Beer, P. D.; Keefe, A. D. *Journal of Organometallic Chemistry* **1989**, *375*, C40.

(24) Worm, K.; Schmidtchen, F. P.; Schier, A.; Schäfer, A.; Hesse, M. *Angewandte Chemie International Edition in English* **1994**, *33*, 327.

(25) Worm, K.; Schmidtchen, F. P. *Angewandte Chemie International Edition in English* **1995**, *34*, 65.

(26) McNaught, A. D. W., A. *IUPAC. Compendium of Chemical Terminology, 2nd ed. (the "Gold Book")*; Blackwell Scientific Publications Oxford, 1997.

(27) Emsley, J. *Chemical Society Reviews* **1980**, *9*, 91.

(28) Larson, J. W.; McMahon, T. B. *Inorganic Chemistry* **1984**, *23*, 2029.

(29) Kollman, P. A. *Journal of the American Chemical Society* **1972**, *94*, 1837.

(30) Dreyfus, M.; Pullman, A. *Theoretical Chemistry Accounts* **1970**, *19*, 20.

(31) Pascal Jr, R. A.; Spergel, J.; Van Engen, D. *Tetrahedron Letters* **1986**, *27*, 4099.

(32) Gale, P. A.; Sessler, J. L.; Král, V.; Lynch, V. *Journal of the American Chemical Society* **1996**, *118*, 5140.

(33) A. Gale, P.; A. Gale, P.; J. Twyman, L.; I. Handlin, C.; L. Sessler, J. *Chemical Communications* **1999**, 1851.

(34) Camiolo, S.; Gale, P. A. *Chemical Communications* **2000**, 1129.

(35) Graf, E.; Lehn, J. M. *Journal of the American Chemical Society* **1976**, *98*, 6403.

(36) Lehn, J. M.; Sonveaux, E.; Willard, A. K. *Journal of the American Chemical Society* **1978**, *100*, 4914.

(37) Lewis, G. N. *Valence and the structure of atoms and molecules*; Chemical Catalogue Company: New Yorl, 1923.

(38) Isaacs, E. D.; Shukla, A.; Platzman, P. M.; Hamann, D. R.; Barbiellini, B.; Tulk, C. A. *Physical Review Letters* **1999**, *82*, 600.

(39) Cordier, F.; Rogowski, M.; Grzesiek, S.; Bax, A. *Journal of Magnetic Resonance* **1999**, *140*, 510.

(40) Jonas, V.; Frenking, G.; Reetz, M. T. *Journal of the American Chemical Society* **1994**, *116*, 8741.

(41) Pearson, R. G. *Journal of the American Chemical Society* **1963**, *85*, 3533.

(42) Pearson, R. G. *Journal of Chemical Education* **1968**, *45*, 581.

(43) Pearson, R. G. *Journal of Chemical Education* **1968**, *45*, 643.

(44) Parr, R. G.; Pearson, R. G. *Journal of the American Chemical Society* **1983**, *105*, 7512.

(45) Miessler, G. L. T., D. A. *Inorganic Chemistry, 2nd Edition*; Prentice-Hall: Upper Saddle River, NJ, 1999.

(46) Beer, P. D. G., P. A.; Smith, D. K. *Supramolecular Chemistry*; Oxford Univesity Press: Oxford, 1999.

(47) Steed, J. W. A., J. L. *Supramolecular Chemistry*; Wiley VCH: New York, 2000.

(48) Kim, Y.-H.; Hong, J.-I. *Chemical Communications* **2002**, 512.

(49) Langmuir, I. *Science* **1921**, *54*, 59.

(50) Liu, H.; Shao, X.-B.; Jia, M.-X.; Jiang, X.-K.; Li, Z.-T.; Chen, G. *Tetrahedron* **2005**, *61*, 8095.

(51) Ahlers, B.; Cammann, K.; Warzeska, S.; Krämer, R. *Angewandte Chemie International Edition in English* **1996**, *35*, 2141.

(52) Motekaitis, R. J.; Martell, A. E.; Dietrich, B.; Lehn, J. M. *Inorganic Chemistry* **1984**, *23*, 1588.

(53) Evers, A.; Hancock, R. D.; Murase, I. *Inorganic Chemistry* **1986**, *25*, 2160.

(54) Wüst, J. D.; Zacharie, B. *Organometallics* **1985**, *4*, 410.

(55) Shur, V. B.; Tikhonova, I. A.; Yanovsky, A. I.; Struchkov, Y. T.; Petrovskii, P. V.; Panov, S. Y.; Furin, G. G.; Volpin, M. E. *Journal of Organometallic Chemistry* **1991**, *418*, C29.

(56) Lewis, G. N. *Journal of the American Chemical Society* **1916**, *38*, 762.

(57) Langmuir, I. *Journal of the American Chemical Society* **1919**, *41*, 868.

(58) Jensen, W. B. *Journal of Chemical Education* **2006**, *83*, 1751.

(59) Perkins, C. W.; Martin, J. C.; Arduengo, A. J.; Lau, W.; Alegria, A.; Kochi, J. K. *Journal of the American Chemical Society* **1980**, *102*, 7753.

(60) Musher, J. I. *Angewandte Chemie International Edition in English* **1969**, *8*, 54.
(61) Magnusson, E. *Journal of the American Chemical Society* **1990**, *112*, 7940.
(62) Gillespie, R. J.; Silvi, B. *Coordination Chemistry Reviews* **2002**, *233–234*, 53.
(63) Azuma, Y.; Newcomb, M. *Organometallics* **1984**, *3*, 9.
(64) Newcomb, M.; Blanda, M. T.; Azuma, Y.; Delord, T. J. *Journal of the Chemical Society, Chemical Communications* **1984**, 1159.
(65) Newcomb, M.; Madonik, A. M.; Blanda, M. T.; Judice, J. K. *Organometallics* **1987**, *6*, 145.
(66) Newcomb, M.; Horner, J. H.; Blanda, M. T. *Journal of the American Chemical Society* **1987**, *109*, 7878.
(67) Newcomb, M.; Blanda, M. T. *Tetrahedron Letters* **1988**, *29*, 4261.
(68) Newcomb, M.; Horner, J. H.; Blanda, M. T.; Squattrito, P. J. *Journal of the American Chemical Society* **1989**, *111*, 6294.
(69) Horner, J. H.; Squatritto, P. J.; McGuire, N.; Riebenspies, J. P.; Newcomb, M. *Organometallics* **1991**, *10*, 1741.
(70) Tamao, K.; Hayashi, T.; Ito, Y.; Shiro, M. *Journal of the American Chemical Society* **1990**, *112*, 2422.
(71) Tamao, K.; Hayashi, T.; Ito, Y. *Journal of Organometallic Chemistry* **1996**, *506*, 85.
(72) Adamczyk-Woźniak, A.; Jakubczyk, M.; Sporzyński, A.; Żukowska, G. *Inorganic Chemistry Communications* **2011**, *14*, 1753.
(73) Li, W.; Nelson, D. P.; Jensen, M. S.; Hoerrner, R. S.; Cai, D.; Larsen, R. D.; Reider, P. J. *The Journal of Organic Chemistry* **2002**, *67*, 5394.
(74) Bresner, C.; Day, J. K.; Coombs, N. D.; Fallis, I. A.; Aldridge, S.; Coles, S. J.; Hursthouse, M. B. *Dalton Transactions* **2006**, 3660.
(75) Hudnall, T. W.; Bondi, J. F.; Gabbaï, F. P. *Main Group Chemistry* **2007**, *5*, 319.
(76) Xu, Z.; Kim, S. K.; Han, S. J.; Lee, C.; Kociok-Kohn, G.; James, T. D.; Yoon, J. *European Journal of Organic Chemistry* **2009**, *2009*, 3058.
(77) Dusemund, C.; Sandanayake, K. R. A. S.; Shinkai, S. *Journal of the Chemical Society, Chemical Communications* **1995**, 333.
(78) Katz, H. E. *Journal of the American Chemical Society* **1985**, *107*, 1420.
(79) Katz, H. E. *The Journal of Organic Chemistry* **1985**, *50*, 5027.
(80) Aldridge, S.; Bresner, C.; Fallis, I. A.; Coles, S. J.; Hursthouse, M. B. *Chem. Commun. (Cambridge, U. K.)* **2002**, 740.
(81) Bresner, C.; Aldridge, S.; Fallis, I. A.; Jones, C.; Ooi, L.-L. *Angewandte Chemie International Edition* **2005**, *44*, 3606.
(82) Aldridge, S.; Fallis, I. A.; Bresner, C.; Day, J. K.; American Chemical Society: 2006, p INOR.
(83) Bresner, C.; Aldridge, S.; Fallis, I. A.; Day, J. K.; Coombs, N. D.; American Chemical Society: 2006, p INOR.
(84) Bresner, C.; Day, J. K.; Coombs, N. D.; Fallis, I. A.; Aldridge, S.; Coles, S. J.; Hursthouse, M. B. *Dalton Transactions* **2006**, 3660.
(85) Broomsgrove, A. E. J.; Addy, D. A.; Bresner, C.; Fallis, I. A.; Thompson, A. L.; Aldridge, S. *Chemistry – A European Journal* **2008**, *14*, 7525.

(86) Aldridge, S.; Fallis, I. A.; Bresner, C.; Day, J. K.; Tatchell, T.; Broomsgrove, A. E. J.; Loveday, M. J.; University College Cardiff Consultants Ltd., UK . 2008, p 132pp.

(87) Coombs, N. D.; Watkin, D. J.; Aldridge, S. *Analytical Science.: X-Ray Structural Anaysis Online* **2008**, *24*, x167.

(88) Day, J. K.; Bresner, C.; Coombs, N. D.; Fallis, I. A.; Ooi, L.-L.; Aldridge, S. *Inorganic Chemistry* **2008**, *47*, 793.

(89) Broomsgrove, A. E. J.; A. Addy, D.; Di Paolo, A.; Morgan, I. R.; Bresner, C.; Chislett, V.; Fallis, I. A.; Thompson, A. L.; Vidovic, D.; Aldridge, S. *Inorganic Chemistry* **2009**, *49*, 157.

(90) Broomsgrove, A. E. J.; Bresner, C.; Morgan, I. R.; Fallis, I. A.; Aldridge, S.; American Chemical Society: 2009, p INOR.

(91) Morgan, I. R.; Broomsgrove, A. E. J.; Fitzpatrick, P.; Vidovic, D.; Thompson, A. L.; Fallis, I. A.; Aldridge, S. *Organometallics* **2010**, *29*, 4762.

(92) Bresner, C.; Haynes, C. J. E.; Addy, D. A.; Broomsgrove, A. E. J.; Fitzpatrick, P.; Vidovic, D.; Thompson, A. L.; Fallis, I. A.; Aldridge, S. *New Journal of Chemistry* **2010**, *34*, 1652.

(93) Broomsgrove, A. E. J.; Addy, D. A.; Di Paolo, A.; Morgan, I. R.; Bresner, C.; Chislett, V.; Fallis, I. A.; Thompson, A. L.; Vidovic, D.; Aldridge, S. *Inorganic Chemistry* **2010**, *49*, 157.

(94) Siewert, I.; Fitzpatrick, P.; Broomsgrove, A. E. J.; Kelly, M.; Vidovic, D.; Aldridge, S. *Dalton Transactions* **2011**, *40*, 10345.

(95) Kelly, M. J.; Broomsgrove, A. E. J.; Morgan, I. R.; Siewert, I.; Fitzpatrick, P.; Smart, J.; Vidovic, D.; Aldridge, S. *Organometallics* **2013**, *32*, 2674.

(96) Tirfoin, R.; Aldridge, S. *Dalton Transactions* **2013**, *42*, 12836.

(97) Vei, I. C.; Pascu, S. I.; Green, M. L. H.; Green, J. C.; Schilling, R. E.; Anderson, G. D. W.; Rees, L. H. *Dalton Transactions* **2003**, 2550.

(98) Huh, J. O.; Do, Y.; Lee, M. H. *Organometallics* **2008**, *27*, 1022.

(99) Zhao, H.; Leamer, L. A.; Gabbai, F. P. *Dalton Transactions* **2013**, *42*, 8164.

(100) Zhao, H.; Reibenspies, J. H.; Gabbai, F. P. *Dalton Transactions* **2013**, *42*, 608.

(101) Zhao, H.; Gabbaï, F. P. *Organometallics* **2012**, *31*, 2327.

(102) Wade, C. R.; Gabbaï, F. *Organometallics* **2011**, *30*, 4479.

(103) Kim, Y.; Huh, H.-S.; Lee, M. H.; Lenov, I. L.; Zhao, H.; Gabbaï, F. P. *Chemistry – A European Journal* **2011**, *17*, 2057.

(104) Wade, C. R.; Zhao, H.; Gabbai, F. P. *Chemical Communications* **2010**, *46*, 6380.

(105) Matsumoto, T.; Wade, C. R.; Gabbaï, F. *Organometallics* **2010**, *29*, 5490.

(106) Wade, C. R.; Gabbai, F. P. *Dalton Transactions* **2009**, 9169.

(107) Kim, Y.; Zhao, H.; Gabbaï, F. P. *Angewandte Chemie International Edition* **2009**, *48*, 4957.

(108) Kim, Y.; Gabbaï, F. P. *Journal of the American Chemical Society* **2009**, *131*, 3363.

(109) Chiu, C.-W.; Kim, Y.; Gabbaï, F. P. *Journal of the American Chemical Society* **2008**, *131*, 60.

(110) Hudnall, T. W.; Chiu, C.-W.; Gabbaï, F. P. *Accounts of Chemical Research* **2009**, *42*, 388.

(111) Chiu, C.-W.; Gabbai, F. P. *Dalton Transactions* **2008**, 814.

(112) Hudnall, T. W.; Gabbaie, F. P. *Journal of the American Chemical Society* **2007**, *129*, 11978.

(113) Lee, M. H.; Gabbaie, F. P. *Inorganic Chemistry* **2007**, *46*, 8132.

(114) Lee, M. H.; Agou, T.; Kobayashi, J.; Kawashima, T.; Gabbai, F. P. *Chemical Communications (Cambridge, U. K.)* **2007**, 1133.

(115) Chiu, C.-W.; Gabbaie, F. P. *Journal of the American Chemical Society* **2006**, *128*, 14248.

(116) Melaiemi, M.; Sole, S.; Chiu, C.-W.; Wang, H.; Gabbaie, F. P. *Inorganic Chemistry* **2006**, *45*, 8136.

(117) Hudnall, T. W.; Melaiemi, M.; Gabbaie, F. P. *Organic Letters* **2006**, *8*, 2747.

(118) Melaimi, M.; Gabbaie, F. P. *Journal of the American Chemical Society* **2005**, *127*, 9680.

(119) Sole, S.; Gabbai, F. P. *Chemical Communications (Cambridge, U. K.)* **2004**, 1284.

(120) Holleman, A. F. W., Egon; Wiberg, Nils *Lehrbuch Der Anorganischen Chemie, 91-100 "Bor"*; Walter de Gruyter, 1985.

(121) Brown, H. C.; Schlesinger, H. I.; Cardon, S. Z. *Journal of the American Chemical Society* **1942**, *64*, 325.

(122) Dusemund, C.; Sandanayake, K. R. A. S.; Shinkai, S. *Journal of the Chemical Society, Chemical Communications* **1995**, 333.

(123) Yamamoto, H.; Ori, A.; Ueda, K.; Dusemund, C.; Shinkai, S. *Chemical Communications (Cambridge)* **1996**, 407.

(124) Arimori, S.; Davidson, M. G.; Fyles, T. M.; Hibbert, T. G.; James, T. D.; Kociok-Kohn, G. I. *Chemical Communications (Camb)* **2004**, 1640.

(125) Galbraith, E.; Fyles, T. M.; Marken, F.; Davidson, M. G.; James, T. D. *Inorganic Chemistry* **2008**, *47*, 6236.

(126) Hofmann, A. W. *Proceedings of the Royal Society of London* **1856**, *8*, 1.

(127) Schleyer, P. v. R. *Chemical Reviews* **2001**, *101*, 1115.

(128) Kekulé, A. *Justus Liebigs Annalen der Chemie* **1872**, *162*, 77.

(129) Schleyer, P. v. R. *Chemical Reviews* **2005**, *105*, 3433.

(130) Veltheer, J. E.; Burger, P.; Bergman, R. G. *Journal of the American Chemical Society* **1995**, *117*, 12478.

(131) Timoshkin, A. Y.; Frenking, G. *Organometallics* **2008**, *27*, 371.

(132) Krossing, I.; Raabe, I. *Chemistry – A European Journal* **2004**, *10*, 5017.

(133) Yamaguchi, S.; Akiyama, S.; Tamao, K. *Journal of the American Chemical Society* **2001**, *123*, 11372.

(134) Chen, M.-C.; Roberts, J. A. S.; Marks, T. J. *Organometallics* **2004**, *23*, 932.

(135) Taube, R.; Wache, S.; Sieler, J. *Journal of Organometallic Chemistry* **1993**, *459*, 335.

(136) Miyasaka, S.; Kobayashi, J.; Kawashima, T. *Tetrahedron Letters* **2009**, *50*, 3467.

(137) Zhao, Q.; Li, F.; Liu, S.; Yu, M.; Liu, Z.; Yi, T.; Huang, C. *Inorganic Chemistry* **2008**, *47*, 9256.

(138) Beer, P. D.; Tite, E. L.; Drew, M. G. B.; Ibbotson, A. *Dalton Transactions* **1990**, 2543.

(139) Beer, P. D.; Hesek, D.; Hodacova, J.; Stokes, S. E. *Journal of the Chemical Society, Chemical Communications* **1992**, 270.

(140) Beer, P. D.; Drew, M. G. B.; Hazlewood, C.; Hesek, D.; Hodacova, J.; Stokes, S. E. *Journal of the Chemical Society, Chemical Communications* **1993**, 229.

(141) Shriver, D. F.; Biallas, M. J. *Journal of the American Chemical Society* **1967**, *89*, 1078.

(142) Williams, V. C.; Piers, W. E.; Clegg, W.; Elsegood, M. R. J.; Collins, S.; Marder, T. B. *Journal of the American Chemical Society* **1999**, *121*, 3244.

(143) Williams, V. C.; Irvine, G. J.; Piers, W. E.; Li, Z.; Collins, S.; Clegg, W.; Elsegood, M. R. J.; Marder, T. B. *Organometallics* **2000**, *19*, 1619.

(144) Herberich, G. E.; Fischer, A.; Wiebelhaus, D. *Organometallics* **1996**, *15*, 3106.

(145) Herberich, G. E.; Englert, U.; Fischer, A.; Wiebelhaus, D. *European Journal of Inorganic Chemistry* **2004**, 4011.

(146) Katz, H. E. *Journal of the American Chemical Society* **1986**, *108*, 7640.

(147) Kawachi, A.; Tani, A.; Shimada, J.; Yamamoto, Y. *Journal of the American Chemical Society* **2008**, *130*, 4222.

(148) Glidewell, C. *Inorganica Chimica Acta* **1975**, *12*, 219.

(149) Huh, J. O.; Kim, H.; Lee, K. M.; Lee, Y. S.; Do, Y.; Lee, M. H. *Chemical Communications* **2010**, *46*, 1138.

(150) Lam, S.-T.; Zhu, N.; Yam, V. W. *Inorganic Chemistry* **2009**, *48*, 9664.

(151) Yamaguchi, S.; Shirasaka, T.; Akiyama, S.; Tamao, K. *Journal of the American Chemical Society* **2002**, *124*, 8816.

(152) Bai, D.-R.; Liu, X.-Y.; Wang, S. *Chemistry – A European Journal* **2007**, *13*, 5713.

(153) Sakuda, E.; Funahashi, A.; Kitamura, N. *Inorganic Chemistry* **2006**, *45*, 10670.

(154) Cummings, S. A.; Iimura, M.; Harlan, C. J.; Kwaan, R. J.; Trieu, I. V.; Norton, J. R.; Bridgewater, B. M.; Jäkle, F.; Sundararaman, A.; Tilset, M. *Organometallics* **2006**, *25*, 1565.

(155) Ashley, A. E.; Herrington, T. J.; Wildgoose, G. G.; Zaher, H.; Thompson, A. L.; Rees, N. H.; Krämer, T.; O'Hare, D. *Journal of the American Chemical Society* **2011**, *133*, 14727.

(156) Chu, T. L.; Weismann, T. J. *Journal of the American Chemical Society* **1956**, *78*, 23.

(157) Brown, H. C.; Dodson, V. H. *Journal of the American Chemical Society* **1957**, *79*, 2302.

(158) Leffler, J. E.; Watts, G. B.; Tanigaki, T.; Dolan, E.; Miller, D. S. *Journal of the American Chemical Society* **1970**, *92*, 6825.

(159) Olmstead, M. M.; Power, P. P. *Journal of the American Chemical Society* **1986**, *108*, 4235.

(160) Kwaan, R. J.; Harlan, C. J.; Norton, J. R. *Organometallics* **2001**, *20*, 3818.

(161) Dorsey, C. L.; Jewula, P.; Hudnall, T. W.; Hoefelmeyer, J. D.; Taylor, T. J.; Honesty, N. R.; Chiu, C.-W.; Schulte, M.; Gabbai, F. P. *Dalton Transactions* **2008**, 4442.

(162) Carpenter, B. E.; Piers, W. E.; Parvez, M.; Yap, G. P. A.; Rettig, S. J. *Canadian Journal of Chemistry* **2001**, *79*, 857.

Chapter Two: Experimental Techniques

2. Experimental Techniques

2.1. General remarks on reaction conditions

The majority of the syntheses described in this thesis were conducted under inert atmospheric conditions. This was necessitated by the sensitivity of the reagents, intermediates or products to the presence of even small amounts of either oxygen or water. Unless specifically stated, it should be assumed that a reaction has been performed under an inert, anhydrous atmosphere of either argon or nitrogen. All inert-atmosphere experiments were performed, as outlined in the literature, using either a Saffron Omega Scientific glove-box or a standard dual-manifold Schlenk line.[1] One manifold of the Schlenk line was provided with a baseline vacuum of 10^{-3} mbar by a Leybold D2.5E two-stage, oil-sealed, rotary-vane pump, which was monitored by a Thermovac TTR 91 active-vacuum sensor attached to a Leybold display. The second manifold of the Schlenk-line was provided with pure, anhydrous argon from a cylinder at pressure slightly greater than atmospheric, which was regulated by a standard regulator and vented through a mercury-filled bubbler. All glassware used for reactions carried out under inert-atmosphere conditions was washed in a base bath (a saturated solution of potassium hydroxide in *iso*-propanol), then a dilute acid bath (2 M hydrochloric acid solution in water), water and finally with acetone. The washed glassware was dried on a rack for at least one hour, followed by drying overnight in an oven at 50°C. Glassware attached to, or part of, the Schlenk-line was subjected to three cycles of evacuation and filling with

argon, with the glassware heated during the first evacuation. If it is stated that a reaction or work-up is performed under "bench-top" conditions, it is to be assumed that the techniques were performed in air and in accordance with appropriate, standard literature protocols.[2,3] All glassware used under "bench-top" conditions was washed first with water, then with acetone and finally dried for two hours in an oven at 50°C.

2.2. Physical measurements

2.2.1. Nuclear Magnetic Resonance (NMR) spectroscopy

NMR spectra were measured using either a Varian 'Mercury' 300, a Varian 'Venus' 300, a Varian 'Unity' 500 FT-NMR or a Bruker AVII500 with cryoprobe spectrometer. For ^{1}H and ^{13}C NMR spectra, signals were referenced to the residual solvent signal(s) of the deuterated solvent.[4] For ^{11}B, ^{19}F, ^{29}Si and ^{31}P NMR spectra, signals were referenced against $Et_2O{\cdot}BF_3$, $CFCl_3$, dilute $SiMe_4$ in $CDCl_3$ and 85% H_3PO_4 in H_2O, respectively. J. Young's NMR tubes were used for compounds requiring inert-atmosphere techniques and conditions.[1]

2.2.2. Elemental analyses (EA)

Elemental analyses were carried out at London Metropolitan University using a Carlo Erba CE1108 Elemental Analyser.

2.2.3. Mass spectrometry (MS)

The mass spectra of all novel compounds were provided by the EPSRC National Mass Spectrometry Service Centre, Swansea University.

2.2.4. Infrared spectroscopy (IR)

Infrared spectra were measured using a Nicolet 500 FT-IR spectrometer. Samples were added to ten equivalents of potassium bromide, ground to a fine powder and pressed into a potassium bromide disk according to standard literature procedures.[3]

2.2.5. Ultra-violet and visible spectroscopy (UV/Vis)

UV spectra were measured using a Scintio UV S-2100 UV/Vis spectrometer and Spectrosil® or quartz cuvettes. Air-sensitive samples were prepared in a J. Young's tap-adapted Spectrosil® cuvette inside a glovebox.

2.2.6. Fluorescence spectroscopy

Fluorescence spectra were collected on a Jobin Yvon-Horiba Fluorolog spectrometer in a Spectrosil® or quartz curvette.

2.2.7. Electrochemistry

Electrochemical measurements were performed on a PAR AMETEK VersaSTAT 3 potentiostat under anhydrous nitrogen within a Saffron Omega Scientific glovebox. Unless otherwise stated, the measurements were performed in a supporting electrolyte of a 0.1 M solution of tetrabutylammonium hexafluorophosphate in tetrahydrofuran as the

solvent. Cyclic voltammetry (CV) measurements were carried out as outlined in the literature,[5] with a silver quasi-reference electrode, a glassy-carbon working electrode and a platinum auxiliary electrode. All electrodes were sourced from Bioanalytical Systems. The quasi-reference electrode was prepared for use by immersion in the electrolyte solution for 48 h prior to commencing the experiment. Ferrocene was used as an internal reference. CV experiments were performed at three different scan rates of 0.05, 0.1 and 0.2 V s^{-1}, both before the addition of the ferrocene internal reference and afterwards, in order to ensure good reproducibility of the results.

2.2.8. X-ray crystallography

Unless otherwise stated, all solid-state structural elucidations were performed by the author. Diffraction data were collected using a Nonius Kappa CCD or Oxford Diffraction (Agilent) SuperNova diffractometer at 150 K;[6] data were reduced using either DENZO, SCALEPACK or CrysAlisPro.[7] The structures were solved with either SIR92[8] or SuperFlip[9] and refined with full-matrix least squares within CRYSTALS[10-12] as described in the CIF.

2.3. Experimental techniques

2.3.1. UV/Vis binding constant determination

Binding constants were determined by titration using UV/Vis spectra measured for either a tetrahydrofuran or a dichloromethane solution. A stock solution of receptor was prepared (typically 20 mg in 20 mL), from which exactly 3 mL was transferred to a UV

cuvette (Spectrosil® or quartz) along with a stirrer bead. A first absorption spectrum was measured, then a known volume of a known concentration of $[^nBu_4N]F{\cdot}3H_2O$ or $[^nBu_4N][CN]{\cdot}2H_2O$ was added (typically 25 μL of a 3×10^{-2} M solution), followed by stirring of the sample for 2 min, and measurement of a second spectrum. Further spectra were collected as subsequent aliquots were added to the cuvette until a total of 2.5 equivalents had been added. The various absorption spectra were collated using Microsoft Excel. The wavelength corresponding to the maximum absorption of the receptor was determined and 99 data points centred on this wavelength, for each aliquot, were selected for data analysis. Binding constants were determined using the REACTLAB™ software package of Jplus Consulting which takes dilution into account in the calculations. It is notable that the error margins on the binding constants are typically lower than the experimental errors associated with the actual measurements, so caution has been taken in making comparisons between binding constants with the same order of magnitude throughout this thesis, i.e. not to over-interpret data of similar magnitude.

2.3.2. UV/Vis kinetic studies

An aliquot of known concentration of the anion, sufficient to provide an excess, was added to 3 mL of receptor solution of known concentration in either a quartz or Spectrosil® cuvette. Individual UV/Vis spectra were collected at 15 s intervals for a period of 300 s.

2.3.3. Specialist drying methods

Many of the target materials synthesised under inert-atmosphere conditions were intractable oils, tars or waxes, which proved difficult to handle or weigh under inert-atmosphere conditions. However, these materials were converted to a sticky powder or nodular material using the technique described below. This manipulation enabled higher isolated yields of the desired reaction product to be obtained and also facilitated much easier manipulation of the target materials under an inert atmosphere.

Caution: The following procedure has an **inherent risk of explosion**, due to the rapid increase of pressure on conversion of the condensed phases of argon to the gas phase in a sealed system, coupled with the low temperatures at which these transitions can occur (Mp = −189°C, Bp = −186°C). Therefore, this procedure should only be attempted by competent inert-atmosphere chemists. For the following protocol the bottom half of the **glassware must be immersed in liquid nitrogen until the system is placed under vacuum. The use of a blast shield is recommended.**

Liquid argon is condensed onto the oil, tar or wax by immersing the glassware containing the product into liquid nitrogen under a high internal flow rate of argon gas. The solid material is now covered by a thick blanket of liquid argon, which means that the system can be briefly opened to an inert-atmosphere without compromising the material's chemical composition. The mechanical manipulation of the solid under a blanket of argon, with the glassware still immersed in liquid nitrogen, renders the solid into a powder. Resealing the system and immediately placing the system under vacuum turns the liquid argon into a solid argon matrix. The glassware is gradually and very carefully removed

from the liquid nitrogen over a period of 10 minutes. The solid argon gradually sublimes under dynamic vacuum over a period of typically one hour to yield the reaction product as a tractable powder.

NOTE: The system must not be heated in any way, which also includes touching the glassware. The system must be retained under dynamic vacuum for at least one hour. Under no circumstances should the system be backfilled before being certain that there is no residual solid argon within the system.

2.4. Purification of solvents and reagents

Commercially available materials used in chemical reactions described in this thesis are listed in Appendix II (CD), which also includes details of the commercial supplier, the purity of the material supplied and whether any further purification was required before use. All solvents for inert-atmosphere chemistry were sparged with anhydrous argon for 30 min and then stored in ampoules. All air- and/or moisture-sensitive reagents were stored under an inert atmosphere, with liquids contained in ampoules and solids stored in a Saffron Omega Scientific glove-box. Commercially available compounds that were used in this thesis are included in Appendix III (CD), along with the source, stated purity and purification protocol where relevant.

Literature compounds that were synthesised for use in this thesis are described in this section. Syntheses that followed the literature methods exactly are presented in tabulated form in section 2.4.1. Syntheses that followed literature procedures with minor modification are described in section 2.4.2. Syntheses of literature compounds that were made without following a literature procedure are presented in Section 2.4.2.

2.4.1. Unmodified literature syntheses

The compounds in this section were synthesised as described in the literature, conserving both the relative stoichiometry and concentration of reagents. The results are summarised in Table 2.1, with the yields obtained alongside the method of characterisation utilised to confirm the identity and, in some cases, the purity of the isolated compounds. The yields were typically within 20% of the values reported in the literature, although it must be noted that some of the reactions were performed only once. In all cases, the characterising spectroscopic data were found to be fully consistent with those presented in the literature.

Table 1 Compounds Synthesised following literature procedures

Compound	Yield	Analysis	Literature
2-Lithio[(dimethylamino)methyl]ferrocene	35 to 45%	Colour/further reactivity (methanol-d_4 quench, ^{1}H integration)	Rausch *et al.*[13]
1,7-Bis(trifluoroactyl)-1,4,7-triazoheptane	90 to 95%	^{1}H, ^{13}C and ^{19}F NMR and mass spectrometry	Platzek *et al.*[14]
1,7-Bis(*tert*-butylactyl)-1,4,7-triazoheptane	95%	^{1}H NMR and mass spectrometry	Wilcock *et al.*[15]
$[1,2\text{-fc}(CH_2NMe_3)BMes_2]^+\cdot I^-$	60%	^{1}H, ^{11}B, ^{13}C NMR and mass spectrometry	Broomsgrove *et al.*[16]
$Me_2Sn(C_6F_5)_2$	90%	^{1}H and ^{19}F NMR	Yap *et al.*[17]
$(C_6F_5)_2BCl$	50 to 65%	^{1}H, ^{11}B and ^{19}F NMR	Yap *et al.*[17]
$FcBMes_2$	55%	^{1}H and ^{11}B NMR and mass spectrometry	Broomsgrove *et al.*[18]
$1,1'\text{-fc}(BMes_2)_2$	55 to 65%	^{1}H and ^{11}B NMR	Broomsgrove *et al.*[19]
IMes-N_2O	80 to 90%	^{1}H and ^{13}C NMR	Tskhovrebov *et al.*[20]
Cl-IMes	75 to 80%	^{1}H and ^{13}C NMR	Arduengo *et al.*[21]
$B(C_6F_5)_3$	45 to 50%	^{1}H, ^{11}B, ^{13}C and ^{19}F NMR	Wang *et al.*[22]
Me_2SnPh_2	20%	^{1}H and ^{13}C NMR	Wursthorn *et al.*[23]
Ph_2BCl	55 to 60%	^{1}H, ^{11}B and ^{13}C NMR	Thomas *et al.*[24]
$(C_6Cl_5)_2BCl$	40 to 50%	^{11}B and ^{13}C NMR	Ashley *et al.*[25]

2.4.2. Modified literature syntheses

The compounds in this section were broadly synthesised as described in the literature, with minor modifications as noted. Many of these modifications were undertaken to increase either the purity or yield compared with the values cited in the literature. In some cases, a modification resulted in a lower yield than that reported the literature, but was still considered expedient as it reduced the number of steps needed to obtain the desired compounds.

$FBMes_2$: Following the work of Brown *et al*.,[26] a solution of 2-bromomesitylene (25.2 ml, 32.80 g, 165 mmol) in THF (70 mL) was added to a suspension of freshly prepared magnesium turnings (4.00 g, 165 mmol, 1 equiv.) in THF (50 mL) at a rate sufficient to induce and maintain reflux. The resulting grey solution was stirred for 2 h, cooled to −78°C and boron trifluoride diethyl etherate (10.3 mL, 11.80 g, 82 mmol, 0.5 equiv.) added dropwise at −78°C. The reaction mixture was allowed to gradually warm to room temperature overnight. Volatiles were removed *in vacuo* from the white suspension, the product extracted with hexane (3 × 50 mL) and the solvent removed *in vacuo* from the combined extracts to afford a white powder. Yield 11.70 g, 60%. ^{1}H, ^{11}B, ^{13}C and ^{19}F NMR data were consistent with composition and literature values.[27]

1,1'-$fcLi_2$·TMEDA: Following the work of Bishop *et al*. *n*-BuLi (56.5 mL of a 1.6 M solution in hexanes, 86 mmol) was added dropwise to a suspension of ferrocene (8.0 g, 43 mmol, 1 equiv.) and tetramethylethylenediamine (TMEDA) (13 mL, 17.2 g, 86 mmol, 2 equiv.) in hexane (50 mL) at room temperature. The resultant reaction mixture was stirred for 16 h, after which the orange precipitate was isolated by filtration, washed with

hexane (3 × 50 mL) and then dried *in vacuo* to afford a pyrophoric, orange powder. Yield 11.50 g, 68%. Purity was assayed by further reactivity.[28]

1,1'-fcBr$_2$: Following the work of Shafir *et al*.,[29] 1,1,2,2-tetrabromoethane (5.8 mL, 17.20 g, 51 mmol, 2 equiv.) was added dropwise to a solution of 1,1'-fcLi$_2$·TMEDA (7.10 g, 23 mmol) in diethyl ether (75 mL) at -60°C. The resulting suspension was allowed to warm to room temperature overnight. The dark red suspension was then quenched with water (50 mL) and from this point handled under "bench-top" conditions. The mixture was stirred for a further 10 min, during which time a dark oil formed. Both phases were decanted from the dark oil and the organic fraction isolated. The solvent was removed *in vacuo* from the red solution to afford a red oil. This was taken up in a minimal amount of methanol and cooled to −30°C to afford yellow crystals, which were isolated by filtration at −30°C and dried *in vacuo* to afford a yellow powder. Yield 4.70 g, 60%. ^{1}H and ^{13}C NMR data were consistent with literature values.[29]

1,1'-fc(BMes$_2$)Br: Following the work of Broomsgrove *et al*.,[16] *n*-BuLi (2.7 mL of a 1.6 M solution in hexanes, 4.4 mmol, 1 equiv.) was added dropwise to a solution of 1,1′-fcBr$_2$ (1.50 g, 4.38 mmol) in THF (30 mL) at −78°C. The purple reaction mixture was stirred for 30 min at −78°C. A solution of FBMes$_2$ (1.23 g, 4.6 mmol, 1.05 equiv.) in THF (30 mL) was then added to the suspension at −78°C. The resulting mixture was allowed to warm to room temperature over 4 h, then quenched with water (50 mL). From this point forward, the reaction was handled under "bench-top" conditions. The organic layer was diluted with diethyl ether (100 mL), isolated, washed with water (2 × 25 mL) and then brine (2 × 25 mL), dried with magnesium sulphate and filtered. The organic solvent was

removed *in vacuo* to yield the crude product as a red solid, purification of which by column chromatography (flash, hexanes untill the yellow band was eluted, then hexanes/diethyl ether 9:1 to elute the red fraction) followed by removal of the solvent *in vacuo* afforded the desired product as a red powder. Yield 1.40 g, 47%. ^{1}H, ^{11}B and ^{13}C NMR data were consistent with literature values.[16]

***rac*-1,2-fc(BMes$_2$)Br:** Following the work of Morgan *et al.,*[30] *n*-BuLi (3.6 mL of a 1.6 M solution in hexanes, 5.8 mmol, 1 equiv.) was added dropwise to a solution of 1,1'-fcBr$_2$ (2.00 g, 5.8 mmol) in THF (40 mL) at −78°C. The resulting mixture was stirred for 30 min at −78°C and then 2,2,6,6-tetramethylpiperidine (TMP) (1.0 mL, 0.84 g, 5.8 mmol, 1 equiv) was added, also at −78°C. The resulting purple solution was warmed to −40°C quickly and then maintained at a temperature between -30 and −40°C for 2 h. The purple reaction solution was then cooled to −78°C again and a solution of FBMes$_2$ (2.10 g, 7.7 mmol, 1.3 equiv.) in THF (30 mL) added dropwise at −78°C. The resulting red mixture was allowed to gradually attain room temperature overnight and then quenched with water (25 mL). From this point forward, the reaction was handled under "bench-top" conditions. The organic fraction was diluted with diethyl ether (100 mL), washed with water (2 × 25 mL), brine (2 × 25 mL), dried over magnesium sulphate and filtered, and the solvent removed *in vacuo* to yield the crude product as a red solid. Further purification was effected by column chromatography (flashed with hexanes to elute a yellow band that was discarded, followed by hexanes/diethyl ether 9:1 to elute the desired red fraction) followed by removal of the solvent *in vacuo* to afford the target material as a red powder. Yield was 1.40 g, 47%. ^{1}H, ^{11}B and ^{13}C NMR data were consistent with literature values.[30]

1,8-Bis(trifluoroactyl)-1,4,8-triazooctane: Following the work of Paltzek *et al*.,[14] ethyl trifluoroacetate (4.8 mL, 5.7 g, 40 mmol) in THF (50 mL) was added to a solution of *N*-(2-aminoethyl)-1,3-propanediamine (2.5 mL, 2.3 g, 20 mmol) also in THF (50 mL) at 0°C. The resultant reaction mixture was allowed to gradually attain room temperature and then stirred for 15 h. Volatiles were removed *in vacuo* to afford a yellow, waxy solid. Yield 5.07 g, 82%. ^{1}H NMR data were consistent with literature values.[31,32]

1,9-Bis(trifluoroactyl)-1,5,9-triazononane: Following the work of Paltzek *et al*.,[14] ethyl trifluoroacetate (4.8 mL, 5.7 g, 40 mmol) in THF (50 mL) was added to a solution of *bis*-(3-aminopropyl)amine (2.8 mL, 2.60 g, 20 mmol) also in THF (50 mL) at 0°C. The resulting mixture was warmed to room temperature and stirred for 15 h. Volatiles were removed *in vacuo* to afford a yellow, waxy solid. Yield 5.42 g, 84%.^{1}H NMR data were consistent with literature values.[31,32]

[FcCH$_2$NMe$_3$]I: Following the work of Lindsay *et al*.,[33] iodomethane (1.0 mL, 2.3 g, 17 mmol) was added dropwise to a solution of (dimethylaminomethyl)ferrocene (1.6 mL, 2.00 g, 8.3 mmol) in hexane (30 mL). The resulting mixture was stirred for 24 h, during which time a yellow precipitate formed, which was isolated by filtration, washed with hexane (2 × 10 mL) and dried *in vacuo* to give a light yellow powder. Yield 2.75 g, 86%.^{1}H NMR data were consistent with literature values.[33]

(C$_6$Cl$_5$)$_2$BCl: Following the work of Ashley and coworkers,[25] *n*-BuLi (22.1 mL of a 1.6 M solution in hexane, 35.3 mmol) was added dropwise over 30 min at −78°C to a suspension of C_6Cl_6 (10.07 g, 35.3 mmol) in a mixture of diethyl ether (100 mL) and hexane (100 mL). The resulting suspension was quickly warmed to −40°C, resulting in

consumption of the insoluble material. The yellow reaction solution was cooled back to −78°C and cold (−78°C) hexane (80 mL) added. BCl_3 (17.65 mL of a 1.0 M soliution in hexane, 17.65 mmol) was added slowly to this suspension at −78°C and the resulting suspension allowed to gradually warm to room temperature. After stirring for 15 h total, volatiles were removed *in vacuo* to afford a tan solid that was extracted with dichloromethane (3 × 100 mL) to afford an orange solution. This was cooled to -30 °C to give a peach-yellow precipitate that was isolated by filtration at -30 °C and dried *in vacuo* to afford a tan solid. Yield 2.79 g, 12%. Further concentration at room temperature and cooling gave additional batches of material, to give overall yields in the range of 30 to 40%. ^{1}H and ^{11}B NMR data were fully consistent with the literature values.[25]

$FcBBr_2$: Following the work of Renk *et al*.,[34] boron tribromide (5.0 mL, 13.0 g, 52.6 mmol) was added dropwise to a solution of ferrocene (9.84 g, 52.6 mmol) in toluene (80 mL), and the resulting mixture stirred at 40°C for 3 h. The dark red suspension was cooled to room temperature and volatiles removed *in vacuo* to afford a dark solid, which was extracted into hexanes (3 × 50 mL). After filtration, the combined extracts were concentrated *in vacuo* to ~50 mL, then cooled to −30°C, to afford the target material as a dark red crystalline material. Yield 7.27 g, 39%. ^{1}H and ^{11}B NMR data were fully consistent with the literature values.[34]

1,1'-$fc(BBr_2)_2$: Following the work of Appel *et al*.[35], boron tribromide (10.2 mL, 26.5 g, 107 mmol) was added slowly to a slurry of ferrocene (10.00 g, 53.8 mmol) in hexane (120 mL) at room temperature, and the resulting slurry heated under reflux for 5 h. The red reaction suspension was cooled to room temperature, filtered and extracted with further hexanes (4 × 50 mL). The combined extracts were concentrated *in vacuo* to

~100 mL and cooled to −30°C, which afforded the target material as a dark red, crystalline solid that was isolated by filtration and dried *in vacuo*. Yield 15.20 g, 80 %. ^{1}H and ^{11}B NMR data were fully consistent with literature values.[35]

Tri-tert-butylphosphine oxide: Caution: As dry mixtures of organic materials and hydrogen peroxide are potentially explosive, any dry reaction products from reactions, where hydrogen peroxide was used as a reagent, such as this one, were not manipulated until complete degradation of hydrogen peroxide was confirmed by ^{1}H NMR spectroscopy (δ_H = 9.5 ppm in d_4-methanol). Following the work of Bendle *et al*.[36], hydrogen peroxide (4.2 mL, 35% by weight in water, 4.31 mmol) was added over 15 min at 0°C to a solution of PBu_3 (0.58 g, 2.87 mmol) in dichloromethane (20 mL). The resulting solution was allowed to warm gradually to room temperature and then heated under reflux for 3 d to ensure complete degradation of residual hydrogen peroxide. Volatiles were then removed *in vacuo* to afford a white solid, which was first analysed by ^{1}H NMR to confirm the absence of hydrogen peroxide, then taken up in dichloromethane, dried over magnesium sulphate, filtered and volatiles removed *in vacuo* to afford a white powder. Yield 0.42 g, 67%. The ^{1}H, ^{31}P and ^{13}C NMR data were fully consistent with the literature values.[36,37]

3-Pyridyl boroxin: Following the work of Li *et al*.,[38] *n*-BuLi (37.5 mL of a 1.6 M solution in hexane, 60 mmol) was added dropwise at –40°C over 30 min to a solution of tri-*iso*-propyl borate (13.9 mL, 11.30 g, 60 mmol) and 3-bromo-pyridine (4.9 mL, 4.00 g, 51 mmol) in a mixture of toluene (80 mL) and THF (20 mL). The resulting mixture was stirred for an additional 30 min at –40°C, then warmed to −20°C and quenched with 2 M aqueous hydrochloric acid (100 mL). From this point forward, the reaction was handled under “bench-top” conditions. The reaction mixture was warmed to room temperature, the

aqueous phase separated and then neutralised by the addition of 5 M aqueous sodium hydroxide (~15 mL). The aqueous phase was extracted with THF (6 × 50 mL), saturated with sodium chloride and further extracted with THF (2 × 100 mL). The combined organic extracts were dried with magnesium sulphate, filtered and volatiles removed *in vacuo* to afford a white solid (8.90 g), which was taken up in acetonitrile (40 mL). The resulting solution was refluxed for 1 h, cooled to room temperature and volatiles removed *in vacuo* to afford the target material as a white powder. Yield 7.10 g, 65%. ^{1}H and ^{11}B NMR data were fully consistent with the literature values.[38]

3-Pyridinyl boronic acid pinacol ester: Following the work of Li *et al*.,[38] this reaction was conducted under "bench-top" conditions. 3-Pyridinyl boroxime (2.51 g, 7.9 mmol) and pinacol (3.45 g, 29.2 mmol) were suspended in toluene (100 mL) and the resulting mixture heated under reflux for 2.5 h, with water being continuously removed using a Dean–Stark apparatus. The mixture was cooled to room temperature and volatiles removed *in vacuo* to afford a tan solid, which was then taken up in cyclohexane (17 mL). The solution was refluxed for 30 min, then gradually cooled to room temperature and the resulting precipitate isolated by filtration. This solid product was washed with cold cyclohexane, then dried *in vacuo* to afford a white powder. Yield 2.50 g, 52%. The ^{1}H, ^{11}B and ^{13}C NMR data were fully consistent with the literature values.[38]

3-Quinolinyl boronic acid: Following the work of Li *et al*.,[38] *n*-BuLi (16.0 mL of a 1.6 M solution in hexane, 26 mmol) was added dropwise at −70°C over 1 h to a solution of tri-*iso*-propyl borate (6.0 mL, 4.89 g, 26 mmol) and 3-bromoquinoline (2.9 mL, 4.45 g, 22 mmol) in a mixture of toluene (32 mL) and THF (8 mL). The mixture was stirred for a further 30 min at −70°C, then warmed to −20°C. The reaction mixture was then quenched

with 2 M aqueous hydrochloric acid (100 mL) and warmed to room temperature. From this point forward, the reaction was handled under "bench-top" conditions. The aqueous phase was isolated and neutralised with 5 M sodium hydroxide (15 mL) and then extracted with THF (3 × 20 mL). The combined organic extracts were dried with magnesium sulphate, filtered and volatiles removed *in vacuo* to afford a tan solid, which was taken up in acetonitrile (20 mL) and refluxed for 30 minutes. The mixture was then cooled to room temperature and volatiles removed *in vacuo* to afford the target material as a white solid. Yield 1.25 g, 33%. The ^{1}H and ^{11}B NMR, and mass spectrometry data were fully consistent with the literature values.[38]

3-Quinolinyl boronic acid pinacol ester: Following the work of Li *et al*.,[38] this reaction was performed under "bench-top" conditions. A suspension of 3-quinoline boronic acid (0.50 g, 2.9 mmol) and pinacol (0.34 g, 2.9 mmol) in toluene (100 mL) was refluxed for 16 h in a Dean–Stark apparatus. The reaction mixture was cooled to room temperature and volatiles removed *in vacuo* to afford the target material as an off-white powder. Yield 0.34 g, 45%. The ^{1}H NMR shifts and mass spectrometry data were fully consistent with the literature.[38]

Lithium diisopropylamide: *n*-BuLi (20 mL of a 1.6 M solution in hexanes, 32.4 mmol, 0.91 equiv.) was added dropwise at -78°C to a solution of diisopropylamine (5 mL, 3.61 g, 35.6 mmol) in diethyl ether (100 mL). The resulting solution was brought to room temperature over 3 h and volatiles then removed *in vacuo*. The residue dried *in vacuo* at 60°C for 1 h to afford the desired target material. Yield 3.16 g, 83%. Purity was assayed by further reactivity.

MesLi: *n*-BuLi (36 mL of a 1.6 M solution in hexane, 57.6 mmol) was added to a solution of 2-bromomesitylene (7.2 mL, 9.37 g, 47 mmol) in diethyl ether (100 mL). The resulting mixture was refluxed for 3 h, and then cooled to room temperature to afford a white precipitate, which was isolated by filtration. The solid product was dried *in vacuo* to afford the target material as a pyrophoric, floccular powder. Yield 4.86 g, 82%. Purity was assayed by further reactivity.

2.4.3. Other sources of precursors

Several compounds were used in this body of work which were not synthesised by the author, but were supplied by colleagues. The author is grateful for their contribution of time and effort.

Table 2 contains a list of compounds that were donated, alongside the name of the person who donated them and their current affiliation. The purity of the compounds was taken on trust as specified by the donor.

Table 2 Chemicals obtained from donations

Compound	Donor	Current affiliation
Hexachlorobenzene	Dr Hasna Zaher	Danone
Hexachlorobenzene	Dr Andrew Ashley	Imperial College London
IMes carbene	Dr Nick Phillips	Imperial College London
Triphenylphosphine oxide	Dr Joshua Bates	Oxford University
Tris(perfluorophenyl)borane	Dr Ian Riddlestone	University of Bath

2.5. References

(1) Shriver, D. F. *The Manipulation of Air-Sensitive Compounds (McGraw-Hill Series in Advanced Chemistry)*; McGraw-Hill, 1969.

(2) Pirrung, M. C. *The Synthetic Organic Chemists' Companion*; John Wiley & Sons, Inc., 2007.

(3) Harwood, L. M.; Percy, J. *Experimental Organic Chemistry: Preparative and Microscale, 2nd ed*; Blackwell Scientific, 1998.

(4) Fulmer, G. R.; Miller, A. J. M.; Sherden, N. H.; Gottlieb, H. E.; Nudelman, A.; Stoltz, B. M.; Bercaw, J. E.; Goldberg, K. I. *Organometallics* **2010**, *29*, 2176.

(5) Bard, A. J.; Faulkner, L. R. *Electrochemical Methods: Fundamentals and Applications*; Masson, 1982.

(6) Cosier, J.; Glazer, A. M. *Journal of Applied Crystallography* **1986**, *19*, 105.

(7) Otwinowski, Z.; Minor, W. *Methods Enzymology* **1997**, *276*, 307.

(8) Altomare, A.; Cascarano, G.; Giacovazzo, C.; Guagliardi, A. *Journal of Applied Crystallography* **1994**, *27*, 1045.

(9) Palatinus, L.; Chapuis, G. *Journal of Applied Crystallography* **2007**, *40*, 786.

(10) Betteridge, P. W.; Carruthers, J. R.; Cooper, R. I.; Prout, K.; Watkin, D. J. *Journal of Applied Crystallography* **2003**, *36*, 1487.

(11) Cooper, R. I.; Thompson, A. L.; Watkin, D. J. *Journal of Applied Crystallography* **2010**, *43*, 1100.

(12) Thompson, A. L.; Watkin, D. J. *Journal of Applied Crystallography* **2011**, *44*, 1017.

(13) Rausch, M. D.; Moser, G. A.; Meade, C. F. *Journal of Organometallic Chemistry* **1973**, *51*, 1.

(14) Platzek, J.; Niedballa, U.; Radeuchel, B.; Schering A.-G., Germany. 1996, p 13 pp.

(15) Willcock, H.; Cooper, A. I.; Adams, D. J.; Rannard, S. P. *Chemical Communications* **2009**, 3095.

(16) Broomsgrove, A. E. J.; A. Addy, D.; Di Paolo, A.; Morgan, I. R.; Bresner, C.; Chislett, V.; Fallis, I. A.; Thompson, A. L.; Vidovic, D.; Aldridge, S. *Inorganic Chemistry* **2009**, *49*, 157.

(17) Parks, D. J.; Piers, W. E.; Yap, G. P. A. *Organometallics* **1998**, *17*, 5492.

(18) Broomsgrove, A. E. J.; Addy, D. A.; Bresner, C.; Fallis, I. A.; Thompson, A. L.; Aldridge, S. *Chemistry – A European Journal* **2008**, *14*, 7525.

(19) Aldridge, S.; Fallis, I. A.; Bresner, C.; Day, J. K.; Tatchell, T.; Broomsgrove, A. E. J.; Loveday, M. J.; University College Cardiff Consultants Ltd., UK . 2008, p 132pp.

(20) Tskhovrebov, A. G.; Solari, E.; Wodrich, M. D.; Scopelliti, R.; Severin, K. *Angewandte Chemie International Edition in English* **2012**, *51*, 232.

(21) Arduengo, A. J.; Davidson, F.; Dias, H. V. R.; Goerlich, J. R.; Khasnis, D.; Marshall, W. J.; Prakasha, T. K. *Journal of the American Chemical Society* **1997**, *119*, 12742.

(22) Wang, C.; Erker, G.; Kehr, G.; Wedeking, K.; Fröhlich, R. *Organometallics* **2005**, *24*, 4760.

(23) Wursthorn, K. R.; Kuivila, H. G.; Smith, G. F. *Journal of the American Chemical Society* **1978**, *100*, 2779.

(24) Thomas, J. C.; Peters, J. C. *Inorganic Chemistry* **2003**, *42*, 5055.

(25) Ashley, A. E.; Herrington, T. J.; Wildgoose, G. G.; Zaher, H.; Thompson, A. L.; Rees, N. H.; Krämer, T.; O'Hare, D. *Journal of the American Chemical Society* **2011**, *133*, 14727.

(26) Brown, H. C.; Dodson, V. H. *Journal of the American Chemical Society* **1957**, *79*, 2302.

(27) Eisch, J. J.; Shafii, B.; Odom, J. D.; Rheingold, A. L. *Journal of the American Chemical Society* **1990**, *112*, 1847.

(28) Bishop, J. J.; Davison, A.; Katcher, M. L.; Lichtenberg, D. W.; Merrill, R. E.; Smart, J. C. *Journal of Organometallic Chemistry* **1971**, *27*, 241.

(29) Shafir, A.; Power, M. P.; Whitener, G. D.; Arnold, J. *Organometallics* **2000**, *19*, 3978.

(30) Morgan, I. R.; Di Paolo, A.; Vidovic, D.; Fallis, I. A.; Aldridge, S. *Chemical Communications* **2009**, 7288.

(31) Xu, D.; Prasad, K.; Repic, O.; Blacklock, T. J. *Tetrahedron Letters* **1995**, *36*, 7357.

(32) An, H.; Cummins, L. L.; Griffey, R. H.; Bharadwaj, R.; Haly, B. D.; Fraser, A. S.; Wilson-Lingardo, L.; Risen, L. M.; Wyatt, J. R.; Cook, P. D. *Journal of the American Chemical Society* **1997**, *119*, 3696.

(33) Lindsay, J. K.; Hauser, C. R. *The Journal of Organic Chemistry* **1957**, *22*, 355.

(34) Renk, T.; Ruf, W.; Siebert, W. *Journal of Organometallic Chemistry* **1976**, *120*, 1.

(35) Appel, A.; Nöth, H.; Schmidt, M. *Chemische Berichte* **1995**, *128*, 621.

(36) Bendle, M.; Huynh, K.; Haddow, M. F.; Manners, I. *Inorganic Chemistry* **2011**, *50*, 10292.

(37) Schmidbaur, H.; Blaschke, G. *Zeitschrift Naturforsch., B: Anoranische. Chemie., Organische Chemie.* **1978**, *33B*, 1556.

(38) Li, W.; Nelson, D. P.; Jensen, M. S.; Hoerrner, R. S.; Cai, D.; Larsen, R. D.; Reider, P. J. *The Journal of Organic Chemistry* **2002**, *67*, 5394.

Chapter Three: 1,2-Functionalised Ferrocenes

3.1. Introduction

Following the work of Beer *et al.*[1-3] on the use of metallocenium derivatives to electrochemically recognize anions in non-aqueous media, Shinkai and coworkers have sought to exploit both the Lewis acidity and the electrochemical potential of ferroceneboronic acid $FcB(OH)_2$ (Figure 3.1) for anion binding.[4] Addition of fluoride anions to a solution of $FcB(OH)_2$ in an aqueous electrolyte led to a shift in the polarographic half-wave potential of approximately 200 mV. A binding constant, K_2, could be determined from this data, with a value of 700 (±50) for fluoride revealing a marked preference over potentially competing anions such as Cl^-, Br^-, SCN^-, SO_4^{2-} or $H_2PO_4^-$ (which have binding constants ranging from <2 through to 20 (±10)). Combining $FcB(OH)_2$ with a redox-active dye, such as methylene blue, allows for the transduction of the electrochemical response to the complexation of fluoride to a colorimetric response *viz* the loss of blue colour from solution.[5]

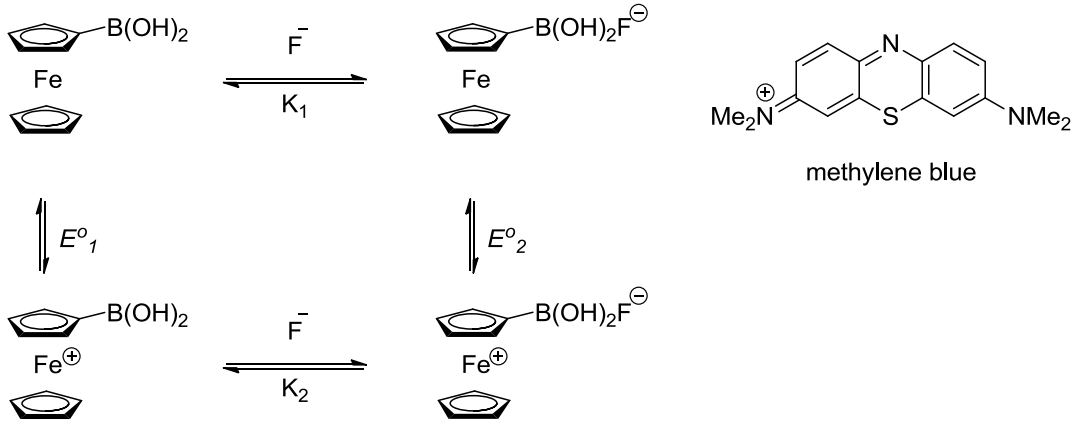

Figure 3.1. The fluoride binding and electrochemical equilibria of $FcB(OH)_2$.

Aldridge *et al.*, with the synthesis of 1,1'-*bis*(dialkoxyboryl)ferrocene (Figure 3.2), explored the capacity of *bis*-borane-functionalized ferrocenes as electrochemical sensors for selective fluoride detection.[6] This system binds two equivalents of fluoride in chloroform solution with a corresponding 146 mV anodic shift of the oxidation potential of the ferrocene substituent. Under anaerobic conditions this occasions no colour change, however, in aerobic conditions, a colour change from orange to green is observed. The signal transduction from electrochemical to colorimetric was, therefore, seen to be possible in the absence of an external dye, relying instead upon the ferrocene/ferrocenium chromophore itself. It was also of note that no other anions screened (Cl^-, Br^-, I^-, PF_6^-, $H_2PO_4^-$, HSO_4^- or NO_3^-) elicited a comparable response, either colorimetrically or by NMR analysis.

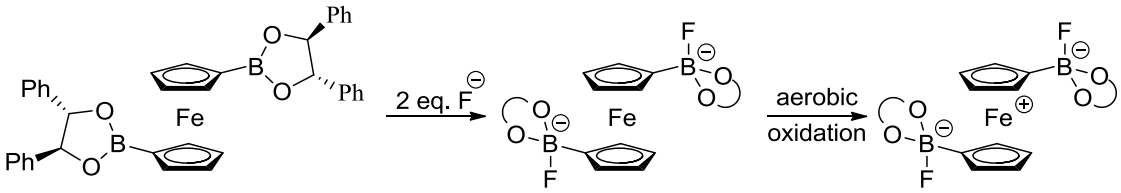

Figure 3.2. The fluoride anion binding of 1,1'-*bis*(dialkoxyboryl)ferrocene.

Further work by Bresner *et al.,* sought to augment the ferrocene-functionalized boranes with a Lewis-basic component, so as to bind HF, either intact or as F^- and H^+.[7] Compounds **I**, **II** and 1,2-fc($B(OH)_2$)(CH_2NMe_2) (Figure 3.3) were synthesized and reacted with hydrogen fluoride as the collidine complex (2,4,6-trimethylpyridine·$(HF)_{1.5}$). All three compounds were found to react with three equivalents of fluoride, with **I** and **II** yielding the $FcBF_3^-$ borate anion. 1,2-fc($B(OH)_2$)(CH_2NMe_2) also undergoes B-O bond cleavage to yield

zwitterionic 1,2-fc(BF_3)(CH_2NHMe_2), containing a related BF_3^- borate anion. Although systems initially containing compounds **I**, **II** or 1,2-fc-($B(OH)_2$)(CH_2NMe_2) exhibit changes in the electrochemistry upon exposure to fluoride, the cleavage of the B-O bonds left scope for development of more chemically robust systems.

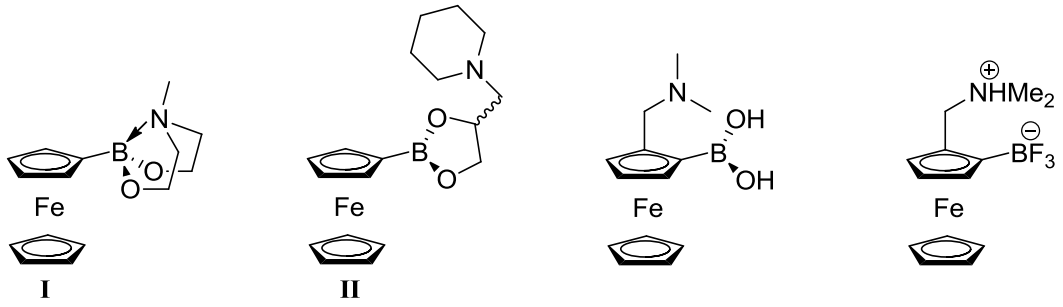

Figure 3.3. Ferrocenyl boranes **I**, **II** and 1,2-fc($B(OH)_2$)(CH_2NMe_2) that are capable of binding fluoride anions and the zwitterionic compound 1,2-fc(BF_3)(CH_2NHMe_2).

The development of a more chemically robust class of ferrocene functionalized boranes was brought about by the incorporation of the $BMes_2$ unit in the work of Broomsgrove *et al.*[8] $ArBMes_2$ units are known to be air- and moisture-stable and have been previously exploited in binding both fluoride[9-16] and cyanide.[17,18] Furthermore, these units also tend to exhibit changes in the UV/Vis spectra upon binding fluoride or cyanide. Incorporation of the $BMes_2$ unit into a metallocene was achieved by Broomsgrove *et al.* in their synthesis of the Lewis acid $FcBMes_2$ (Figure 3.4).[8]

Anion receptor $FcBMes_2$ binds fluoride anions in dichloromethane solution, with binding reported by a colour change from dark red $FcBMes_2$ to pale yellow $[FcBMes_2{\cdot}F]^-$.[19]

The ^{11}B NMR spectrum of $FcBMes_2$ (δ = 76 ppm) changes on addition of fluoride to δ = 5 ppm.[19] Anion receptor $FcBMes_2$ also binds cyanide anions in dichloromethane solution, with binding reported to yield a similar colour change and a shift in the ^{11}B signal to δ = -16 ppm.[8] The UV-Vis response in each case to the presence of fluoride or cyanide in dichloromethane solution allowed for binding constant determination (K_F = 7.8(1.2) x 10^4 M^{-1} and K_{CN} = 8.3(2.0) x 10^4 M^{-1}.).[19] Moreover, although these numbers are similar, treatment of $[FcBMes_2{\cdot}F]^-$ with cyanide results in the formation of $[FcBMes_2{\cdot}CN]^-$, whereas treatment of $[FcBMes_2{\cdot}CN]^-$ with fluoride does not result in the formation of $[FcBMes_2{\cdot}F]^-$. Thus $FcBMes_2$ binds cyanide more strongly than fluoride.[8]

$FcBMes_2$ is reversibly oxidised at a potential E^o_1 of +181 mV (*vs*. FcH/FcH^+), which shifts by -550 mV on the addition of fluoride anions (E^o_2 = -369 *vs*. FcH/FcH^+) (Figure 3.4).[8] $FcBMes_2$ also exhibits a shift of -564 mV on addition of cyanide (E^o_3 = -383 mV cf. FcH/FcH^+).[8] The difference in the oxidation potentials of $[FcBMes_2{\cdot}F]^-$ and $[\mathbf{8}{\cdot}CN]^-$ of 14 mV is not sufficient to allow for discrimination between the two adducts at a reasonable cost, and hence for anion receptor $FcBMes_2$ cannot selectively report the presence of fluoride or cyanide anions through electrochemical means.

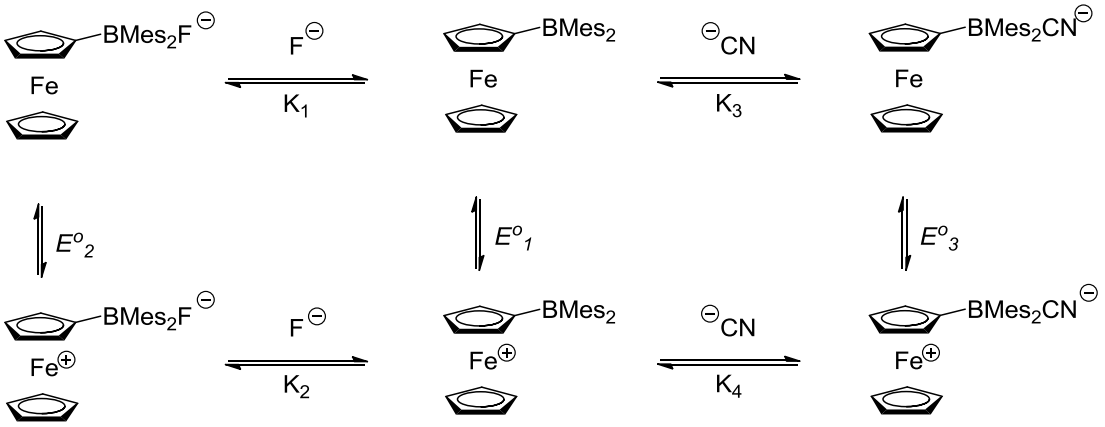

Figure 3.4. The anion binding and electrochemical oxidation equilibria exhibited by anion receptor $FcBMes_2$ with fluoride and cyanide anions.[8,19]

The work of Broomsgrove *et al.* also probed the role of electrostatics on the anion binding propensities of $FcBAr_2$ systems, by utilising 4-functionalised 2,6-xylyl boranes $FcB(Mes)_2$, $FcB(Xyl)_2$, $FcB(Xyl^F)_2$ and $FcB(Xyl^{OMe})_2$.[20] Key properties of these four anion receptors are shown in Table 3.1, ordered according to the Hammett parameter (σ_p) of the substituent in the *para* position of the aryl groups.[21] It is clear that on increasing the electron withdrawing nature of the *para* substituent (increasing σ_p), the reversible oxidation potential increases.[20] This would be expected to result in greater Lewis acidity at the borane, and hence increasing anion binding constants (K_F and K_{CN}), as is indeed exhibited by these four anion receptors.[20] The binding constants of these four receptors tend to be greater for cyanide than fluoride anions.[20]

Lewis Acid	Hammett Parameter σ_p	E^o_1	K_F (mol^{-1} dm^{-3})	K_{CN} (mol^{-1} dm^{-3})
$FcB(Xyl^{OMe})_2$	-0.27	+95	$6.6(0.4) \times 10^4$	$1.5(0.2) \times 10^5$
$FcB(Mes)_2$	-0.17	+131	$7.8(1.2) \times 10^4$	$8.3(2.0) \times 10^4$
$FcB(Xyl)_2$	0.00	+153	$4.4(0.5) \times 10^5$	$1.4(0.2) \times 10^5$
$FcB(Xyl^F)_2$	0.06	+184	$4.3(0.7) \times 10^5$	$7.7(1.8) \times 10^5$

Table 3.1. Hammett parameters (σ_p), oxidation potential (E^o_1) [*vs.* FcH/FcH^+], fluoride anion binding constant (K_F) and cyanide binding constant (K_{CN}) [in dichloromethane solution ca. 4×10^{-4} mol dm^{-3}] for ferrocenyl boranes.[20]

Ferrocenyl systems featuring an ancillary hydrogen bond designed to interact with fluoride anions bound at the borane centre have also been reported by Broomsgrove *et al.* (Figure 3.5).[20] The cationic anion receptor [1,2-fc($BMes_2$)(CH_2NMe_3)]I and its related isomer [1,1'-Fc($BMes_2$)(CH_2NMe_3)]I were synthesised and their anion binding properties evaluated by NMR spectroscopy and UV/Vis titration. As with related triarylboranes, the inclusion of a proximal cationic moiety to the borane results in an increase in the anion binding affinity (K_F and K_{CN}) relative to the neutral borane (Table 3.2).[20,22-25] In addition, [1,2-fc($BMes_2$)(CH_2NMe_3)]I exhibits a dramatic (*ca.* 1000-fold) increase in anion binding affinity (K_F and K_{CN}) relative to [1,1'-Fc($BMes_2$)(CH_2NMe_3)]I (Table 3.2).[20] As anion receptors [1,2-fc($BMes_2$)(CH_2NMe_3)]I and [1,1'-Fc($BMes_2$)(CH_2NMe_3)]I have similar reversible oxidation potentials (E^o_1 = +367 and +314 mV vs. FcH/FcH^+), the difference in binding constants presumably reflects the differing proximities of the cationic NMe_3 moiety, and the possibility for a secondary H-bonding interaction.[20]

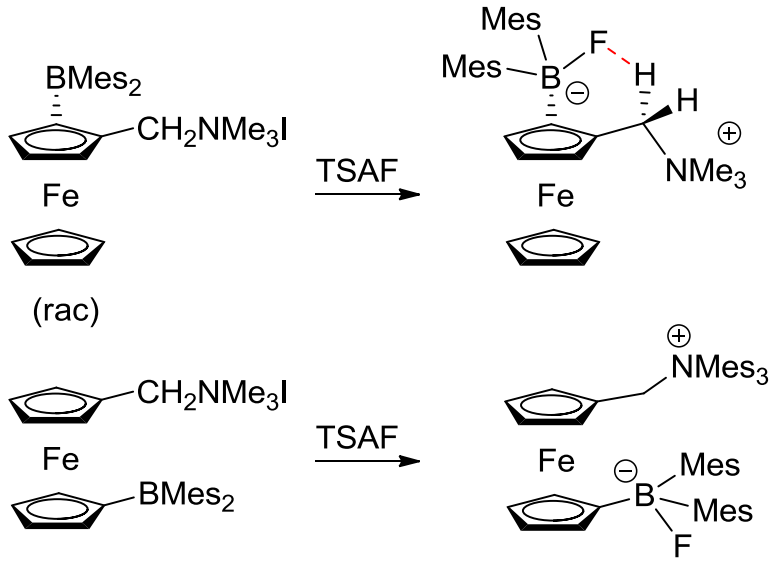

Figure 3.5. Hydrogen bonding to fluoride anions bound at ferrocenyl boranes [1,2-fc($BMes_2$)(CH_2NMe_3)]I and [1,1'-Fc($BMes_2$)(CH_2NMe_3)]I.[20]

The ^{11}B NMR spectrum of [1,2-fc($BMes_2$)(CH_2NMe_3)]I in *d*-chloroform exhibits a broad resonance centred at 80 ppm, which shifts to a sharper resonance at 6 ppm on treatment with fluoride, consistent with binding at the borane.[20] The ^{1}H NMR spectrum of [1,2-fc($BMes_2F$)(CH_2NMe_3)] in *d*-chloroform features a doublet of doublets centred at 5.54 ppm ($^{1}J_{HF}$ = 6.6 Hz, $^{2}J_{HH}$ = 12.2 Hz), which collapses to a doublet ($^{2}J_{HH}$ = 12.2 Hz) on broad-band fluorine decoupling, illustrative of ancillary hydrogen bonding to the boron bound fluoride.[20] Anion binding association and competition studies of [1,2-fc($BMes_2$)(CH_2NMe_3)]I, [1,2-fc($BMes_2F$)(CH_2NMe_3)] and [1,2-fc($BMes_2CN$)(CH_2NMe_3)] suggest that cyanide is bound slightly more strongly by [1,2-fc($BMes_2$)(CH_2NMe_3)]$^{+}$ than fluoride, but to a lesser degree than $FcBMes_2$.[20]

Lewis Acid	K_F	K_{CN}	E^o_1 (mV)
$FcBMes_2$	$7.8(1.2) \times 10^4$	$8.3(2.0) \times 10^4$	+131
[1,2-fc($BMes_2$)(CH_2NMe_3)]I	$5.6(2.3) \times 10^9$	$5.6(2.4) \times 10^9$	+367
[1,1'-fc($BMes_2$)(CH_2NMe_3)]I	$9.4(3.6) \times 10^5$	$5.8(1.7) \times 10^5$	+314

Table 3.2. Oxidation potential (E^o_1) [*vs.* FcH/FcH^+], fluoride anion binding constant (K_F) and cyanide binding constant (K_{CN}) [in dichloromethane solution ca. 4×10^{-4} mol dm^{-3}] for three boranes.[20]

Further probes of the nature of 1,2-functionalised systems are complicated by hydrolysis of the borane function; thus, treatment of 1,2-fc($BMes_2$)(CH_2NMe_2) with wet sources of fluoride gives borinic acid [1,2-fc(BMes(OH)F)(CH_2NMe_2H)] (Figure 3.6.).[19] The concomitant formation of mesitylene was confirmed by ^1H NMR spectroscopy. This degradation of the receptor has not been observed with the related 1,1'-isomer, suggesting that the proximity of the Lewis acid and (protonated) Lewis base function are key to the degradation process.[19]

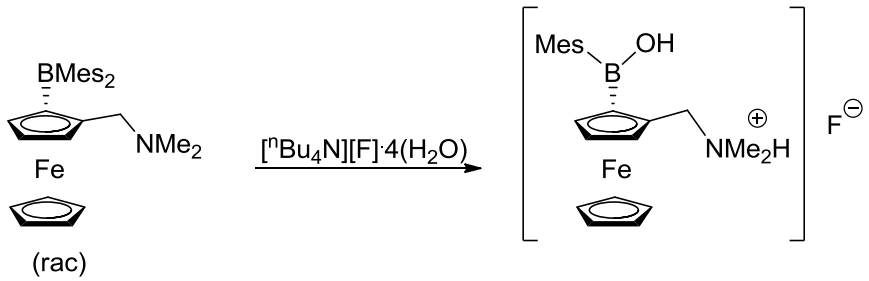

Figure 3.6. Hydrolysis of 1,2-functionalised ferrocene [1,2-fc($BMes_2$)(CH_2NMe_2)] to give [1,2-fc(BMes(OH)F)(CH_2NMe_2H)].

Attempts to exploit the chelate effect utilising two borane receptor sites on a ferrocene backbone to were undertaken by Morgan *et al.* using Lewis acid 1,2-fc($BMes_2$)$_2$ (Figure 3.7).[26] 1,2-fc($BMes_2$)$_2$ was shown to readily bind cyanide to give the adduct [1,2-fc($BMes_2$)$_2$·CN]$^-$, which exhibits two resonances in the ^{11}B NMR spectrum at -15 and 78 ppm indicative of the absence of chelation in solution.[26] The non-chelating nature of cyanide binding in the solid state was confirmed by X-ray crystallography, with the cyanide clearly sitting in an *exo* position, viz the pocket between the two boron centres.[26] The binding event was reported both colorimetrically and electrochemically.[26] 1,2-fc($BMes_2$)$_2$ also reacts with fluoride to give [1,2-fc($BMes_2$)$_2$·F]$^-$, although the binding event was observed to be slow (reaction rate k_{obs} = 1.64 x 10^2 s^{-1} with a 20-fold excess of fluoride). The boron bound fluoride was observed to reside *endo* with respect to the pocket between the two centres, although there was little evidence of chelation in the solid state. This absence of the chelate effect is perhaps not unexpected given the large B-B separation in 1,2-fc($BMes_2$)$_2$ [3.684 Å] compared to typical B-F distances for a bridging fluoride (e.g. 1.585(5) and 1.633(5) for [1,8-$C_{10}H_8$($BMes_2$)($BC_{12}H_8S$)(μ-F)]$^-$).[26,27] Further investigation of the anion binding propensities of 1,2-bisborylferrocenes was undertaken by Aldridge and co-workers.[28]

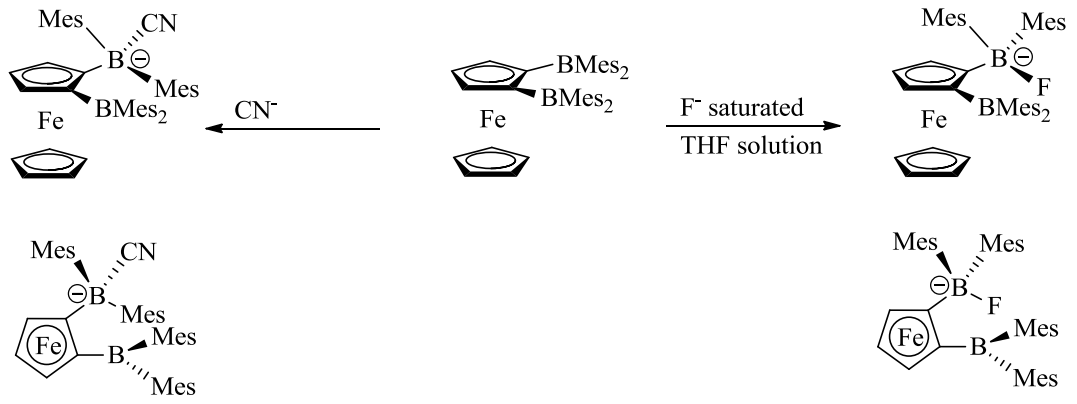

Figure 3.7. The binding of cyanide and fluoride anions by bisborylferrocene 1,2-fc$(BMes_2)_2$.[26]

A ferrocenyl borane capable of binding fluoride via an ancillary interaction with a proximal Lewis acid (in the 2-position) was reported by Jäkle and co-workers (Figure 3.8).[29] 1,2-fc(BMePh)($SnMe_2Cl$) was shown to react with one equivalent of potassium fluoride and 18-crown-6 gave the fluoride bridged system [1,2-fc(BMePh)($SnMe_2Cl$)·F]$^-$, while reaction with an excess of potassium fluoride at an elevated temperature (50 ºC) led to the additional substitution of the Sn-Cl bond to give the fluoride bridged complex [1,2-fc(BMePh)($SnMe_2F$)·F]$^-$ (Figure 3.8).[29] X-ray crystallographic studies of the [K(18-crown-6)]$^+$ salts of [1,2-fc(BMePh)($SnMe_2Cl$)·F]$^-$ and [1,2-fc(BMePh)($SnMe_2F$)·F]$^-$ unambiguously establish that one fluoride in each adduct binds in a μ-bridging fashion.[29] The B-F bond distances of 1.530(3) and 1.530(9) Å, respectively, are as expected.[29] Moreover, the $F_{bridging}$-Sn-$(F/Cl)_{terminal}$ angles for [1,2-fc(BMePh)($SnMe_2Cl$)·F]$^-$ and [1,2-fc(BMePh)($SnMe_2F$)·F]$^-$ are 171.11(4) and 175.21(15)º respectively, closely resembling the case of [1,2-{$C_6H_4BMes_2$(μ_2-F)$SiMe_2F$)]$^-$ reported by Kawchi *et al*,[29,30] and indicative of donation from the fluoride guest into the Sn-F σ* orbital of the host. The Sn-$F_{bridging}$ distances for [1,2-fc(BMePh)($SnMe_2Cl$)·F]$^-$ and [1,2-fc(BMePh)($SnMe_2F$)·F]$^-$ are 2.420(2) and

2.379(4) Å respectively, which are within the range of typical fluoro-bridged tin compounds.[29] Both the Sn-Cl and the Sn-$F_{terminal}$ bonds of complexes [1,2-fc(BMePh)($SnMe_2Cl$)·F]$^-$ and [1,2-fc(BMePh)($SnMe_2F$)·F]$^-$ exhibit bond lengths [2.4346(9) and 2.013(4) Å respectively] that are elongated with respect to typical Sn-Cl and Sn-F bonds.[29]

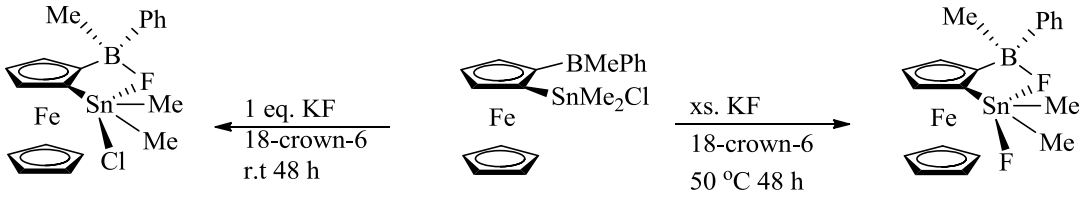

Figure 3.8. The reaction of receptor 1,2-fc(BMePh)($SnMe_2Cl$) to potassium fluoride in the presence of 18-crown-6.[29]

The ^1H, ^{11}B, ^{19}F and ^{119}Sn NMR spectra of both [1,2-fc(BMePh)($SnMe_2Cl$)·F]$^-$ and [1,2-fc(BMePh)($SnMe_2F$)·F]$^-$ suggest that the bridging-binding motif is retained by the fluoride adducts in d_3-acetonitrile solution.[29] The adduct **[**1,2-fc(BMePh)($SnMe_2Cl$)·F]$^-$ exhibits a resonance at 6 ppm in the ^{11}B NMR spectrum, consistent with a borane-bound fluorine anion. The ^{119}Sn NMR spectrum of [1,2-fc(BMePh)($SnMe_2F$)·F**]**$^-$ exhibits two sets of signals arising from diastereoisomerism, with each set comprised of a doublet of doublets (at 30.8 ppm: dd, $^1J_{Sn\text{-}F(terminal)}$ = 2038 Hz, $^1J_{Sn\text{-}F(bridging)}$ = 342 Hz; at 26.6 ppm: dd, $^1J_{Sn\text{-}F(terminal)}$ = 2046 Hz, $^1J_{Sn\text{-}F(bridging)}$ = 372 Hz). That the tin resonances exhibit coupling to two separate fluorine atoms suggests that chelation is retained in solution. The ^{19}F NMR spectrum exhibits two sets of signals due to diastereoisomerism, with peaks at -169.8 (br, B-F), -171.6 (br, B-F), -183.5 (d/pst, $^1J_{SnF}$ = 2049,1951 Hz, $^2J_{FF}$ = 51.7 Hz) and -184.2 (d/pst, $^1J_{SnF}$ = 2040/1950 Hz,

$^{2}J_{FF}$ = 51.7 Hz).[29] The broadened signals are typical of boron-bound fluoride anions and the F-F coupling is further indicative that the chelation of fluoride is retained in d_3-acetonitrile.

3.2. Aims

At the outset, the objective of the research presented in this chapter was to investigate the possibility of selectively binding fluoride anions in preference to cyanide anions in solution, together with transduction of this binding event into a colorimetric response.

Using the ferrocene appended bis-aryl borane moiety as the primary binding site, it was envisioned that hydrogen bond donor(s) included in our receptor might interact with a boron-bound fluoride in an intra-molecular fashion, hence increasing the fluoride anion binding affinity. Therefore, a primary aim was to devise synthetic routes to novel 1,2-difunctionalised ferrocenes featuring both a bis-aryl borane and a flexible group containing amide functions, and then evaluate their anion binding properties.

It was also of interest to explore the capacity of 1,2-difunctionalised ferrocenes containing both a primary bis-aryl borane anion binding site and a secondary Lewis acidic centre. It was thought that these two Lewis acidic centres would favour the binding of fluoride over cyanide, as fluoride was envisioned as likely to be chelated, whereas cyanide was not. Therefore, a second aim was to devise synthetic routes to novel 1,2-difunctionalised ferrocenes featuring two Lewis acidic centres, one boron-based, the other featuring an element giving rise to a longer E-F bond (given that 1,2-fc($BMes_2$)$_2$ does not chelate fluoride). To disambiguate the role of chelation over electronic effects in anion binding, the isomeric 1,1'-difunctionalised ferrocenyl receptors were also to be synthesised (where possible) and their anion binding capabilities evaluated.

3.3. Experimental

$[NH_2(CH_2CH_2NHCOCF_3)_2][CF_3CO_2]$: Following a protocol reported by O'Sullivan and coworkers to synthesise $NH(CH_2CH_2NHCOCF_3)_2$,[31] ethyl trifluoroacetate (12.1 mL, 101 mmol) and distilled water (0.6 mL, 35 mmol) were added dropwise to $NH(CH_2CH_2NH_2)_2$ (3.15 mL, 29 mmol) in acetonitrile (45 mL). The mixture was refluxed for 20 h. The mixture was cooled to room temperature and volatiles removed *in vacuo* to afford the target material as an off-white solid. Yield 7.9 g, 92%. Spectroscopic analyses were fully consistent with salt formation, corroborating the findings of Dalrymple and coworkers.[31]

$Fc(CH_2N(CH_2CH_2NHCOCF_3)_2$ (5): A solution of **1** (0.765 g, 2.6 mmol) and **4** (1.00 g, 2.6 mmol) in acetonitrile (50 mL) was refluxed for 24 h. The resulting black suspension was cooled to room temperature, diluted with diethyl ether, dried over magnesium sulphate and filtered, and the volatiles removed *in vacuo* to afford a brown solid. TLC (100% diethyl ether) gave rise to three bands, the first, orange band (R_f = 0.85) was found to correspond to the target material. Column chromatography with diethyl ether allowed the isolation of the target material as a solution in diethyl ether. Volatiles were then removed *in vacuo* to afford the target material as an orange solid. Yield 0.26 g, 18%. Crystals suitable for single crystal X-ray analysis were grown from slow diffusion of hexane into a saturated chloroform solution of **5**, which were isolated by filtration.

^{1}H NMR (300 MHz, $CDCl_3$, 20 ºC): δ_H 6.73 (br s, 2H, NH), 4.08 (t, $^3J_{H\text{-}H}$ = 1.8 Hz, 2H, C_5H_4C), 4.60 (s, 5H, C_5H_5), 4.02 (t, $^3J_{H\text{-}H}$ = 1.8 Hz, 2H, C_5H_4C), 3.41 (s, 2H, $FcC\underline{H}_2$), 3.15 (q, $^3J_{H\text{-}H}$ = 5.7 Hz, 4H, $NC\underline{H}_2$), 2.55 (t, $^3J_{H\text{-}H}$ = 5.7 Hz, 4H, $C\underline{H}_2NHCO$).

^{13}C NMR (125 MHz, $CDCl_3$, 20 ºC): δ_C 157.6 (q, $^2J_{C-F}$ = 5 Hz, NHCO), 115.8 (q, $^1J_{C-F}$ = 286 Hz, CF_3), 82.2 (quaternary carbon of C_5H_4C), 69.6 (C_5H_4C), 68.7 (C_5H_5), 68.6 (C_5H_4C), 53.0 ($FcCH_2N$), 51.6 (NCH_2R), 37.4 (CH_2NHAc).

^{19}F NMR (282 MHz, $CDCl_3$, 20 ºC): δ_F -76.0 (s, CF_3).

MS (ESI^+) 199.0 (100%) $[FcCH_2]^+$, 494.1 (97%) $[M]^+$. Exact mass (calculated for M^+, ^{14}N, ^{16}O, ^{19}F, ^{56}Fe, isotopomer) 494.0960, (measured) 494.0955.

Elemental microanalysis: calc. for $C_{19}H_{21}F_6FeN_3O_2$ C 46.27% H 4.29% N 8.52%, meas. C 46.18, 46.25%, H 4.27, 4.26%, N 8.53, 8.52%.

Crystallographic data: $C_{19}H_{21}F_6FeN_3O_2$, M_r = 493.23, orthorhombic, P 2_1 2_1 2_1, a = 7.66080(10), b = 10.54380(10), c = 25.4990(4) Å, V = 2059.65(5) Å^3, Z = 4, ρ_c = 1.591 Mg m^{-3}, T = 150 K, λ = 0.71073 Å. 22347 reflections collected, 4700 independent [R(int) = 0.060] used in all calculations. R_1 = 0.0346, wR_2 = 0.0734 for observed unique reflections [I>2σ(I)] and R_1 = 0.0427, wR_2 = 0.0781 for all unique reflections. Max. and min. residual electron densities 0.42 and -0.46 e Å^3.

Li[1,2-fc(CH_2NMe_2)] (6): ^{n}BuLi (3.9 mL of a 1.6 M solution in hexanes, 6.2 mmol) was added dropwise to a solution of $FcCH_2NMe_2$ (1.2 mL, 6.2 mmol, 1 equiv.) in diethyl ether (50 mL) at 0 ºC. The reaction mixture was stirred at 0 ºC for 1 h, then warmed to room temperature and stirred for a further 12 h. Volatiles were removed *in vacuo* from the orange suspension, the orange solid washed with hexanes (3 x 15 mL) and dried *in vacuo* to afford an

orange, pyrophoric powder. Yield 1.42 g, 92%. Purity could be assayed by treating the lithiate with an excess of d_4-methanol with subsequent ^{1}H NMR spectroscopy showing a 2:1 ratio for the proton resonances corresponding to the η^5-C_5H_3DR unit.

[1,2-fc(BMes$_2$)(CH$_2$NMe$_3$)]I (7): A solution of $FBMes_2$ (0.210 g, 0.8 mmol) in diethyl ether (20 mL) was added dropwise at -78 ºC to a suspension of **6** (0.102 g, 0.4 mmol) also in diethyl ether (20 mL) at -78 ºC. The yellow suspension was stirred at -78 ºC for 1 h. After warming to room temperature, the dark red suspension was stirred for a further 14 h. Iodomethane (0.5 mL, 80 mmol) was then added dropwise to the suspension at room temperature. Stirring for 5 h at room temperature was accompanied by precipitation of a purple solid and lightening of the solution to a straw yellow color. The purple solid was isolated by filtration, washed with diethyl ether (2 x 30 mL) and the volatiles removed *in vacuo*. The solid was taken up in minimal dichloromethane (~100 mL) and filtered off from a colorless insolute. The solvent was removed *in vacuo* to afford the target material. Yield 0.383 g, 76%. ^{1}H, ^{11}B and ^{13}C NMR spectra were fully consistent with literature values.[20]

1,2-fc(BMes$_2$)(CH$_2$N(CH$_2$CH$_2$NHCOCF$_3$)$_2$) (8): **7** (0.200 g, 0.32 mmol), K_2CO_3 (0.043 g, 3.2 mmol, 10 equiv.) and **1** (0.127 g, 0.42 mmol, 1.3 equiv.) were suspended in acetonitrile (20 mL) and the resulting mixture refluxed for 5 h. After cooling to room temperature, the dark solution was isolated by filtration, and the volatiles removed *in vacuo*. Column chromatography (dry column vacuum chromatography over pre-dried silica, with hexanes:diethyl ether elutant (50 mL portions, starting with 100% hexanes, increasing volume % of diethyl ether by 10% per elution) followed by removal of volatiles *in vacuo*

afforded the target material as a red powder. Yield 0.029 g, 10%. Attempts to grow crystals suitable for single crystal X-ray studies proved unsuccessful.

^{1}H NMR (300 MHz, $CDCl_3$, 20 ºC): δ_H 6.79 (s, 4H, 4 x Mes), 6.49 (br. s, 2H, 2 x NH), 4.85 (s, 1H, C_5H_3BC), 4.65 (s, 1H, C_5H_3BC), 4.50 (s, 1H, C_5H_3BC), 4.20 (s, 5H, C_5H_5), 3.67 (d, $^{2}J_{H\text{-}H}$ = 15 Hz, 1H, $FcCH_2N$), 3.20 (m, 5H, $FcCH_2N$ and 2 x NCH_2R), 3.09 (m, 4H, 2 x $C\underline{H}_2NHAc$), 2.33 (s, 6H, 2 x *para* CH_3 of Mes), 2.27 (s, 12H, 4 x *ortho* CH_3 of Mes).

^{11}B NMR (96 MHz, $CDCl_3$, 20 ºC): δ_B 76 (br.s, $FcBMes_2$).

^{13}C NMR (125 MHz, $CDCl_3$, 20 ºC): δ_C 157.6 (q, $^{2}J_{C\text{-}F}$ = 37.5 Hz, 2 x NHCO), 143.2 (Mes), 139.4 (Mes), 137.5 (Mes), 128.1 (Mes), 115.8 (q, $^{1}J_{C\text{-}F}$ = 285 Hz, 2 x CF_3), 91.9 (C_5H_3BC), 80.2 (C_5H_3BC), 72.6 (C_5H_3BC), 70.2 (C_5H_3BC), 51.3 ($FcCH_2N$), 37.7 (NCH_2R), 34.7 (CH_2NH), 24.5 (*para* CH_3 of Mes), 20.9 (*ortho* CH_3 of Mes). Note neither of the two quaternary carbon signals of C_5H_3BC were observed.

^{19}F NMR (282 MHz, $CDCl_3$, 20 ºC): δ_F -75.9 (s, CF_3).

MS (EI^+) 249.1 (7%) $[BMes_2]^+$, 327.1 (17%) $[C_5H_3(BMes_2)(CH_2)]^+$, 447.2 (24%) $[1,2\text{-}fc(BMes_2)(CH_2)]^+$, 481.1 (12%), $[C_5H_3(BMes_2)(CH_2N(CH_2CH_2NHCOCF_3))]^+$, 741.3 (100%) $[M]^+$. Isotopic profile for $[M]^+$ was fully consistent with a theoretical profile for $C_{37}H_{42}BFeN_3O_2F_6$. MS (HEIP) Exact mass (calculated for $C_{37}H_{42}BFeN_3O_2F_6$, ^{10}B, ^{14}N, ^{16}O, ^{19}F, ^{54}Fe, isotopomer) 738.2701, (measured) 738.2692.

[K(18-crown-6)][1,2-fc($BMes_2F$)($CH_2N(CH_2CH_2NHCOCF_3)_2$)],

[K(18-crown-6)][8·F]: Compound **8** (30 mg, 40 μmol), KF (26 mg, 450 μmol) and 18-crown-6 (10 mg, 40 μmol) were dissolved in $CDCl_3$ (1 mL). The mixture was stirred at room temperature for 24 h, with a gradual colour change to yellow being observed. The solution was isolated by filtration. The solid could be obtained by removal of volatiles *in vacuo*. Yield 0.023 g, 56%.

^{1}H NMR (300 MHz, CD_3CN, 20 ºC): δ_H 6.75 (s, 2H, NHCO), 6.70 (s, 1H, Mes), 6.57 (s, 1H, Mes), 6.54 (s, 1H, Mes), 6.38 (s, 1H, Mes), 4.42 (s, 1H, C_5H_3BC), 4.16 (s, 1H, C_5H_3BC), 3.55 (s, 24H, 18-crown-6), 4.01 (d, $^2J_{H-H}$ = 6.0 Hz, 1H, $FcCH_2N$), 3.90 (s, 5H, C_5H_5), 3.30 (br. m, 4H, NCH_2R), 2.29 (d, $^2J_{H-H}$ = 6.0 Hz, 1H, $FcCH_2N$), 2.72 (m, 2H, C<u>H</u>$_2$NH), 2.48 (m, 2H, C<u>H</u>$_2$NH), 2.31 (s, 3H, *ortho* CH_3 of Mes), 2.25 (s, 3H, *ortho* CH_3 of Mes), 2.22 (s, 3H, *ortho* CH_3 of Mes), 2.08 (s, 3H, *ortho* CH_3 of Mes), 1.89 (s, 3H, *para* CH_3 of Mes), 1.82 (s, 3H, *para* CH_3 of Mes).

^{11}B NMR (96 MHz, CD_3CN, 20 ºC): δ_B 8 (br s).

^{19}F NMR (282 MHz, CD_3CN, 20 ºC): δ_F -76.4 (s, 6F, CF_3), -170 (br. s, 1F, $FcBMes_2F$).

[K(18-crown-6)][1,2-fc($BMes_2CN$)($CH_2N(CH_2CH_2NHCOCF_3)_2$)],

[K(18-crown-6)][8·CN]: 8 (30 mg, 40 μmol), KCN (29 mg, 446 μmol) and 18-crown-6 (10 mg, 40 μmol) were dissolved in $CDCl_3$ (1 mL). The mixture was stirred at room temperature

for 24 h, with a gradual colour change to yellow observed. The solution was isolated by filtration. Layering a concentrated $CDCl_3$ solution with hexane led to the formation of yellow crystals. Yield not determined.

^{1}H NMR (500 MHz, CD_3CN, 20 ºC): δ_H 6.73 (s, 1H, Mes), 6.50 (s, 2H, Mes), 6.39 (s, 1H, Mes), 4.24 (s, 1H, C_5H_3BC), 4.19 (s, 1H, C_5H_3BC), 3.95 (s, 5H, C_5H_5), 3.92 (s, 1H, C_5H_3BC), 3.57 (s, 24H, 18-crown-6), 3.40 (m, 4H, $CH_2C\underline{H_2}NH$), 3.33 (m, 2H, $FcC\underline{H_2}NR_2$), 3.04 (s, 3H, CH_3), 2.76 (m, 2H, $C\underline{H_2}CH_2NH$), 2.62 (m, 2H, $C\underline{H_2}CH_2NH$), 2.18 (s, 3H, CH_3), 2.14 (s, 3H, CH_3), 2.09 (s, 3H, CH_3), 1.69 (s, 3H, CH_3), 1.67 (s, 3H, CH_3).

^{11}B NMR (96 MHz, CD_3CN, 20 ºC): δ_B -15 (s, $FcBMes_2CN$).

^{13}C NMR (125 MHz, CD_3CN, 20 ºC): δ_C 156.5 (q, $^{2}J_{C\text{-}F}$ = 36.3 Hz, 2 x $\underline{C}OCF_3$), 143.0 (Ar-C of Mes), 142.1 (Ar-C of Mes), 141.9 (Ar-C of Mes), 141.7 (Ar-C of Mes), 131.7 (Ar-C of Mes), 131.6 (Ar-C of Mes), 129.1 (Ar-C of Mes), 129.0 (Ar-C of Mes), 128.6 (Ar-C of Mes), 128.5 (Ar-C of Mes), 112.8 (Ar-C of Mes), 90.2 (C_5H_3BC), 76.5 (C_5H_3BC), 69.9 (CH_2 of 18-crown-6), 68.6 (C_5H_5), 65.2 (C_5H_3BC), 55.3 (CH_2), 52.5 (CH_2), 38.8 (CH_2), 26.4 (CH_3 of Mes), 25.1 (CH_2), 24.6 (CH_3 of Mes), 24.0 (CH_3 of Mes), 23.4 (CH_3 of Mes), 23.3 (CH_3 of Mes), 19.8 (CH_3 of Mes), 19.7 (CH_3 of Mes). One resonance arising from CF_3 and one resonance arising from the mesityl rings were not observed.

^{19}F NMR (282 MHz, CD_3CN 20 ºC): δ_F -76.7 (s, CF_3), -76.9 (s, CF_3).

1,2-fc($BMes_2$)($CH_2N(CH_2CH_2NHCOCF_3)(CH_2CH_2CH_2NHCOCF_3)$) 9: **7** (0.200 g, 0.32 mmol), K_2CO_3 (0.050 g, 3.2 mmol, 10 equiv.) and **2** (0.140 g, 0.45 mmol, 1.4 equiv.) were suspended in acetonitrile (20 mL) and the resulting mixture refluxed for 5 h. The suspension was cooled to room temperature, the dark solution isolated by filtration and the volatiles removed *in vacuo*. Column chromatography (dry column vacuum chromatography over pre-dried silica, with hexanes:diethyl ether elutant (50 mL portions, starting with 100% hexanes, increasing volume % of diethyl ether by 10% per elution) followed by removal of volatiles *in vacuo* afforded the target material as a red powder. Yield 0.019 g, 8%. Attempts to grow crystals suitable for X-ray diffraction studies by slow evaporation and slow solvent mixing failed.

^{1}H NMR (300 MHz, CD_3CN, 20 ºC): δ_H 7.95 (br s, 1H, NH), 7.46 (br s, 1H, NH), 6.95 (s, 4H, Mes), 5.20 (s, 1H, C_5H_3BC), 4.82 (s, 1H, C_5H_3BC), 4.48 (s, 1H, C_5H_3BC), 4.36 (s, 5H, C_5H_5), 3.82 (d, $^2J_{H\text{-}H}$ = 14.1 Hz, 1H, FcC$\underline{H}_2$N), 3.34 (m, 2H, NC$\underline{H}_2CH_2$NH), 3.24 (m, 3H, FcC$\underline{H}_2$N and NC$\underline{H}_2CH_2CH_2$NH), 2.47 (s, 18H, *ortho*-CH_3), 2.40 (m, 8H, *para*-CH_3 and $NCH_2C\underline{H}_2CH_2NH$), 2.13 (m, 2H, $NCH_2C\underline{H}_2NH$), 1.63 (m, 2H, $NCH_2CH_2C\underline{H}_2NH$).

^{11}B NMR (96 MHz, CD_3CN, 20 ºC): δ_B 76 (br s).

^{13}C NMR (125 MHz, CD_3CN, 20 ºC): δ_C 158.0 (q, $^2J_{C\text{-}F}$ = 30 Hz, $\underline{C}OCF_3$), 144.0 (Ar-C of Mes), 140.0 (Ar-C of Mes), 138.2 (Ar-C of Mes), 129.5 (Ar-C of Mes), 117.3 (q, $^1J_{C\text{-}F}$ = 477 Hz, $CO\underline{C}F_3$), 91.4 (C_5H_3BC), 79.8 (C_5H_3BC), 77.5 (C_5H_3BC), 71.0 (C_5H_5), 55.6 (NCH_2),

53.8 (NCH_2), 52.8 (NCH_2), 39.2 ($CH_2\underline{C}H_2CH_2$), 38.3 ($CH_2\underline{C}H_2CH_2$), 26.5 ($\underline{C}H_2NHCO$), 24.5 ($\underline{C}H_2NHCO$), 20.9 ($\underline{C}H_2NHCO$).

^{19}F NMR (282 MHz, CD_3CN, 20 ºC): δ_F -76.5 (s, CF_3), -76.7 (s, CF_3).

MS (EI^+) 308.0 (100%) $[N(CH_2CH_2NHCOCF_3)(CH_2CH_2CH_2NHCOCF_3)]^+$, 755.3 (100%) $[M]^+$. Isotopic profile for $[M]^+$ was fully consistent with a theoretical profile for $C_{38}H_{44}BFeN_3O_2F_6$. MS (HEIP) Exact mass (calculated for $C_{38}H_{44}BFeN_3O_2F_6$, ^{10}B, ^{14}N, ^{16}O, ^{19}F, ^{54}Fe, isotopomer) 738.2701, (measured) 738.2692.

[K(18-crown-6)][1,2-fc($BMes_2F$)($CH_2N(CH_2CH_2NHCOCF_3)$ ($CH_2CH_2CH_2NHCOCF_3$))], [K(18-crown-6)] [9·F]: Compound **9** (30 mg, 40 μmol), KF (25 mg, 430 μmol) and 18-crown-6 (10 mg, 40 μmol) were dissolved in $CDCl_3$ (1 mL). The resulting mixture was stirred at room temperature for 24 h, with a gradual colour change to yellow observed. The compound was isolated by filtration. Slow evaporation under inert atmosphere conditions resulted in one crystal suitable for X-ray diffraction. Yield not determined.

^1H NMR (300 MHz, CD_3CN, 20ºC): δ_H 8.19 (br s, 1H, NHCO), 7.85 (br s, 1H, NHCO), 6.9-6.7 (br m, 4H, Mes), 5.00 (m, 1H, $FcCH_2N$), 4.60 (m, 2H, C_5H_3BC), 4.38 (s, 5H, C_5H_5), 4.15 (m, 1H, C_5H_3BC), 3.71 (m, 1H, $FcCH_2N$), 3.6-3.00 (br m, 22H, 18-crown-6 + NCH_2R), 2.59 (s, 3H, CH_3), 2.42 (s, 3H, CH_3), 2.4-1.6 (br m., 12H, $CH_2C\underline{H}_2CH_2$ + $C\underline{H}_2NHCO$ + CH_3), 1.54 (s, 3H, CH_3), 1.10 (s, 3H, CH_3).

^{11}B NMR (96 MHz, CD_3CN, 20 ºC): δ_B 8 (br s, $fcBMes_2F$).

^{19}F NMR (282 MHz, CD_3CN, 20 ºC): δ_F -75.8 (s, 3F, CF_3), -75.9 (s, 3F, CF_3), -172.9 (br s, 1F, BF).

MS (ESI⁻) 560.1 (61) [**9** – (2 x $COCF_3$)], 660.2 (57) [**9** – ($COCF_3$)], 674 (100) [**9**·**F** – $COCF_3$] 755 (45) [**9**], 760 (43) [unknown], 776 (44) [**9**·**F**]. MS (ESI) Exact mass (calculated for $C_{38}H_{46}BF_7FeN_3O_2$, ^{10}B, ^{14}N, ^{16}O, ^{19}F, ^{54}Fe, isotopomer) 776.2934, (measured) 776.2299.

[K(18-crown-6)][1,2-fc($BMes_2CN$)($CH_2N(CH_2CH_2NHCOCF_3)$ ($CH_2CH_2CH_2NHCOCF_3$))], [K(18-crown-6)][9·CN]: Compound **9** (30 mg, 40 μmol), KCN (28 mg, 430 μmol) and 18-crown-6 (10 mg, 40 μmol) were dissolved in $CDCl_3$ (1 mL). The reaction mixture was stirred at room temperature for 24 h, with a gradual colour change to yellow observed. The compound was isolated by filtration. Slow diffusion of pentane into a saturated $CDCl_3$ solution under inert atmosphere conditions led to the formation of yellow crystals suitable to X-ray crystallography as well as a brown tar. Yield not determined.

^{1}H NMR (300 MHz, CD_3CN, 20 ºC): δ_H 7.63 (br s, 2H, NH), 6.73 (s, 1H, Mes), 6.50 (s, 2H, Mes), 6.39 (s, 1H, Mes), 4.26 (m, 1H, C_5H_4BC), 4.19 (m, 1H, C_5H_4BC), 3.95 (s, 5H, C_5H_5), 3.92 (m, 2H, 1H of C_5H_4BC and 1H of $FcCH_2N$), 3.56 (s, 24 H, 18-crown-6), 3.39 (br m, 3H, 1H of $FcCH_2N$ and $NC\underline{H}_2CH_2N$), 3.31 (m, 2H, $NC\underline{H}_2CH_2CH_2N$), 3.05 (s, 3H, CH_3), 2.78 (m, 2H, $NCH_2C\underline{H}_2CH_2N$), 2.64 (m, 2H, $NCH_2C\underline{H}_2N$), 2.54 (m, 2H, $NCH_2CH_2C\underline{H}_2N$), 2.18 (s, 3H, CH_3), 2.14 (s, 3H, CH_3), 2.09 (s, 3H, CH_3), 1.69 (s, 3H, CH_3), 1.67 (s, 3H, CH_3).

^{11}B NMR (96 MHz, CD_3CN, 20 ºC): δ_B -15 (s, $fcBMes_2CN$).

^{13}C NMR (75 MHz, CD_3CN, 20 ºC): δ_C 158.0 (q, $^2J_{C\text{-}F}$ = 28 Hz, $\underline{C}OCF_3$), 144.0 (Mes), 143.0 (Mes), 142.9 (Mes), 142.6 (Mes), 132.7 (Mes), 130.2 (Mes), 129.7 (Mes), 129.5 (Mes), 119.2 (Mes), 115.4 (Mes), 91.4 (C_5H_3BC), 77.5 (C_5H_3BC), 71.0 (C_5H_5), 69.7 (C_5H_3BC), 69.6 (C_5H_3BC), 66.3 (C_5H_3BC), 55.6 (CH_2), 53.8 (CH_2), 52.8 (CH_2), 39.2 (CH_2), 38.3 (CH_2), 27.5 (CH_3), 26.5 (CH_3), 24.9 (CH_3), 24.4 (CH_3), 20.9 (CH_3), 20.8 (CH_3). Two Mes quaternary carbon resonances were not observed.

^{19}F NMR (282 MHz, CD_3CN, 20 ºC): δ_F -76.3 (s, CF_3), -76.5 (s, CF_3).

1,2-fc($BMes_2$)($CH_2N(CH_2CH_2CH_2NHCOCF_3)_2$), 10: **7** (0.017 g, 0.27 mmol), K_2CO_3 (0.090 g, 5.8 mmol, 21 equiv.) and **3** (0.150 g, 0.45 mmol, 1.7 equiv.) were suspended in acetonitrile (10 mL) and the reaction mixture refluxed for 5 h. The suspension was cooled to room temperature, the dark solution isolated by filtration and volatiles removed *in vacuo*. Column chromatography (dry column vacuum chromatography over pre-dried silica, with hexanes:diethyl ether elutant (50 mL portions, starting with 100% hexanes, increasing volume % of diethyl ether by 10% per elution) followed by removal of volatiles *in vacuo* afforded the target material as a red powder. Yield 0.033 g, 16%.

^{1}H NMR (300 MHz, CD_3CN, 20 ºC): δ_H 8.02 (br s, 2H, NH), 6.79 (s, 4H, Mes), 5.02 (m, 1H, C_5H_3BC), 4.66 (m, 1H, C_5H_3BC), 4.33 (m, 1H, C_5H_3BC), 4.21 (s, 5H, C_5H_5), 3.70 (d,

$^{2}J_{H\text{-}H}$ = 13.2 Hz, 1H, $FcCH_2N$), 3.13 (m, 5H, 1H of $FcCH_2N$, $NC\underline{H}_2CH_2CH_2NH$), 2.32-2.16 (br m, 22H, CH_3 + $NCH_2C\underline{H}_2CH_2NH$), 1.49-39 (br m, 4H, $NCH_2CH_2C\underline{H}_2NH$).

^{11}B NMR (96 MHz, CD_3CN, 20 ºC): δ_B 79 (s, $fcBMes_2$).

^{13}C NMR (75 MHz, CD_3CN, 20 ºC): δ_C 156.8 (q, $^{2}J_{C\text{-}F}$ = 36 Hz, $\underline{C}OCF_3$), 139.5 (Mes), 138.6 (Mes), 137.5 (Mes), 136.7 (Mes), 129.1 (Mes), 128.1 (Mes), 116.4 (q, $^{1}J_{C\text{-}F}$ = 286 Hz, CF_3), 94.2 (C_5H_3BC), 79.4 (C_5H_3BC), 77.3 (C_5H_3BC), 72.3 (C_5H_3BC), 69.5 (C_5H_5), 55.0 (C_5H_3BC), 51.6 (CH_2), 50.7 (CH_2), 49.5 (CH_2), 38.8 (CH_2), 25.2 (CH_3), 24.9 (CH_3), 24.1 (CH_3), 22.0 (CH_3), 20.5 (CH_3), 20.2 (CH_3).

^{19}F NMR (282 MHz, CD_3CN, 20 ºC): δ_F -76.5

[K(18-crown-6)][1,2-fc($BMes_2F$)($CH_2N(CH_2CH_2CH_2NHCOCF_3)_2$)],

[K(18-crown-6)] [10·F]: Compound **10** (30 mg, 40 μmol), KF (25 mg, 430 μmol) and 18-crown-6 (10 mg, 40 μmol) were dissolved in $CDCl_3$ (1 mL). The reaction mixture was stirred at room temperature for 24 h, with a gradual colour change to yellow observed. The compound was isolated by filtration. Attempts to form crystals suitable to X-ray diffraction analyses by slow diffusion and slow evaporation under inert atmosphere conditions failed. Yield not determined.

^{1}H NMR (300 MHz, CD_3CN, 20 ºC): δ_H 6.93 (s, 1H, Mes), 6.85 (s, 1H, Mes), 6.67 (br. s, 2H, NH), 6.48 (br. s, 2H, Mes), 4.26 (m, 1H, C_5H_3BC), 4.19 (m, 1H, C_5H_3BC), 4.05 (m, 1H, $FcCH_2N$), 3.98 (m, 1H, C_5H_3BC), 3.91 (s, 5H, C_5H_5), 3.87 (m, 1H, $FcCH_2N$), 3.71 (s,

3H, CH_3), 3.68 (s, 3H, CH_3), 3.64 (s, 21H, 18-crown-6 + CH_3), 3.24 (m, 4H, NCH_2), 2.55 (m, 4H, $CH_2C\underline{H}_2CH_2$), 2.44 (s, 3H, CH_3), 2.29 (s, 3H, CH_3),2.16 (s, 3H, CH_3), 1.72 (s, 3H, CH_3).

^{11}B NMR (96 MHz, CD_3CN, 20 ºC): δ_B 6 (br s).

^{19}F NMR (282 MHz, CD_3CN, 20 ºC): δ_F -75.8 (s, 3F, CF_3), -76.1 (s, 3F, CF_3), -172.9 (br s, 1F, BF).

[K(18-crown-6)][1,2-fc($BMes_2CN$)($CH_2N(CH_2CH_2CH_2NHCOCF_3)_2$)],

[K(18-crown-6)][10·CN]: Compound **10** (30 mg, 40 μmol), KCN (28 mg, 430 μmol) and 18-crown-6 (10 mg, 40 μmol) were dissolved in $CDCl_3$ (1 mL). The reaction mixture was stirred at room temperature for 24 h, with a gradual colour change to yellow observed. The compound was isolated by filtration. Slow diffusion of hexane into a saturated $CHCl_3$ solution led to the formation of yellow crystals. Yield not determined.

^{1}H NMR (300 MHz, CD_3CN, 20 ºC): δ_H 8.17 (br s, 2H, NH), 6.73 (s, 1H, Mes), 6.49 (s, 2H, Mes), 6.37 (s, 1H, Mes), 4.21 (m, 2H, C_5H_3BC), 3.95 (s, 5H, C_5H_5), 3.91 (m, 1H, C_5H_3BC), 4.15 (m, 1H, $FcCH_2N$), 3.59 (s, 3H, CH_3), 3.37 (m, 1H, $FcCH_2N$), 3.32 (m, 4H, NCH_2), 3.03 (s, 3H, CH_3), 2.59 (m, 4H, $CH_2C\underline{H}_2CH_2$), 2.18 (s, 3H, CH_3), 2.14 (s, 3H, CH_3), 2.13 (s, 3H, CH_3), 2.08 (s, 3H, CH_3), 1.74 (m, 4H, CH_2NHCO), 1.69 (s, 3H, CH_3), 1.67 (s, 3H, CH_3).

^{11}B NMR (96 MHz, CD_3CN, 20 ºC): δ_B -13 (sharp s).

^{13}C NMR (125 MHz, CD_3CN, 20 ºC): δ_C 156.3 (q, $^2J_{C\text{-}F}$ = 28 Hz, $\underline{C}OCF_3$), 143.4 (Mes), 142.5 (Mes), 142.4 (Mes), 142.2 (Mes), 138.9 (Mes), 132.2 (Mes), 129.7 (Mes), 129.4 (Mes), 129.3 (Mes), 129.0 (Mes), 127.4 (Mes), 127.2 (Mes), 117.9 (18-crown-6), 116.7 (q, $^1J_{C\text{-}F}$ = 477 Hz, CF_3), 90.7 (C_5H_3BC), 87.4 (C_5H_3BC), 77.0 (C_5H_3BC), 75.3 (C_5H_3BC), 70.4 (C_5H_5), 69.1 ($FcCH_2N$), 65.7 (C_5H_3BC), 55.9 (CH_3), 53.0 (CH_3), 49.8 (CH_2), 39.3 (CH_3), 38.3 (CH_2), 26.9 (CH_2), 25.6 (CH_3), 25.2 (CH_2), 24.5 (CH_2), 23.9 (CH_3), 22.3 (CH_2), 20.3 (CH_3). The resonance corresponding to the cyanide bound at boron was not observed.

^{19}F NMR (282 MHz, CD_3CN, 20 ºC): δ_F -76.3 (CF_3), -76.5 (CF_3).

MS(ESI$^-$) *m*/*z* (%): 795.3 (100) [**10**·CN]$^-$, 1591.6 (23) [(**10**·**CN)$_2$**]$^-$. Exact mass (calculated for $C_{40}H_{46}BF_6FeN_4O_2$, ^{10}B, ^{12}C, ^{14}N, ^{16}O, ^{19}F, ^{54}Fe isotopomer) 793.3027, (measured) 793.3023.

Crystallographic data: [K(18-crown-6)][**10**·CN], $C_{51}H_{67}BF_6FeKN_4O_9$, M_r = 1099.86, triclinic, *P -1*, *a* = 14.72430(10), *b* = 15.1354(2), *c* = 17.1534(2) Å, α = 95.1693(5), β = 111.5310(5), γ = 112.0650(5)º, *V* = 3178.26 Å^3, *Z* = 2, ρc = 1.149 Mg m^{-3}, *T* = 150 K, λ = 0.71073 Å. 14524 independent reflns [R(int) = 0.043935] used in all calcns. R_1 = 0.0647, wR_2 = 0.1792 for observed unique reflns [I>2σ(I)] and R_1 = 0.1148, wR_2 =0.2042 for all unique reflns. Max./min. residual electron densities 0.74 and -0.66 e Å^3.

1,1'-fc(BMes$_2$)(PPh$_2$) (11): A known compound synthesised by a novel route.[32] *n*-BuLi (0.61 mL of a 1.6 M solution in hexanes, 1.0 mmol, 1 equiv.) and

tetramethylethylenediamine (TMEDA) (0.15 mL, 1.0 mmol, 1 equiv.) were added dropwise to a solution of 1,1'-fc($BMes_2$)Br (0.500 g, 1.0 mmol) in diethyl ether (25 mL) at -78 ºC. The resulting reaction mixture was stirred for 1 h at-78 ºC. Diphenylchlorophosphine ($ClPPh_2$; 0.27 mL, 1.5 mmol, 1.5 equiv.) was added to this purple solution at -78 ºC and the resulting red suspension allowed to reattain room temperature overnight. Volatiles were removed *in vacuo* to yield a red tar, purification of which by column chromatography (flash with hexanes to elute a yellow band that was discarded, hexanes/diethyl ether 95:5 to elute a red band that was isolated), followed by removal of volatiles *in vacuo* yielded the crude product as a red powder, which was taken up in a minimal amount of hexane and cooled to -30 ºC. The resulting red crystals were isolated by filtration at -30 ºC and dried *in vacuo* to afford the desired target compound as a red solid. Yield 0.395 g, 66%. The NMR data were collected in a solvent differing from the literature, and are therefore presented below:[32]

^{1}H NMR (300 MHz, $CDCl_3$, 20 ºC): δ_H 7.26-7.33 (m, 10H, CH of Ph), 6.80 (s, 4H, *meta*-CH of Mes), 4.61 (t, 2H, $^{1}J_{H\text{-}H}$ = 1.9 Hz, C_5H_4B), 4.46 (t, 2H, $^{1}J_{H\text{-}H}$ = 1.7 Hz, C_5H_4P), 4.41 (t, 2H, $^{1}J_{H\text{-}H}$ = 1.9 Hz, C_5H_4B), 4.04 (m, 2H, C_5H_4P), 2.34 (s, 12H, *ortho*-CH_3 of Mes), 2.29 (s, 6H, *para*-CH_3 of Mes).

^{13}C NMR (125 MHz, $CDCl_3$, 20 ºC): δ_C 142.6 (*para*-CH of Ph), 137.0 (quaternary carbon of Mes), 133.4 (d, $^{2}J_{C\text{-}P}$ = 18.9 Hz, *ortho*-CH of Ph), 128.4 (d, $^{1}J_{C\text{-}P}$ = 46.6 Hz, *ipso*-C of Ph), 128.1 (*meta*-CH of Mes), 80.0 (CH of C_5H_4B), 77.3 (d, $^{1}J_{C\text{-}P}$ = 37.8 Hz, phosphorus-bound, quaternary carbon of C_5H_4P), 77.2 (boron-bound, quaternary carbon of C_5H_4B), 75.3 (CH of C_5H_4B), 73.9 (d, $^{2}J_{C\text{-}P}$ = 13.9 Hz, CH of C_5H_4P), 72.4 (d, $^{3}J_{C\text{-}P}$ = 3.8 Hz, CH of

C_5H_4P), 24.5 (*ortho*-CH_3 of Mes), 21.0 (*para*-CH_3 of Mes). The boron-bound, quaternary, *ipso* carbon of Mes could not be observed. Assignments were assisted by the use of gCOSY, HSQC and HMBC NMR.

^{11}B NMR (96 MHz, $CDCl_3$, 20 ºC): δ_B 81 (br. s).

^{31}P NMR (121 MHz, $CDCl_3$, 20 ºC): -17.6 (s).

[K(18-crown-6)][1,1'-fc(BMes$_2$·F)(PPh$_2$)], [K(18-crown-6)][11·F]: A solution of 1,1'-fc($BMes_2$)(PPh_2) (0.050 g, 80 μmol) in $CDCl_3$ (1.0 mL) was added to a mixture of KF (0.094 g, 1.60 mmol, 20 equiv.) and 18-crown-6 (0.021 g, 80 μmol) and the resulting reaction mixture stirred for 4 hours at room temperature. The reaction solution was isolated by filtration and NMR analysis indicated complete consumption of 1,1'-fc($BMes_2$)(PPh_2).

NOTE: this compound degrades with time, so the ^{13}C data is incomplete. The peaks listed for ^{13}C are of the target material, with those corresponding to the degradation compound omitted. These peaks could be identified by the change in their relative intensities over time.

^1H NMR (300 MHz, $CDCl_3$, 20 ºC): δ_H 7.23-7.35 (m, 10H, *ortho*-, *meta*- and *para*-CH of Ph), 6.52 (s, 4H, *meta*-CH of Mes), 4.10 (m, C_5H_4P), 3.88 (m, 2H, C_5H_4B), 3.76 (m, 2H, C_5H_4B), 3.62 (s, 24H, CH_2 of 18-crown-6), 2.19 (v br s, 18H, *ortho*-CH_3 and *para*-CH_3 of Mes).

^{13}C NMR (125 MHz, $CDCl_3$, 20 ºC): δ_C 141.4 (boron-bound, *ipso*-carbon of Mes), 138.9 (carbon-bound, quaternary of Mes), 138.6 (d, $^4J_{C\text{-}P}$ = 10.1 Hz, *para*-CH of Ph), 133.4 (d, $^2J_{C\text{-}P}$ = 18.9 Hz, *ortho*-CH of Ph), 129.8 (d, $^3J_{C\text{-}P}$ = 12.6 Hz, *meta*-CH of Ph), 128.6 (*meta*-bound CH of Mes), 128.1 (carbon-bound, quaternary carbon of Mes), 77.2 (CH of C_5H_4P), 73.8 (d, $J_{C\text{-}P}$ = 15.1 Hz, CH of C_5H_4P), 69.1 (CH of C_5H_4B), 68.6 (CH of C_5H_4B), 70.3 (CH_2 of 18-crown-6), 24.7 (*ortho*-CH_3 of Mes), 20.7 (*para*-CH_3 of Mes). The boron-bound, quaternary carbons of C_5H_4B and BCN as well as phosphorus-bound, quaternary carbons of C_5H_4P and Ph were not observed.

^{11}B NMR (96 MHz, $CDCl_3$, 20 ºC): δ_B 4 (br. s).

^{31}P NMR (121 MHz, $CDCl_3$, 20 ºC): δ_P -15.3 (s).

^{19}F NMR (282 MHz, $CDCl_3$, 20 ºC): δF -174 (m).

MS(ESI$^-$): 637.2 (100%) [1,1'-fc($BMes_2F$)(PPh_2)]$^-$, exact mass (calculated for ^{10}B, ^{57}Fe isotopomer) 637.2307; (measured) 637.2307.

[K(18-crown-6)][1,1'-fc($BMes_2$·CN)(PPh_2)], [K(18-crown-6)][11·CN]: A solution of 1,1'-fc($BMes_2$)(PPh_2) (0.050 g, 80 μmol) in $CDCl_3$ (1.0 mL) was added to a mixture of KCN (0.052 g, 810 μmol, 10 equiv.) and 18-crown-6 (0.021 g, 80 μmol, 1 equiv.), and the resulting suspension stirred for 19 h at room temperature. The yellow solution was isolated by filtration and NMR analysis indicated complete consumption of 1,1'-fc($BMes_2$)(PPh_2). Slow diffusion of pentane into a saturated $CHCl_3$ solution led to the formation of a yellow powder.

Yield 0.062 mg, 82%. Attempts to grow crystals suitable for X-ray diffraction studies from slow diffusion and evaporation failed.

^{1}H NMR (300 MHz, $CDCl_3$, 20 ºC): δ_H 7.21-7.34 (m, 10H, *ortho-, meta-* and *para*-CH of Ph), 6.51 (s, 4H, *meta*-CH of Mes), 4.29 (m, 2H, C_5H_4B), 4.1 (m, 2H, C_5H_4B), 3.85 (m, 4H, C_5H_4P), 3.57 (s, 24H, CH_2 of 18-crown-6), 2.13 (br. s, 12H, *ortho*-CH_3 of Mes), 2.11 (s, 6H, *para*-CH_3 of Mes).

^{13}C NMR (125 MHz, $CDCl_3$, 20 ºC): δ_C 141.5 (boron-bound, *ipso*-carbon of Mes), 140.3 (d, $^{3}J_{C\text{-}P}$ = 10.1 Hz, *meta*-CH of Ph), 133.5 (d, $^{2}J_{C\text{-}P}$ = 18.9 Hz, *ortho*-CH of Ph), 131.3 (carbon-bound, quaternary carbon of Mes), 131.3 (d, $^{4}J_{C\text{-}P}$ = 8.8 Hz, *para*-CH of Ph), 128.6 (*meta*-CH of Mes), 127.8 (carbon-bound, quaternary carbon of Mes), 76.8 (d $^{1}J_{C\text{-}P}$ = 107.1 Hz, phosphorus-bound, quaternary carbon of C_5H_4P), 76.4 (boron-bound, quaternary carbon of C_5H_4B), 72.4 (d, $J_{C\text{-}P}$ = 3.8 Hz, CH of C_5H_4P), 72.2 (CH of C_5H_4B), 72.1 (d, $J_{C\text{-}P}$ = 2.5 Hz, CH of C_5H_4P), 69.9 (CH_2 of 18-crown-6), 68.9 (CH of C_5H_4B), 25.1 (*ortho*-CH_3 of Mes), 20.6 (*para*-CH_3 of Mes). The phosphorus-bound, *ipso*-carbon of Ph was not observed.

^{11}B NMR (96 MHz, $CDCl_3$, 20 ºC): δ_B -16 (s).

^{31}P NMR (121 MHz, $CDCl_3$, 20 ºC): δ_P -15.2 (s).

MS (ESI$^-$): 644.2 (100%) $[fc(BMes_2CN)(PPh_2)]^-$, exact mass (calculated for ^{10}B, ^{57}Fe isotopomer) 644.2354; (measured) 644.2360.

[1,1'-fc(BMes$_2$)(PPh$_2$Me)]I (12): Methyl iodide (1.0 mL, 16 mmol, 20 equiv.) was added to a solution of 1,1'-fc(BMes$_2$)(PPh$_2$) (0.500 g, 0.81 mmol) in diethyl ether (25 mL) and the resulting reaction mixture stirred for 15 h at room temperature. The resulting red precipitate isolated by filtration, washed with hexane (3 x 50 mL) and diethyl ether (3 x 50 mL), and dried *in vacuo* to afford the target material as a red powder. Yield 0.455 g, 74 %.

^{1}H NMR (300 MHz, $CDCl_3$. 20 ºC): δ_H 7.54-7.73 (m, 10 H, CH of Ph), 6.84 (s, 4H, *meta*-CH of Mes), 4.85 (m, 2H, C_5H_4P), 4.68 (m, 2H, C_5H_4P), 4.62 (t, 2H, $^1J_{H-H}$ = 1.7 Hz, C_5H_4B), 4.37 (t, 2H, $^1J_{H-H}$ = 1.7 Hz, C_5H_4B), 2.43 (d, 3H, $^2J_{H-P}$ = 13.5 Hz, CH_3 of PPh_2Me^+),2.30 (s, 6H, *para*-CH_3 of Mes), 2.28 (s, 12H, *ortho*-CH_3 of Mes).

^{13}C NMR (125 MHz, $CDCl_3$, 20 ºC): δ_C 141.7 (boron-bound, *ipso*, quaternary carbon of Mes), 138.7 (carbon-bound, quaternary carbon of Mes), 138.0 (carbon-bound, quaternary carbon of Mes), 134.8 (d, $^4J_{C-P}$ = 2.1 Hz, *para*-CH of Ph), 132.5 (d, $^3J_{C-P}$ = 10.7 Hz, *meta* CH of Ph), 130.2 (d, $^2J_{C-P}$ = 12.9 Hz, *ortho*-CH of Ph), 128.5 (*meta*-CH of Mes), 120.9 (d, $^1J_{C-P}$ = 90.7 Hz, phosphorus-bound, *ipso*, quaternary carbon of Ph), 81.1 (CH of C_5H_4B), 78.8 (boron-bound, quaternary carbon of C_5H_4B), 76.4 (d, $^3J_{C-P}$ = 10.5 Hz, CH of C_5H_4P), 75.8 (CH of C_5H_4B), 73.4 (d, $^2J_{C-P}$ = 12.6 Hz, CH of C_5H_4P), 60.7 (d, $^1J_{C-P}$ = 103.8 Hz, phosphorus-bound, quaternary carbon of C_5H_4P), 24.5 (*para*-CH_3 of Mes), 21.0 (*ortho*-CH_3 of Mes), 9.6 (d, $^1J_{C-P}$ = 59.6 Hz, CH_3 of PPh_2Me^+).

^{11}B NMR (96 MHz, $CDCl_3$, 20 ºC): δ_B 80 (br. s).

^{31}P NMR (121 MHz, $CDCl_3$, 20 ºC): δ_P 22.4 (s).

MS (ESI$^+$) 265.1 (75%) $[C_5H_4(PPh_2Me)]^+$, 385.1 (100 %) $[Fc(PPh_2Me)]^+$, 634.8 (90 %) $[1,1'fc(BMes_2)(PPh_2Me)]^+$, exact mass (calculated for M^+, ^{10}B, ^{57}Fe isotopomer) 633.2547, (measured) 633.2549.

Crystallographic data: M_r = 999.08, triclinic, P -1, a = 9.9034(2) Å, b = 21.2853(7) Å, c = 22.6799(7) Å, α = 70.211(3)º, β = 86.756(2)º, γ = 82.600(2)º, V = 4460.6(2) Å^3, Z = 4, ρ_c = 1.488 Mg m^{-3}, T = 150 K, λ = 1.54180 Å, 45364 reflections collected, 18514 independent [R(int) = 0.050]. R = 0.059, wR^2 = 0.175 for observed unique reflections [$F^2>2\sigma(F^2)$]. Max. and min. residual electron densities 3.52 and -2.83 e Å^3.

UV-vis (dichloromethane): λ_{max} = 496 nm, ε = 950 mol^{-1} cm^{-1} dm^3.

1,1'-fc(BMes$_2$·F)(PPh$_2$Me) (12·F) (obtained as a 50:50 mixture with [K(18-crown-6)]I): A solution of [1,1'-fc(BMes$_2$)(PPh$_2$Me)]I (0.020 g, 27 μmol) in $CDCl_3$ (1.0 mL) was added to a mixture of KF (0.016 g, 270 μmol, 10 equiv.) and 18-crown-6 (0.007 g, 27 μmol, 1 equiv.) and the reaction mixture stirred for 4 h at room temperature. The resulting yellow solution was isolated from the colourless insolute by filtration, and NMR analysis showed complete consumption of [1,2-fc(BMes$_2$)(PPh$_2$Me)]I. Attempts to separate the two salts were unsuccessful.

^{1}H NMR (300 MHz, $CDCl_3$, 20 ºC): δ_H 7.44-7.73 (m, 10H, *ortho*-, *meta*- and *para*-CH of Ph), 6.59 (s, 4H, *meta*-CH of Mes), 4.61 (m, 4H, C_5H_4P), 4.27 (m, 4H, C_5H_4B), 3.67 (s, 24H, CH_2 of 18-crown-6), 2.20 (v br. s, 21H, *ortho*-CH_3 and *para*-CH_3 of Mes and CH_3 of PPh_2Me^+).

^{13}C NMR (125 MHz, $CDCl_3$, 20 ºC): δ_C 141.4 (boron-bound, *ipso*-carbon of Mes), 134.3 (carbon-bound, quaternary carbon of Mes), 132.6 (carbon-bound, quaternary carbon of Mes), 129.8 (d, $^{4}J_{C\text{-}P}$ = 8.8 Hz, *para*-CH of Ph), 128.7 (*meta*-CH of Mes), 128.1 (d, $^{1}J_{C\text{-}P}$ = 52.9 Hz, *ipso*-carbon of Ph), 76.3 (d, $J_{C\text{-}P}$ = 5.0 Hz, CH of C_5H_4P), 74.6 (d, $J_{C\text{-}P}$ = 12.6 Hz, CH of C_5H_4P), 72.2 (CH of C_5H_4B), 70.3 (CH_2 of 18-crown-6), 69.7 (CH of C_5H_4B), 24.7 (*ortho*-CH_3 of Mes), 20.7 (*para*-CH_3 of Mes), 12.6 (d, $^{1}J_{C\text{-}P}$ = 40.8 Hz, CH_3 of PPh_2Me^+). The boron- and phosphorus-bound, quaternary carbons of C_5H_4B and C_5H_4P, respectively, were not observed.

^{11}B NMR (96 MHz, $CDCl_3$, 20 ºC): δ_B 4 (br s, actually broadened doublet).

^{31}P NMR (121 MHz, $CDCl_3$, 20 ºC): δ_P 23.3 (s).

^{19}F NMR (282 MHz, $CDCl_3$, 20 ºC): δ_F -175 (m).

MS (ESI^-): 127.0 (100%) I^-, 779.2 (30%) [1,1'-fc$(BMes_2F)^-$(PPh_2Me)I], exact mass (calculated for ^{10}B, ^{57}Fe isotopomer) 779.1587; (measured) 779.1609.

1,1'-fc($BMes_2$·CN)(PPh_2Me) (12·CN) (obtained as a 50:50 mixture with [K(18-crown-6)]I): A solution of [1,1'-fc($BMes_2$)(PPh_2Me)]I (0.040 g, 53 μmol) in $CDCl_3$ (2.0 mL) was added to a mixture of KCN (0.034 g, 530 μmol, 10 equiv.) and 18-crown-6 (0.014 g, 53 μmol, 1 equiv.), and the resulting reaction mixture stirred for 4 h at room temperature. The sample was filtered and NMR analysis indicated the complete consumption of [1,1'-fc($BMes_2$)(PPh_2Me)]I. Separation of the target material from [K(18-crown-6)]I could not be achieved.

^{1}H NMR (300 MHz, $CDCl_3$, 20 ºC): δ_H 7.44-7.74 (m, 10H, Ph), 6.59 (br. s, 4H, *meta*-CH of Mes), 4.76 (m, 4H, C_5H_4B), 4.30 (m, 4H, C_5H_4P), 3.65 (s, 24H, CH_2 of 18-crown-6), 2.13 (v br. s, 21H, *ortho*-CH_3 of Mes, *para*-CH_3 of Mes and CH_3 of PPh_2Me^+).

^{13}C NMR (125 MHz, $CDCl_3$, 20 ºC): δ_C 141.6 (carbon-bound, *ipso*-carbon of Mes), 134.4 (d, $^4J_{C\text{-}P}$ = 2.9 Hz, *para*-CH of Ph), 132.1 (carbon-bound, quaternary carbon of Mes), 131.8 (d, $^3J_{C\text{-}P}$ = 10.6 Hz, *meta*-CH of Ph), 129.9 (d, $^2J_{C\text{-}P}$ = 12.6 Hz, *ortho*-CH of Ph), 129.1 (*meta*-CH of Mes), 122.7 (d $^1J_{C\text{-}P}$ = 90.0 Hz, *ipso*-carbon of Ph), 77.9 (CH of C_5H_4B), 75.2 (d, $^3J_{C\text{-}P}$ = 11.3 Hz, CH pf C_5H_4P), 72.5 (d, $^2J_{C\text{-}P}$ = 14.0 Hz, CH of C_5H_4P), 70.4 (CH of C_5H_4B), 70.0 (CH_2 of 18-crown-6), 55.5 (d, $^1J_{C\text{-}P}$ = 59.6 Hz, phosphorus-bound, quaternary carbon of C_5H_4P), 25.4 (*ortho*-CH_3 of Mes), 20.7 (*para*-CH_3 of Mes), 8.2 (d, $^1J_{C\text{-}P}$ = 62.1 Hz, CH_3 of PPh_2Me^+). The boron-bound, quaternary carbons of C_5H_4B, CN and Mes could not be observed.

^{11}B NMR (96 MHz, $CDCl_3$, 20 ºC): δ_B -17 (s).

^{31}P NMR (121 MHz, $CDCl_3$, 20 ºC): δ_P 23.5 (s).

MS (ESI^+): 682.2 (20%) [1,1'-fc($BMes_2CN$)(PPh_2Me)Na^+], exact mass (calculated for ^{10}B, ^{23}Na, ^{57}Fe isotopomer) 682.2476; (measured) 682.2463.

***rac*-1,2-fc($BMes_2$)(PPh_2) (13):** *n*-BuLi (1.22 mL of a 1.6 M solution in hexanes, 2.0 mmol, 1 equiv.) and tetramethylethylenediamine (TMEDA) (0.29 mL, 2.0 mmol, 1 equiv.) was added dropwise to a solution of 1,2-fc($BMes_2$)Br (1.00 g, 2.0 mmol) in diethyl ether (50 mL) at -78 ºC. The resulting reaction mixture was stirred for 1 hour at -78 ºC. Diphenylchlorophosphine ($ClPPh_2$) (0.29 mL, 0.360 g, 2.0 mmol, 1 equiv.) was added to the purple solution at -78 ºC and the resulting suspension allowed to reattain room temperature overnight. The volatiles were removed *in vacuo* from the red suspension to give a sticky, red solid. Purification of which by column chromatography (flash with hexanes to elute a yellow band that was discarded, followed by hexanes/ethyl acetate 97:3 to elute a red band that was collected, with volatiles subsequently removed *in vacuo*) yielded the crude product as a red powder, which was then taken up in a minimal amount of hexanes, cooled to -30 ºC and the red crystals that formed isolated by filtration at -30 ºC and dried *in vacuo*. Yield 0.850 g, 70 %.

^{1}H NMR (300 MHz, $CDCl_3$, 20 ºC): δ_H 6.80-7.42 (m, 10 H, Ph), 6.62 (s, 4H, *meta*-CH of Mes), 4.69 (m, 1H, C_5H_3BP), 4.66 (m, 1H, C_5H_3BP), 4.20 (s, 5H, C_5H_5), 4.11 (m, 1H, C_5H_3BP), 2.24 (s, 6H, *para*-CH_3 of Mes), 2.18 (br. s, 12H, *ortho*-CH_3 of Mes).

^{13}C NMR (125 MHz, $CDCl_3$, 20 ºC): δ 142.9 (boron-bound, quaternary carbon of Mes), 139.5 (carbon-bound, quaternary carbon of Mes), 139.1 (d, $^{1}J_{C\text{-}P}$ = 73.1, phosphorus-bound, *ipso*-carbon of Ph), 138.8 (d, $^{1}J_{C\text{-}P}$ = 70.6 Hz, phosphorus-bound, *ipso*-carbon of Ph), 136.9 (carbon-bound, quaternary carbon of Mes), 134.1 (d, $^{3}J_{C\text{-}P}$ = 20.2 Hz, *ortho*-CH of Ph), 133.2 (d, $^{2}J_{C\text{-}P}$ = 21.4 Hz, *ortho*-CH of Ph), 128.2 (d, $^{3}J_{C\text{-}P}$ = 5.0 Hz, *meta*-CH of Ph), 127.9 (d, $^{3}J_{C\text{-}P}$ = 6.3 Hz, *meta*-CH of Ph), 127.8 (*meta*-CH of Mes), 127.5 (*para*-CH of Ph), 127.4 (*para*-CH of Ph), 88.1 (d $^{2}J_{C\text{-}P}$ = 17.6 Hz, boron-bound, quaternary carbon of C_5H_3BP), 83.2 (d, $^{2}J_{C\text{-}P}$ = 5.0 Hz, CH of C_5H_3BP), 78.5 (d, $^{3}J_{C\text{-}P}$ = 3.8 Hz, CH of C_5H_3BP), 72.7 (CH of C_5H_3BP), 70.6 (d, $^{1}J_{C\text{-}P}$ = 98.3 Hz, phosphorus-bound, quaternary carbon of C_5H_3BP), 70.5 (CH of C_5H_5), 24.4 (*ortho*-CH_3 of Mes), 21.0 (*para*-CH_3 of Mes). Signal assignment assisted by gCOSY, HMBC and HSQC.

^{11}B NMR (96 MHz, $CDCl_3$, 20 ºC): δ_B 81 (br. s).

^{31}P NMR (121 MHz, $CDCl_3$, 20 ºC): δ_P -20.6 (s).

***rac*-[1,2-fc(BMes$_2$)(PPh$_2$Me)]I (14)**: Methyl iodide (1.0 mL, 16 mmol, 20 equiv.) was added to a solution of 1,2-fc(BMes$_2$)(PPh$_2$) (0.500 g, 0.8 mmol) in diethyl ether (25 mL) and the resulting reaction mixture stirred for 48 h at room temperature. The resulting orange-red precipitate was isolated by filtration, washed with hexane (3 x 50 mL) and diethyl ether (3 x 50 mL), then dried *in vacuo* to yield the desired product as an orange-red powder (0.400 g, 67 %).

^{1}H NMR (300 MHz, CD_2Cl_2, 20 ºC): δ_H 7.39-7.90 (m, 10H, Ph), 6.77 (br s, *meta*-CH of Mes), 5.14 (m , 1H, C_5H_3BP), 4.95 (m, 1H, C_5H_3BP), 4.89 (m, 1H, C_5H_3BP), 4.24 (s, 5H, C_5H_5), 2.55 (d, 3H, $^{2}J_{C\text{-}P}$ = 12.0 Hz, CH_3 of PPh_2Me^{+}), 2.17 (v br. s, 18H, *ortho*-CH_3 and *para*-CH_3 of Mes).

^{13}C NMR (96 MHz, CD_2Cl_2, 20 ºC): δ_C 135.1 (carbon-bound, quaternary carbon of Mes, 135.0 (carbon-bound, quaternary carbon of Mes), 134.7 (d, $^{4}J_{C\text{-}P}$ = 2.9 Hz, *para*-CH of Ph), 134.2 (d, $^{4}J_{C\text{-}P}$ = 3.8 Hz, *para*-CH of Ph), 134.0 (carbon-bound, quaternary carbon of Mes), 133.8 (d, $^{3}J_{C\text{-}P}$ = 12.5 Hz, *meta*-CH of Ph), 132.9 (d, $^{3}J_{C\text{-}P}$ = 11.5 Hz, *meta*-CH of Ph), 132.1 (carbon-bound, quaternary carbon of Mes), 131.0 (d, $^{2}J_{C\text{-}P}$ = 15.4 Hz, *ortho*-CH of Ph), 130.8 (carbon-bound, quaternary carbon of Mes), 130.2 (d, $^{2}J_{C\text{-}P}$ = 14.4 Hz, *ortho*-CH of Ph), 128.7 (*meta*-CH of Mes), 128.3 (*meta*-CH of Mes), 128.3 (*meta*-CH of Mes), 128.2 (*meta*-CH of Mes), 127.5 (d, $^{1}J_{C\text{-}P}$ = 39.2 Hz, *ipso*- carbon of Ph), 88.4 (d, $J_{C\text{-}P}$ = 15.9 Hz, CH of C_5H_3BP), 81.4 (d, $J_{C\text{-}P}$ = 18.8 Hz, CH of C_5H_3BP), 76.7 (d, $J_{C\text{-}P}$ = 13.8 Hz, CH of $_5H_3BP$), 74.4 (CH of C_5H_5), 25.7 (*ortho*-CH_3 of Mes), 20.9 (*para*-CH_3 of Mes), 13.6 (d, $^{1}J_{C\text{-}P}$ = 77.3 Hz, CH_3 of PPh_2Me^{+}). The boron- and phosphorus-bound, quaternary carbons of C_5H_3BP were not observed. One phosphorus-bound, *ipso*-carbon of Ph and the boron-bound, *ipso*-carbon of Mes were also not observed. Assignments assisted by gCOSY, HSQC and HMBC NMR.

^{11}B NMR (96 MHz, CD_2Cl_2, 20 ºC): δ 83 (br. s).

^{31}P NMR (121 MHz, CD_2Cl_2, 20 ºC): δ_P 20.8 (s).

MS (ESI^+) 632.2 (100%) $[1,2\text{-fc}(BMes_2)(PPh_2Me)]^+$, exact mass (calculated for M^+, ^{10}B, ^{57}Fe isotopomer) 633.2547; (measured) 633.2541.

UV-Vis (dichloromethane): λ_{max} = 455 nm, ε = 880 mol^{-1} cm^{-1} dm^3.

***rac*-1,2-fc($BMes_2$·F)(PPh_2Me) (14·F) (obtained as a 50:50 mixture with [K(18-crown-6)]I):** A solution of [1,2-fc($BMes_2$)(PPh_2Me)]I (0.150 g, 0.20 mmol) in $CDCl_3$ (4 mL) was added to a mixture of KF (0.114 g, 2.0 mmol, 10 equiv.) and 18-crown-6 (0.052 g, 0.2 mmol, 1 equiv) and the reaction mixture stirred for 4 hours. The resulting yellow solution was isolated from the colourless insolute by filtration and NMR analysis showed complete consumption of [1,2-fc($BMes_2$)(PPh_2Me)]I. Attempts to separate the two salts were unsuccessful.

^1H NMR (300 MHz, $CDCl_3$, 20 ºC): δ_H 7.18-7.96 (m, 10H, Ph), 6.70 (s, 1H, CH of Mes), 6.63 (s, 1H, CH_3 of Mes), 6.49 (s, 1H, *meta*-CH of Mes), 6.32 (s, 1H, *meta*-CH of Mes), 4.74 (m, 1H, C_5H_3BP), 4.43 (m, 1H, C_5H_3BP), 3.93 (m, 1H, C_5H_3BP), 3.84 (s, 5H, C_5H_5), 3.66 (s, 24H, CH_2 of 18-crown-6), 2.74 (br. s, 3H, *ortho*-CH_3 of Mes), 2.68 (d, 3H, $^2J_{H\text{-}P}$ = 8.4 Hz, CH_3 of PPh_2Me^+),2.21 (s, 3H, *para*-CH_3 of Mes), 2.13 (s, 3H, *ortho*-CH_3 of Mes), 2.10 (s, 3H, *para*-CH_3 of Mes), 2.00 (s, 3H, *ortho*-CH_3 of Mes), 1.66 (s, 3H, *ortho*-CH_3 of Mes).

^{13}C NMR (125 MHz, $CDCl_3$, 20 ºC): δ_C 143.4 (boron-bound, *ipso*-carbon of Mes), 141.8 (carbon-bound, quaternary carbon of Mes), 139.3 (carbon-bound, quaternary carbon of

Mes), 139.0 (carbon-bound, quaternary carbon of Mes), 134.8 (d, $^{4}J_{C\text{-}P}$ = 3.0 Hz, *para*-CH of Ph), 133.1 (d, $^{4}J_{C\text{-}P}$ = 4.5 Hz, *para*-CH of Ph), 133.0 (carbon-bound, quaternary carbon of Mes), 132.7 (d, $^{3}J_{C\text{-}P}$ = 10.0 Hz, *meta*-CH of Ph), 132.5 (carbon-bound, quaternary carbon of Mes), 131.9 (carbon-bound, quaternary carbon of Mes), 131.8 (carbon-bound, quaternary carbon of Mes), 130.3 (d, $^{3}J_{C\text{-}P}$ = 12.5 Hz, *meta*-CH of Ph), 128.9 (m, *ortho*-CH of Ph), 128.7 (*meta*-CH of Mes), 128.6 (*meta*-CH of Mes), 128.5 (*meta*-CH of Mes), 128.4 (*meta*-CH of Mes), 128.3 (br. m, *ortho*-CH of Ph), 126.1 (d, $^{1}J_{C\text{-}P}$ = 89.6 Hz, *ipso*-carbon of Ph), 124.2 (d, $^{1}J_{C\text{-}P}$ = 88.2 Hz, *ipso*-carbon of Ph), 80.4 (dd, J_1 = 15.1 Hz, J_2 = 11.5 Hz, CH of C_5H_3BP), 75.1 (d, $^{3}J_{C\text{-}P}$ = 19.7 Hz, CH of C_5H_3BP), 72.3 (d, $^{2}J_{C\text{-}P}$ = 12.3 Hz, CH of C_5H_3BP), 70.2 (CH of C_5H_5), 70.0 (CH_2 of 18-crown-6), 62.1 (d, $^{1}J_{C\text{-}P}$ = 102.7 Hz, phosphorus-bound, quaternary carbon of C_5H_3BP), 26.4 (*ortho*-CH_3 of Mes), 25.3 (d, $J_{C\text{-}F}$ = 14 Hz, *ortho*-CH_3 of Mes), 24.3 (*ortho*-CH_3 of Mes), 23.6 (*ortho*-CH_3 of Mes), 20.8 (*para*-CH_3 of Mes), 20.7 (*para*-CH_3 of Mes), 15.9 (dd, $^{1}J_{C\text{-}P}$ = 64.0 Hz, $^{2}J_{C\text{-}F}$ = 20.0 Hz, CH_3 of PPh_2Me^+). The boron-bound, carbon of C_5H_3BP and one of the Mes substituents were not observed.

^{11}B NMR (96 MHz, $CDCl_3$, 20 ºC): δ_B 5 (br s).

^{19}F NMR (282 MHz, $CDCl_3$, 20 ºC): δ_F -158 (br m).

^{31}P NMR (121 MHz, $CDCl_3$, 20 ºC): δ_P 28.6 (d, $^{1}J_{P\text{-}F}$ = 8.6 Hz).

MS(ESI$^-$): 126.9 (90%) [I$^-$], 786.2 (100%) [1,2-fc($BMes_2F$)(PPh_2Me)I], exact mass (calculated for ^{11}B isotopomer + I$^-$) 779.1587, (measured) 779.1606.

***rac*-1,2-fc(BMes$_2$·CN)(PPh$_2$Me) (14·CN) (obtained as a 50:50 mixture with [K(18-crown-6)]I)**: A solution of [1,2-fc(BMes$_2$)(PPh$_2$Me)]I (0.150 g, 0.2 mmol) in $CDCl_3$ (4 mL) was added to a mixture of KCN (0.128 g, 2.0 mmol, 10 equiv.) and 18-crown-6 (0.052 g, 0.2 mmol, 1 equiv.) and the reaction mixture stirred for 4 h at room temperature. The resulting yellow solution was isolated from the colourless insolute by filtration and NMR analysis showed complete consumption of [1,2-fc(BMes$_2$)(PPh$_2$Me)]I. Attempts to separate the two salts were unsuccessful.

^{1}H NMR (300 MHz, $CDCl_3$, 20 ºC): δ_H 7.40-8.00 (m, 10H, *ortho*-, *meta*- and *para*-CH of Ph), 6.77 (s, 1H, *meta*-H of Mes), 6.58 (s, 2H, *meta*-CH of Mes), 6.23 (s, 1H, *meta*-CH of Mes), 4.62 (m, 1H, C_5H_3BP), 4.58 (m, 1H,C_5H_3BP), 4.32 (m, 1H, C_5H_3BP), 3.67 (s, 5H, C_5H_4), 3.61 (s, 24H, CH_2 of 18-crown-6), 3.11 (s, 3H, *ortho*-CH_3 of Mes), 2.64 (d, 3H, $^2J_{H\text{-}P}$ =13.8 Hz, CH_3 of PPh_2Me^+), 2.35 (s, 3H, *ortho*-CH_3 of Mes), 2.18 (s, 3H, *para*-CH_3 of Mes), 2.01 (s, 3H, *para*-CH_3 of Mes), 1.82 (s, 3H, *ortho*-CH_3 of Mes), 1.71 (s, 3H, *ortho*-CH_3 of Mes).

^{13}C NMR (125 MHz, $CDCl_3$, 20 ºC): δ_C 143.6 (carbon-bound, quaternary carbon of Mes), 142.5 (carbon-bound, quaternary-carbon of Mes), 142.4 (carbon-bound, quaternary carbon of Mes), 140.3 (carbon-bound, quaternary carbon of Mes), 134.7 (d, $^4J_{C\text{-}P}$ = 3.0 Hz, *para*-CH of Ph), 133.5 (d, $^3J_{C\text{-}P}$ = 9.6 Hz, *meta*-CH of Ph), 133.2 (d, $^4J_{C\text{-}P}$ = 2.9 Hz, *para*-CH of Ph), 133.0 (carbon-bound, quaternary carbon of Mes), 132.9 (carbon-bound, quaternary carbon of Mes), 132.8 (d, $^3J_{C\text{-}P}$ = 6.9 Hz, *meta*-CH of Ph), 132.4 (d, $^3J_{C\text{-}P}$ = 10.1 Hz, *meta*-CH of Ph), 130.2 (d, $^2J_{C\text{-}P}$ = 12.5 Hz, *ortho*-CH of Ph), 129.8 (d, $^2J_{C\text{-}P}$ =11.5 Hz, *ortho*-CH of Ph),

129.4 (*meta*-CH of Mes), 129.2 (*meta*-CH of Mes), 129.1 (*meta*-CH of Mes), 129.0 (d, $^{1}J_{C\text{-}P}$ = 90.6 Hz, *ipso*-carbon of Ph), 128.8 (d, $^{2}J_{C\text{-}P}$ = 12.0 Hz, *ortho*-CH of Ph), 126.3 (d, $^{1}J_{C\text{-}P}$ = 87.1 Hz, *ipso*-carbon of Ph), 128.4 (*meta*-CH of Mes), 82.4 (d, $J_{C\text{-}P}$ = 15.2 Hz, CH of C_5H_3BP), 75.1 (d, $J_{C\text{-}P}$ = 16.5 Hz, CH of C_5H_3BP), 72.4 (d, $J_{C\text{-}P}$ = 11.8 Hz, CH of C_5H_3BP), 71.4 (boron-bound, quaternary carbon of C_5H_3BP), 70.9 (CH of C_5H_5), 70.0 (CH_2 of 18-crown-6), 62.3 (d, $^{1}J_{C\text{-}P}$ = 96.3 Hz, phosphorus-bound, quaternary carbon of C_5H_3BP), 27.1 (*ortho*-CH_3 of Mes), 25.6 (*ortho*-CH_3 of Mes), 24.8 (*ortho*-CH_3 of Mes), 24.2 (*ortho*-CH_3 of Mes), 20.7 (*para*-CH_3 of Mes), 20.5 (*para*-CH_3 of Mes), 14.2 (d, $^{1}J_{C\text{-}P}$ = 56.2 Hz, CH_3 of PPh_2Me^{+}). One *ortho*-CH of Ph, one *meta*-CH of Ph, and both boron-bound *ipso*-carbons of Mes were not observed.

^{11}B NMR (96 MHz, $CDCl_3$, 20 ºC): δ_B -16 (s).

^{31}P NMR (121 Mhz, $CDCl_3$, 20 ºC): δ_P 31.4 (s).

MS (ESI$^-$): 126.9 (90%) [I$^-$], 786.2 (100%) [1,2-fc($BMes_2CN$)$^-$(PPh_2Me)I], exact mass (calculated for ^{10}B, ^{57}Fe isotopomer) 786.1634; (measured) 786.1645.

***rac*-1,2-fc($BMes_2$)($SiMe_2Cl$) (15):** *t*-BuLi (1.72 ml of a 1.9 M solution in pentane, 3.27 mmol, 2 equiv.) was added dropwise to a solution of *rac*-1,2-fc($BMes_2$)Br (0.842 g, 1.64 mmol) in diethyl ether (100 ml) at -78 ºC. The resulting solution was stirred at -78 ºC for 30 minutes. Me_2SiCl_2 (2 ml, 16.6 mmol, 1 equiv.) was then added to the purple reaction solution at -78 ºC. The reaction mixture was allowed to re-attain room temperature overnight.

Volatiles were removed *in vacuo* and the residue extracted with pentane (3 x 20 ml). Volatiles were removed *in vacuo* from the combined extracts to afford the target material as an orange solid. Yield: 0.795 g, 91%.

^{1}H NMR (500 MHz, $CDCl_3$, 20 ºC): δ_H 6.74 (s, 4H, CH of Mes), 4.83 (m, 1H, C_5H_3BSi), 4.73 (m, 1H, C_5H_3BSi), 4.58 (m, 1H, C_5H_3BSi), 4.22 (s, 5H, C_5H_5), 2.26 (s, 6H, *para*-CH_3 of Mes), 2.12 (br. s, 12 H, *ortho*-CH_3 of Mes), 0.36 (s, 3H, CH_3 of $SiMe_2Cl$), 0.21 (s, 3H, CH_3 of $SiMe_2Cl$).

^{13}C NMR (125 MHz, $CDCl_3$, 20 ºC): δ_C 142.7 (*ipso*-carbon of Mes), 139.7 (*ortho*-carbon of Mes), 138.0 (*para*-carbon of Mes), 128.2 (*meta*-CH of Mes), 94.1 (boron-bound, quaternary carbon of C_5H_3BSi), 87.2 (CH of C_5H_3BSi), 80.8 (CH of C_5H_3BSi), 73.1 (CH of C_5H_3BSi), 71.7 (silicon-bound, quaternary carbon of C_5H_3BSi), 70.7 (Cp), 23.6 (*para*-CH_3 of Mes), 21.1 (*ortho*-CH_3 of Mes), 4.0 (CH_3 of $SiMe_2Cl$), 3.6 (CH_3 of $SiMe_2Cl$). Assignments assisted by gCOSY, HSQC, HMBC NMR (500 MHz (^{1}H) /125 MHz (^{13}C), $CDCl_3$, 20 ºC).

^{11}B NMR (96 MHz, $CDCl_3$, 20 ºC): δ_B 82 (br. s).

^{29}Si NMR (60 MHz, $CDCl_3$, 20 ºC): δ_{Si} 24.5 (s).

MS (EI^{+}) 526.2 (100%) M^{+}; exact mass (calc. for M^{+}, ^{10}B, ^{35}Cl, ^{28}Si isotopomer) 523.1795; (meas) 523.1794. Isotopic profile consistent with assignment. Elemental microanalysis: (calc. for $C_{30}H_{36}BClFeSi$) C 68.40, H 6.89; (meas.) C 68.42, 68.31, H 6.84, 6.77.

***rac*-1,2-fc(BMes$_2$)(SiMe$_2$F) (16):** A solution of *rac*-1,2-fc(BMes$_2$)(SiMe$_2$Cl) (0.500 g, 1 mmol) in dichloromethane (10 mL) was added to CuF_2 (0.200 g, 1 mmol, 1 equiv.) and the reaction mixture stirred at room temperature for 3 h. Volatiles were then removed *in vacuo*, the solid residue extracted with hexane (3 x 20 mL) and volatiles removed *in vacuo* from the combined extracts to afford the target material as a red tar. Yield 0.450 g, 93 %, [98 % pure with 2 % *rac*-1,2-fc(BMes$_2$)(SiMe$_2$Cl)].

^{1}H NMR (500 MHz, $CDCl_3$, 20 ºC): δ_H 6.76 (s, 4H, C-H of Mes), 4.78 (m ,1H, C_5H_3BSi), 4.77 (m, 1H, C_5H_3BSi), 4.61 (m, 1H, C_5H_3BSi), 4.21 (s, 5H, C_5H_5), 2.28 (s, 6H, *para*-CH_3 of Mes), 2.15 (s, 12 H, *ortho*-CH_3 of Mes), 0.15 (d, $^3J_{F\text{-}H}$ = 7.5 Hz, 3H, CH_3 of SiMe$_2$F), 0.11 (d, $^3J_{F\text{-}H}$ = 7.5 Hz, 3H, CH_3 of SiMe$_2$F).

^{13}C NMR (125 MHz, $CDCl_3$, 20 ºC): δ_C 142.8 (boron-bound, *ipso*-carbon of Mes), 139.6 (*ortho*-carbon of Mes), 137.7 (*para*-carbon of Mes), 128.0 (*meta*-CH of Mes), 92.2 (boron-bound, quaternary carbon of C_5H_3BSi), 86.8 (CH of C_5H_3BSi), 80.0 (CH of C_5H_3BSi), 73.6 (CH of C_5H_3BSi), 70.4 (C_5H_5), 69.4 (silicon-bound, quaternary carbon of C_5H_4BSi), 23.7 (*ortho*-CH_3 of Mes), 21.0 (*para*-CH_3 of Mes), 0.2 (d, $^2J_{C\text{-}F}$ = 16 Hz, CH_3 of SiMe$_2$F), -0.1 (d, $^2J_{C\text{-}F}$ = 16 Hz, CH_3 of SiMe$_2$F).

^{11}B NMR (96 MHz, $CDCl_3$, 20 ºC): δ_B 83 (s).

^{19}F NMR (282 MHz, $CDCl_3$, 20 ºC): δ_F -152.0 (triplet of septets, $^1J_{F\text{-}Si}$ = 275 Hz, $^3J_{H\text{-}F}$ = 7.0 Hz).

^{29}Si (60 MHz, $CDCl_3$, 20 ºC): δ_{Si} 23.4 (d, $^1J_{F\text{-}Si}$ = 275 Hz).

[K(18-crown-6)][*rac*-1,2-fc($BMes_2$)($SiMe_2F$)·F], [K(18-crown-6)][16·F]: A solution of *rac*-1,2-fc($BMes_2$)($SiMe_2F$) (0.290 g, 0.57 mmol) in toluene (10 mL) was added to a mixture of KF (0.033 g, 0.57 mmol, 1 equiv.) and 18-crown-6 (0.150 g, 0.57 mmol, 1 equiv.) and the reaction mixture stirred for 5 h. The solvent was then removed *in vacuo*, the residue washed with hexane (10 mL), then toluene (10 mL) and dried *in vacuo* to give an orange solid. Yield 0.250 g, 53 %. Attempts to grow crystals suitable for X-ray diffraction studied by slow diffusion and slow evaporation failed.

^{1}H NMR (500 MHz, CD_3CN, 20 ºC): δ_H 6.63 (br.s, 1H, CH of Mes), 6.49 (br.s, 1H, CH of Mes), 6.42 (br.s, 1H, CH of Mes), 6.27 (br.s, 1H, CH of Mes), 4.22 (m, 1H, C_5H_3BSi), 4.18 (m, 1H, C_5H_3BSi), 3.99 (m, 1H, C_5H_3BSi), 3.81 (s, 5H, C_5H_5), 3.57 (s, 24H, CH_2 of 18-crown-6), 2.81 (s, 3H, *ortho*-CH_3 of Mes), 2.19 (s, 3H, *para*-CH_3 of Mes), 2.05 (m, 6H, *ortho*-CH_3 and *para*-CH_3 of Mes), 1.79 (s, 3H, *ortho*-CH_3 of Mes), 1.55 (s, 3H, *ortho*-CH_3 of Mes), 0.50 (dd, $^3J_{F\text{-}H}$ = 4.0 Hz, $^3J_{F\text{-}H}$ = 8.0 Hz, 3H, CH_3 of $SiMe_2F$), -0.07 (dd, $^3J_{F\text{-}H}$ = 2.5 Hz, $^3J_{F\text{-}H}$ = 8.0 Hz, 3H, CH_3 of $SiMe_2F$).

^{13}C NMR (125 MHz, CD_3CN, 20 ºC): δ_C 131.8 (*meta*-CH of Mes), 131.4 (*meta*-CH of Mes), 127.7 (*meta*-CH of Mes), 127.6 (*meta*-CH of Mes), 76.5 (CH of C_5H_3BSi), 73.3 (CH of C_5H_3BSi), 69.9 (CH of C_5H_3BSi), 68.8 (CH of C_5H_5), 70.1 (CH_2 of 18-crown-6), 25.1 (*ortho*-CH_3 of Mes), 24.3 (*ortho*-CH_3 of Mes), 23.0 (*ortho*-CH_3 of Mes), 20.0 (*para*-CH_3 of Mes), 19.8 (*para*-CH_3 of Mes), 2.2 (CH_3 of $SiMe_2F$), 1.0 (CH_3 of $SiMe_2F$).

The signals for the quaternary carbons of Mes, the boron-bound and the silicon bound carbon atoms in the C_5H_3BSi unit were not observed. Assignments were assisted by gCOSY, HSQC and HMBC spectra.

^{11}B NMR (96 MHz, CD_3CN, 80 ºC): δ_B +5 (d, $^1J_{B\text{-}F}$ = 85 Hz).

^{19}F NMR (282 MHz, CD_3CN, 20 ºC): δ_F -164.6 (br. m, B-F), -153.3 (sept. $^3J_{F\text{-}H}$ = 8.0 Hz, $SiMe_2F$).

^{29}Si NMR (60 MHz, CD_3CN, 20 ºC): δ_{Si} 25.2 (dd, $^1J_{F\text{-}Si}$ = 190 Hz, $^1J_{F\text{-}Si}$ = 70 Hz).

MS(ES^-) 529.24 (M^-, 100 %).

[^{n}Bu$_4$N][*rac*-1,2-fc(BMes$_2$)(SiMe$_2$F)·F], [^{n}Bu$_4$N][16·F]: A solution of *rac*-1,2-fc($BMes_2$)($SiMe_2F$) (0.050 g, 0.1 mmol) in CD_3CN (0.75 mL) was added to [^{n}Bu$_4$N][F]·4(H_2O) (0.031 g, 0.1 mmol, 1 equiv.) at room temperature and the resulting reaction mixture stirred for 5 h. NMR studies were then conducted. The volatiles were removed *in vacuo*, taken up in minimal THF and layered with pentanes. Slow diffusion of pentane into a saturated THF solution lead to a yellow precipitate. Yield 0.035 g, 50%.

^{1}H NMR (300 MHz, $CDCl_3$, 20 ºC): δ_H 6.59 (s, 1H, *meta*-CH of Mes), 6.46 (s, 1H, *meta*-CH of Mes), 6.43 (s, 1H, *meta*-CH of Mes), 6.34 (s, 1H, *meta*-CH of Mes), 4.11 (m, 1H, C_5H_3BSi), 3.97 (m, 1H, C_5H_3BSi), 3.84 (s, 5H, C_5H_5), 3.74 (m, 1H, C_5H_3BSi), 2.99 (m, 8H,

CH_2 of $^nBu_4N$), 2.73 (br. s, 3H, CH_3 of Mes), 2.11 (br. m, 9H, CH_3 of Mes), 1.97 (s, 3H, CH_3 of Mes), 1.75 (s, 3H, CH_3 of Mes), 1.67 (m, 8H, CH_2 of $^nBu_4N$), 1.45 (m, 8H, CH_2 of $^nBu_4N$), 0.89 (m, 12 H, CH_3 of $^nBu_4N$), 0.24 (br. s, 3H, CH_3 of $SiMe_2F$), 0.01 (br. s, 3H, CH_3 of $SiMe_2F$).

^{11}B NMR (96 MHz, $CDCl_3$, 20 ºC): δ_B 5 (br. s).

^{19}F NMR (282 MHz, $CDCl_3$, 20 ºC): δ_F -156 (br. m), 163 (br. m).

[K(18-crown-6)][*rac*-1,2-fc($BMes_2$)($SiMe_2F$)·CN], [K(18-crown-6)][16·CN]: A solution of *rac*-1,2-fc($BMes_2$)($SiMe_2F$) (0.100 g, 0.2 mmol) in toluene (20 mL) was added to a mixture of KCN (0.015 g, 0.2 mmol, 1 equiv.) and 18-crown-6 (0.050 g, 0.2 mmol, 1 equiv) and the reaction mixture stirred for 5 h. Volatiles were then removed from the resulting orange suspension *in vacuo* and the solid residue washed with hexane (3 x 10 mL), dried *in vacuo*, and then extracted with toluene (10 mL). Removal of the solvent *in vacuo* afforded the desired product as an orange solid. Yield 0.080 g, 75 %.

^1H NMR (300 MHz, CD_3CN, 20 ºC): δ_H 6.76 (s, 1H, *meta*-CH of Mes), 6.61 (s, 1H, *meta*-CH of Mes), 6.54 (s, 1H, *meta*-CH of Mes), 6.39 (s, 1H, *meta*-CH of Mes), 4.43 (m, 1H, C_5H_3BSi), 4.31 (m, 1H, C_5H_3BSi), 4.02 (s, 5H, C_5H_5), 3.86 (m, 1H, C_5H_3BSi), 3.57 (s, 24H, CH_2 of 18-crown-6), 3.07 (s, 3H, *ortho*-CH_3 of Mes), 2.24 (s, 3H, *para*-CH_3 of Mes), 2.20 (s, 3H, *para*-CH_3 of Mes), 2.13 (s, 3H, *ortho*-CH_3 of Mes), 1.69 (s, 3H, *ortho*-CH_3 of Mes), 1.61

(s, 3H, *ortho*-CH_3 of Mes), 0.67 (d, 3H, $^3J_{H\text{-}F}$ = 7.8 Hz, CH_3 of $SiMe_2F$), 0.30 (d, 3H, $^3J_{H\text{-}F}$ = 7.8 Hz, CH_3 of $SiMe_2F$).

^{13}C NMR (75 MHz, CD_3CN, 20 ºC): δ_C 131.6 (*meta*-CH of Mes), 131.4 (*meta*-CH of Mes), 129.3 (*meta*-CH of Mes), 128.4 (*meta*-CH of Mes), 79.8 (CH of C_5H_3BSi), 75.7 (CH of C_5H_3BSi), 70.8 (CH of C_5H_3BSi), 70.0 (CH_2 of 18-crown-6), 68.5 (CH of C_5H_5), 26.8 (*ortho*-CH_3 of Mes), 25.0 (*ortho*-CH_3 of Mes), 24.6 (*ortho*-CH_3 of Mes), 24.3 (*ortho*-CH_3 of Mes), 19.9 (*para*-CH_3 of Mes), 19.8 (*para*-CH_3 of Mes), 3.1 (d, $^2J_{C\text{-}F}$ = 17.8 Hz, CH_3 of $SiMe_2F$), 1.6 (d, $^2J_{C\text{-}F}$ = 17.8 Hz, CH_3 of $SiMe_2F$).

^{11}B NMR (96 MHz, CD_3CN, 20 ºC): δ_B -16 (s).

^{19}F NMR (282 MHz, CD_3CN, 20 ºC): δ_F -149.3 (septet, $^3J_{F\text{-}H}$ = 7.8 Hz).

^{29}Si NMR (60 MHz, CD_3CN, 20 ºC): δ_{Si} 27.5 (d, $^1J_{Si\text{-}F}$ = 260 Hz, $SiMe_2F$).

MS(ESI$^-$): 536.2 (100%) [1,2-fc($BMes_2$)($SiMe_2F$)·CN].

Crystallographic data: [K(18-crown-6)][1,2-fc($BMes_2CN$)($SiMe_2F$)], $C_{427}H_{71}BF_2FeKO_7Si$, M_r = 777.67, monclinic, P 21/c, a = 12.81310(10), b = 17.3681(2), c = 20.2116(2) Å, β = 90.3773(10)º, V = 4497.78(8) Å^3, Z = 4, ρ_c = 1.148 Mg m^{-3}, T = 150 K, λ = 1.54180 Å. 8232 independent reflns [R(int) = 0.03562] used in all calcns. R_1 = 0.0524, wR_2 = 0.1191 for observed unique reflns [I>2σ(I)] and R_1 = 0.0584, wR_2 = 0.1268 for all unique reflns. Max./min. residual electron densities 1.27 and -0.96 e Å^3.

***rac*-1,2-fc(BMes$_2$)(SiMe$_2$OMe) (17)**: A suspension of *rac*-1,2-fc(BMes$_2$)(SiMe$_2$Cl) (0.300 g, 0.57 mmol) in methanol (50 mL) was stirred for 1 h. Diethyl ether (50 mL) was added and the reaction mixture stirred for 3 h. Volatiles were then removed *in vacuo* and the residue extracted with hexane (3 x 20 mL). The solvent was removed *in vacuo* from the combined extracts to afford the target material as a red solid. Yield 0.244 g, 82 %.

^{1}H NMR (300 MHz, $CDCl_3$, 20 ºC): δ_H 6.73 (s, 4H, *meta*-CH of Mes), 4.70 (m, 1H, C_5H_3BSi), 4.65 (m, 1H, C_5H_3BSi), 4.51 (m, 1H, C_5H_3BSi), 4.15 (s, 5H, C_5H_5), 3.31 (s, 3H, CH_3 of SiMe$_2$O<u>Me</u>), 2.25 (s, 6H, *para*-CH_3 of Mes), 2.12 (s, 12 H, *ortho*-CH_3 of Mes), 0.03 (s, 3H, CH_3 of Si<u>Me$_2$</u>OMe), 0.02 (s, 3H, CH_3 of Si<u>Me$_2$</u>OMe).

^{13}C NMR (75 MHz, $CDCl_3$, 20 ºC): δ_C 143.0 (boron-bound, *ipso*-carbon of Mes), 139.7 (*ortho*-carbons of Mes), 137.7 (*para*-carbon of Mes), 128.0 (*meta*-CH of Mes), 85.9 (CH of C_5H_3BSi), 80.1 (CH of C_5H_3BSi), 72.7 (CH of C_5H_3BSi), 71.7 (silicon-bound, quaternary carbon of C_5H_3BSi), 70.1 (C_5H_5), 50.2 (SiMe$_2$O<u>Me</u>), 23.6 (*ortho*-CH_3 of Mes), 21.1 (*para*-CH_3 of Mes), -1.0 (Si<u>Me$_2$</u>OMe), -1.2 (Si<u>Me$_2$</u>OMe). The signal for the boron-bound, quaternary carbon of the C_5H_3BSi unit was not observed. Assignments were assisted by gCOSY, HMQC and HSQC NMR spectra.

^{11}B NMR (96 MHz, $CDCl_3$, 20 ºC): δ_B 87 (br. s).

^{29}Si NMR (60 MHz, $CDCl_3$, 20 ºC): δ_{Si} 11 (s).

MS (EI^+) 522.2 (100 %) M^+; exact mass (calc for M^+, ^{10}B, ^{28}Si isotopomer) 519.2290, (meas.) 519.2288.

Crystallographic data: $C_{31}H_{39}BFeOSi$, M_r = 522.39, monoclinic, *-P 2ybc*, a = 14.9853(2), b = 8.91110(10), c = 20.9000(3) Å, V = 2773.12(6) $Å^3$, Z = 4, ρ_c = 1.251 Mg m^{-3}, T = 150 K, λ = 0.71073 Å. 92997 reflections collected, 6283 independent [R(int) = 0.024] used in all calculations. R_1 = 0.0434, wR_2 = 0.0902 for observed unique reflections [I>2σ(I)] and R_1 = 0.0556, wR_2 = 0.0981 for all unique reflections. Max. and min. residual electron densities 0.47 and -0.45 e $Å^3$.

[K(18-crown-6)][*rac*-1,2-fc($BMes_2$)($SiMe_2OMe$)·F], [K(18-crown-6)][17·F]: A solution of *rac*-1,2-fc($BMes_2$)($SiMe_2OMe$) (0.370 g, 0.7 mmol) in CD_3CN (3 mL) was added to a mixture of KF (0.042 g, 0.7 mmol, 1 equiv) and18-crown-6 (0.190 g, 0.71 mmol, 1 equiv.) and the reaction mixture stirred for 16 h. The reaction was deemed to be complete on observation of a colour change to yellow. NMR analysis showed complete consumption of *rac*-1,2-fc($BMes_2$)($SiMe_2OMe$). Attempts to grow crystals suitable for X-ray diffraction analyses by slow diffusion and evaporation failed due to gradual decomposition of the material.

^{1}H NMR (300 MHz, CD_3CN, 20 ºC): δ_H 6.46 (s, 1H, *meta*-CH of Mes), 6.62 (s, 1H, *meta*-CH of Mes), 6.40 (s, 1H, *meta*-CH of Mes), 6.25 (s, 1H, *meta*-CH of Mes), 4.22 (m, 1H, C_5H_3BSi), 4.14 (m, 1H, C_5H_3BSi), 3.91 (m, 1H, C_5H_3BSi), 3.78 (s, 5H, C_5H_5), 3.54 (s, 24H, CH_2 of 18-crown-6), 3.44 (s, 3H, CH_3 of $SiMe_2O\underline{Me}$), 2.83 (s, 3H, *orhto*-CH_3 of Mes), 2.18 (s, 3H, *para*-CH_3 of Mes), 2.08 (s, 3H, *ortho*-CH_3 of Mes), 2.05 (s, 3H, *para*-CH_3 of Mes), 1.76 (s, 3H, *orhto*-CH_3 of Mes), 1.55 (s, 3H, *ortho*-CH_3 of Mes), 0.50 (d, 3H, 1.8 Hz, CH_3 of $Si\underline{Me_2}OMe$), -0.17 (d, 3H, 1.8 Hz, CH_3 of $Si\underline{Me_2}OMe$).

^{13}C NMR (75 MHz, CD_3CN, 20 ºC): δ_C 127.7 (br. m, *meta*-CH of Mes), 76.8 (CH of C_5H_3BSi), 74.3 (CH of C_5H_3BSi), 73.3 (CH of C_5H_3BSi), 70.0 (CH_2 of 18-crown-6), 67.7 (CH of C_5H_5), 25.1 (*ortho*-CH_3 of Mes), 24.6 (*ortho*-CH_3 of Mes), 24.0 (*ortho*-CH_3 of Mes), 20.3 (*para*-CH_3 of Mes), 20.0 (*ortho*-C_3 of Mes), 19.8 (*ortho*-CH_3 of Mes), 2.9 (d, 8.8 Hz, CH_3 of $Si\underline{Me_2}OMe$), -0.8 (d, 8.8 Hz, CH_3 of $Si\underline{Me_2}OMe$).

^{11}B NMR (96 MHz, CD_3CN, 20 ºC): δ_B 5 (br. s).

^{19}F NMR (282 MHz, CD_3CN, 20 ºC): δ_F -163.8 (br. m).

^{29}Si NMR (60 MHz, CD_3CN, 20 ºC): δ_{Si} 10 (br).

[K(18-crown-6)][*rac*-1,2-fc($BMes_2$)($SiMe_2OMe$)·CN] [K(18-crown-6)][17·CN]: A solution of *rac*-1,2-fc($BMes_2$)($SiMe_2OMe$) (0.370 g, 0.7 mmol) in CD_3CN (3 mL) was added to a mixture of KCN (0.046 g, 0.7 mmol, 1 equiv) and18-crown-6 (0.190 g, 0.71 mmol, 1 equiv.) and the reaction mixture stirred for 10 min. The reaction was deemed complete on

colour change to yellow and NMR analysis showed complete consumption of *rac*-1,2-fc($BMes_2$)($SiMe_2OMe$).

^{1}H NMR (300 MHz, CD_3CN, 20 ºC): δ_H 6.72 (s, 1H, *meta*-CH of Mes), 6.50 (s, 1H, *meta*-CH of Mes), 6.47 (m, 1H, *meta*-CH of Mes), 6.30 (s, 1H, *meta*-CH of Mes), 4.32 (m, 1H, C_5H_3BSi), 4.21 (m, 1H, C_5H_3BSi), 4.00 (m, 1H, C_5H_3BSi), 3.92 (s, 5H, CH of C_5H_5), 3.57 (s, 24H, CH_2 of 18-crown-6), 3.43 (s, 3H, CH_3 of $SiMe_2O\underline{Me}$), 3.02 (s, 3H, *ortho*-CH_3 of Mes), 2.18 (s, 3H, *para*-CH_3 of Mes), 2.07 (s, 3H, *para*-CH_3 of Mes), 2.05 (s, 3H, *orhto*-CH_3 of Mes), 1.63 (s, 3H, *ortho*-CH_3 of Mes), 1.59 (s, 3H, *ortho*-CH_3 of Mes), 0.67 (CH_3 of $Si\underline{Me_2}OMe$), 0.08 (CH_3 of $Si\underline{Me_2}OMe$).

^{13}C NMR (75 MHz, CD_3CN, 20 ºC): δ_C 143.3 (*ortho*-quaternary carbon of Mes), 166.3 (CN), 143.0 (*ortho*-quaternary carbon of Mes), 142.8 (*ortho*-quaternary carbon of Mes), 142.2 (*ortho*-quaternary carbon of Mes), 132.4 (*para*-quaternary carbon of Mes), 132.2 (*para*-quaternary carbon of Mes), 130.1 (*meta*-CH of Mes), 129.7 (*meta*-CH of Mes), 129.5 (*meta*-CH of Mes), 129.2 (*meta*-CH of Mes), 80.4 (CH of C_5H_3BSi), 77.2 (CH of C_5H_3BSi), 75.2 (silicon-bound, quaternary carbon of C_5H_3BSi), 70.8 (CH_2 of 18-crown-6), 70.4 (CH of C_5H_3BSi), 69.2 (boron-bound, quaternary carbon of C_5H_3BSi), 69.0 (CH of C_5H_5), 50.5 (CH_3 of $SiMe_2O\underline{Me}$), 27.8 (*ortho*-CH_3 of Mes), 25.9 (*ortho*-CH_3 of Mes), 25.2 (*ortho*-CH_3 of Mes), 24.5 (*ortho*-CH_3 of Mes), 20.7 (*para*-CH_3 of Mes), 20.6 (*para*-CH_3 of Mes), 3.6 (CH_3 of $Si\underline{Me_2}OMe$), 0.9 (CH_3 of $Si\underline{Me_2}OMe$). The boron-bound, quaternary carbons of Mes were not observed.

^{11}B NMR (96 MHz, CD_3CN, 20 ºC): δ_B -16 (s).

^{29}Si NMR (60 MHz, CD_3CN, 20 ºC): δ_{Si} 16.5 (s).

MS(ESI$^-$): 548.2 (100%) [1,2-fc($BMes_2$)($SiMe_2OMe$)·CN^-].

Competition reactions between potassium cyanide and potassium fluoride with *rac*-1,2-fc($BMes_2$)($SiMe_2OMe$) 17:

A solution of [K(18-crown-6)][1,2-fc($BMes_2$)($SiMe_2OMe$)F] (0.380 g, 0.7 mmol) in CD_3CN (3 mL) was added to potassium cyanide (0.046 g, 0.7 mmol, 1 equiv) and the reaction mixture stirred for 3 h. NMR analysis revealed quantitative conversion of [K(18-crown-6)][1,2-fc($BMes_2$)($SiMe_2OMe$)F] to [K(18-crown-6)][1,2-fc($BMes_2$)($SiMe_2OMe$)CN]. The clearest evidence for this reaction was a shift in the ^{11}B NMR resonance from δ 5 (br s) to δ -16 (s) ppm.

A solution of [K(18-crown-6)]$^+$[1,2-fc($BMes_2$)($SiMe_2OMe$)CN] (0.390 g, 0.7 mmol) in CD_3CN (3 mL) was added to potassium fluoride (0.420 g, 0.7 mmol, 1 equiv) and the reaction mixture stirred for 48 h. NMR analysis revealed no conversion of [K(18-crown-6)][1,2-fc($BMes_2$)($SiMe_2OMe$)CN] to [K(18-crown-6)][1,2-fc($BMes_2$)($SiMe_2OMe$)F]. The clearest evidence for this reaction was the lack of any change in either the ^{1}H or the ^{11}B NMR spectrum.

[K(18-crown-6)][*rac*-1,2-fc($BMes_2$)($SiMe_2OH$)·F], [K(18-crown-6)][18·F]:

A solution of *rac*-1,2-fc($BMes_2$)($SiMe_2OH$) (0.053 g, 0.1 mmol) in $CDCl_3$ (2 mL) was added to of KF (0.006 g, 0.1 mmol, 1 equiv.) and 18-crown-6 (0.026 g, 0.1 mmol, 1 equiv) at room temperature and the resulting reaction mixture stirred for 5 h. The volatiles were removed *in vacuo* and the yellow solid taken up in $O(SiMe_3)_2$ (10 mL). Slow evaporation under inert amtmosphere led to the formation of three yellow crystals. Yield not determined.

Crystallographic data: [K(18-crown-6)][1,2-fc($BMes_2F$)($SiMe_2OH$)], $C_{42}H_{61}BFFeKO_7Si$, M_r = 830.78, monclinic, P 21/c, a = 12.4769(2), b = 14.4345(2), c = 24.4216(4) Å, β = 92.3848(5)º, V = 4394.47(12) $Å^3$, Z = 4, ρ_c = 1.256 Mg m^{-3}, T = 150 K, λ = 0.71073 Å. 9984 independent reflns [R(int) = 0.036411] used in all calcns. R_1 = 0.0495, wR_2 = 0.0980 for observed unique reflns [I>2σ(I)] and R_1 = 0.0820, wR_2 =0.1099 for all unique reflns. Max./min. residual electron densities 0.66 and -0.66 e $Å^3$.

[^{n}Bu_4N][*rac*-1,2-fc($BMes_2$)($SiMe_2OH$)·F]·MeCN [^{n}Bu_4N][18·F]·MeCN:

A solution of *rac*-1,2-fc($BMes_2$)($SiMe_2Cl$) (0.051 g, 0.1 mmol) in THF (2 mL) was added to [^{n}Bu_4N][F]·4(H_2O) (0.031 g, 0.1 mmol, 1 equiv.) at room temperature and the resulting reaction mixture stirred for 5 h. NMR studies were then conducted. The volatiles were removed *in vacuo*, taken up in minimal MeCN. Slow evaporation under inert atmosphere conditions gave yellow crystals. Yield 0.015 g, 21%.

Crystallographic data: $[Bu_4N][1,2\text{-fc}(BMes_2F)(SiMe_2OH)]\cdot MeCN$, $C_{44}H_{64}BFFeKO_7Si_1$, M_r = 830.78, monclinic, P 21/c, a = 15.4080(3), b = 12.2378(2), c = 24.3125(5) Å, β =90.01º, V = 4584.37 Å^3, Z = 4, ρ_c = 1.256 Mg m^{-3}, T = 150 K, λ = 0.71073 Å. 15243 independent reflns [R(int) = 0.00] used in all calcns. R_1 = 0.0556, wR_2 = 0.1118 for observed unique reflns [I>2σ(I)] and R_1 = 0.0794, wR_2 = 0.1322 for all unique reflns. Max./min. residual electron densities 0.63 and -0.64 e Å^3.

[K(18-crown-6)][*rac*-1,2-fc(BMes$_2$)(SiMe$_2$OH)·CN], [K(18-crown-6)][18·CN]:

A solution of *rac*-1,2-fc(BMes$_2$)(SiMe$_2$Cl) (0.051 g, 0.1 mmol) in THF (2 mL) was added to [^{n}Bu$_4$N][CN]˙3(H$_2$O) (0.030 g, 0.1 mmol, 1 equiv.) at room temperature and the resulting reaction mixture stirred for 5 h. Slow diffusion of pentane into a saturated THF solution led to formation of yellow crystals. Yield not determined.

Crystallographic data: $[Bu_4N][1,2\text{-fc}(BMes_2CN)(SiMe_2OH)]$, $C_{47}H_{72}BFeN_2O_1Si$, M_r = 775.93, monclinic, P 21/c, a = 12.81313(12), b = 17.36807(16), c = 20.2116(2) Å, β = 90.3773(10)º, V = 4497.78(8) Å^3, Z = 4, ρ_c = 1.146 Mg m^{-3}, T = 150 K, λ = 1.54184 Å. 9386 independent reflns [R(int) = 0.036] used in all calcns. R_1 = 0.0536, wR_2 = 0.1236 for observed unique reflns [I>2σ(I)] and R_1 = 0.0598, wR_2 = 0.1315for all unique reflns. Max./min. residual electron densities 1.53 and -0.85 e Å^3.

***rac*-1,2-fc(BMes$_2$)(SiMe$_2$OC$_6$H$_4$I) and FcBMes(OC$_6$H$_4$I):** 4-Iodophenol (0.021 g, 95 μmol, 1 equiv.) was added to a solution of *rac*-1,2-fc(BMes$_2$)(SiMe$_2$Cl) (0.050 g, 95 μmol) in acetonitrile at room temperature and the reaction mixture stirred for 3 hours, concomitant

with a lightening in colour to form a pale orange solution. Volatiles were then removed *in vacuo* and the orange residue taken up in $CDCl_3$ (0.75 mL). NMR analysis showed complete consumption of *rac*-1,2-fc($BMes_2$)($SiMe_2Cl$). Attempts to obtain the clean material failed due to rapid decomposition of 1,2-fc($BMes_2$)($SiMe_2OC_6H_4I$) to FcBMes(OC_6H_4I).

^{1}H NMR (300 MHz, $CDCl_3$, 20 ºC): δ_H 7.50 (br. m, 2H, CH of Ar), 6.74 (s, 4H, *meta*-CH of Mes), 6.70 (br. m, 2H, CH of Ar), 4.83 (m, 1H, C_5H_3BSi), 4.73 (m, 1H, C_5H_3BSi), 4.58 (m, 1H, C_5H_3BSi), 4.22 (s, 5H, C_5H_5), 2.27 (s, 6H, *para*-CH_3 of Mes), 2.12 (s, 12H, *ortho*-CH_3 of Mes), 0.01 (s, 3H, CH_3 of $SiMe_2OAr$), 0.00 (s, 3H, CH_3 of $SiMe_2OAr$).

^{11}B NMR (96 MHz, $CDCl_3$, 20 ºC): δ_B 63 (s).

Orange crystals, which had formed upon standing for approximately 2 days, were isolated by filtration.

Crystallographic data: FcBMes(OC_6H_4I), $C_{50}H_{48}B_2Fe_2I_2O_2$ M_r = 1068.05, triclinic, *P*-1, *a* = 7.8776(1), *b* = 10.3724(2), *c* = 13.8718(3) Å, α = 94.2750(7), β = 96.1673(7), γ = 102.3538(9)º, *V* = 1095.24(3) Å^3, *Z* =1, ρc = 1.619 Mg m^{-3}, *T* = 150 K, λ = 0.71073 Å. 4949 independent reflns [R(int) = 0.027] used in all calcns. R_1 = 0.0260, wR_2 = 0.0461 for observed unique reflns [$I>2\sigma(I)$] and R_1 = 0.0339, wR_2 = 0.0545 for all unique reflns. Max./min. residual electron densities 0.84 and -0.61 e Å^3.

***rac*-1,2-fc(BMes$_2$)(SiPh$_2$Cl):** ^{t}BuLi (0.245 mL of a 1.6 M solution in hexane, 0.39 mmol, 2 equiv.) was added dropwise to 1,2-fc(Br)BMes$_2$ (0.1 g, 0.196 mmol) in THF (20 mL) at -78ºC. The purple solution was stirred for 5 min, then dichlorodiphenylsilane (0.81 mL, 3.9 mmol, 10 equiv.) was added dropwise at -78ºC. The solution was warmed to room temperature and stirred for a further 16 h, gradually changing to a red colour. The solvent was removed *in vacuo*, extracted with hexane (2 x 50 mL) and dried *in vacuo* to yield a mixture of products.

NOTE: A mixture of 1,2-fc(BMes$_2$)(SiPh$_2$Cl) and 1,2-fc(BMes$_2$)Br was obtained with a ratio of 10:1, as well as an excess of ClPPh$_2$. The peaks corresponding to 1,2-fc(BMes$_2$)Br and ClPPh$_2$ are omitted for clarity.

^{1}H NMR (96 MHz, CDCl$_3$, 20 ºC): δ_H 7.24 (br. m. co-incident with ClPPh$_2$), 7.60 (br. m, co-incident with ClPPh$_2$), 6.66 (s, 4H, *meta*-CH of Mes), 4.52 (m, 1H, CH of C$_5$H$_3$BSi), 4.38 (m, 1H, CH of C$_5$H$_3$BSi), 4.07 (m, 1H, CH of C$_5$H$_3$BSi), 3.99 (s, 5H, CH of C$_5$H$_5$), 2.27 (s, 12H, *ortho*-CH$_3$ of Mes), 2.12 (s, 6H, *para*-CH$_3$ of Mes).

^{11}B NMR (96 MHz, CDCl$_3$, 20 ºC): δ_B 80 (s).

3.4. Results and Discussion

3.4.1. Proximal Hydrogen Bond Donor(s)

3.4.1.1. Syntheses

The initial focus of this chapter was aimed at establishing synthetic routes to ferrocenyl systems bearing both amide and borane functionalities (**8**, **9** and **10**) as outlined in Figure 3.9. These target compounds are similar to the 1,2-difunctionalised systems bearing an amine and a borane function which were shown by Addy *et al.* to exhibit hydrogen bonding to boron-bound fluoride[20] and it was thought that an auxiliary hydrogen bonding motif might enable selective detection of fluoride over cyanide, for example.

The conversion of $NH(CH_2CH_2NH_2)_2$ to $NH(CH_2CH_2NHCOCF_3)_2$ (**1**) was attempted by the protocol described by O'Sullivan and co-workers[33]. Contrary to the results which these authors reported, we obtained the salt $[NH_2(CH_2CH_2NHCOCF_3)_2][CF_3CO_2]$ in almost quantitative yield (92%). This result corroborates the work of Dalrymple and co-worker,[31] in their investigation of this reaction. ^1H and ^{19}F NMR spectra are fully consistent with salt formation and mass spectroscopic results also exhibit peaks corresponding to both components of the salt. The conversion of $NH(CH_2CH_2NH_2)_2$ to $NH(CH_2CH_2NHCOCF_3)_2$ (**1**) was successfully completed by following the protocol described by Platzek *et al*.,[34] giving the target material in yields of ca. 95%. This protocol was modified to give the longer chain analogues $NH(CH_2CH_2NHCOCF_3)(CH_2CH_2CH_2NHCOCF_3)$ (**2**) and $NH(CH_2CH_2CH_2NHCOCF_3)_2$ (**3**), also in good yields (80-90%).

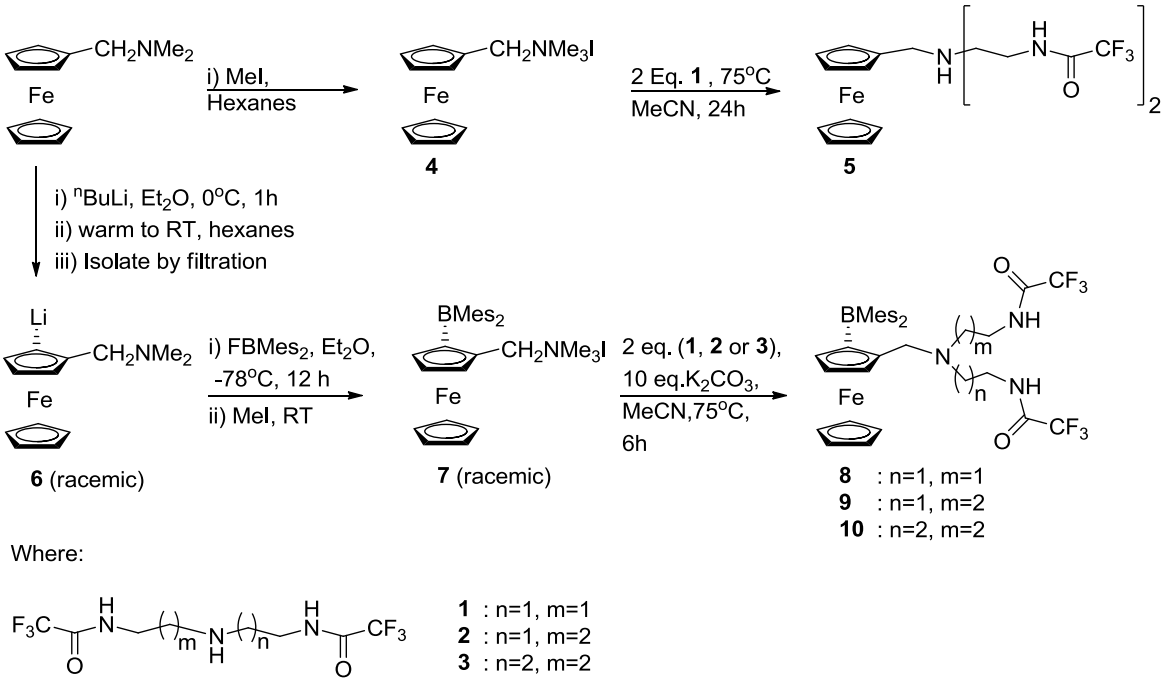

Figure 3.9. The syntheses of amine/amide functionalised ferrocene and ferrocenyl borane complexes.

$[FcCH_2NMe_3]I$ (**4**) was synthesised following a slightly modified protocol of Brocard and co-workers[35] (Figure 3.9). The synthesis of compound **5** was initially conducted as a proof-of-principle reaction, to determine whether a ferrocene-bound, quaternary-ammonium cation could undergo substitution with a neutral amine (**1**). Refluxing a one-to-one mixture of **1** and **4** gave rise to $FcCH_2N(CH_2CH_2NHCOCF_3)_2$ (**5**), although in a low yield of 18%. The ^1H, ^{13}C and ^{19}F NMR spectra were fully consistent with the formation of the desired compound. X-ray studies of single crystals of **5** (Figure 3.10) further confirmed its identity, with elemental analysis confirming bulk purity. The UV-Vis spectrum of **5** in chloroform solution does not exhibit a change upon addition of excess fluoride anions.

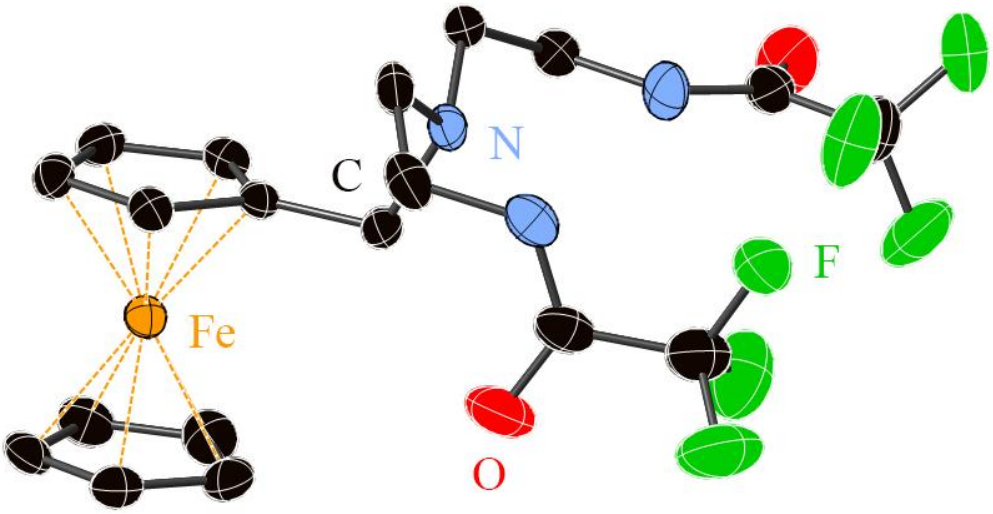

Figure 3.10 The crystal structure of **5**. Ellipsoids drawn at the 50% probability level, with hydrogen atoms omitted for clarity. Carbon in black, nitrogen in blue, oxygen in red, fluorine in green and iron in orange.

The synthesis of 1,2-fc($BMes_2$)(CH_2NMe_2) was achieved following a slightly modified procedure of Aldridge and co-workers.[20] Synthesis of the literature compound **7** *via* the isolation of the lithiate **6** was found to simplify purification of **7** and gave moderate overall conversion (60 to 70%). Attempts to synthesise 1,2-fc($BMes_2$)($CH_2N(CH_2CH_2NHCOCF_3)_2$) (**8**) following the same reaction pathway as **5** proved unsuccessful, instead yielding a complex mixture of compounds from which no target material could be isolated. Variation of the timescale and temperature of the reaction was explored, with no notable successes. Only upon addition of an excess of potassium carbonate (*ca*. 10 equivalents), does the reaction proceed in a fashion that allows for the isolation of **8**, although with low isolated yields (5–16%). Again, optimisation of timescale and temperature

was explored. The reaction conditions of 75 ºC and 6 hours led to the highest yields of the target material (10 - 16 %).

1,2-fc($BMes_2$)($CH_2N(CH_2CH_2NHCOCF_3)(CH_2CH_2CH_2NHCOCF_3)$) (**9**) and 1,2-fc($BMes_2$)($CH_2N(CH_2CH_2CH_2NHCOCF_3)_2$) (**10**) could be synthesised in similarly low yields (5-10 %) under similar reaction conditions by replacement of the amine **1** by the longer-chain analogues **2** and **3** (Figure 3.9). The compounds **8**, **9** and **10** are all air stable in the solid state, however they tend to decompose in solution, with decomposition products observable in the ^{1}H and ^{11}B NMR spectra after 12 hours. This decomposition is ascribed to hydrolysis of the $BMes_2$ unit, initially to BMes(OH), supported by a resonance in the ^{11}B NMR spectrum at +36 ppm, and resonances corresponding to mesitylene in the ^{1}H NMR spectrum. This chemistry has previously been observed by the Aldridge research group, and is notable for systems featuring both an amine and a borane in the 1 and 2-positions of ferrocene respectively; such behaviour has not been observed for the analogous 1,1' isomers.[36]

These ferrocenyl systems bearing both amide and borane functionalities, i.e. compounds **8**, **9** and **10,** were characterised using a combination of ^{1}H, ^{11}B, ^{13}C, ^{19}F, COSY, HMBC and HSQC NMR spectroscopy and mass spectrometry. All three compounds exhibit a broad resonance in the ^{11}B NMR spectrum at 75 to 80 ppm, which is fully consistent with a three-coordinate, ferrocene-appended $BMes_2$ unit. This allayed fears that the pendant arms of the amine would form dative bonds to the borane and thereby limit the capacity of **8**, **9** and **10** to bind anions, such as fluoride and cyanide. The ^{19}F NMR spectra of these compounds

exhibited peaks between -75 and -77 ppm, typical of the $C(O)CF_3$ groups. The ^{1}H and ^{13}C NMR spectra were fully consistent with the structures shown in Figure 3.11. Of note in the ^{1}H NMR spectrum were the resonances for the aromatic protons of the mesityl rings, with the resonance for all four protons being coincident at 25 ºC, consistent with fast rotation about the mesityl C_{ipso}-B bond, relative to the NMR timescale. The identities of **8** and **9** were confirmed by high resolution mass spectrometry.

3.4.1.2. Anion Binding

All three compounds, **8**, **9** and **10**, react with an excess of fluoride in the presence of one equivalent of 18-crown-6, as shown in Figure 3.11, accompanied by a change in colour from dark red to yellow. For compound **8**, conversion to the fluoride adduct in d_3-acetonitrile was evidenced by a change in the chemical shift in the ^{11}B NMR spectrum from 76 ppm to a broad signal at 8 ppm, which is typical for four-coordinate boranes of the type $[FcBMes_2F]^-$.[8] That a well-resolved doublet is not observed (as might be expected from coupling to ^{19}F (I = ½)) is not unusual, and seems to be a feature of systems of this ilk.[28] Further evidence for the binding of a fluoride anion at the boron atom is obtained from the ^{19}F NMR spectrum of $[\mathbf{8}\cdot F]^-$, with a signal at -170 ppm that integrates to one fluorine (*cf.* the resonance of -76.4 ppm that integrates to six, corresponding to the two CF_3 groups). The chemical shift of -170 ppm is typical of systems such as $[FcBAr_2F]^-$, as is the unresolved coupling to ^{11}B (I = $^3/_2$).[28] Compound $[\mathbf{8}\cdot F]^-$ no longer exhibits fast rotation around the C_{ipso}-B bonds of the mesityl substituents at room temperature on the ^{1}H NMR timescale, as the four resonances of the C-H protons, as well as the four sets for the *ortho* CH_3 groups are found to be inequivalent. Whether this arises from hydrogen bonding of the pendant arms of the amine to the fluoride

atom or whether this arises simply from steric congestion has not been elucidated. No evidence for hydrogen bonding was observed in the ^{1}H NMR spectrum.

The corresponding fluoride adducts [**9**·F]$^{-}$ and [**10**·F]$^{-}$ exhibit broad resonances in the respective ^{11}B NMR spectra at 8 and 6 ppm respectively, typical of systems containing a [FcBAr$_2$F]$^{-}$ unit.[28] As with [**8**·F]$^{-}$, [**9**·F]$^{-}$ features a broad resonance at -173 ppm typical of a boron-bound fluoride anion.[28] This signal integrates to one fluorine atom, as compared to resonances at -75.8 and -75.9 ppm that correspond to the two CF_3 units, both of which integrate to three fluorine atoms. Confidence in the identity of the fluoride adduct, [**9**·F]$^{-}$, was provided by high resolution mass spectrometry, in which the molecular ion [**9**·F]$^{-}$ could be observed. These adducts do, however, decompose over time in acetonitrile-d_3 solution, presumably through hydrolysis.

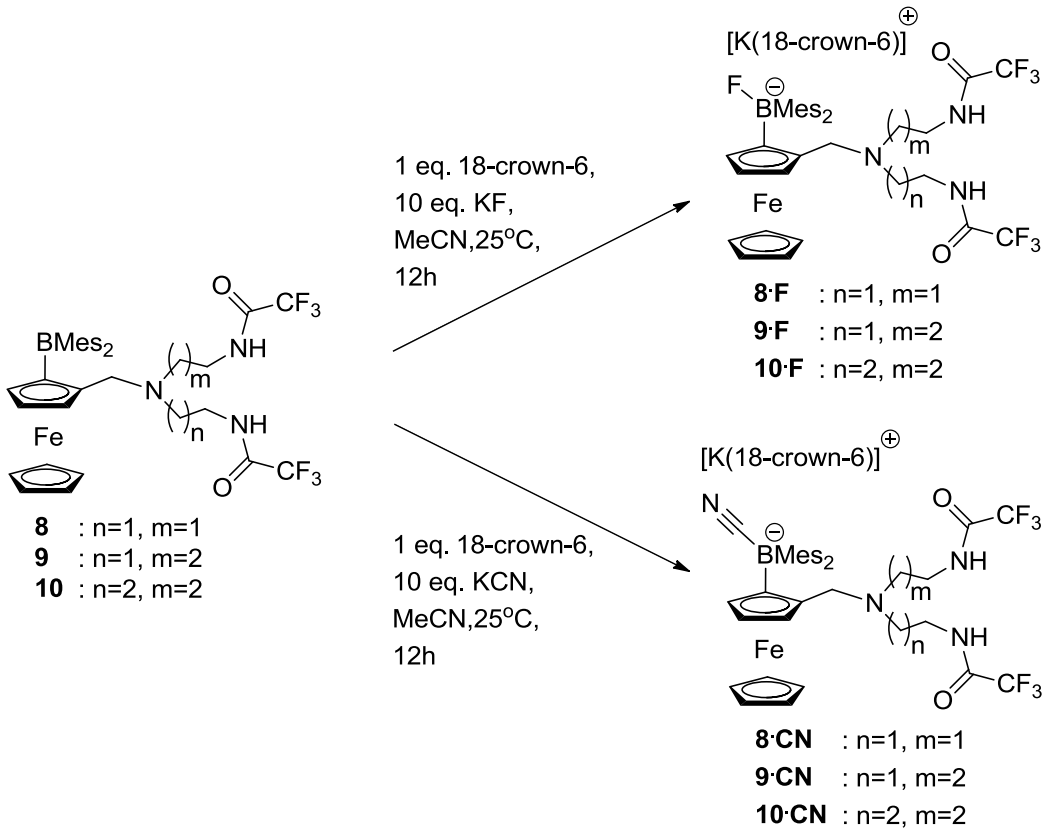

Figure 3.11. The reaction of **8**, **9** and **10** with sources of fluoride and cyanide in acetonitrile solution to form the adducts **8·F**, **9·F**, **10·F, 8·CN**, **9·CN** and **10·CN**.

In addition to binding fluoride, all three compounds **8**, **9** and **10** react with an excess of potassium cyanide and one equivalent of 18-crown-6, yielding [**8·**CN]$^-$, [**9·**CN]$^-$ and [**10·**CN]$^-$ respectively, as shown in Figure 3.11. These reactions are accompanied by a change in colour from dark red to yellow. For all three adducts, the ^{11}B NMR spectrum in acetonitrile exhibits a sharp peak in the range -13 to -15 ppm, which is typical for systems of the type [$FcBAr_2(CN)$]$^-$.[28] Compounds [**8·**CN]$^-$ and [**9·**CN]$^-$ no longer exhibit fast rotation around the C_{ipso}-B bonds of the mesityl substituents at room temperature on the ^{1}H NMR timescale. This is evident from the four distinct resonances of the C-H protons of the mesityl substituents, as

well as the four inequivalent sets for the *ortho* CH_3 groups. As with the fluoride adducts, whether this arises from hydrogen bonding of the pendant arms of the amine to the fluoride atom or whether this arises simply from steric congestion has not been elucidated. No evidence for hydrogen bonding was observed in the ^{1}H NMR spectra.

Attempts to react **8** and **9** with one equivalent of $[^nBu_4N]F{\cdot}3(H_2O)$ in d_3-acetonitrile and d_1-chloroform solution did not lead to clean conversion to the respective fluoride adducts. The ^{1}H NMR spectrum in each case exhibited a complicated mixture of products in the ferrocenyl region. As both **8** and **9** slowly decompose in solution by reaction with water, this could be ascribed to the reaction of **8** and **9** with both fluoride and residual water in $[^nBu_4N]F{\cdot}3(H_2O)$. Similarly, attempts to react **8** and **9** with one equivalent of $[^nBu_4N][CN]{\cdot}2(H_2O)$ in d_3-acetonitrile and d_1-chloroform did not lead to clean conversion to the cyanide adducts. The ^{1}H NMR spectra were consistent with a complicated mixture of products in the ferrocenyl region. This is similarly ascribed to **8** and **9** reacting with both cyanide and residual water in $[^nBu_4N][CN]{\cdot}2(H_2O)$.

As both **8** and **9** do not react cleanly with either $[^nBu_4N]F{\cdot}3(H_2O)$ or $[^nBu_4N][CN]{\cdot}2(H_2O)$, reliable binding constants could not be determined for these compounds. However, the rate of hydrolysis is much slower than that of anion assimilation, as decomposition due to hydrolysis in d_3-acetonitrile is not complete after 12 h, whereas consumption of either receptor **8** or **9** is complete within 10 minutes with 1.1 equivalents of fluoride or cyanide as the tetrabutylammonium salts. The effect of sequential addition of aliquots of $[^nBu_4N][CN]{\cdot}2(H_2O)$ to a solution of **8** in THF is shown in Figure 3.12. Thus, a

rough estimate of the cyanide binding strength in dichloromethane solution could be obtained and is of the order of 10^5.

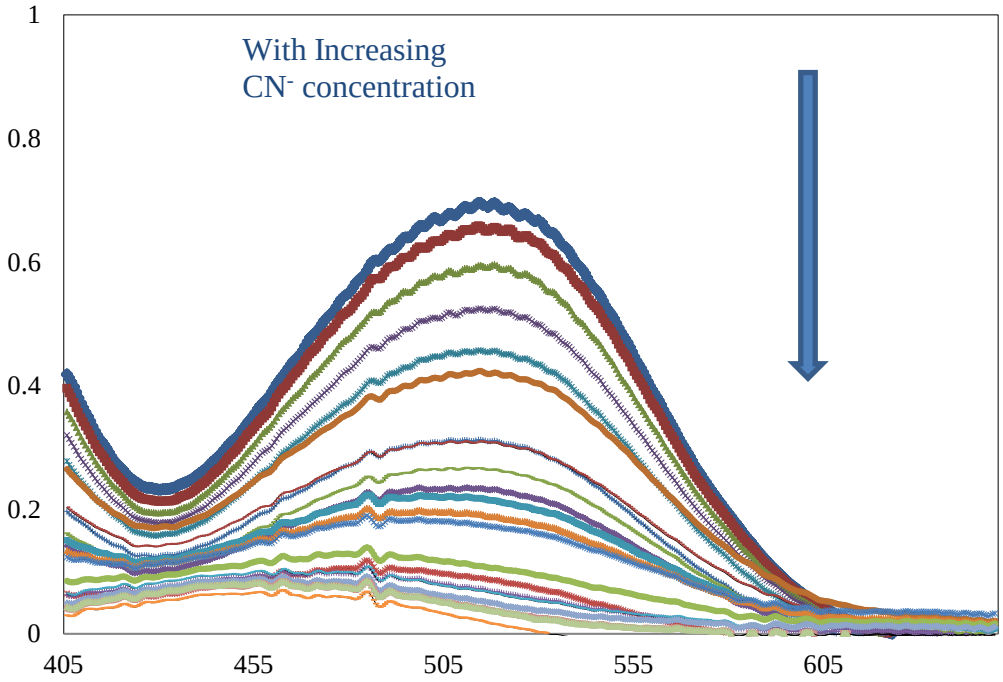

Figure 3.12. A series of the UV-visible absorption spectra for a solution of **8** in THF, showing the sequential decrease in signal intensity on addition of aliquots of cyanide.

The cyanide adduct [K(18-crown-6)][**10**·CN] was structurally characterised by X-ray crystallography (Figure 3.13 and Figure 3.14.). The key angles and distances of [K(18-crown-6)][**10**·CN] are listed in Table 3.3. Of note in the crystal structure is the direct bond established by the carbon of cyanide to boron (1.634(6) Å), giving rise to a four coordinate boron centre which is fully consistent with the solution state ^{11}B NMR spectra. The pyramidalization of boron is exhibited, with a sum of the C-B-C angles (excluding cyanide) of [K(18-crown-6)][**10**·CN] equal to 335.3(9)º. The crystal structure to the adduct reveals dimerization of the molecular unit, in which the monomer units are bound together through

inter-molecular N-H···NC-B hydrogen bonds [d(N-N) = 2.883(5) Å] (illustrated by red dashed lines in Figures 3.13-15). The crystal structure of the cyanide adduct also features one intra-molecular N-H···NRR′R″ hydrogen bond, to form a six-membered ring [d(N-N) = 2.854(4) Å)] (illustrated by red dashed lines in Figures 3.13-15), and close approaches from the oxygen atoms of all $NHCOCF_3$ groups to the potassium cation of $[K(18\text{-crown-6})]^+$ [d(O-K) = 2.706(3), 2.863(4) Å].

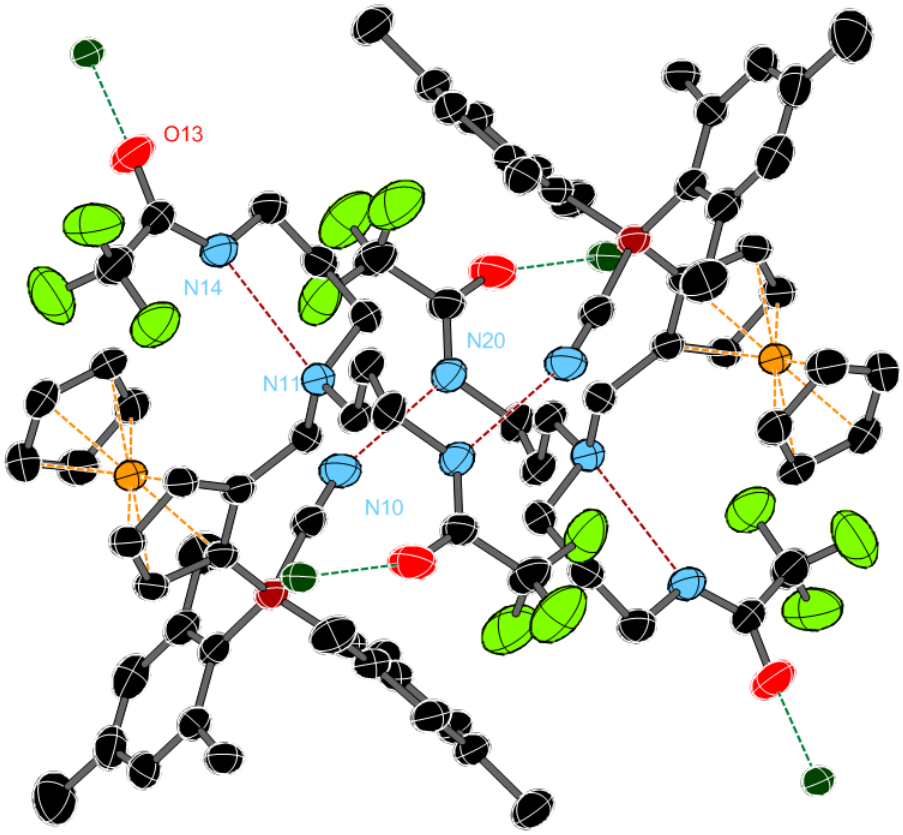

Figure 3.13. The crystal structure of [**10·CN][K(18-crown-6)]**. Ellipsoids are drawn at the 50% probability level, with hydrogen atoms and the atoms of the 18-crown-6 rings omitted for clarity. Presumed hydrogen bonding is illustrated with red dashed lines. Close approaches of the oxygen atoms to the potassium cations is illustrated in green dashed lines. Boron drawn in maroon, carbon in black, nitrogen in blue, oxygen in red, fluorine in light green, potassium in dark green and iron in orange.

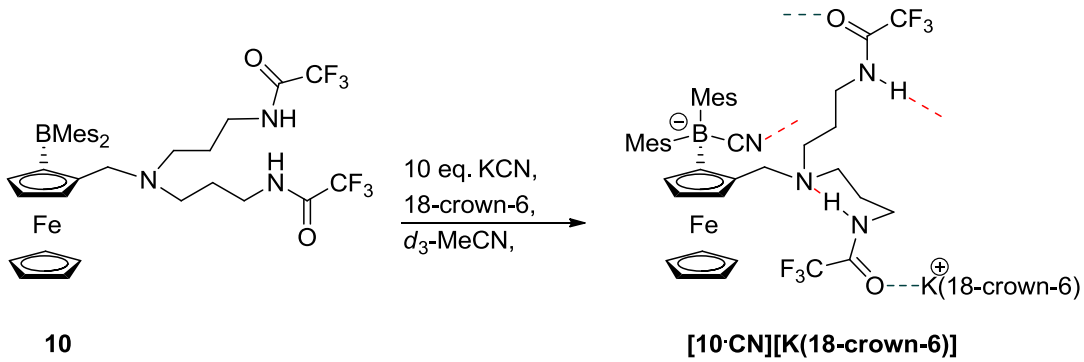

Figure 3.15. The reactions **10** with KCN and 18-crown-6 to yield [K(18-crown-6)][**10**·CN]. Hydrogen bonding is illustrated with red dashed lines. Close approaches of the oxygen atoms to the potassium atoms is illustrated in green dashed lines.

Bond/Angle	[K(18-crown-6)][10·CN]
B-C_{aryl}	1.660(6), 1.688(4)
B-C_{Fc}	1.661(6)
B-$C_{cyanide}$	1.634(6)
B-Fe	3.445(4)
$C_{cyanide}$-$N_{cyanide}$	1.144(6)
N_{amide}-N_{amine}	2.854(4), 4.371(3)
B-N_{amine}	4.830(6)
O_{amide}-K	2.706(3), 2.863(4)
C_{aryl}-B-C_{aryl}	109.8(3)
C_{aryl}-B-C_{Fc}	109.6(3), 115.9(3)
$C_{cyanide}$-B-C_{Fc}	115.3(3), 101.7(3)
$C_{cyanide}$-B-C_{aryl}	104.5(3)
Σ(C-B-C) excluding cyanide	335.3(9)

Table 3.3. Important bond lengths (Å) and angles (º) of the crystal structure of [K(18-crown-6)][**10**·CN].

Given that no quantitative comparison of the anion affinities of **8**, **9** or **10** for either cyanide or fluoride could be determined, the fact that **8**, **9** and **10** degrade in the presence of water, and that each appears to bind cyanide via an *inter*-molecular hydrogen bonding motif, further investigation into this class of compounds was halted. We thought to broaden our investigation from auxilliary hydrogen bonding motifs, to anion binding utilising (more pre-organized) Lewis acid chelation. In broadening our investigation from the utilisation of a proximal Brønstead acid to the utilisation of a proximal Lewis acid to afford selective binding, we sought to synthesise a library of *bis*-functionalised ferrocenyl systems.

3.5. Proximal Lewis Acids

The syntheses of a library of *bis*-functionalised ferrocenyl systems are summarised in Figure 3.16, with all yields ranging from moderate (46 %) through to quantitative. The preliminary work centred on the synthesis of mixed phosphine/boron Lewis-acid-functionalised ferrocene derivatives. It was of interest to synthesise both the 1,1' and 1,2 isomers of mixed boron/phosphine and boron/phosphonium systems, so as to be able to identify the effect of proximity on anion binding. The syntheses are summarised in Figure 3.16.

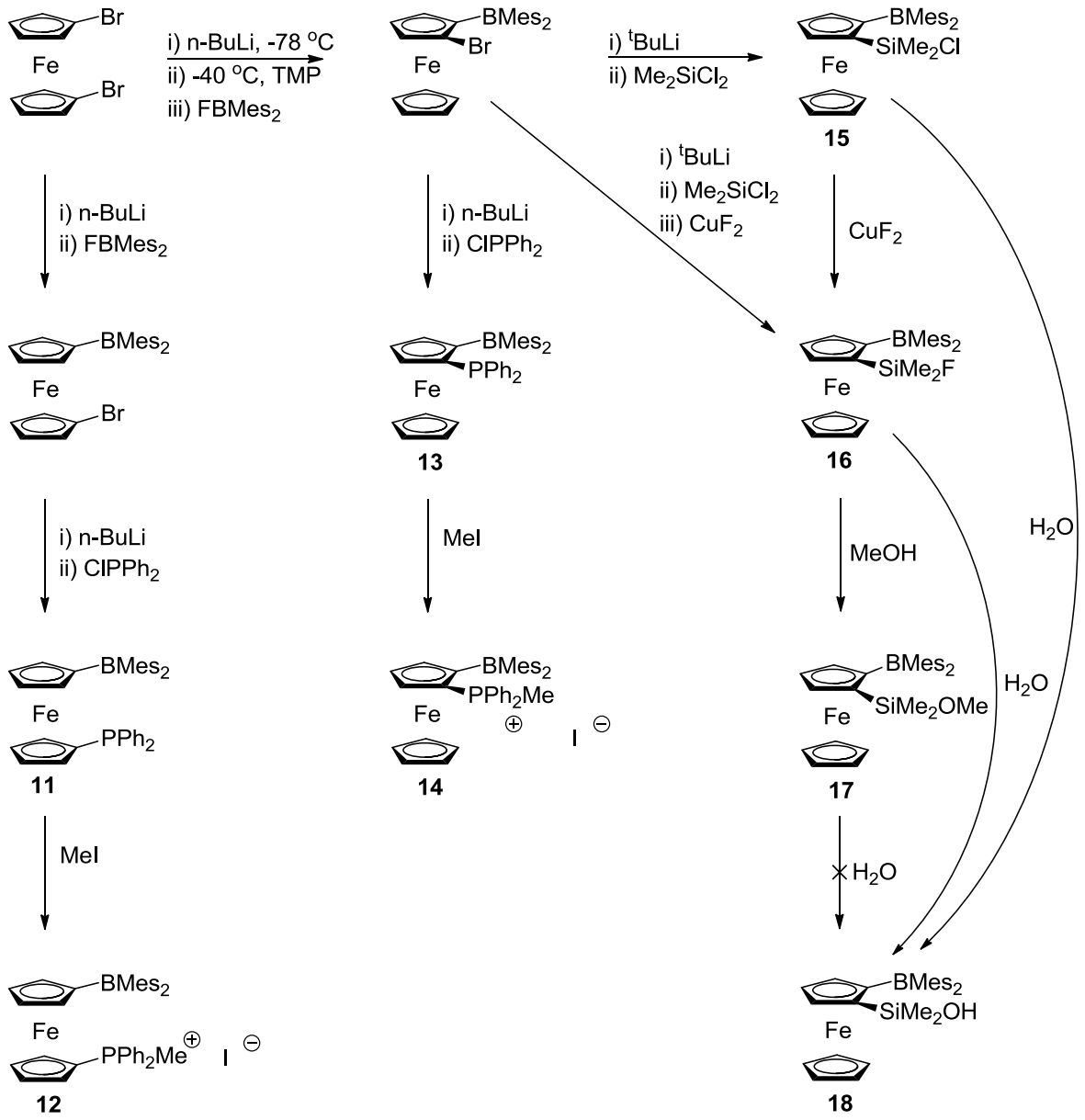

Figure 3.16 The syntheses of a range of difunctionalised ferrocenyl compounds (**11-18**).

3.5.1. Proximal Phosphorus-containing Lewis Acids

3.5.1.1. Syntheses of Proximal Phosphorus Lewis Acids

Wishing to explore the effect of an additional Lewis acid on the binding of fluoride and cyanide, we sought to exploit a ferrocenyl-bound boron as our primary site for anion binding, with the incorporation of an additional phosphonium function at either the 2- or the 1'-position relative to the $BMes_2$ unit. The literature compound 1,1'-fc($BMes_2$)(PPh_2) (**11**) was synthesised, although we exploited an alternative synthetic pathway (yield: 66%) due to the availability of the 1,1'-fc($BMes_2$)Br starting material (Figure 3.16). The ^{1}H, ^{11}B, ^{13}C and ^{31}P NMR spectra were fully consistent with the literature values.[32]

Conversion of **11** to the methylated compound, [1,1'-fc($BMes_2$)(PPh_2Me)]I (**12**) with iodomethane proved facile and proceeds in a quantitative fashion. The methylated compound thus obtained was fully characterised using a combination of ^{1}H, ^{13}C, ^{11}B and ^{31}P NMR spectroscopy and mass spectrometry. A peak at -22.4 ppm in the ^{31}P NMR spectrum is characteristic of a methylated, four-coordinate phosphonium system. The ^{11}B NMR spectrum exhibits a broad resonance at 81 ppm, that is indicative of a three-coordinate boron centre. The ^{1}H NMR spectrum exhibits a doublet centred at 2.43 ppm ($^{2}J_{H\text{-}P}$ = 13.5 Hz) that integrates to three protons, indicating that the methyl group is bound directly to the phosphorus centre. The ^{1}H and ^{13}C NMR spectra are also fully consistent with the proposed structure. Moreover accurate mass ESI-MS clearly reveals a peak corresponding to the

molecular ion, for added confirmation of identity. Single crystals suitable for X-ray diffraction were grown from d_1-chloroform solution layered with hexane (Figure 3.17). Selected bond lengths and angles are included in Table 3.4.

The three-coordinate nature of the boron centre suggested by analysis of the ^{11}B NMR spectrum in solution is present in the solid state. The sum of angles around boron is 359.9º, which, in concert with the absence of unremarkable shifts in the ^{1}H, ^{13}C and ^{31}P NMR spectra, suggests that there is no significant interaction between the phosphorus and the boron centres. This observation is, perhaps, unsurprising taking into account the fact that a phosphorus-boron distance of 5.229(5) Å is observed in the solid state.

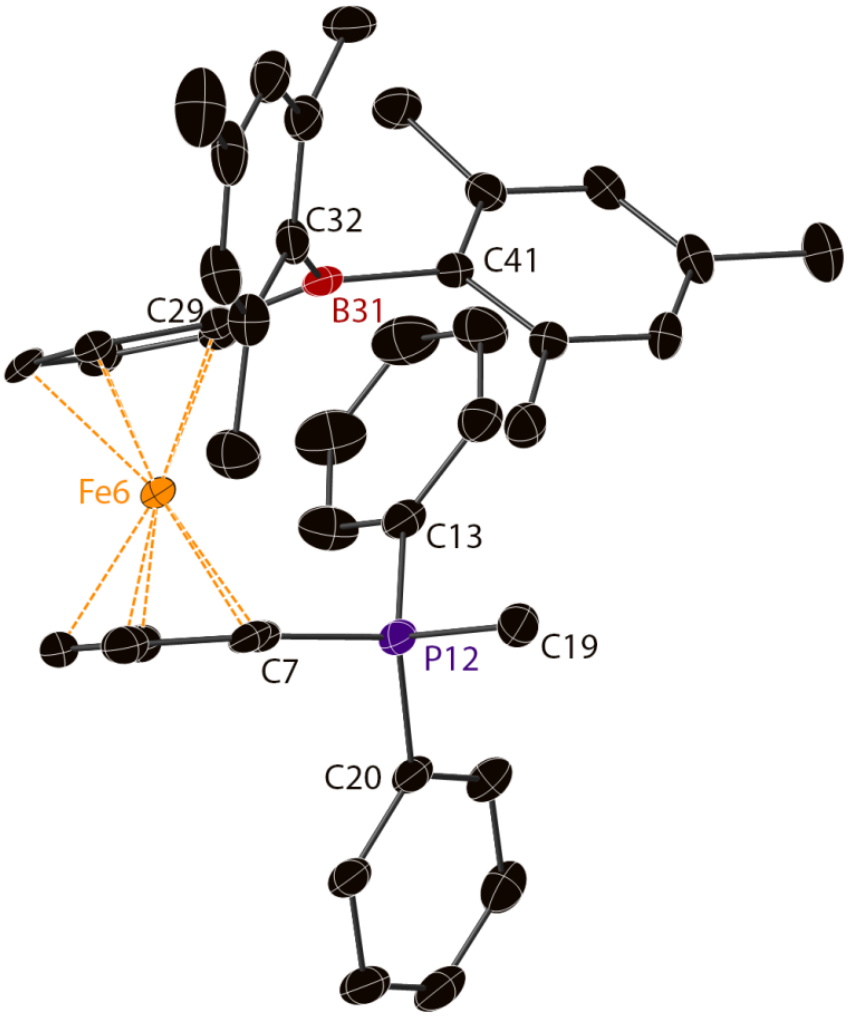

Figure 3.17 The crystal structure of **12**. Hydrogen atoms, Iodine anion and chloroform solvate molecule omitted for clarity. Thermal ellipsoids drawn at the 50% probability level. Boron in maroon, carbon in black, phosphorus in purple and iron in orange.

Bond/Angle	[1,1'-fc($BMes_2$)(PPh_2Me)]I·$CHCl_3$ (**12**·$CHCl_3$)
B-C_{aryl}	1.582(7), 1.589(7), 1.584(7), 1.594(7)
B-C_{Fc}	1.558(6), 1.553(6)
B-Fe	3.347(5), 3.365(5)
P-C_{alkyl}	1.781(5), 1.795(4)
P-C_{aryl}	1.785(5), 1.788(4), 1.795(4), 1.780(4)
P-C_{Fc}	1.781(5), 1.768(5)
P-Fe	3.474(2), 3.450(1)
B-P	5.229(5), 5.076(5)
B-C_{PMe}	4.743(9), 4.779(7)
H-I	2.89, 2.86, 2.95, 2.82
C_{aryl}-B-C_{aryl}	123.5(4), 121.4(4)
C_{aryl}-B-C_{Fc}	118.7(4), 117.7(4), 120.0(4), 118.4(4)
C_{Me}-P-C_{Aryl}	109.6(2), 109.6(3), 111.4(2), 109.5(2)
C_{Me}-P-C_{Fc}	108.5(3), 107.6(2)
C_{aryl}-P-C_{aryl}	109.8(2), 106.4(2)
C_{aryl}-P-C_{Fc}	106.9(2), 112.4(2), 111.8(2) , 110.1(2)
Σ(C-B-C)	360, 360
Σ(C-P-C) (excluding C_{PMe})	329, 328
$Cp_{centroid}$-C_{ipso}-B	175.85, 174.25
$Cp_{centroid}$-C_{ipso}-P	173.27, 176.42
Plane Cp_B - Plane Cp_P	7.26, 8.07
Torsion (B-$Cp_{centroid}$-$Cp_{centroid}$-P)	-76.10, 68.47 (two different chiralities)

Table 3.4. Pertinent bond lengths (Å) and angles (º) for [1,1'-fc($BMes_2$)(PPh_2Me)]I·$CHCl_3$ (**12**·$CHCl_3$).

The phosphorus centre is approximately tetrahedral with C-P-C angles ranging from 106.9(2)º through to 112.4(2)º. The largest angle of 112.4(2)º corresponds to the angle between the *ipso*-carbon (C51) of the ferrocenyl fragment and the *ipso*-carbon (C57) of a phenyl group orientated towards the $BMes_2$ unit. The distortion in the bond angle from the ideal value of 109.5º for this group can be rationalised by taking into account the steric repulsion between the -$BMes_2$ and the -PPh_2Me^+ units. This significant steric repulsion is not, however, reflected in the room temperature ^{1}H NMR spectrum of this compound, which shows equivalence of both *para* and all *ortho*-CH_3 groups on the NMR timescale, indicative of fast rotation about the ferrocenyl and both mesityl C-B bonds on the NMR timescale. The presence of a weak hydrogen bond between one of the hydrogen atoms of the methyl group of the -PPh_2Me^+ moiety and the iodide counter-ion is indicated by a bond distance of 3.06 Å, which is within the sum of the Van der Waals radii of these two elements.

The isomeric systems derived from 1,2-fc($BMes_2$)(PPh_2) (**13**) were synthesised following the procedure of Aldridge and co-workers (Scheme 3.2.8). [37]. Reaction of **13** with an excess of iodomethane allowed for the synthesis of the novel phosphonium salt [1,2-fc($BMes_2$)(PPh_2Me)]I, **14**. The methylation of **13** to **14** was observed to take longer than that of the 1,1' isomer (48 h vs. 15 h respectively), which presumably arises from the sterically more demanding environment about the phosphorus centre in **13**. Spectroscopically, the ^{11}B NMR spectrum of **14** exhibits a broad resonance at 81 ppm, typical of the three coordinate boron centres of $FcBMes_2$ systems.[38] The ^{31}P NMR spectrum features a resonance at -20.6 ppm, typical of a four coordinate phosphonium unit. in a similar fashion to **12**, the ^{1}H NMR spectrum exhibits a doublet resonance centred at 2.55 ppm ($^2J_{H\text{-}P}$ = 12.0 Hz) that integrates to

three protons and corresponds to a methyl group directly bound to a phosphorus atom. The remaining features of the ^{1}H and ^{13}C NMR spectra are fully consistent with the structure shown in Scheme 3.2.8. Confirmation of identity was provided by accurate mass ESI-MS, which reveals a peak corresponding to the molecular ion. Attempts to grow crystals suitable for single crystal structural elucidation were unsuccessful.

Analysis of the ^{1}H NMR spectrum of **14** highlights the increased steric demands of the 1,2-disubstituted isomer compared to its 1,1' counterpart. The signals for all the *para* and *ortho*-CH_3 groups of the mesityl unit are broadened into one broad multiplet for the 1,2-isomer in the ^{1}H NMR spectrum, which suggests that the rate of rotation around the ferrocenyl-boron and mesityl-boron bonds is comparable to that of the NMR measurement timescale. The resonances are noticeably broader than is the case for **12**. The barrier to rotation about the B-C_{aryl} bond for [1,2-fc($BMes_2$)(PPh_2Me)]I (**14**) was estimated by variable temperature NMR analysis by calculating the rate constant for rotation at the coalescence temperature. The barrier to rotation was thus calculated to be $\Delta G^{\ddagger}$ = 59 kJ mol^{-1}, which is higher than that seen for 1,2-fc($BXyl)_2$ ($\Delta G^{\ddagger}$ = 42.2 kJ mol^{-1}),[19] indicating that the -PPh_2Me moiety is more a sterically demanding molecular fragment than the corresponding -$BXyl_2$ substituent.[28]

3.5.1.2. NMR Studies of Anion Binding of Proximal Phosphorus Lewis Acids

Once viable synthetic routes had been established, the responses to exposure to either cyanide or fluoride of the cationic borane/phosphonium systems **12** and **14** were investigated;

the corresponding anion binding capabilities of the neutral phosphine precursors **13** and **11** were also examined for comparative purposes.

The reaction of 1,1'-fc($BMes_2$)(PPh_2) (**11**) with one equivalent of 18-crown-6 and ten equivalents of either potassium fluoride or potassium cyanide proceeds cleanly, as indicated by multinuclear NMR spectroscopy. The reaction is accompanied by a colour change from red to yellow for both anions. In the case of the cyanide adduct [**11**·CN]$^-$, a diagnostic peak at -16 ppm was observed in the ^{11}B NMR spectrum. The fluoride adduct [**11**·F]$^-$ exhibits a typically broad signal at 5 ppm in the ^{11}B NMR spectrum and a broad unresolved resonance at 174 ppm in the ^{19}F NMR. These NMR spectra show that the boron centre binds the anion in each case, leading to an increase in the coordination number to four. In each case, the ^{31}P NMR signal corresponding to the PPh_2 function remains little changed from that observed for the free receptor with a chemical shift of *ca.* -15 ppm. Mass spectrometry provides further evidence for the adduct formation, with the molecular ion [**11**·F]$^-$ observed in the ESI spectrum, with confirmation by high resolution measurements.

The reaction of the methylated phosphonium cation **14** with 18-crown-6 and either potassium cyanide or potassium fluoride under analogous conditions proceeds cleanly, as indicated by multinuclear NMR spectroscopy. The reaction is accompanied by a colour change from red to yellow for either anion. The ^{11}B NMR spectrum for both adducts illustrate the four-coordinate nature of the boron centre, with a characteristic sharp singlet at -16 ppm for the cyanide adduct **14**·CN and a broad signal at 5 ppm for the fluoride adduct **14**·F. The broad signal at -175 ppm in the ^{19}F NMR spectrum of the fluoride adduct **14**·F suggests the

presence of a single bond between the fluoride and the boron-centre and the absence of any auxiliary binding motif.[39] As with the non-methylated derivative, the ^{31}P NMR signal corresponding to the PPh_2Me^+ function is little changed from that of the free receptor, with a chemical shift of *ca.* 22 ppm. This observation suggests that in both cases, there is little perturbation of the phosphorus centre upon binding of the anion. Analysis of the mass spectra further substantiate the conclusion that a one-to-one adduct had been formed during this reaction, as the molecular ions of **14**·F and **14**·CN were observed in the ESI spectra and their identity confirmed via high resolution measurements.

The reaction of isomeric [1,2-fc($BMes_2$)(PPh_2Me)]I (**12**) with one equivalent of 18-crown-6 and ten equivalents of potassium cyanide is also accompanied by a colour change from orange-red through to yellow. The ^{11}B NMR spectrum exhibits a peak at -16 ppm for the cyanide adduct **12**·CN, which is indicative of the presence a four-coordinate boron-centre. Unlike either **11** or **14**, the ^{31}P NMR spectrum of **12**·CN, however exhibits a significant shift on cyanide binding (from 20.8 ppm for the receptor to 31.4 ppm in the adduct), which is implies a perturbation of the phosphorus centre. In the absence of a crystal structure, the nature of this interaction (be it electrostatic or involving significant orbital overlap) cannot be definitively established, although a σ*-π interaction between the phosphorus centre and cyanide comparable to that found in the adduct [1,2-C_6H_4($BMes_2CN$)(SMe_2)]$^-$ cannot be ruled out.[40]

The reaction of **12** with fluoride under analogous conditions is also accompanied by a gradual colour change to yellow. The ^{11}B NMR spectrum of the fluoride adduct **12**·F exhibits a broad peak at 5 ppm, and its ^{31}P resonance shows a marked shift on binding fluoride, from 20.8 ppm for the receptor to a doublet at 28.6 ppm ($^{1}J_{P\text{-}F}$ = 8.6 Hz) for the adduct. The ^{19}F NMR spectrum is also markedly different than that recorded for each of the fluoride adducts [**11**·F]$^{-}$ and **14**·F, being shifted upfield by approximately 17 ppm (to a broad multiplet at -158 ppm). The identity of the adduct is also confirmed using mass spectrometry as the molecular ion [**12**·F]$^{-}$ was observed in the ESI mass spectrum, with the identity confirmed by high resolution accurate mass spectrometry.

A range of decoupling experiments were performed to probe the nature of **12**·F in solution. The ^{19}F NMR spectrum exhibits a broad signal, which noticeably sharpened on decoupling to boron, although not to a well-resolved doublet. The ^{31}P{^{1}H} NMR spectrum features a doublet ($^{1}J_{P\text{-}F}$ = 8.6 Hz), and the ^{31}P{^{19}F} NMR spectrum a broadened quartet ($^{2}J_{P\text{-}H}$ = 30 Hz), which is indicative of coupling to the three protons of the phosphorus bound methyl group (Figure 3.18). The ^{13}C NMR spectrum also features a diagnostic pattern for the methyl carbon atom, namely a doublet of doublets, with coupling both to phosphorus ($^{1}J_{C\text{-}P}$ = 64.0 Hz) and fluorine ($^{2}J_{C\text{-}F}$ = 20.0 Hz), which in turn suggests retention of the interaction between the phosphonium moiety and the boron-bound fluorine.

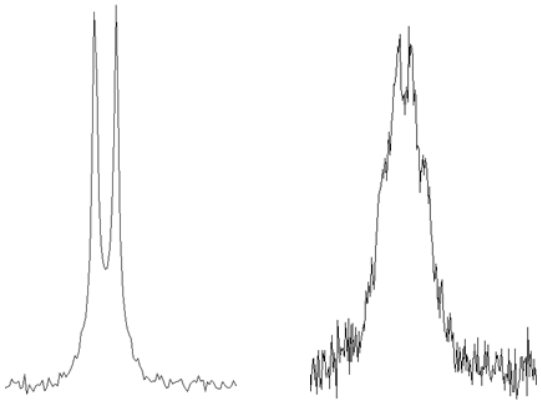

Figure 3.18. The $^{31}P\{^{1}H\}$ NMR spectrum of **12**·F illustrating coupling to the bound fluoride anion (J= ½) (left) and the $^{31}P\{^{19}F\}$ NMR spectrum of **12**·F illustrating coupling to the three protons of the phosphorus bound methyl group (J = ½) (right).

In the absence of a definitive crystal structure determination of the fluoride adduct, discussion of the exact nature of the interaction must necessarily be speculative. However, the chemical shifts observed for this system (δ_B = 5 ppm, δ_F = -158 ppm) show a remarkable similarity to those exhibited by Gabbai's fluoride adduct [1,2-C_6H_4($BMes_2F$)(PPh_2Me)]$^-$ (δ_B= 5.7 ppm, δ_F = -158 ppm).[41] This fact could well imply that both systems bind fluoride in an analogous fashion, whereby the fluoride anion is chelated by between the boron and phosphorus centres. The nature of the interaction between the phosphorus centre and fluoride is expected to be dominated by donation of electron density into the σ* orbital of the phosphorus-methyl bond. With this in mind, the most obvious difference between the two systems is the size of the P-F coupling constant, with **12**·F exhibiting a J value of 8.6 Hz and [1,2-C_6H_4($BMes_2F$)(PPh_2Me)]$^-$ 24.3 Hz.[41] This difference suggests that the interaction between the phosphonium function and fluoride is weaker in our system, which would be

consistent with a greater separation between the phosphorus and boron centres in **12**·F (r_2) than in [1,2-C_6H_4($BMes_2F$)(PPh_2Me)]$^-$ (r_1), due to the differing geometries enforced by the different backbone ring sizes (Figure 3.19).

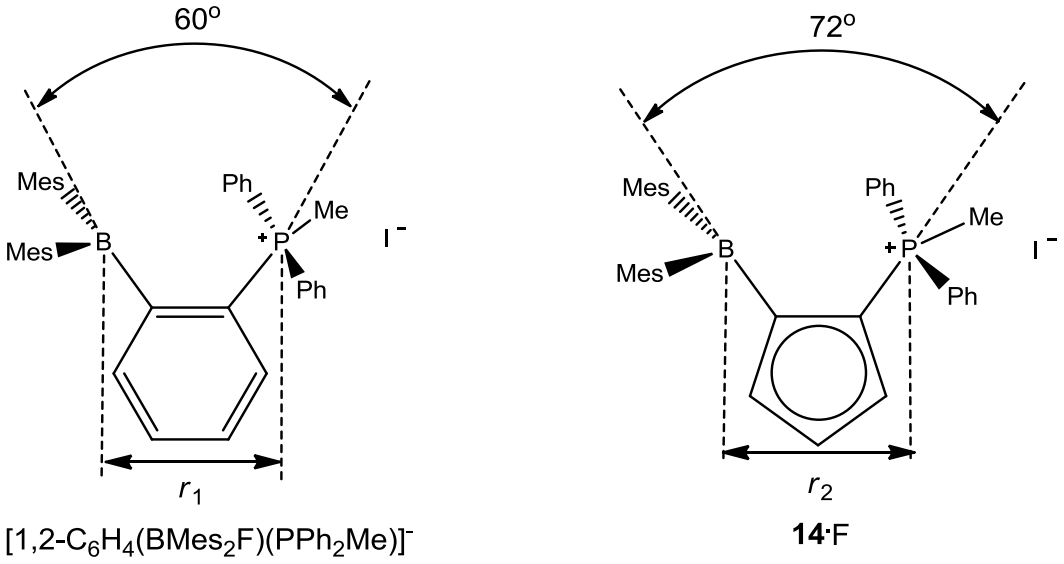

Figure 3.19. The geometries of **14** and that of 1,2-C_6H_4($BMes_2$)(PPh_2Me).[41]

Unlike the free receptor, the ^{1} NMR spectra of both the cyanide and fluoride adducts, **12**·CN and **12**·F, exhibit very well resolved signals for the mesityl groups at 25 ºC. The *ortho*- and *para*-CH_3 groups are separated into six separate signals, each of which is integrated as three protons. This observation suggests the presence of a higher barrier to rotation around both the ferrocenyl- and mesityl-boron bonds for the adducts **12**·CN and **12**·F compared to that found for the free receptor **12**. This interpretation would be in good agreement with an increase in steric bulk at the boron atom on transitioning from a three-coordinate to a four-coordinate system. Variable temperature ^{1}H NMR studies conducted on the cyanide adduct

12·CN showed that these signals remain inequivalent up to 60 ºC, suggesting the existence of a high barrier to rotation ($\Delta G^{\ddagger} > 80$ kJ mol^{-1}), which presumably reflects the high degree of steric bulk borne by the boron centre. In comparison, the fluoride adduct **12**·F exhibits a lower barrier to rotation ($\Delta G^{\ddagger} = 66.6$ kJ mol^{-1}) for both mesityl-boron bonds (Figure 3.20). This barrier to rotation is not connected to the B-F-P interaction, and merely reflects the steric loading around the mesityl groups.

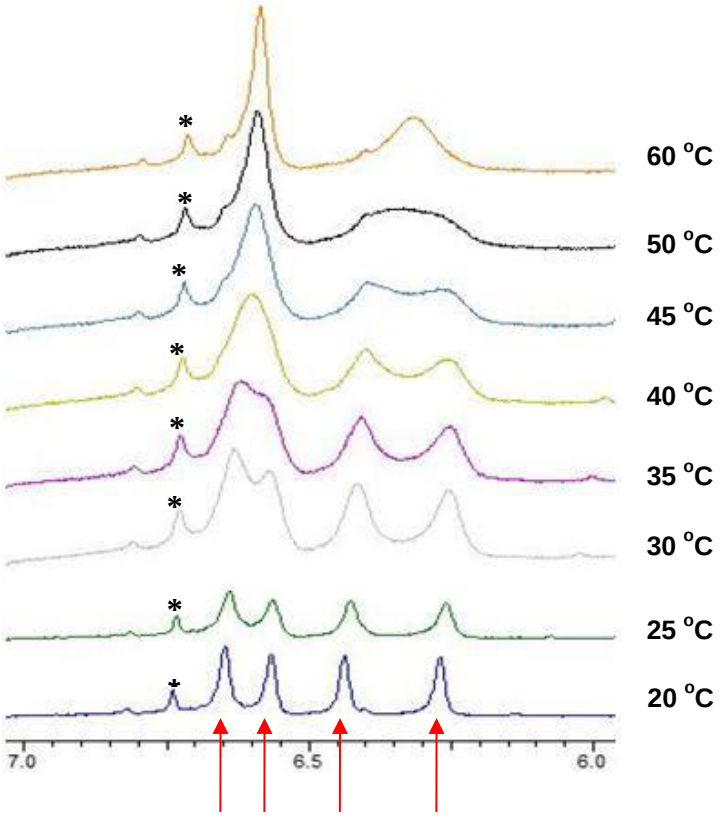

Figure 3.20. The *meta*-CH region of the ^{1}H NMR spectrum of **12**·F in $CDCl_3$ over a range of temperatures. The peaks marked * indicate an impurity.

3.5.1.3. UV-Vis Titration and Competition Studies of Anion Binding of Proximal Phosphorus Lewis Acids

Since all the 1,2-functionalised systems exhibit a marked colour change upon binding one equivalent of either fluoride or cyanide, it was of interest to explore the potential for these systems to act as selective colorimetric sensors for these two anions. In order to gauge the anion association constants of these systems, titrations were performed using UV-Vis spectra to determine the relative concentration of free receptor to adduct (see chapter two for a description of the standard test protocol and Table 3.5 for a summary of the results of the tests carried out). All three receptors were shown to bind only one equivalent of either fluoride or cyanide anions – representative spectra for **12** together with the titration curve and predicted speciation plot are included in Figures 3.21-22. The fluoride/cyanide binding constant data for all three systems are summarized in Table 3.5.

Receptor	K_{CN} (M^{-1})	K_F (M^{-1})
1,1'-fc($BMes_2$)(PPh_2), 11	$6.3(0.4) \times 10^4$	$4.5(0.4) \times 10^4$
[1,1'-fc($BMes_2$)(PPh_2Me)]I, 12	$1.0(0.4) \times 10^6$	$8.2(4.0) \times 10^6$
[1,2-fc($BMes_2$)(PPh_2Me)]I, 14	$1.1(0.1) \times 10^6$	$4.2(1.5) \times 10^6$

Table 3.5. Anion binding constants determined in THF.

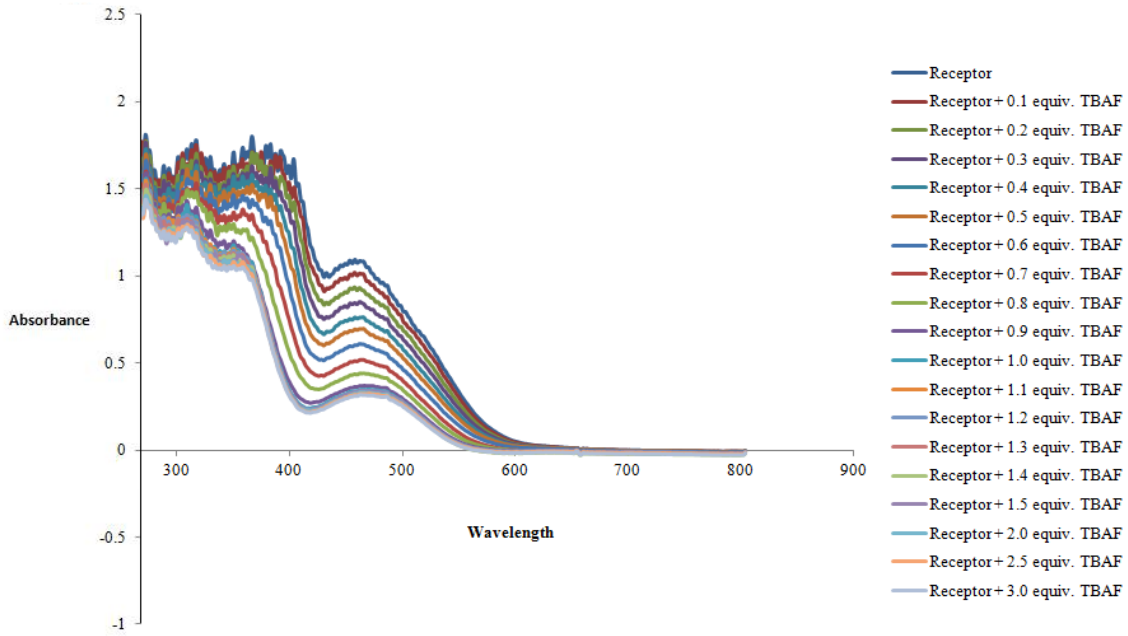

Figure 3.21. Changes in the UV-Vis spectrum of **12** upon sequential addition of aliquots of $[^{n}Bu_4N]F{\cdot}3H_2O$.

As can be seen from Table 3.5, phosphonium borane **12** gives rise to binding constants approximately two orders of magnitude greater than that determined for its charge neutral counterpart **11**, for both cyanide and fluoride anions. Given the lack of perturbation of the phosphorus centre in these adducts implied by their NMR spectra, this can probably be largely ascribed to Coulombic effects. For the isomeric phosphonium receptors, it might be expected that, on transitioning from the 1,1'-disubstituted system (**12**) to its 1,2-disubstituted counterpart (**14**), the increase in steric bulk that accompanies anion binding would be less readily accommodated. Consequently, on a steric basis alone, one might expect a higher binding constant for the 1,1'-isomer. However, as the Coulombic force is proportional to r^{-2}, and the phosphonium centre is likely to be closer to the primary borane binding site in the 1,2

isomer, electrostatic factors would favour stronger binding by **14**. The situation is complicated further by the auxillary binding motif exhibited by the **14** in the presence of fluoride. These competing factors presumably underpin the observation, then, that there is little difference between **12** and **14** in their affinities for either anion.

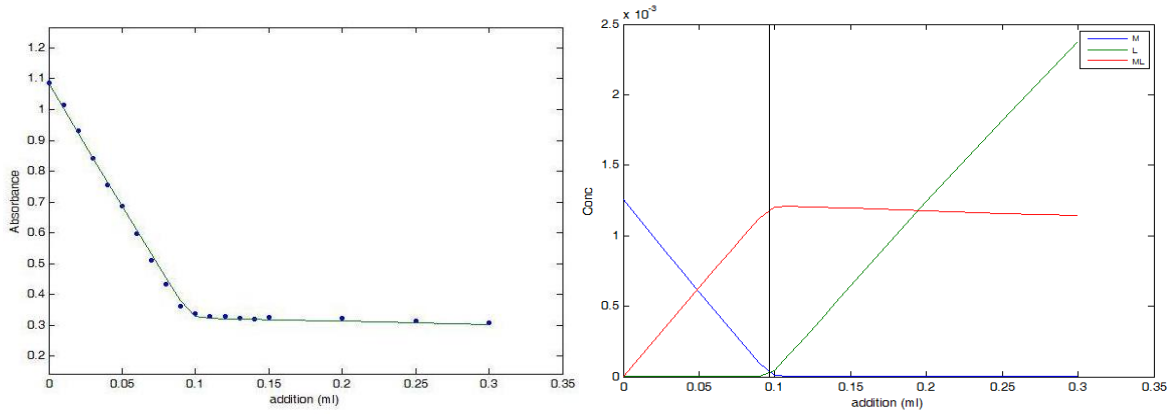

Figure 3.22. (left) Representative example of anion binding isotherm, based on UV-Vis measurements on sequential additions of aliquots of $[^nBu_4N]F{\cdot}3H_2O$ to a solution of **12** in THF solution. Key - points: experimental measurement; line: best calculated fit. (right) Calculated changes in concentrations of receptor **12** (blue), adduct **12**·F (red) and $[^nBu_4N]F{\cdot}3H_2O$ (green).

For all three receptors, the difference between the binding constants for fluoride and cyanide is small. Therefore, competition experiments were performed on an NMR scale to confirm that the relative affinities for the two anions are in line with that predicted from UV-Vis titration (Table 3.6). These tests show that excess cyanide reacts with $[\mathbf{11}{\cdot}F]^-$ to give the corresponding cyanide adduct $[\mathbf{11}{\cdot}CN]^-$. The converse reaction of $[\mathbf{11}{\cdot}CN]^-$ with an excess of fluoride did not lead to a reaction. Moreover, the reaction of the free receptor with equimolar

cyanide/fluoride led to exclusive formation of the cyanide adduct. Hence, we can conclude that **11** binds cyanide more strongly than fluoride.

The results for the competition reactions for the adducts **12**·CN and **12**·F are less clear, and presumably complicated by kinetic factors. On the addition of excess cyanide anions to **12**·F, no significant change was observed after 1 h. However, after 24 h, a roughly one-to-one ratio of **12**·F and **12**·CN was observed. The addition of excess fluoride anions to **12**·CN did not show any discernible formation of **12**·F after 24 h. The slow kinetics of exchange can presumably be accounted for by the high anion binding strength of **12** (as compared to **11**) as the mechanism of anion exchange presumably requires first the loss of the bound anion before the second anion can compete for the free borane (i.e. S_N1-like rather than S_N2). As the binding strength of **12** is high for both anions, the concentration of free **12** in these cross-over experiments is assumed to be very low, and hence provides a kinetic impediment to anion exchange. The competition experiments for receptor **14** show that treatment of **14**·F with excess cyanide did not result in any change in the ^{1}H or ^{11}B NMR spectra after 24 h, nor did treating **14**·CN with excess fluoride anions. Treating **14** with a one-to-one mixture of fluoride and cyanide anions led primarily to the formation of adduct **14**·F (0.83 equiv.), but also **14**·CN (0.17 equiv.). It is therefore difficult to attribute the anion binding preferences of either **12** or **14** to solely thermodynamic or kinetic effects.

Receptor	Fluoride adduct + excess cyanide	Cyanide adduct + excess fluoride	Receptor plus a one-to-one ratio of fluoride and cyanide
1,1'-fc($BMes_2$)(PPh_2) (11)	Complete displacement	No reaction	Exclusive formation of the cyanide adduct
[1,1'-fc($BMes_2$)(PPh_2Me)]I (12)	One-to-one mixture of adducts formed	No reaction	Two-to-one mixture of the fluoride adduct to the cyanide adduct
[1,2-fc($BMes_2$)(PPh_2Me)]I (14)	No reaction	No reaction	Five-to-one mixture of the fluoride adduct to the cyanide adduct.

Table 3.6. Results of ^{1}H and ^{11}B NMR spectroscopic studies of anion binding competition experiments.

3.5.2. Proximal Silicon Lewis Acids

3.5.2.1. Syntheses and Characterization of Proximal Silicon Lewis Acids

Given the precedent for use of silane functions as auxilliary Lewis acid binding sites, we sought to probe the use of such groups as charge-neutral alternatives to the phosphonium group in bidentate receptors. Accordingly, the silyl-appended borane 1,2-fc($BMes_2$)($SiMe_2Cl$) (**15**) be synthesised in good overall yield from the known compound 1,2-fc($BMes_2$)(Br) (Figure 3.16). The ^{11}B NMR spectrum of **15** features a peak at 82 ppm consistent with a three

coordinate borane, and the ^{29}Si NMR spectrum a signal centred at 24.5 ppm, consistent with a ferrocene bound $SiMe_2Cl$ unit. The ^{1}H and ^{13}C NMR spectra of **15** are also fully consistent with the structure shown in Figure 3.16, and the mass spectrum shows the molecular ion peak with the expected isotopic distribution.

Attempts to convert **15** to 1,2-fc($BMes_2$)($SiMe_2F$) (**16**) proved non trivial, with a successful route being developed using CuF_2. This reagent is a sufficiently mild fluorinating reagent so as not to give the fluoride adduct [**16**·F]$^-$, although reaction times have to be kept short to minimise side reactions giving a paramagnetic material presumably formed by oxidation of the ferrocene centre by Cu^{2+}. The ^{11}B NMR spectrum of **16** exhibits a broad resonance at 83 ppm, typical of a three coordinate borane, while the ^{19}F NMR spectrum shows septet with silicon satellites centred at -152 ppm, indicative of coupling to silicon ($^{1}J_{F\text{-}Si}$ = 275 Hz) and the two sets of three protons corresponding to the two methyl groups ($^{2}J_{H\text{-}F}$ = 7.0 Hz for both groups). The ^{29}Si NMR spectrum features a doublet centred at 23.4 ppm, with the coupling to the silicon-bound fluorine being consistent with a direct Si-F bond ($^{1}J_{F\text{-}Si}$ = 275 Hz). The ^{1}H and ^{13}C NMR spectra are also fully consistent with the structure shown in Figure 3.16.

The synthesis of 1,2-fc($BMes_2$)($SiMe_2OMe$) (**17**) was achieved by treating **15** with methanol (Figure 3.23). In similar fashion to **16**, the ^{11}B NMR spectrum of **17** exhibits a broad peak at 87 ppm typical of a three coordinate borane, and the ^{29}Si NMR spectrum features a peak at 11 ppm consistent with a ferrocene appended $SiMe_2OMe$ group. The ^{1}H

and ^{13}C NMR spectra are also fully consistent with the structure shown in Figure 3.23. The molecular ion was observed in mass spectrometry studies of **17**.

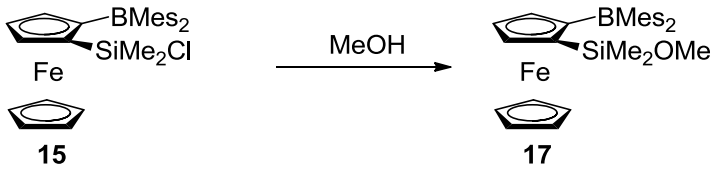

Figure 3.23. The synthesis of 1,2-fc($BMes_2$)($SiMe_2OMe$) (**17**).

Single crystals of **17** were grown from a saturated solution in hexamethdisiloxane, and analysed by X-ray crystallography (Figure 3.24). A list of bond distances and angles of the crystal structure of **17** are included in Table 3.7: none of these deviates markedly from expected values. Thus, the sum of the angles (ΣC-B-C) around boron is 358.9(6)º as would be expected for a three coordinate borane. Of note is the B···Si distance of 3.660(3) Å, which compares to a B···B distance of 3.702 Å in 1,2-fc$(BMes_2)_2$.[28]

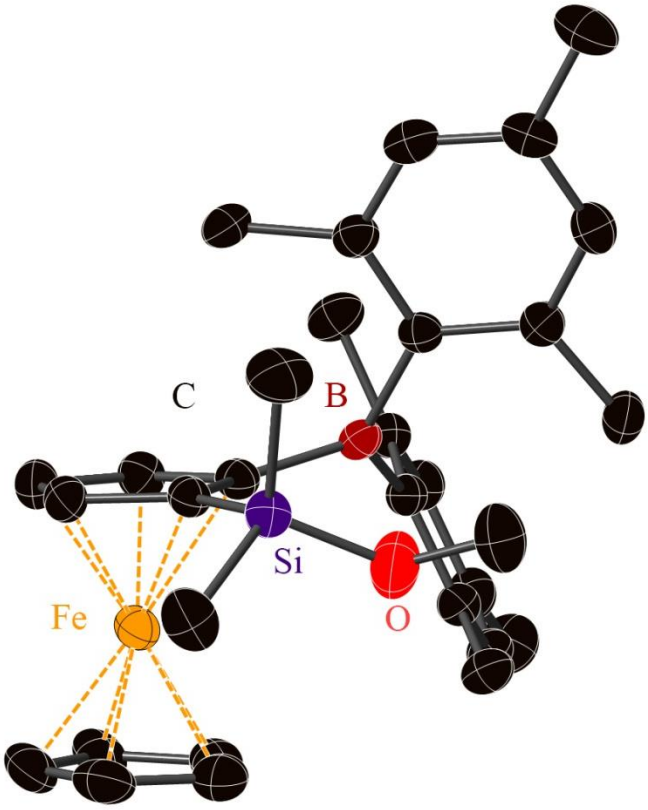

Figure 3.24. The crystal structure of **17**. The hydrogen atoms have been omitted for clarity. Ellipsoids are drawn at the 50% probability level, with boron in maroon, carbon in black, silicon in purple and iron in orange.

Bond/Angle	
B-C_{aryl}	1.587(3), 1.585(3)
B-C_{Fc}	1.572(3)
B-Fe	3.432(2)
B-Si	3.660(3)
B-O	3.352(3)
Si-C_{Me}	1.894(3), 1.855(3)
Si-C_{Fc}	1.844(2)
Si-Fe	3.4920(7)
Si-O	1.640(2)
O-C_{Me}	1.388(3)
C_{Mes}-B-C_{Mes}	122.2(2)
C_{Mes}-B-C_{Fc}	119.8(2), 116.9(2)
C_{Me}-Si-C_{Me}	107.8(1)
C_{Me}-Si-C_{Fc}	111.2(1), 109.9(1)
C_{Me}-Si-O	110.0(1), 111.9(1)
C_{Fc}-Si-O	106.0(1)
Si-O-C_{Me}	127.3(2)
Σ(C-B-C)	358.9(6)
Σ(C-Si-C)	328.9(3)
Torsion (B-C_{Fc}-C_{Fc}-Si)	+17.0(3)

Table 3.7. Pertinent bond lengths (Å) and angles (º) of 1,2-fc($BMes_2$)($SiMe_2OMe$) (**17**).

3.5.2.2. NMR Studies of Anion Binding by Proximal Silicon Lewis Acids

Various NMR studies of the reactions of 1,2-fc($BMes_2$)($SiMe_2Cl$) (**15**) with cyanide and fluoride anion sources were conducted. When **15** was treated with one equivalent of [$^nBu_4N$]F·$3H_2O$ in acetonitrile-d_3 the predominant product formed was 1,2-fc($BMes_2$)($SiMe_2F$) (**16**), along with unreacted **15** and [K(18-crown-6][**17**·F]. When **15** was treated with a ten-fold excess of KF and one equivalent of 18-crown-6 in acetonitrile-d_3 this resulted in clean conversion to [K(18-crown-6][**16**·F]. The reaction of **15** with sources of the cyanide anion resulted in a colour change to yellow and a new signal in the ^{11}B NMR spectrum at -13 ppm, typical of ferrocene appended $BMes_2CN^-$ unit. The ^{1}H NMR spectrum of this reaction mixture, however, is complicated, implying that a range of compounds were formed. It is possible that the cyanide partially replaces the silicon bound chloride in a similar fashion to the fluoride anion. Attempts to isolate clean products from this mixture proved unsuccessful. Given the complexity of the reactions of **15** with either cyanide and fluoride, no meaningful UV-Vis binding data could be obtained, nor were NMR anion competition studies attempted.

The fluorosilyl receptor 1,2-fc($BMes_2$)($SiMe_2F$) (**16**) is competent at binding both fluoride and cyanide in acetonitrile-d_3 and this binding event is transduced into a colour change from red to yellow for both anions. When **16** was treated with one equivalent of potassium cyanide and one equivalent of 18-crown-6 in chloroform-d_1, acetonitrile-d_3 or toluene, the result was the formation of the cyanide adduct [**16**·CN]$^-$ (Figures 3.25-26). The ^{11}B NMR spectrum exhibits a peak at -16 ppm, which is consistent with the formation of a

ferrocene appended -$BMes_2CN^-$ unit. The ^{19}F NMR spectrum, however, shows a septet at -149.3 ppm ($^3J_{F\text{-}H}$ = 7.8 Hz), close to the value of the free receptor **16** (-152.0 ppm, $^3J_{F\text{-}H}$ = 7.0 Hz), which confirms that the fluoride group has not been displaced from silicon. This is further substantiated by a ^{29}Si NMR spectrum that shows a doublet centred at 27.5 ppm ($^1J_{Si\text{-}F}$ = 260 Hz), again similar to that of the free receptor **16** (23.4 ppm (d, $^1J_{F\text{-}Si}$ = 275 Hz)). The implication of the ^{19}F and ^{29}Si NMR spectra is that the $SiMe_2F$ group does not interact greatly with the boron bound cyanide anion, which is not unexpected given the relative sizes of the cyanide ion and the B···Si cavity.

The ^1H NMR spectrum of [**16**·CN]$^-$ exhibits four separate signals for the *meta*-CH protons of the mesityl groups, unlike the free receptor **16** that has four equivalent *meta*-CH protons. This suggests that the increased steric demands of binding the cyanide anion have imposed a greater barrier to rotation around the B-C_{ipso} and the B-C_{Fc} bonds. The ^{13}C NMR spectrum is fully consistent with the postulated structure. The mass spectrum of [**16**·CN]$^-$ exhibits a well-defined molecular ion envelope.

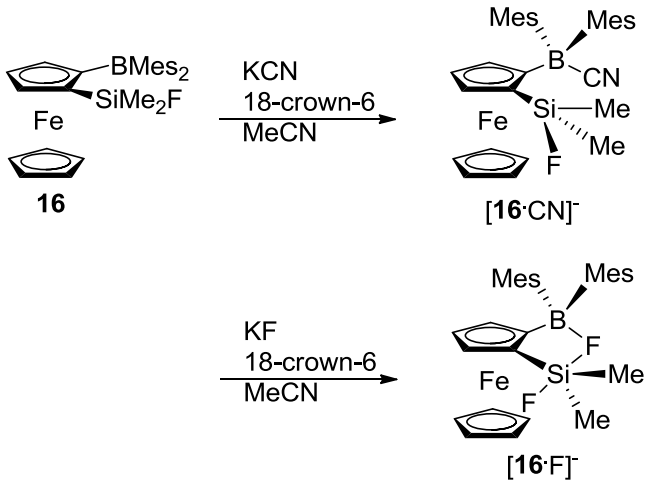

Figure 3.25. The binding of fluoride and cyanide anions by **16**.

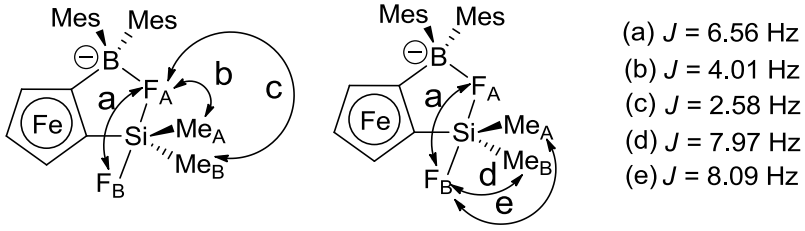

Figure 3.26. Diagnostic coupling constants for [**16**·F]$^-$.

When **16** was treated with one equivalent of potassium fluoride and one equivalent of 18-crown-6 in chloroform-d_1 the result was a mixture of unreacted **16** and the fluoride anion adduct [**16**·F]$^-$. In acetonitrile-d_3 solution, the same reaction proceeds to give [**16**·F]$^-$ cleanly (Figure 3.25). When this adduct was isolated as, an orange solid and then re-dissolved in chloroform-d_1, the red solution was shown by ^{1}H, ^{11}B and ^{19}F NMR spectroscopic studies to be composed of both free receptor **16** and fluoride adduct [**16**·F]$^-$. This reversibility of fluoride binding, that was not exhibited by the cyanide adduct, possibly suggests that the receptor **16** binds cyanide more strongly than fluoride.

The ^{11}B NMR spectrum of [**16**·F]$^-$ in $CDCl_3$ exhibits a broadened doublet centered at 5 ppm ($^1J_{B\text{-}F}$ = 85 Hz), typical of a ferrocene appended -$BMes_2F^-$ unit, and comparable to the resonance observed for [K(18-crown-6)][1,2-fc{($BMes_2$)(μ-F)($SnMe_2F$)}] (6 ppm).[29] The ^{29}Si NMR spectrum features a doublet of doublets centred at 25.2 ppm, clearly showing coupling to two NMR inequivalent fluorine atoms ($^1J_{F\text{-}Si}$ = 190 Hz, $^1J_{F\text{-}Si}$ = 70 Hz).

The ^{19}F NMR spectrum of [**16**·F]$^-$ exhibits two separate resonances, a broad signal centered at -164.6 ppm corresponding to the boron bound, chelating fluoride anion and a septet centered at -153.3 ppm corresponding to the solely silicon bound fluoride. The latter exhibits coupling to the six protons of the methyl groups of $SiMe_2F$ ($^3J_{F\text{-}H}$ = 8.0 Hz). This parallels the ^{19}F NMR spectrum of [K(18-crown-6)][1,2-fc{($BMes_2$)(μ-F)($SnMe_2F$)}] in acetonitrile-d_3, that exhibits broad resonances at -169.8 and -171.6 ppm, and exhibits better resolved peaks at -183.5 and -184.2 ppm (two sets arise due to diasteroisomerism for the tin complex that we do not observe for [**16**·F]$^-$).[29]

The ^{1}H NMR spectrum of [**16**·F]$^-$ provides further evidence that the fluoride anion is chelated by both borane and silane groups in a similar manner to [1,2-fc{($BMes_2$)(μ-F)($SnMe_2F$)}]$^-$, with each of the silicon-bound methyl groups giving rise to a doublet of doublets resonance (at 0.50 and -0.07 ppm; Figure 3.27). This coupling pattern groups arises from each inequivalent methyl group coupling to two distinct fluorine atoms ($^3J_{F\text{-}H}$ = 4.0 Hz, 8.0 Hz and $^3J_{F\text{-}H}$ = 2.5 Hz, 8.0 Hz), further implying that the boron-bound fluoride anion is also bonded to the silicon atom to which the methyl groups are bound. Additionally, the ^{13}C NMR is fully consistent with the formation of [**16**·F]$^-$, and the ESI mass spectrum reveals the presence of the molecular ion [**16**·F]$^-$.

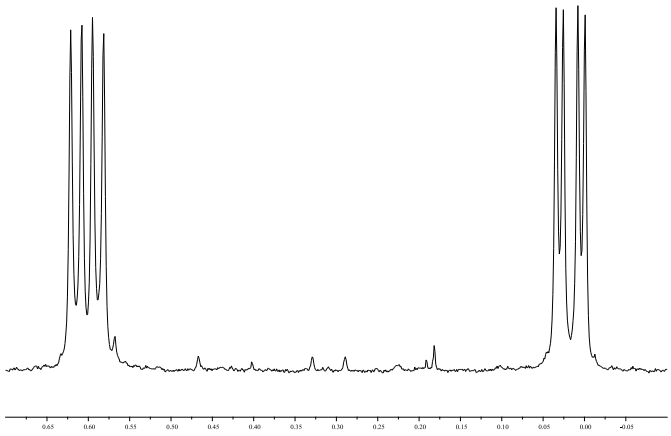

Figure 3.27. A section of the ^{1}H NMR spectrum of [**16**·F]$^{-}$ in $CDCl_3$ showing the two doublet of doublets signals corresponding to the silicon bound methyl groups.

The ^{1}H, ^{11}B, ^{19}F and ^{29}Si NMR spectroscopic studies of [**16**·F]$^{-}$ allowed for the accurate determination of coupling constants by Dr. Nick Rees and Jessica Smart using the gNMR software suite (Table 3.8, Figures 3.28-29).

	$^{1}H_A$	$^{1}H_B$	$^{19}F_A$
$^{19}F_A$	4.01 Hz	2.58 Hz	-
$^{19}F_B$	8.09 Hz	7.97 Hz	6.56 Hz
^{11}B	-	-	82.6 Hz
^{29}Si	257 Hz	257 Hz	-

Table 3.8. Coupling constants obtained from modelling of the ^{1}H, ^{11}B, ^{19}F and ^{29}Si NMR spectra.

This modelling is consistent with two distinct ^{19}F NMR environments, with the magnitude of the couplings to the methyl groups being significantly lower for the chelating fluoride anion

($^3J_{H\text{-}F}$ = 4.01 and 2.58 Hz) than the terminal, solely silicon bound fluorine atom ($^3J_{H\text{-}F}$ = 7.97 and 8.09 Hz). This further supports the idea that there is a bonding interaction between the boron bound fluoride anion and the silicon centre, although weaker than that to the terminal, solely silicon bound fluorine atom.

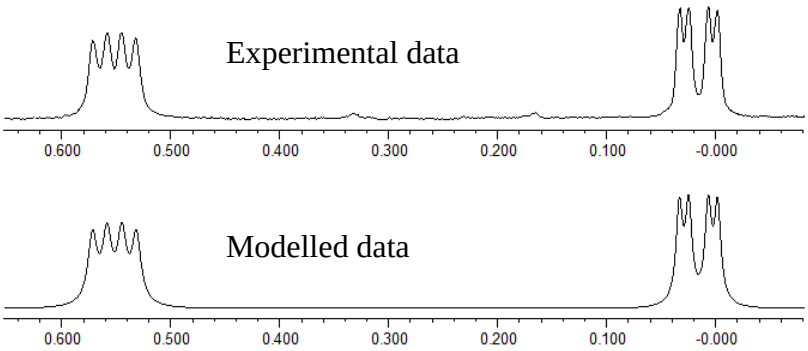

Figure 3.27. Sections of the experimentally obtained and theoretical modelled ^{1}H NMR spectrum of [**16**·F]$^-$.

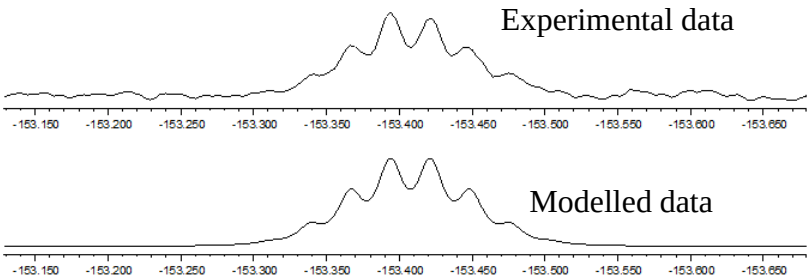

Figure 3.28. Sections of the experimentally obtained and theoretical modelled ^{19}F NMR spectrum of [**16**·F]$^-$.

The ^{1}H NMR spectrum of [**16**·F]$^-$ in acetonitrile-d_3 at room temperature exhibits four separate, but broad, signals between 6.9 and 6.2 ppm for the four *meta* CH protons of the mesityl groups. This suggest that the barrier to rotation around the B-C_{ipso} and B-C_{Fc} bonds is high compared to the energy available to the system, resulting in slow rotation on the NMR timescale.

Variable temperature ^{1}H NMR spectroscopic studies were therefore conducted to probe the magnitudes of these barriers to rotation (Figure 3.30).

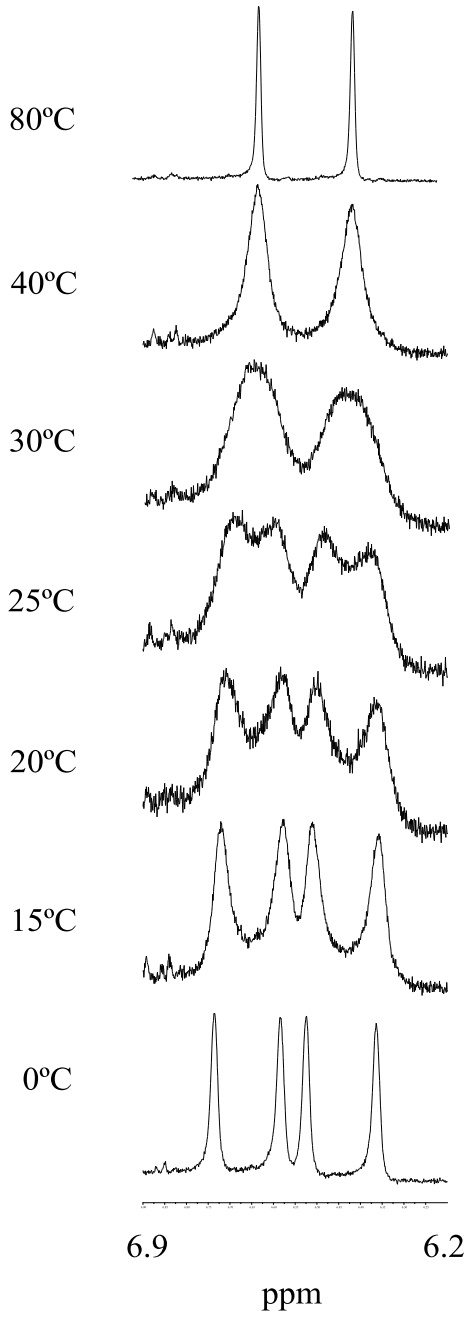

Figure 3.30. Selected region of the ^{1}H NMR spectrum of [**16**·F]$^{-}$ in $CDCl_3$ at temperatures in the range 0ºC to 80ºC.

. The barrier to rotation around the B-C_{ipso} bonds ($\Delta G^{\ddagger}$) thus determined by VT-NMR was shown to be 33 kJ mol^{-1}. This is lower than that of the corresponding zwitterionic system 1,2-fc($BMes_2F$)(PPh_2Me) ($\Delta G^{\ddagger}$ = 66.6 kJ mol^{-1}), and suggests that the conformationally constrained -$SiMe_2F$ group imposes less sterically on the mesityl groups of $BMes_2F$ than does a PPh_2Me group. At 80ºC there is no observable rotation around the B-C_{Fc} bond, which is consistent with the idea that fluoride chelation is retained even at these higher temperatures. Moreover, the coupling of the silicon-bound methyl groups to both fluorines is unchanged at 80ºC, which strongly suggests that the chelating mode of anion binding is retained at elevated temperatures.

The related anion receptor 1,2-fc($BMes_2$)($SiMe_2OMe$) (**17**) is also capable of binding both cyanide and fluoride anions in acetonitrile-d_3 solution and reporting the binding event via a colour change from red to yellow (Figure 3.31). In addition, **17** can be shown, in contrast to **15** and **16**, to be water stable. When **17** is treated with one equivalent of potassium cyanide and one equivalent of 18-crown-6, the cyanide adduct [**17**·CN]$^-$ is formed cleanly. The ^{11}B NMR spectrum of [**17**·CN]$^-$ exhibits a sharp peak at -16 ppm, indicative of the cyanide binding at the boron centre. Moreover, the ^{1}H, ^{13}C and ^{29}Si NMR spectra are fully consistent with the formation of [**17**·CN]$^-$, with the four inequivalent *meta* CH proton signals in the ^{1}H NMR spectrum being illustrative of high barriers to rotation around the B-C_{ipso} and B-C_{Fc} bonds. The ESI mass spectrum shows a peak envelope corresponding to [**17**·CN]$^-$.

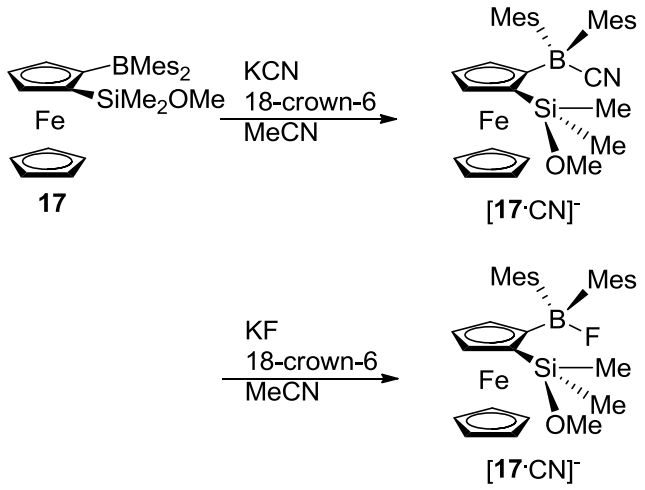

Figure 3.31. The binding of cyanide and fluoride anions by **17**.

When receptor **17** is treated with one equivalent of fluoride and one equivalent of 18-crown-6, the fluoride anion adduct [**17**·F]$^-$ is formed cleanly. The ^{11}B NMR spectrum exhibits a resonance at 5 ppm, which is consistent with a ferrocene appended -$BMes_2F^-$ unit. The ^{19}F NMR exhibits a broad multiplet centred at -163.8 ppm, which is similar to that observed for the adduct [**16**·F]$^-$ (-164.6 ppm) which features chelation of the bound fluoride anion. This resonance in the ^{19}F NMR spectrum is sharpened on decoupling to ^{11}B, although not sufficiently to resolve the coupling constants. The ^{29}Si NMR exhibits a broad resonance at 10 ppm. The ^{1}H NMR spectrum provides evidence that the fluoride anion is chelated by the boron and silicon centre, as both the silicon bound methyl groups are doublets ($^3J_{HF}$ = 1.8 Hz), which are consistent with coupling to fluorine. The ^{13}C is fully consistent with the formation of [**17**·F]$^-$. ESI mass spectrometry allowed for observation of the molecular ion [**17**·F]$^-$.

3.5.2.3. UV-Vis Titration Studies of Anion Binding by Proximal Silicon Lewis Acids

Attempts were made to determine e binding constants for the receptors $FcBMes_2$, 1,1'-$fc(BMes_2)_2$ 1,2-$fc(BMes_2)(SiMe_2F)$ (**16**) and 1,2-$fc(BMes_2)(SiMe_2OMe)$ (**17**) in a range of solvents by measuring UV-Vis spectra as function of added cyanide or fluoride. For reasons of solubility $[^nBu_4N]F\cdot 3(H_2O)$ and $[^nBu_4N][CN]\cdot 2(H_2O)$ were used as the sources for these anions. As both are hygroscopic, they were weighed out accurately in a glove box.

The binding constants so determined are listed in Table 3.9, and representative data used for the binding constant determinations is shown in Figure 3.32. $FcBMes_2$ was used as the standard against which the other receptors can be assessed. 1,1'-$fc(BMes_2)_2$ possesses a greater first anion binding constant (K_1) for both cyanide and fluoride than $FcBMes_2$, a finding which can be attributed to the increased Lewis acidity at boron due to the incorporation of a second (π electron-withdrawing) $BMes_2$ unit. All of the receptors tested bound cyanide anions more strongly than fluorine anions in THF solution, perhaps reflecting the stronger solvation of fluorine anions by THF. That both the fluoride anion binding constants are lower for **16** and **17** relative to $FcBMes_2$ probably reflects the increased steric repulsion that anion binding causes for **16** and **17** compared to $FcBMes_2$.

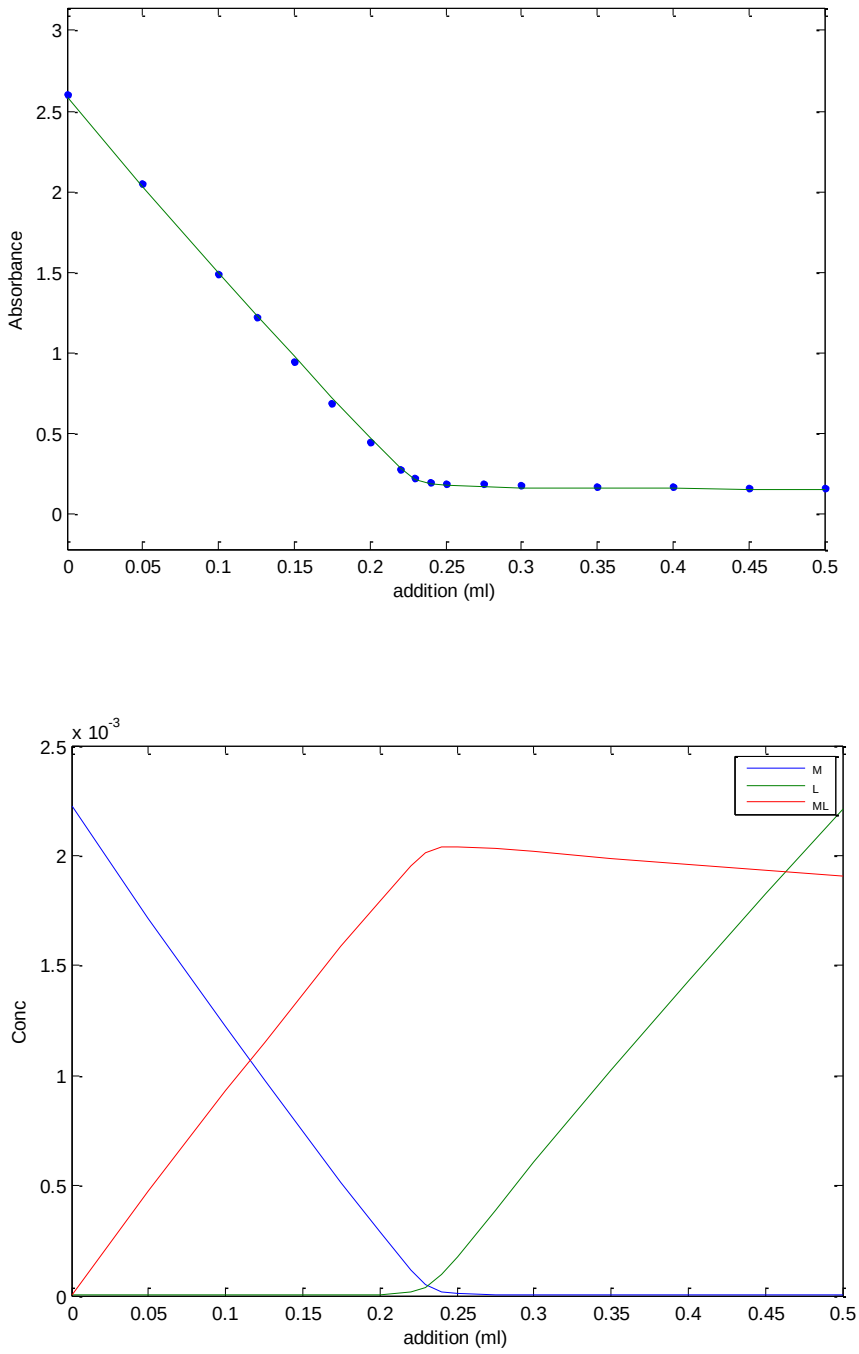

Figure 3.32. Plot of absorbance measured (blue) and fitted (green) for the UV-Vis titration of $[^{n}Bu_4N]F{\cdot}3(H_2O)$ against $FcBMes_2$ in THF solution (above) and the calculated concentrations of $FcBMes_2$ (blue), $FcBMes_2{\cdot}F$ (red) and $[^{n}Bu_4N]F{\cdot}3(H_2O)$ (green) (below).

Receptor	$\log_{10} K_F$ (THF)	$\log_{10} K_{CN}$ (THF)
$FcBMes_2$	**6.06** (0.06)/**5.90** (0.07)	**6.55** (0.15)
$1,1'\text{-}fc(BMes_2)_2$	[K_1 = **8.26** (0.09)* K_2 = **5.60** (0.06)**] /[K_1 = **7.79** (0.61)* K_2 = **5.01** (0.44)**]	[K_1 = **8.88** (0.20)* K_2 = **5.90** (0.11)**] /[K_1 = **9.72** (2.1)* K_2 = **6.72** (2.0)**]
16	**5.34** (0.03)/**5.39** (0.07)	**5.63** (0.024)
17	**5.34** (0.02)/**5.42** (0.08)	**6.21** (0.39)/**6.36** (0.24)

Table 3.9. Anion binding constants determined by UV-Vis titration. Please note that where two sets of values are presented this represents the results of two independent titrations with separately prepared stock solutions of both receptor and anion. The symbol * denotes that the binding constant that has been calculated by the software is unrealistic, and should be interpreted as being equal too/or greater than 7. The symbol ** denotes that the determination of the second binding constant K_2 has been impacted by that calculated for K_1, and is therefore also unreliable.

3.5.2.4. Crystallographic Studies of Anion Binding by Proximal Silicon Lewis Acids

The crystal structure of $[^nBu_4N][1,2\text{-}fc(BMes_2{\cdot}CN)(SiMe_2F)]$ was obtained and the fragment [**16**·CN)]$^-$ is shown in Figure 3.33 with pertinent bond lengths and angles included in Table 3.10. The crystal structure clearly shows the cyanide anion bound at the boron centre, with a B-C bond length of 1.617(3) Å typical of a $FcBMes_2CN$ unit.[8,19,20,26,28,38,42] The pyramidalization around boron is revealed in the sum of C-B-C angles excluding cyanide being equal to 337.2(6)º. The $SiMe_2F$ unit has been modelled over two positions, differing primarily in whether the fluoride sits above the Cp ring relative to iron (occupancy calculated as 0.333) or below the Cp ring (occupancy calculated as 0.667). There is no indication of a secondary binding event to the silicon centre in the solid state. The boron-silicon distance in

[^{n}Bu$_4$N][**16**·CN)] of 3.821(2) Å is significantly greater than that in the receptor **17** of 3.660(3) Å, and presumably reflects the increasing steric demands of the BMes$_2$CN unit relative to BMes$_2$.

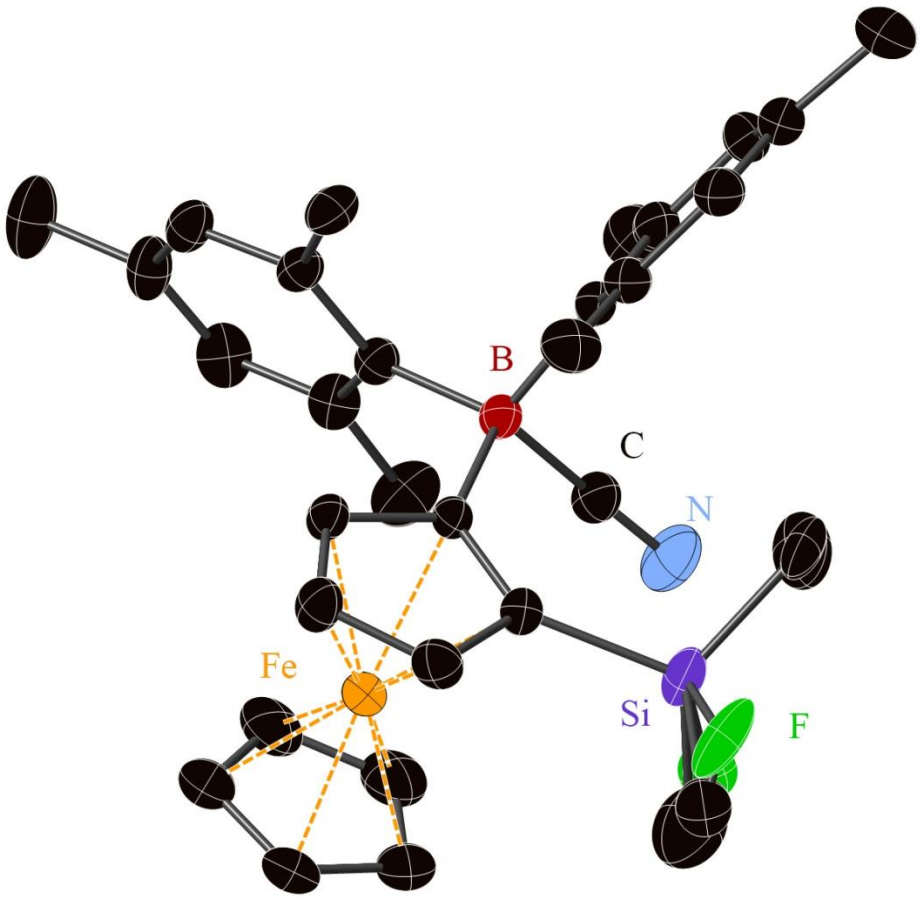

Figure 3.33. The crystal structure of [**16**·CN]$^-$. The hydrogen atoms have been omitted for clarity. The counter cation has been omitted for clarity. Ellipsoids drawn at the 50% probability level, with boron in maroon, carbon in black, nitrogen in light blue, fluorine in green, silicon in purple and iron in orange. The SiMe$_2$F has been modelled as disordered rotationally around the C$_{Fc}$-Si bond in two positions.

Bond/Angle	[$^{n}Bu_4N$][16$^{\cdot}$CN]
B-C_{aryl}	1.665(3), 1.678(3)
B-C_{Fc}	1.636(3)
B-C_{CN}	1.617(3)
B-Fe	1.636(3)
B-Si	3.821(2)
C-N	1.153(3)
Si-C_{Me}	1.902(5), 1.929(6) [0.667 occupancy] 1.873(4), 2.021(3) [0.333 occupancy]
Si-C_{Fc}	1.869(2)
Si-F	1.658(4) [0.667 occupancy] 1.698(2) [0.333 occupancy]
C_{Ar}-B-C_{Ar}	113.1(2)
C_{Ar}-B-C_{Fe}	108.8(2), 115.3(2)
C_{Ar}-B-C_{CN}	136.0(1), 101.4(2)
Σ C-B-C (excluding CN)	337.2(6)
C_{Me}-Si-C_{Me}	115.0(2) [0.667 occupancy] 115.3(2) [0.333 occupancy]
C_{Me}-Si-C_{Fc}	111.2(1), 109.3(1) [0.667 occupancy] 110.7(2), 111.2(2) [0.333 occupancy]
C_{Me}-Si-F	110.3(1), 98.0(1) [0.667 occupancy] 109.5(2), 98.5(2) [0.333 occupancy]
C_{Fc}-Si-F	112.4(1) [0.667 occupancy] 111.0(1) [0.333 occupancy]
Σ C-Si-C	335.5(4) [0.667 occupancy] 337.2(6) [0.333 occupancy]

Table 3.10. Pertinent bond lengths (Å) and angles (°) of [$^{n}Bu_4N$][16$^{\cdot}$CN]

The crystal structure of [^{n}Bu$_4$N][**18**·CN] was also obtained, and the fragment [**18**·CN]$^-$ is shown in Figure 3.34; pertinent bond lengths and angles are contained in Table 3.11. The crystal structure clearly shows the cyanide anion bound at the boron centre, with a B-C bond length of 1.617(3) Å, which is identical to that observed for [^{n}Bu$_4$N][**16**·CN]. The pyramidalization around boron is manifested in the sum of C-B-C angles (excluding cyanide) being equal to 337.1(6)º, which identical to that observed for [^{n}Bu$_4$N][**16**·CN] [337.2(6)º]. Further evidence of the similarity of the binding event at boron is provided by the non-cyanide B-C bond lengths of these two cyanide adducts (Tables 3.10-11). This similarity of the environment around boron would suggest that the binding of cyanide is not significantly different between these two adducts, and hence the proximal SiMe$_2$OH unit is not involved in stabilising the cyanide binding at boron. Although there is a close approach of the freely refined hydrogen atom of SiOH to the nitrogen atom of cyanide (2.16(5) Å), the geometry of crystal structure would seem to preclude any hydrogen bonding event (C-N-H 112(1)º). The boron-silicon distance in [^{n}Bu$_4$N][**18**·CN)] of 3.818(3) Å is not significantly different from that observed in [^{n}Bu$_4$N][**16**·CN)] (3.821(2) Å), although it is significantly greater than that in the receptor **17** of 3.660(3) Å, and presumably reflects the increasing steric demands of the BMes$_2$CN unit relative to BMes$_2$.

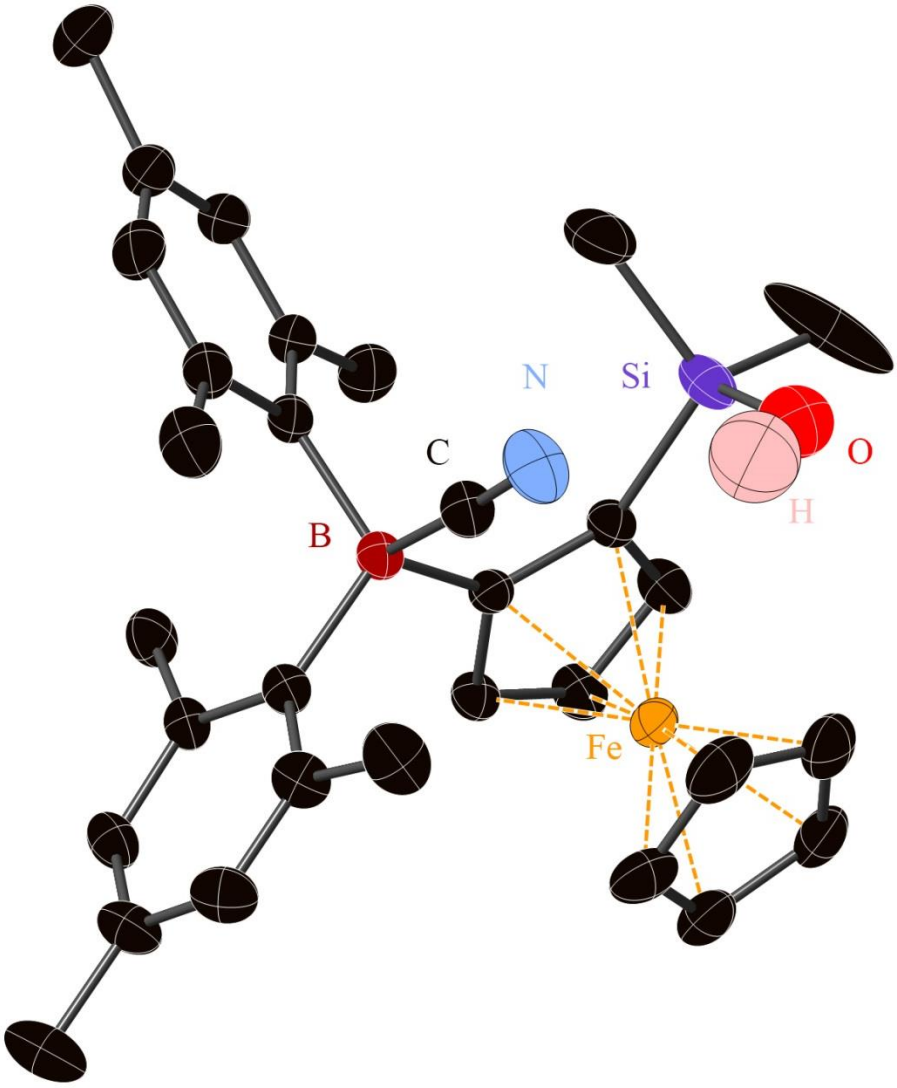

Figure 3.34.. The crystal structure of [^{n}Bu$_4$N][**18**·CN]. The most hydrogen atoms have been omitted for clarity. The counter cation has been omitted for clarity. Ellipsoids drawn at the 50% probability level, with hydrogen in pink, boron in maroon, carbon in black, oxygen in red, fluorine in light green, silicon in purple and iron in orange. The SiOH hydrogen atom has been freely refined against the data.

Bond/Angle	[^{n}Bu$_4$N][**18**·CN]
H-O	1.09(4)
H-N	2.16(5)
B-C$_{aryl}$	1.676(3), 1.665(3)
B-C$_{Fc}$	1.636(3)
B-C$_{CN}$	1.617(3)
B-Si	3.818(3)
B-Fe	3.445(3)
C$_{CN}$-N	1.151(3)
C$_{Bu}$-N (nearest approach)	3.652(4), 3.293(3)
O-N	3.020(4)
Si-C$_{Me}$	1.854(3), 1.787(5)
Si-C$_{Fc}$	1.869(2)
Si-O	1.701(3)
Si-Fe	3.5011(8)
B-C$_{CN}$-N	172.7(3)
C$_{Ar}$-B-C$_{Ar}$	113.1(2)
C$_{Ar}$-B-C$_{Fe}$	108.8(2), 115.2(2)
C$_{Ar}$-B-C$_{CN}$	101.4(2), 114.4(2)
C$_{Fe}$-B-C$_{CN}$	103.5(2)
Σ C-B-C (excluding cyanide)	337.1(6)
C$_{Me}$-Si-C$_{Me}$	106.3(2)
C$_{Me}$-Si-C$_{Fc}$	109.3(2), 111.6(1)
C$_{Me}$-Si-O	105.3(2), 110.0(1)
C$_{Fc}$-Si-O	113.9(1)
Σ C-Si-C	327.2(5)

Table 3.11. Pertinent bond lengths (Å) and angles (°) of [^{n}Bu$_4$N][**18**·CN].

The crystal structure of [K(18-crown-6)][**18**·F] was also obtained, and the fragment [**18**·F]$^-$ is shown in Figure 3.35; pertinent bond lengths and angles are contained in Table 3.12. The crystal structure clearly shows the fluoride anion bound at the boron centre, with a B-F bond length of 1.492(3) Å, which is typical for $ArBMes_2F$ units.[26,39,43] The pyramidalization around boron is exhibited in the sum of C-B-C angles being equal to 338.4(6) º, which is not significantly different from that of 337.1(6)º (excluding cyanide) observed for [^{n}Bu$_4$N][**18**·CN]. This presumably reflects comparable steric loading experienced by the two aryl groups and the ferrocene at boron for both anion adducts. In contrast to [^{n}Bu$_4$N][**18**·CN], [K(18-crown-6)][**18**·F] exhibits a secondary binding event with the $SiMe_2OH$ unit, namely a hydrogen bond to the OH group. That this structural arrangement does not result from packing forces is suggested by the crystal structures of [^{n}Bu$_4$N][**18**·F] and for [K(18-crown-6)][**18**·F]·MeCN. The intramolecular hydrogen bond is reflected in the orientation of the OH group toward the boron bound fluorine atom, with a O-F bond distance of 2.572(2) Å. The distance observed between the freely refined hydrogen of OH and fluorine atom was 1.78(4) Å, which is significantly shorter than the H-F distances of both the inter- and intra-molecular hydrogen bonds (N-H···F-B) observed for the comparable 1,2-fc(BF_3)(CH_2NMe_2H) dimer [2.124 and 2.204 Å respectively].[7] The O-H-F angle is 167(4)º, which suggests that a less than ideal geometry (180º) has been adopted due to the geometric imposition of the receptor framework. It is notable that the B-Si distance of 3.709(2) Å for [K(18-crown-6)][**18**·F] is significantly shorter than that of 3.818(3) Å for [^{n}Bu$_4$N][**18**·CN], further substantiating an ancillasry binding event between the $SiMe_2OH$ unit and the boron bound fluoride anion that is absent in the cyanide analogue.

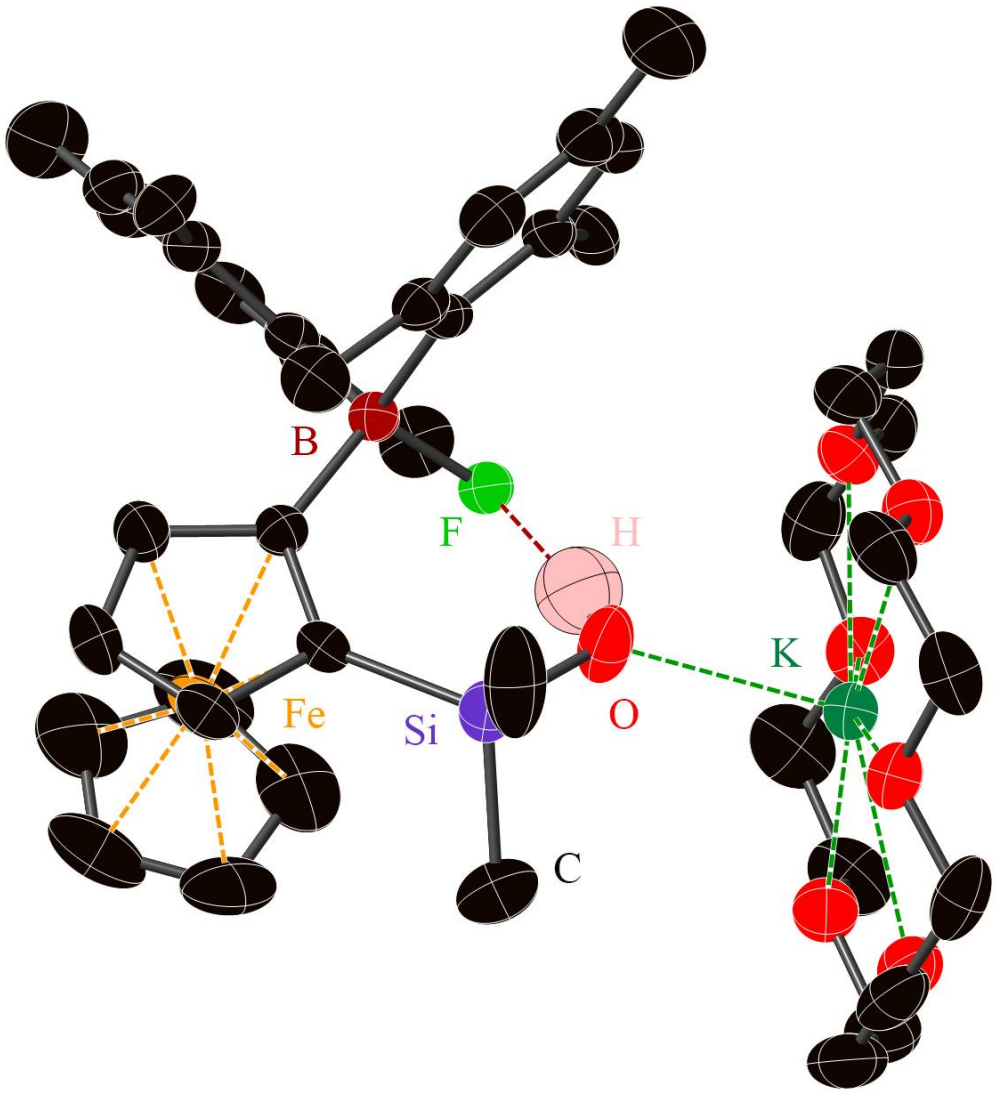

Figure 3.35. The crystal structure of [K(18-crown-6)][**18**·F] Most hydrogen atoms and the counter-cation have been omitted for clarity. Ellipsoids drawn at the 50% probability level, with hydrogen in pink, boron in maroon, carbon in black, oxygen in red, fluorine in light green, silicon in purple and iron in orange. The SiOH hydrogen atom has been freely refined against the data.

Bond/Angle	[K(18-crown-6)][18·F]
H-O	0.80(4)
H-F	1.78(4)
B-C_{aryl}	1.666(3), 1.672(3)
B-C_{Fc}	1.632(3)
B-F	1.492(3)
B-Si	3.709(2)
B-Fe	3.415(2)
O-F	2.572(2)
O-K (excluding 18-crown-6)	2.646(2)
Si-C_{Me}	1.862(3), 1.861(3)
Si-C_{Fc}	1.850(2)
Si-O	1.630(2)
B-F-H	117(1)
B-F-O	113.9(1)
C_{Ar}-B-C_{Ar}	112.8(2)
C_{Ar}-B-C_{Fe}	115.5(2), 110.1(2)
C_{Ar}-B-F	109.2(2), 103.3(2)
Σ C-B-C	338.4(6)
C_{Me}-Si-C_{Me}	106.4(2)
C_{Me}-Si-C_{Fc}	108.9(1), 111.6(1)
C_{Me}-Si-O	109.1(1), 107.7(1)
C_{Fc}-Si-O	112.9(1)
Σ C-Si-C	326.9(4)
O-H-F	167(4)
Si-O-H	112(2)
Si-O-F	103.6(1)
Si-O-K	133.7(1)

Table 3.12. Pertinent bond lengths (Å) and angles (º) of [K(18-crown-6)][**18**·F].

3.6. Conclusions

New synthetic routes to novel ferrocenyl diaryl boranes incorporating hydrogen bond donors have been devised and these systems shown to be competent at binding and colorimetrically reporting both cyanide and fluoride anions. The propensity of these boranes to degrade in the presence of water was established, thereby limiting the scope of investigations into their anion binding properties.

Novel synthetic routes have also been developed to a range of 1,2-functionalised ferrocene receptors, featuring a diaryl borane and a secondary Lewis acidic centre. The corresponding 1,1' isomers were synthesised and the anion binding properties of both the 1,2- and 1,1'- isomers evaluated for fluoride and cyanide. It was established that all the new compounds were capable of binding both cyanide and fluoride, and reporting the presence of these anions colourimetrically. The capacity of 1,2-fc($BMes_2$)($SiMe_2F$) to bind fluoride in a chelating fashion was clearly established by NMR studies.

Interestingly, the 1,2-fc($BMes_2$)($SiMe_2OMe$) receptor was shown to undergo hydrolysis in the presence of wet sources of fluoride and cyanide anions, which was accompanied by anion binding. The crystal structures of these adducts clearly establish that for [Bu_4N][1,2-fc($BMes_2F$)($SiMe_2OH$)] the fluoride accepts a hydrogen bond in an intra-molecular fashion, whereas for the related [K(18-crown-6)][1,2-fc($BMes_2CN$)($SiMe_2OH$)] no intra-molecular hydrogen bond is formed.

3.7. References

(1) Beer, P. D.; Tite, E. L.; Drew, M. G. B.; Ibbotson, A. *Journal of the Chemical Society, Dalton Transactions* **1990**, 2543.

(2) Beer, P. D.; Hesek, D.; Hodacova, J.; Stokes, S. E. *Journal of the Chemical Society, Dalton Transactions* **1992**, 270.

(3) Beer, P. D.; Drew, M. G. B.; Hazlewood, C.; Hesek, D.; Hodacova, J.; Stokes, S. E. *Journal of the Chemical Society, Dalton Transactions* **1993**, 229.

(4) Dusemund, C.; Sandanayake, K. R. A. S.; Shinkai, S. *Journal of the Chemical Society, Dalton Transactions* **1995**, 333.

(5) Yamamoto, H.; Ori, A.; Ueda, K.; Dusemund, C.; Shinkai, S. *Chemical Communications (Cambridge)* **1996**, 407.

(6) Aldridge, S.; Bresner, C.; Fallis, I. A.; Coles, S. J.; Hursthouse, M. B. *Chemical Communications (Cambridge, U. K.)* **2002**, 740.

(7) Bresner, C.; Aldridge, S.; Fallis, I. A.; Jones, C.; Ooi, L.-L. *Angewandte Chemie International Edition* **2005**, *44*, 3606.

(8) Broomsgrove, A. E. J.; Addy, D. A.; Bresner, C.; Fallis, I. A.; Thompson, A. L.; Aldridge, S. *Chemistry – A European Journal* **2008**, *14*, 7525.

(9) Yamaguchi, S.; Akiyama, S.; Tamao, K. *Journal of the American Chemical Society* **2001**, *123*, 11372.

(10) Melaimi, M.; Gabbaï, F. P. *Journal of the American Chemical Society* **2005**, *127*, 9680.

(11) Liu, Z.-Q.; Shi, M.; Li, F.-Y.; Fang, Q.; Chen, Z.-H.; Yi, T.; Huang, C.-H. *Organic Letters* **2005**, *7*, 5481.

(12) Hudnall, T. W.; Melaïmi, M.; Gabbaï, F. P. *Organic Letters* **2006**, *8*, 2747.

(13) Melaiemi, M.; Sole, S.; Chiu, C.-W.; Wang, H.; Gabbaie, F. P. *Inorganic Chemistry* **2006**, *45*, 8136.

(14) Chiu, C.-W.; Gabbaï, F. P. *Journal of the American Chemical Society* **2006**, *128*, 14248.

(15) Lee, M. H.; Agou, T.; Kobayashi, J.; Kawashima, T.; Gabbaï, F. P. *Chemical Communications (Cambridge, U. K.)* **2007**, 1133.

(16) Lee, M. H.; Gabbaie, F. P. *Inorganic Chemistry* **2007**, *46*, 8132.

(17) Parab, K.; Venkatasubbaiah, K.; Jäkle, F. *Journal of the American Chemical Society* **2006**, *128*, 12879.

(18) Hudnall, T. W.; Gabbaï, F. P. *Journal of the American Chemical Society* **2007**, *129*, 11978.

(19) Broomsgrove, A. E. J., University of Oxford, 2010.

(20) Broomsgrove, A. E. J.; A. Addy, D.; Di Paolo, A.; Morgan, I. R.; Bresner, C.; Chislett, V.; Fallis, I. A.; Thompson, A. L.; Vidovic, D.; Aldridge, S. *Inorganic Chemistry* **2009**, *49*, 157.

(21) Hammett, L. P. *Journal of the American Chemical Society* **1937**, *59*, 96.

(22) Zhao, H.; Leamer, L. A.; Gabbaï, F. P. *Dalton Transactions* **2013**, *42*, 8164.

(23) Chiu, C.-W.; Kim, Y.; Gabbaï, F. P. *Journal of the American Chemical Society* **2008**, *131*, 60.

(24) Chiu, C.-W.; Gabbaï, F. P. *Dalton Transactions* **2008**, 814.

(25) Chiu, C.-W.; Gabbaï, F. P. *Journal of the American Chemical Society* **2006**, *128*, 14248.

(26) Morgan, I. R.; Broomsgrove, A. E. J.; Fitzpatrick, P.; Vidovic, D.; Thompson, A. L.; Fallis, I. A.; Aldridge, S. *Organometallics* **2010**, *29*, 4762.

(27) Sole, S.; Gabbaï, F. P. *Chemical Communications (Cambridge, U. K.)* **2004**, 1284.

(28) Kelly, M. J.; Broomsgrove, A. E. J.; Morgan, I. R.; Siewert, I.; Fitzpatrick, P.; Smart, J.; Vidovic, D.; Aldridge, S. *Organometallics* **2013**, *32*, 2674.

(29) Boshra, R.; Venkatasubbaiah, K.; Doshi, A.; Lalancette, R. A.; Kakalis, L.; Jäkle, F. *Inorganic Chemistry* **2007**, *46*, 10174.

(30) Kawachi, A.; Tani, A.; Shimada, J.; Yamamoto, Y. *Journal of the American Chemical Society* **2008**, *130*, 4222.

(31) O'Sullivan, M. C.; Dalrymple, D. M. *Tetrahedron Letters* **1995**, *36*, 3451.

(32) Bebbington, M. W. P.; Bontemps, S.; Bouhadir, G.; Hanton, M. J.; Tooze, R. P.; van Rensburg, H.; Bourissou, D. *New Journal of Chemistry* **2010**, *34*, 1556.

(33) Mitchinson, A.; Golding, B. T.; Griffin, R. J.; O'Sullivan, M. C. *Journal of the Chemical Society, Chemical Communications* **1994**, 2613.

(34) Platzek, J.; Niedballa, U.; Radeuchel, B.; Schering A.-G., Germany . 1996, p 13 pp.

(35) Biot, C.; Delhaes, L.; Abessolo, H.; Domarle, O.; Maciejewski, L. A.; Mortuaire, M.; Delcourt, P.; Deloron, P.; Camus, D.; Dive, D.; Brocard, J. S. *Journal of Organometallic Chemistry* **1999**, *589*, 59.

(36) Addy, D. A. M.Chem, University of Oxford, 2008.

(37) Morgan, I. R.; Di Paolo, A.; Vidovic, D.; Fallis, I. A.; Aldridge, S. *Chemical Communications* **2009**, 7288.

(38) Siewert, I.; Fitzpatrick, P.; Broomsgrove, A. E. J.; Kelly, M.; Vidovic, D.; Aldridge, S. *Dalton Transactions* **2011**, *40*, 10345.

(39) Wade, C. R.; Broomsgrove, A. E. J.; Aldridge, S.; Gabbaï, F. P. *Chemical Reviews* **2010**, *110*, 3958.

(40) Kim, Y.; Zhao, H.; Gabbaï, F. P. *Angewandte Chemie International Edition* **2009**, *48*, 4957.

(41) Hudnall, T. W.; Chiu, C.-W.; Gabbaï, F. P. *Accounts of Chemical Research* **2009**, *42*, 388.

(42) Aldridge, S.; Fallis, I. A.; Bresner, C.; Day, J. K.; Tatchell, T.; Broomsgrove, A. E. J.; Loveday, M. J.; University College Cardiff Consultants Ltd., UK . 2008, p 132pp.

(43) Bresner, C.; Haynes, C. J. E.; Addy, D. A.; Broomsgrove, A. E. J.; Fitzpatrick, P.; Vidovic, D.; Thompson, A. L.; Fallis, I. A.; Aldridge, S. *New Journal of Chemistry* **2010**, *34*, 1652.

Chapter Four: Boronic Esters and Mixed Alkenyl/Aryl Boranes

4.1. Introduction

Boronic esters have been exploited in fluoride anion sensing. Thus, for instance, Shinkai *et al*. developed saccharide esters, $FcB(O_2C_6H_8(OH)_4)$, which were shown to electrochemically sense fluoride anions in mixed methanol/water solutions bearing electrolytes, through the change in the half-cell reduction potential brought about by the complexation of fluoride at the boron centre.[1] When these boronic esters were coupled to redox active dyes (that were complementary to the shift in the ferrocenyl half-wave reduction brought about by fluoride anion complexation) the binding event could be transduced into a colorimetric response.[1]

Further examples of the use of esters include compound $FcB(OR)_2$ (Figure 4.1) that was shown by Bresner *et al*. to reversibly bind and electrochemically indicate the presence of fluoride anions in chloroform solution.[2] Further work on related calixarene boronic esters showed that these systems were susceptible to B-O bond cleavage, reflecting the weaker B-O bonding in B-O-Ar systems as compared to the analogous alkyl B-OR systems.[2-4]

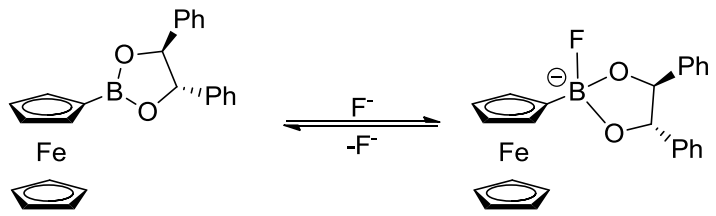

Figure 4.1. The reversible binding of fluoride anions by a ferrocenyl boronic ester in chloroform solution.[2]

Triaryl boranes are chemically more robust than boronic esters and typically stable to hydrolysis. [5-7] Triaryl boranes are also capable of binding both cyanide and fluoride anions and reporting the binding event through changes in the UV-Vis spectrum, as shown by the work of Aldridge, Gabbaï and Tamao with their BArAr'$_2$ systems (Ar = Ph, Mes, Ant, Ar' = Mes, Ant).[5-7] Triarylboranes, such as *para*-$Mes_2B(C_6H_4)NMe_3^+$ and *para*-$Mes_2B(C_6H_4)PMe_3^+$ have been shown by Gabbaï and co-workers to possess intense fluorescence in solution (Figure 4.2).[8,9] On binding fluoride, the boron centres of these receptors no longer possess an empty *p*-orbital, and so fluorescence ceases. This fluorescence "switch off" on binding fluoride was utilised in determining the fluoride anion binding affinity of both *para*-$Mes_2B(C_6H_4)NMe_3^+$ and *para*-$Mes_2B(C_6H_4)PMe_3^+$.

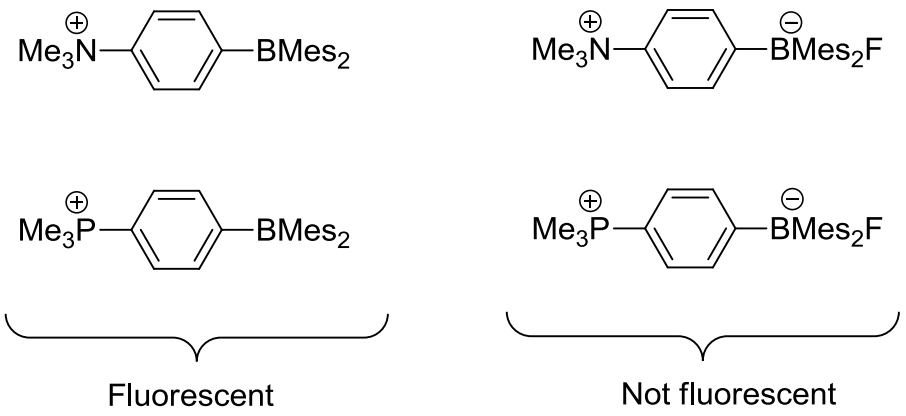

Figure 4.2. The fluorescent fluoride anion receptors *para*-$Mes_2B(C_6H_4)NMe_3^+$ and *para*-$Mes_2B(C_6H_4)PMe_3^+$ and their non-fluorescing fluoride anion adducts.[8,9]

4.2. Aims

The objective of the research presented in this chapter was to investigate the possibility of selectively binding fluoride anions in preference to cyanide anions in solution, with reporting of this binding event through a change in fluorescence.

Using a quinoline appended boronic ester as the anion receptor, it was envisioned that the binding of fluoride or cyanide could be reported through a change in the fluorescence. It was thought that incorporation of a cationic group proximal to the boron center would increase the anion binding affinity of the receptor. Therefore, a primary aim was to devise synthetic routes to novel quinoline appended boronic ester incorporating a proximal cationic center and evaluate the anion binding affinities of these boronic esters.

It was also of interest to explore the capacity of quinoline appended bis aryl boranes to bind and report the presence of fluoride and cyanide anions, given the increased resistance to hydrolysis cf. boronic esters. Hence, new synthetic routes to create these novel quinoline appended bis aryl boranes were to be explored and the anion binding capacity of these novel boranes to be evaluated.

4.3. Experimental

2,4,6-tri(pyridin-3-yl)-1,3,5,2,4,6-trioxatriborinane: *n*-Butyllithium (37.5 mL of a 1.6 M solution in hexanes) was added dropwise over approximately 30 min to a solution of 3-bromopyridine (4.9 mL, 51 mmol) and tri-isopropylborate (13.85 mL, 60 mmol) in THF (20 mL) and toluene (80 mL) at -40 ºC according to a modified literature

procedure.[10] The resulting reaction mixture was stirred at -40 ºC for a further 20 min its temperature raised to -20 ºC and then quenched with a 2 M hydrochloric acid (100 mL). The biphasic mixture was brought to room temperature and the aqueous phase was decanted off. The aqueous phase was neutralized with 5 M sodium hydroxide solution (15 mL) and extracted with THF (6 x 50 mL). The aqueous solution was then saturated with sodium chloride and extracted again with THF (2 x 100mL). The combined organic extracts were dried over magnesium sulfate, filtered and the volatiles removed *in vacuo* to afford a crude product consisting of 3-pyridinyl-boronic acid and associated anhydrides (~8.9 g). The off-white crude product mixture was taken up in acetonitrile (40 mL) and heated to reflux for 90 min, then allowed to come to room temperature and the volatiles removed *in vacuo* to afford the target trimer material as a white powder (7.1 g, 65%).

^{1}H NMR (300 MHz, methanol-d_4, 20 ^{o}C): δ_H 8.64 (s, 1H, Ar), 8.52 (m, 1H, Ar), 8.40 (d, $^{3}J_{H\text{-}H}$ = 7.0 Hz, 1H, Ar), 7.67 (t, $^{3}J_{H\text{-}H}$ = 6.2 Hz, 1H, Ar).

2,4,6-tri(quinolin-3-yl)-1,3,5,2,4,6-trioxatriborinane: *n*-Butyllithium (16.0 mL of a 1.6 M solution in hexanes, 26 mmol) was added portion-wise over 60 min to a solution of 3-bromoquinoline (2.9 mL, 22 mmol), a solution of tri-isopropylborate (5.97 mL, 26 mmol) in THF (8 mL) and toluene (32 mL) at -78 ºC, following a modified literature procedure.[10] The resulting suspension was stirred for a further 30 min at –78 ºC, warmed to -20 ºC, and then quenched with 2 M hydrochloric acid (10 mL). The biphasic mixture was allowed to come to room temperature and the aqueous phase decanted off and neutralized with 5 M sodium hydroxide solution (1.5 mL). The neutralized aqueous phase was saturated with sodium chloride and then extracted with THF (3 x 20 mL). The combined organic extracts were dried with magnesium sulfate, filtered and the volatiles

removed *in vacuo* to afford a crude mixture composed of 3-quinolinyl-boronic acid and associated anhydrides. The off-white crude product was taken up in acetonitrile (20 mL), brought to reflux for 30 min, cooled to 0 ºC, then stirred for 30 min and the white precipitate that formed isolated by filtration. The white solid was dried *in vacuo* to afford the target trimer material as a white powder. Yield 1.2 g, 32%.

^{1}H NMR (300 MHz, DMSO-d_6, 20 ºC): δ_H 9.21 (s, 1H, Ar), 8.91 (s, 1H, Ar), 8.09 (m, 2H, Ar), 7.89 (m, 1H, Ar), 7.70 (m, 1H, Ar).

3-(4,4,5,5-tetramethyl-1,3,2-dioxaborolan-2-yl)pyridine 1: A suspension of 3-pyridinyl boroxin (2.51 g, 7.9 mmol) and pinacol (3.45 g, 29.2 mmol) in toluene (100 mL) was refluxed for 2.5 h in a Dean-Stark apparatus following a modified literature procedure.[10] The reaction mixture was isolated, the volatiles removed *in vacuo* and the resulting yellow residue taken up in cyclohexane (17 mL). The resulting solution was refluxed for 30 min and then allowed to cool to room temperature. The resulting precipitate was filtered off, washed with minimal amount of cold cyclohexane (~10 ºC) and dried *in vacuo* to afford the target material as a white powder. Yield 2.50 g, 52 %.

^{1}H NMR (300 MHz, $CDCl_3$, 20 ºC): δ_H 8.95 (br. s, 1H, Ar), 8.67 (dd, $^3J_{H\text{-}H}$ = 1.8, 4.9 Hz, 1H, Ar), 8.06(dt, $^3J_{H\text{-}H}$ = 1.8, 7.5 Hz, 1H, Ar), 7.29-6 (m, 1H, Ar), 1.36 (s, 12H, CH_3).

MS(ESI) *m*/*z* (%): 206.1 (100) $[C_{11}H_{16}BNO_2, M+H]^+$.

3-(4,4,5,5-tetramethyl-1,3,2-dioxaborolan-2-yl)quinoline 2: A suspension of 3-quinolyl-boroxin (0.50 g, 2.9 mmol) and pinacol (0.34 g, 2.9 mmol) in toluene (100 mL) was refluxed for 16 h in a Dean-Starke apparatus. The reaction mixture was isolated and the volatiles removed *in vacuo*. The resulting off-white crude product was sublimed under reduced pressure over 6 h to afford the target material as an off-white solid. Yield 0.34 g, 45 %.

^{1}H NMR (300 MHz, $CDCl_3$, 20 ^{o}C): δ_H 9.20 (s, 1H, Ar), 8.63 (s, 1H, Ar), 8.12 (d, $^{3}J_{H\text{-}H}$ = 8.1 Hz, 1H, Ar), 7.84 (d, $^{3}J_{H\text{-}H}$ = 8.1 Hz, 1H, Ar), 7.75 (app. t, $^{3}J_{H\text{-}H}$ = 7.7 Hz, 1H, Ar), 7.54 (app. t, $^{3}J_{H\text{-}H}$ = 7.4 Hz, 1H, Ar), 1.40 (s, 12H, CH_3).

MS(ESI) *m*/*z* (%): 256.2 (100) $[C_{15}H_{18}BNO_2, M+H]^{+}$.

1-methyl-3-(4,4,5,5-tetramethyl-1,3,2-dioxaborolan-2-yl)pyridinium iodide [3]I: Methyl iodide (2.2 mL, 43 mmol) was added to a solution of **1** (1.2 g, 5.9 mmol) in chloroform (20 mL) and the result reaction mixture stirred for 24 h. The volatiles were removed *in vacuo* to afford the target material as a pale orange solid. Yield 2.0 g, 98 %. Crystals suitable for single crystal X-ray diffraction were grown by slow diffusion of hexane into a chloroform solution of the target material.

^{1}H NMR (300 MHz, $CDCl_3$, 20 ^{o}C): δ_H 9.74 (d, $^{3}J_{H\text{-}H}$ = 5.9 Hz, 1H, Ar), 8.65 (s, 1H, Ar), 8.65(d, $^{3}J_{H\text{-}H}$ = 7.6 Hz, 1H, Ar), 8.17 (m, 1H, Ar), 4.71 (s, 3H, N-CH_3), 1.35 (s, 12H, CH_3).

$^{13}C[^{1}H]$ NMR (126 MHz, $CDCl_3$, 20 ^{o}C): δ_C 150.3 (C_5H_4NB), 148.9 (C_5H_4NB), 147.9 (C_5H_4NB), 128.1 (C_5H_4NB), 86.1 (O-C), 50.0 (N-Me), 24.9 ($C(CH_3)_2$). Quaternary carbon bound to boron was not observed.

$^{11}B[^{1}H]$ NMR (96 MHz, $CDCl_3$, 20 ^{o}C): δ_B 31 (br).

MS(ESI) *m*/*z* (%): 220 (100) $[C_{12}H_{19}BNO_2, M\text{-}I]^+$. HRMS(ESI) (*m*/*z*): calc. for [(M-I)+] (^{10}B isotopomer), $C_{12}H_{19}BNO_2$ 220.1505; meas. 220.1505.

Elemental microanalysis: calc. for $C_{12}H_{19}BNO_2I$ C 41.54% H 5.52% N 4.04%, meas. C 41.54 % H 5.58% N 4.69%.

Crystallographic data: $C_{12}H_{19}BNO_2I\cdot(CHCl_3)$, *M*r = 466.38, orthorhombic, *P* bca, *a* = 9.21151(8), *b* = 15.51231(13), *c* = 27.2389 Å, α = 90, β = 90, γ = 90º, *V* = 3892.21(5) $Å^3$, *Z* = 4, ρ_c = 1.592 Mg m^{-3}, *T* = 150 K, λ = 1.54180 Å. 76007 reflections collected, 4013 independent [R(int) = 0.000] used in all calculations. R_1 = 0.0553, wR_2 = 0.1524 for observed unique reflections [$I>2\sigma(I)$] and R_1 = 0.0555, wR_2 = 0.1527 for all unique reflections. Max. and min. residual electron densities 2.77 and -3.32 e $Å^3$.

1-methyl-3-(4,4,5,5-tetramethyl-1,3,2-dioxaborolan-2-yl)quinolinium iodide [4]I: Methyl iodide (0.5 mL, 9.8 mmol) was added to a solution of **2** (0.25 g, 0.98 mmol) in chloroform (10 mL) and the resulting mixture stirred for 72 h. Hexane (100 mL) was added to the reaction mixture and the resulting precipitate filtered off and dried *in vacuo* to afford the target material as a pale orange solid. Yield 0.31 g, 80 %.

^{1}H NMR (300 MHz, CD_2Cl_2, 20 ^{o}C): δ_H 9.47 (s, 1H, Ar), 9.28 (s, 1H, Ar), 8.53 (d, $^{3}J_{H\text{-}H}$ = 9.4 Hz, 1H, Ar), 8.36-30 (m, 2H, Ar), 8.05 (m, 1H, Ar), 4.85 (s, 3H, N-CH_3), 1.43 (s, 12H, C(CH_3)$_2$).

^{13}C[^{1}H] NMR (75 MHz, CD_2Cl_2, 20 ^{o}C): δ_C 154.0 (C_9H_8NB), 153.4 (C_9H_8NB), 139.6 (C_9H_8NB), 137.8 (C_9H_8NB), 131.4 (C_9H_8NB), 131.1 (C_9H_8NB), 129.6 (C_9H_8NB), 119.5 (C_9H_8NB), 86.6 (C-O), 48.0 (N-CH_3), 25.0 (C(CH_3)$_2$). Quaternary carbon bound to boron was not observed.

^{11}B[^{1}H] NMR (96 MHz, $CDCl_3$, 20 ^{o}C): δ_B 30 (br).

MS(ESI) *m*/*z* (%): 270 (100) [$C_{16}H_{21}BNO_2$, M-I]$^{+}$. HRMS(ESI) (*m*/*z*): calc. for [(M-I)+] (^{10}B isotopomer), $C_{16}H_{21}BNO_2$ 270.1663; meas. 270.1665.

1-methyl-3-(4,4,5,5-tetramethyl-1,3,2-dioxaborolan-2-yl)pyridinium fluoride [3·F]: Route 1

A mixture of [**3**]I (5.0 mg, 0.014 mmol) and [^{n}Bu_4N]F·3(H_2O) (4.5 mg, 0.014 mmol) was suspended in $CDCl_3$ (1.0 mL) and the resulting suspension stirred at room temperature until all of the material had dissolved.

1-methyl-3-(4,4,5,5-tetramethyl-1,3,2-dioxaborolan-2-yl)pyridinium fluoride [3·F]: Route 2

A mixture of [**3**]I (70 mg, 0.2 mmol), KF (116 mg, 2.0 mmol) and 18-crown-6 (53 mg, 0.2 mmol) was suspended in $CDCl_3$ (2.0 mL) and the resulting suspension stirred at

room temperature for one hour. The reaction solution was isolated by filtration. Yield not determined.

^{1}H NMR (300 MHz, $CDCl_3$, 20 ^{o}C, Route 2): δ_H 8.67 (d, $^{3}J_{H-H}$ = 7.5 Hz, 1H, Ar), 8.57 (s, 1H, Ar), 8.48 (d, $^{3}J_{H-H}$ = 6.6 Hz, Ar-H), 7.69 (m, 1H, Ar), 4.30 (s, 3H, N-CH_3), 1.29 (s, 6H, C(CH_3)$_2$), 1.09 (s, 6H, C(CH_3)$_2$).

^{13}C[^{1}H] NMR (75 MHz, $CDCl_3$, 20^{o}C): δ_C 148.8 (C_5NH_4B), 146.5 (C_5NH_4B), 140.7 (C_5NH_4B), 126.3 (br. C_5NH_4B), 126.1 (C_5NH_4B), 79.2 (O-C), 48.1 (N-CH_3), 26.0 (C(CH_3)$_2$), 25.9 (C(CH_3)$_2$).

^{11}B[^{1}H] NMR (96 MHz, $CDCl_3$, 20^{o}C): δ_B 8 (d, $^{1}J_{B-F}$ = 59 Hz).

^{19}F NMR (282 MHz, $CDCl_3$, 20^{o}C): δ_F -137 (partially collapsed quartet, 1F).

Crystallographic data: $C_{12}H_{19}BNO_2F$, *M*r = 239.10, monoclinic, *P* 2_1/c, *a* = 28.0795(2), *b* = 6.36895(5), *c* = 13.83872(10) Å, β = 94.7553(7), *V* = 2483.92(3) Å^3, *Z* = 4, ρc = 1.279 Mg m^{-3}, *T* = 150 K, λ = 1.54180 Å. 52431 reflections collected, 5183 independent [R(int) = 0.040] used in all calculations. R_1 = 0.0341, wR_2 = 0.0999 for observed unique reflections [I>2σ(I)] and R_1 = 0.0383, wR_2 = 0.1052 for all unique reflections. Max. and min. residual electron densities 0.31 and -0.23 e Å^3.

1-methyl-3-(4,4,5,5-tetramethyl-1,3,2-dioxaborolan-2-yl)pyridinium cyanide [3·CN]: Route 1

A mixture of [**3**]I (5.0 mg, 0.0014 mmol) and [^{n}Bu$_4$N][CN]·2(H$_2$O) (3.6 mg, 0.014 mmol) was suspended in $CDCl_3$ (1.0 mL) and stirred at room temperature until all the material had dissolved (~ 5 h). Slow diffusion of hexanes into a saturated chloroform solution led to the formation of a yellow powder that was isolated by filtration. Yield not determined.

1-methyl-3-(4,4,5,5-tetramethyl-1,3,2-dioxaborolan-2-yl)pyridinium cyanide [3·CN]: Route 2

A mixture of [**3**]I (70 mg, 0.02 mmol), 18-crown-6 (53 mg, 0.2 mmol) and KCN (130 mg, 2.0 mmol) was suspended in $CDCl_3$ (2.0 mL) and stirred at room temperature for 1 h Slow diffusion of hexanes into a saturated chloroform solution led to the formation of a yellow powder that was isolated by filtration. Yield 50 mg, 63%.

^{1}H NMR (300 MHz, $CDCl_3$, 20 ^{o}C, route 2): δ_H 8.65 (d, $^{3}J_{H\text{-}H}$ = 4.7 Hz, 1H, Ar), 8.59 (d, $^{3}J_{H\text{-}H}$ = 7.0 Hz, 1H, Ar), 8.53 (s, 1H, Ar), 7.61 (m, 1H, Ar), 4.27 (s, 3H, N-CH_3), 1.13 (s, 6H, C(CH_3)$_2$), 1.02 (s, 6H, C(CH_3)$_2$).

^{13}C[^{1}H] NMR (75 MHz, $CDCl_3$, 20 ^{o}C, route 2): δ_C 148.5 (C_5NH_4B), 146.7 (C_5NH_4B), 140.0 (C_5NH_4B), 125.8 (C_5NH_4B), 78.4 (O-C), 47.9 (N-CH_3), 25.7 (C(CH_3)$_2$), 24.6 (C(CH_3)$_2$).

^{11}B[^{1}H] NMR (96 MHz, $CDCl_3$, 20^{o}C): δ_B 5

1-methyl-3-(4,4,5,5-tetramethyl-1,3,2-dioxaborolan-2-yl)quinolinium fluoride [4·F]

A mixture of [**4**]I (18.0 mg, 0.04 mmol), 18-crown-6 (12 mg, 0.04 mmol) and KF (26 mg, 0.4 mmol) was suspended in CD_2Cl_2 (1.5 mL) and stirred at room temperature for 4 h. The reaction solution was isolated by filtration. The volatiles were removed *in vacuo* and taken up in minimal THF. Slow diffusion of pentanes into the saturated THF solution led to the formation of a colourless precipitate that was isolated by filtration and dried *in vacuo*. Yield not determined.

^{1}H NMR (300 MHz, $CDCl_3$, 20 ^{o}C): δ_H 9.08 (s, 1H, Ar), 9.04 (s, 1H, Ar), 8.16-11 (m, 2H, Ar), 8.03 (m, 1H, Ar), 7.84 (m, 1H, Ar), 4.50 (s, 3H, N-CH_3), 1.22 (s, 6H, $C(CH_3)_2$), 1.04 (s, 6H, $C(CH_3)_2$).

^{13}C[^{1}H] NMR (75 MHz, $CDCl_3$, 20 ^{o}C): δ_C 153.3 (C_9NH_6B), 150.5 (C_9NH_6B), 137.3 (C_9NH_6B), 133.8 (C_9NH_6B), 130.3 (C_9NH_6B), 130.2 (C_9NH_6B), 129.2 (C_9NH_6B), 117.8 (C_9NH_6B), 79.4 (O-C), 45.6 (N-CH_3), 26.1 ($C(\underline{C}H_3)_2$), 26.0 ($C(\underline{C}H_3)_2$). Quaternary carbon of C_9NH_6B bound to boron was not observed.

^{11}B[^{1}H] NMR (96 MHz, $CDCl_3$, 20 ^{o}C): δ_B 4.1 (d, $^{1}J_{F\text{-}B}$ = 59 Hz).

^{19}F[^{1}H] NMR (282 MHz, $CDCl_3$, 20 ºC): δ_F -137 (partially collapsed quartet).

1-(dimesitylboryl)-5-(dimesitylboryl)-1,2-dihydro-2,3'-bipyridine 5: *n*-BuLi (7.1 mL of a 1.6 M solution in hexanes, 11.4 mmol) was added dropwise to a solution of

3-bromopyridine (1.81 g, 11.4 mmol) in diethyl ether (50 mL) at -78 ºC. The reaction mixture was stirred at -78 ºC for 5 min. A solution of $FBMes_2$ (3.37 g, 12.6 mmol) in diethyl ether (100 mL) was then added dropwise quickly to the reaction mixture at -78 ºC. The resulting reaction mixture was stirred at -78 ºC for 1 h, then allowed to attain room temperature over 12 h. The reaction mixture was diluted with diethyl ether (100 mL) and quenched with water (200 mL). The organic layer was separated, washed with water (2 x 100 mL), then brine (2 x 100 mL), dried over magnesium sulfate, filtered and the volatiles removed *in vacuo* to afford a fluorescent yellow solid. The crude product was purified using column chromatography (2:1 hexanes: diethyl ether, silica 60) to afford the target material as a fluorescent yellow solid. Yield 1.392 g, 37%.

^{1}H NMR (500 MHz, $CDCl_3$, 20 ^{o}C): δ_H 8.48 (dd, $^{3}J_{H\text{-}H}$ = 4.8 Hz, $^{3}J_{H\text{-}H}$ = 1.8 Hz, 1H, C_5NH_4), 8.07 (d, $^{3}J_{H\text{-}H}$ = 1.8 Hz, 1H, C_5NH_4), 7.34 (dt, $^{3}J_{H\text{-}H}$ = 7.5 Hz, $^{3}J_{H\text{-}H}$ = 2.4 Hz, 1H, C_5NH_4), 7.18 (dd, $^{3}J_{H\text{-}H}$ = 7.5 Hz, $^{3}J_{H\text{-}H}$ = 2.4 Hz, 1H, C_5NH_4), 6.93 (s, 1H, Mes), 6.83 (s, 2H, Mes), 6.74 (s, 2H, Mes), 6.59 (s, 2H, Mes), 6.31 (s, 1H, Mes), 6.26 (d, $^{3}J_{H\text{-}H}$ = 9.6 Hz, 1H, C_5NH_4B), 5.57 (m, 2H, C_5NH_4B), 5.46 (dd, $^{3}J_{H\text{-}H}$ = 9.6 Hz, $^{3}J_{H\text{-}H}$ = 5.4 Hz, 1H, C_5NH_4B), 2.59 (s, 3H, CH_3 of Mes), 2.31 (s, 3H, CH_3 of Mes), 2.29 (s, 3H, CH_3 of Mes), 2.22 (s, 6H, CH_3 of Mes), 2.15 (br. s, 6H, 2 x CH_3 of Mes), 2.05 (s, 3H, CH_3 of Mes), 2.00 (s, 3H, CH_3 of Mes), 1.97 (s, 3H, CH_3 of Mes), 1.64 (s, 3H, CH_3 of Mes), 1.49 (s, 3H, CH_3 of Mes).

^{13}C[^{1}H] NMR (125 MHz, $CDCl_3$, 20 ^{o}C): δ_C 154.0, 150.8, 150.3, 149.4, 149.3, 149.2, 142.3, 141.1, 140.6, 139.5, 138.9, 138.5, 138.4, 138.3, 138.2, 137.8, 135.5, 133.5, 132.6, 129.1, 128.4, 128.3, 128.2, 128.1, 127.9, 127.8, 127.7, 127.6, 126.7, 123.7, 123.3, 119.2, 56.9 ($\underline{C}HC_2N$ of C_5NH_3B), 23.0 (CH_3 of Mes), 22.9 (CH_3 of Mes), 22.8 (CH_3 of

Mes), 22.6 (CH_3 of Mes), 22.4 (CH_3 of Mes), 22.0 (CH_3 of Mes), 21.9 (CH_3 of Mes), 21.3 (CH_3 of Mes), 21.2 (CH_3 of Mes), 21.1 (CH_3 of Mes), 21.0 (CH_3 of Mes), 20.9 (CH_3 of Mes).

$^{11}B[^{1}H]$ NMR (96 MHz, $CDCl_3$, 20 ^{o}C): δ_B 74 (br. s.), 49 (br. s.).

Elemental microanalysis: calc. for $C_{46}H_{52}B_2N_2$, C 84.41%, N 4.28%, H 8.01%; meas. C 84.54, 84.57%, N 4.12, 4.21%, H 7.90, 7.94%.

[^{n}Bu$_4$N][5·CN]

Compound **5** (26.8 mg, 0.05 mmol) and [$^{n}Bu_4N$][CN]·2(H_2O) (30.4 mg, 0.10 mmol) were dissolved in d_8-THF (0.75 mL) and the resulting suspension sonicated for 1 h. Slow diffusion of hexanes into the d_8-THF solution led to the formation of an orange precipitate that was isolated by filtration and dried *in vacuo*. Yield not determined.

^{1}H NMR (500 MHz, d_8-THF , 20 ^{o}C): δ_H 8.31(m, 1H, C_5NH_4C), 8.07 (s, 1H, Mes), 7.72 (m, 1H, C_5NH_4C), 7.04 (m, 1H, C_5NH_4C), 6.88 (s, 1H, Mes), 6.79 (m, 1H, C_5NH_4C), 6.68 (s, 1H, Mes), 6.42 (m, 3H, 2 x Mes & 1 x C_5NH_4B), 6.24 (m, 3H, 3 x Mes), 5.46 (m, 3H, C_5NH_4B), 3.25 (m, 16H, 4 x CH_2 of $^{n}Bu_4N$), 2.70 (s, 3H, CH_3 of Mes), 2.24 (m, 12H, 4 x CH_3 of Mes), 2.13 (m, 12H, 4 x CH_3 of Mes), 1.93 (s, 6H, 2 x CH_3 of Mes), 1.80 (m, 3H, CH_3 of Mes), 1.73 (m, 9H, 3 x CH_3 of Mes), 1.63 (m, 16H, 4 x CH_2 of $^{n}Bu_4N$), 1.37 (m, 16H, 4 x CH_2 of $^{n}Bu_4N$), 0.96 (m, 24H, 4 x CH_3 of $^{n}Bu_4N$).

[K(18-crown-6)][5·CN]

A mixture of compound **5** (47 mg, 72 μmol), 18-crown-6 (19 mg, 72 μmol) and KCN (31 mg, 480 μmol) was suspended in d_1-chloroform (2 mL) and stirred for six hours. The reaction solution was separated by filtration from the white insolute. Slow diffusion of hexanes into the chloroform solution led to the formation of an orange precipitate that was isolated by filtration and dried *in vacuo*. Yield not determined.

^{1}H NMR (500 MHz, $CDCl_3$, 20 ^{o}C): δ_H 8.40 (dd, $^{3}J_{H\text{-}H}$ = 4.8 Hz, $^{3}J_{H\text{-}H}$ = 1.8 Hz, 1H, C_5NH_4C), 8.16 (s, 1H, Mes), 7.66 (d, $^{3}J_{H\text{-}H}$ = 5.4 Hz, 1H, C_5NH_4C), 7.07 (dd, $^{3}J_{H\text{-}H}$ = 7.8 Hz, $^{3}J_{H\text{-}H}$ = 4.8 Hz, 1H, C_5NH_4C), 6.89 (s, 1H, Mes), 6.79 (d, $^{3}J_{H\text{-}H}$ = 6.6 Hz, 1H, C_5NH_4C), 6.69 (s, 1H, Mes), 6.53 (br. s, 2H, Mes), 6.48 (s, 1H, Mes), 6.37 (s, 1H, Mes), 6.28 (s, 1H, Mes), 5.50 (br. m., 3H, C_5NH_4B), 3.51 (s, 24H, 18-crown-6), 2.69 (s, 3H, CH_3 of Mes), 2.27 (m, 9H, 3 x CH_3 of Mes), 2.19 (s, 3H, CH_3 of Mes), 2.16 (s, 3H, CH_3 of Mes), 2.13 (s, 3H, CH_3 of Mes), 1.95 (s, 3H, CH_3 of Mes), 1.84 (s, 6H, 2 x CH_3 of Mes), 1.73 (s, 3H, CH_3 of Mes).

^{13}C[^{1}H] NMR (125 MHz, d_8-THF, 20 ^{o}C): δ_C 150.9, 149.9 (Mes), 149.2 (C_5NH_4), 149.0, 148.3 (Mes), 145.7 (Mes), 142.5 (Mes), 140.8 (C_5NH_4), 140.3, 139.8, 139.0 (alkene of $C_5NH_4B_2$), 138.0, 136.8, 136.6 (C_5NH_4), 135.8 (alkene of $C_5NH_4B_2$), 135.7 (Mes), 134.5, 133.5, 133.8, 131.7, 131.1, 129.0, 128.7, 128.6, 128.4, 128.3, 128.0, 127.7, 127.2, 126.7, 122.0 (C_5NH_4), 117.6 (alkene of $C_5NH_4B_2$), 69.9 (18-crown-6), 55.6 (alkane of $C_5NH_4B_2$), 29.7 (CH_3 of Mes), 24.9 (CH_3 of Mes), 24.8 (CH_3 of Mes), 23.1 (CH_3 of Mes), 22.4 (CH_3 of Mes), 22.1 (CH_3 of Mes), 21.1 (CH_3 of Mes), 21.1 (CH_3 of Mes), 20.8 (two nearly coincident signals, 2 x CH_3 of Mes), 20.5 (CH_3 of Mes), 15.9 (CH_3 of Mes).

Only 46 out of the 47 carbon signals were observed. The carbon signal corresponding to the boron bound cyanide was not observed.

$^{11}B[^{1}H]$ NMR (96 MHz, $CDCl_3$, 20 ^{o}C): δ_B 49 (br. s), -14 (s).

[K(18-crown-6)][5·F]

A mixture of compound **5** (47 mg, 72 μmol), 18-crown-6 (19 mg, 72 mmol) and KF (5 mg, 90 mmol) was suspended in d_1-chloroform (2 mL) and the resulting suspension stirred for 24 h. The reaction solution was separated by filtration from the white insolute.

^{1}H NMR (500 MHz, $CDCl_3$, 20 ^{o}C): δ_H 8.53 (m, 1H, CH of C_5NH_4), 8.09 (m, 1H, CH of C_5NH_4), 7.56 (m, 1H, CH of C_5NH_4), 7.35 (m, 1H, CH of C_5NH_4), 6.94 (s, 1H, CH of Mes), 6.82 (s, 1H, CH of Mes), 6.78 (s, 1H, CH of Mes), 6.65 (m, 4H, 4 x CH of Mes), 6.32 (m, 1H, CH of Mes), 6.02 (d, $^{3}J_{H\text{-}H}$ = 12.0 Hz, CH of C_5NH_4B), 5.32 (3, 1H, CH of C_5NH_4B), 4.91 (dd, $^{3}J_{H\text{-}H}$ = 12.0 Hz, $^{3}J_{H\text{-}H}$ = 4.0 Hz, CH of C_5NH_4B), 4.23 (m, 1H, CH of C_5NH_4B), 3.56 (s, 24H, 12 x CH_3 of 18-crown-6), 2.08 (m, 36H, 12 x CH_3 of Mes).

$^{11}B[^{1}H]$ NMR (96 MHz, $CDCl_3$, 20 ^{o}C): δ_B 28 (br. s), 4 (s).

$^{13}C[^{1}H]$ NMR (75 MHz, $CDCl_3$, 20 ^{o}C): δ_C 152.1, 149.3 (Mes), 149.1 (C_5NH_4), 148.9, 148.6 (Mes), 148.2 (Mes), 142.2 (Mes), 140.5 (C_5NH_4), 140.4, 139.0, 138.9 (alkene of $C_5NH_4B_2$), 138.0, 136.7, 136.4 (C_5NH_4), 135.8 (alkene of $C_5NH_4B_2$), 135.7 (Mes), 134.3, 133.3, 132.4, 131.6, 131.2, 129.0, 126.6, 126.5, 126.4, 126.3, 126.2, 126.1, 126.0, 125.8, 121.8 (C_5NH_4), 117.5 (alkene of $C_5NH_4B_2$), 69.9 (18-crown-6), 55.8 (alkane

of $C_5NH_4B_2$), 30.0 (CH_3 of Mes), 25.9 (CH_3 of Mes), 24.6 (CH_3 of Mes), 23.0 (CH_3 of Mes), 22.5 (CH_3 of Mes), 22.0 (CH_3 of Mes), 21.1 (CH_3 of Mes), 20.7 (CH_3 of Mes), 20.5 (CH_3 of Mes), 20.4 (CH_3 of Mes), 20.3 (CH_3 of Mes), 16.0 (CH_3 of Mes). The carbon signal corresponding to the boron bound fluoride was not observed.

$^{19}F[^1H]$ NMR (282 MHz, $CDCl_3$, 20 ºC): δ_F -137.

[^{n}Bu$_4$N][5·F]

5 (26.8 mg, 0.05 mmol) and [^{n}Bu$_4$N]F·3(H_2O) (15.2 mg, 0.05 mmol) were dissolved in d_8-THF (0.75 mL) and the resulting suspension sonicated for 1 h.

$^{11}B[^1H]$ NMR (96 MHz, $CDCl_3$, 20 ^{o}C): δ_B 28 (br. s), 4 (s).

$^{19}F[^1H]$ NMR (282 MHz, $CDCl_3$, 20 ºC): δ_F -137.

4.4. Results and Discussion

4.4.1. Boronic Esters

The boronic esters of pyridine were targeted initially with the aim of synthesizing a pyridine functionalized, three-coordinate borane. The conversion of 3-bromopyridine to the corresponding pyridine pinacol ester (**1**) was a performed according to a literature procedure with an overall yield of 34% (Scheme 4.1.).[10] The corresponding chemistry was also carried out using 3-bromoquinoline to afford the analogous quinoline pinacol ester (**2**) with an overall yield of 14%.

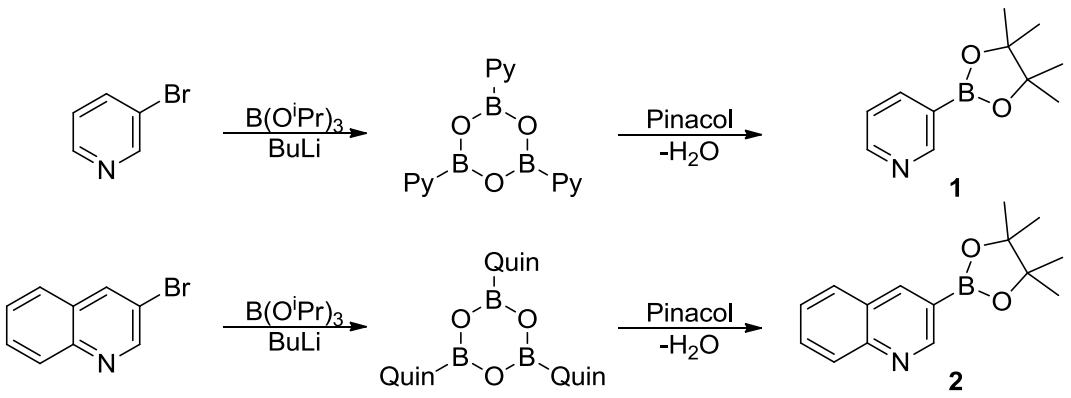

Scheme 4.1. The literature methods of preparation of **1** and **2**.[10]

These boronic esters (**1** and **2**) could readily be methylated with methyl iodide to afford the corresponding pyridinium and quinolinium iodide salts ([**3**]I and [**4**]I) in essentially quantitative yields (Scheme 4.2.). These novel, cationic three-coordinate boranes were characterized by a combination of ^{1}H, ^{11}B and ^{13}C NMR spectroscopy and mass spectrometry. The peaks in the ^{11}B NMR spectrum at 30 and 31 ppm for [**3**]I and

[**4**]I, respectively, are typical of three-coordinate boron centers bound to a single aryl group and a chelating pinacolate function.[11] The molecular structure of [**3**]I in the solid state was obtained *via* single crystal X-ray diffraction, which confirmed connectivity and hence the presence of a three-coordinate borane (Figure 4.3.).

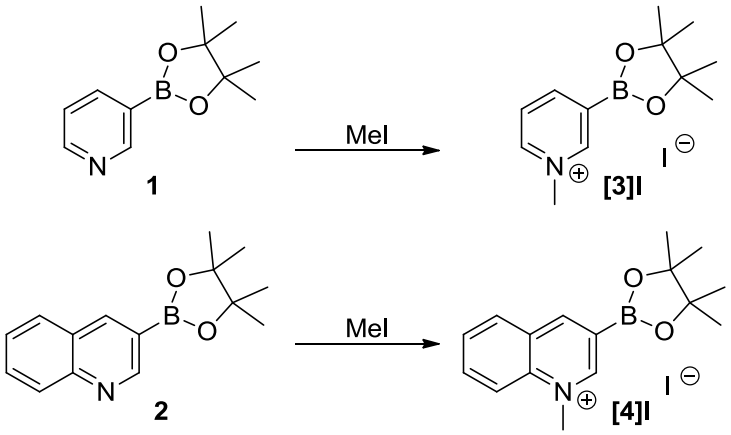

Scheme 4.2. The reactions of **1** and **2** with methyl iodide to give [**3**]I and [**4**]I, respectively.

The crystal structure of [**3**]I exhibits a planar environment around boron, as is suggested by the ^{11}B NMR in chloroform solution, with the sum of the angles approximately equal to 360 º (Table 4.1). The two boron-oxygen and boron-carbon bond distances are typical for this type of compound with values of 1.350(6), 1.363(5) and 1.562(6) Å respectively.[2,12,13]

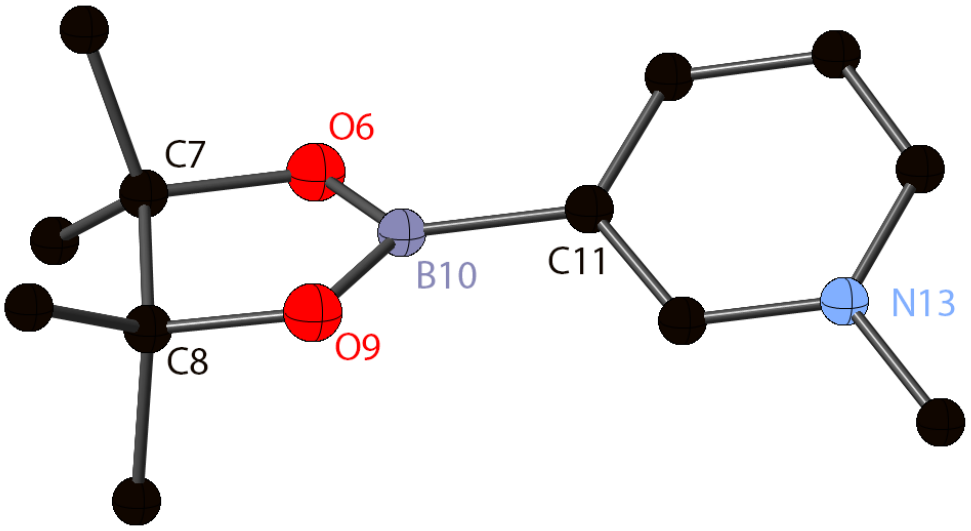

Figure 4.3. The molecular structure of [**3**]I as obtained from X-ray crystallography. The iodine anion and $CHCl_3$ solvate omitted for clarity. Atoms illustrated as isotropic spheres set at the 20 % probability level, with hydrogen atoms omitted, boron in mauve, carbon in black, nitrogen in blue and oxygen in red. Thermal ellipsoids have not been used for reasons of clarity, as they are large and misshapen due to low crystal quality.

Bond/Angle	**Distance (Å) / Angle (º)**
B-O	1.350(6), 1.363(5)
B-C	1.562(6)
N-C	1.477(6)
O-B-C	122.5(3), 122.4(3)
O-B-O	115.1(4)
Σ(O-B-C/O-B-O)	360 (1)

Table 4.1. Pertinent bond lengths and angles for **[3]**I. Σ(O-B-C/O-B-O) is the sum of the angles C_{Aryl}-B-O and O-B-O.

Treating **3** with one equivalent of the fluoride anion in $CDCl_3$ solution gives rise to the fluoride adduct [**3**·F] (Scheme 4.4.). The ^{11}B NMR spectrum exhibits a doublet at 8.3

ppm. The chemical shift and the nature of the coupling are indicative of a fluorine anion being directly bound to the boron center.[12] The ^{19}F NMR spectrum exhibits a partially collapsed quartet at -137 ppm, with the chemical shift and nature of the coupling indicative of a fluorine anion directly bound to the boron center (^{11}B: I = 3/2).[2] The ^{1}H and ^{13}C NMR spectra are fully consistent with this interpretation, with the signals corresponding to the methyl groups of the pinacol exhibiting two chemical environments, i.e. pointing towards/away from the boron bound fluoride anion. The identity of the compound was confirmed *via* single crystal X-ray diffraction, with the crystal structure obtained confirming the presence a fluorine atom bound to boron (Figure 4.5).

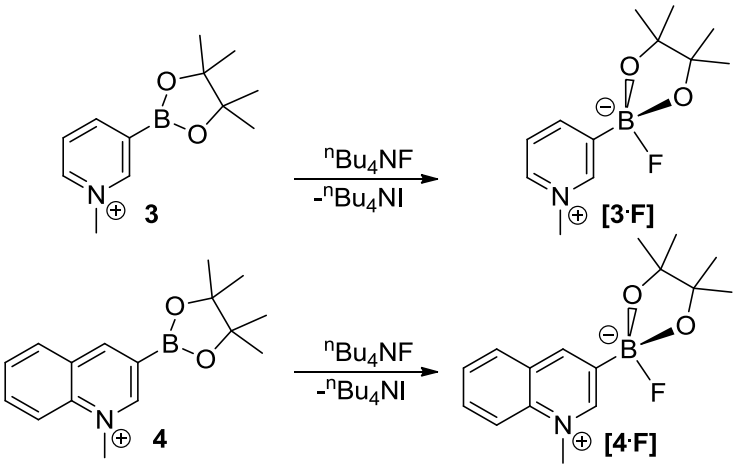

Scheme 4.4. The reaction of **3** and **4** with [^{n}Bu$_4$N]F·4(H$_2$O) to give [**3**·F]$^-$ and [**4**·F]$^-$, respectively.

The crystal structure of [**3**·F] (Figure 4.3), which has two crystallographically unique units, displays two four-coordinate borate molecules with boron-fluorine bond distances of 1.439(1) and 1.445(1) Å respectively. These B-F bond lengths are similar to those found in the crystal structure of **I** (1.407 Å)[14] and are identical to those predicted by DFT (1.439 and 1.445 Å, respectively) for the related systems **II** and **III** (Scheme 4.5.).[13]

The average B-O bond distance (1.46 Å) observed in **[3**·F] is longer the average B-O bond distance (1.36 Å) determined for **3** with the degree of elongation being similar to that (0.1 Å) calculated by DFT for related systems. [13] The sums of the O-B-C and O-B-O angles (approximately 331 and 335 º, respectively) are similar to those observed for **I** (330.5 º), consistent with the boron centre becoming pyramidal (cf 360 ºC for **3**).

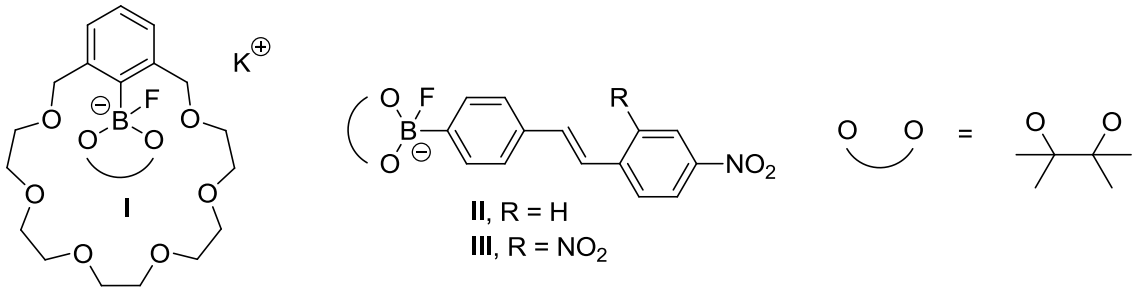

Scheme 4.5. The structures of **I**, **II** and **III**.

The crystal structure of [**3**·F]I also exhibits a close approach of the boron-bound fluorine atom to one of the protons of the pyridine unit, with H···F contacts for the two molecules in the asymmetric unit of 2.47 and 2.50 Å. This suggests that in the solid state at least, the lowest energy conformation features an additional hydrogen bonding motif. There is no evidence in the ^{1}H or ^{19}F NMR spectra that this binding motif is retained in either chloroform or THF solution, even at -40 ºC.

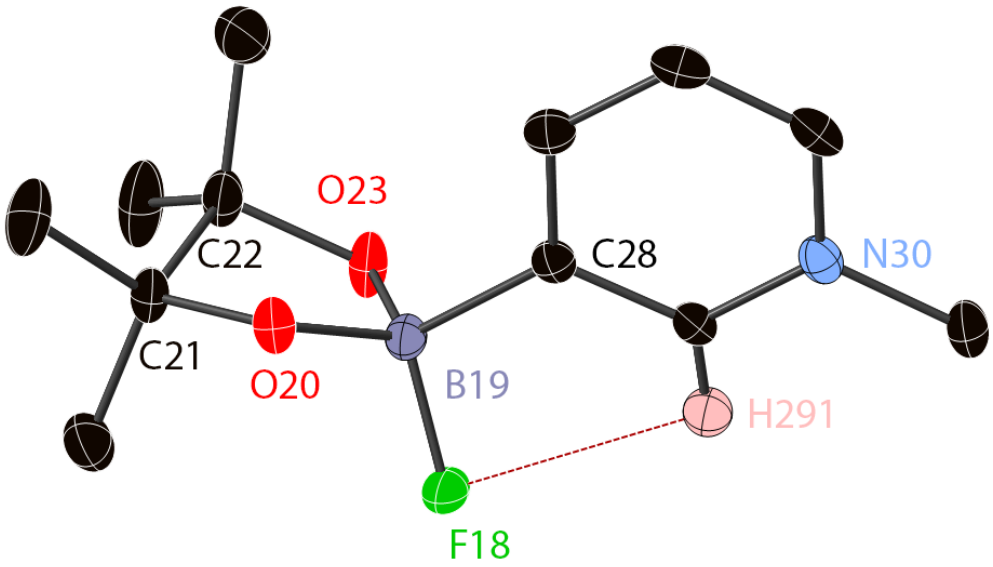

Figure 4.6. The molecular structure of **[3**·F], with one of the crystallographically unique boron containing species omitted for clarity. Ellipsoids drawn at the 50% probability level, with hydrogen in pink, boron in mauve, carbon in black, nitrogen in blue, oxygen in red and fluorine in green.

Bond/Angle	**Distance (Å) / Angle (º)**
B-F	1.439(1), 1.445(1)
B-O	1.450(1). 1.469(1), 1.449(1), 1.4700(1)
B-C	1.647(1), 1.644(1)
N-C	1.477(1), 1.477(1)
F-H	2.468, 2.495
O-B-C	111.97(2), 111.19(7), 111.52(8), 112.91(8)
O-B-O	112.17(7), 106.37(7)
O-B-F	112.14(7), 112.04(7), 112.07(8), 108.65(7)
Σ(O-B-C/O-B-O)	335, 331

Table 4.2. Pertinent bond lengths and angles of [**3**·F]. Σ(O-B-C/O-B-O) is the sum of the angles C_{Aryl}-B-O and O-B-O.

Treating [**3**]I with half an equivalent of fluoride gave rise to a set of equilibrium-weighted chemical shifts in the ^{1}H NMR spectrum, rather than two sets of peaks corresponding to the receptor [**3**]I and the fluoride adduct [**3**·F], which suggests that fluoride binds reversibly and that the rate of exchange between the receptor and the fluoride adduct is fast on the NMR time-scale. This feature allows the fluoride binding constant of **[3**]I to be determined in d_3-acetonitrile by titrating [^{n}Bu$_4$N]F·3(H$_2$O) against [**3**]I, and measuring the ^{1}H NMR spectrum after each addition (Figure 4.7-8). It was thus possible for Stuart Cornes (M.Chem student under my supervision) to estimate the fluoride binding constant (approximately 10^4 M^{-1}) using the WinEQNMR2 software suite by plotting the chemical shift of protons at the 5 (c) and 6 (d) positions of [**3**]I against the concentration of fluoride added (Figure 4.4).[15] The value of 10^4 M^{-1} in d_3-acetonitrile compares relatively well to a value of 10^5 M^{-1} in dichloromethane for **II** and **III** obtained by Spange and coworkers, with due allowance made for the different solvent employed (Scheme 4.5).[13]

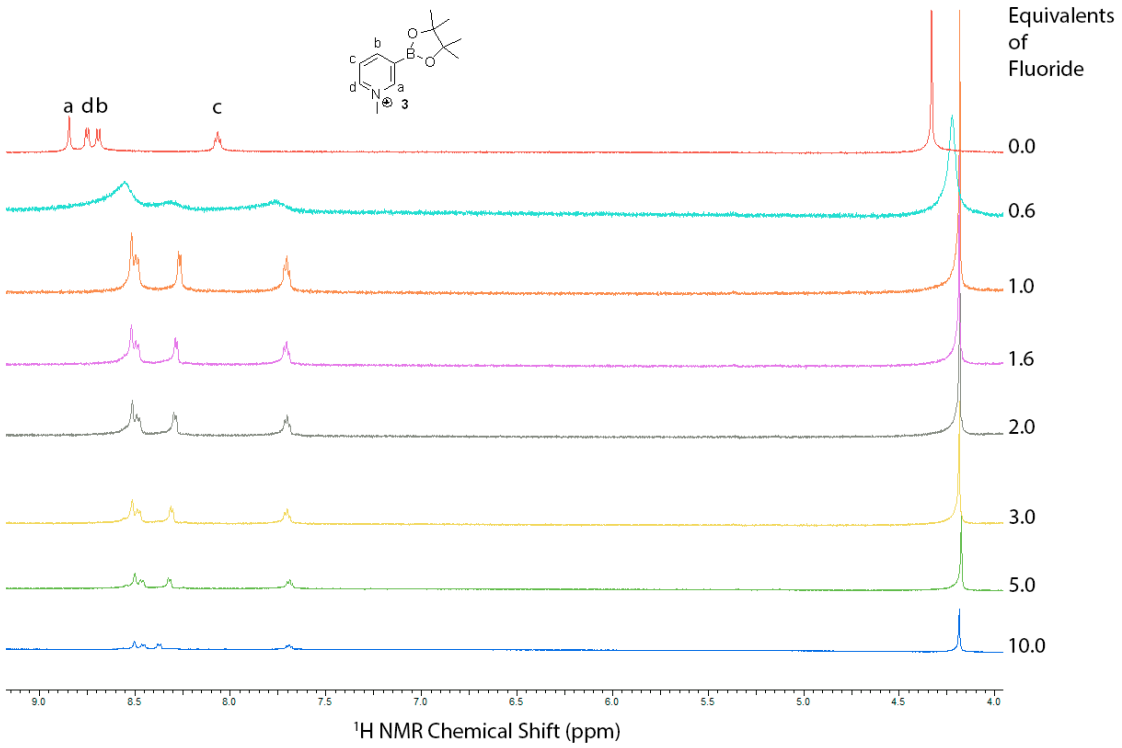

Figure 4.7. The ^{1}H NMR spectra used in the determination of the fluoride binging constant (K_F) of [**3**]I.

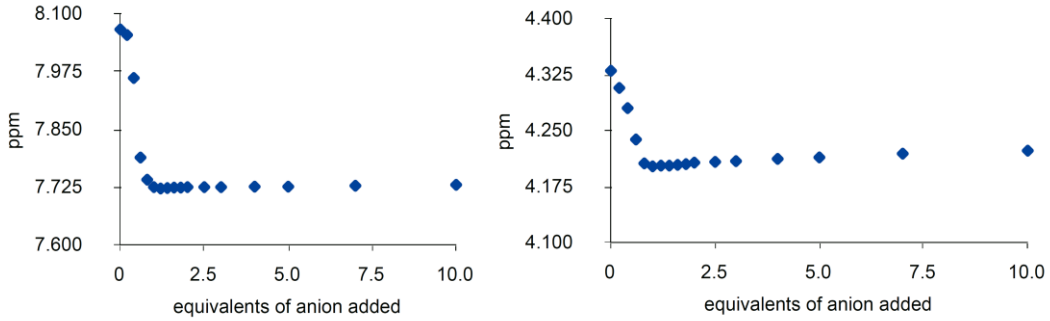

Figure 4.8 Change in the ^{1}H NMR chemical shift of the 5-proton (c, left) and 6-proton (d, right) against equivalents of fluoride added, as used in the WinEQNMR software suite to calculate the binding constant for fluoride.

Treating [**4**]I with one equivalent of the fluoride anion gives the fluoride adduct [**4**·F], which results in a similar binding motif as [**3**·F]. The ^{11}B NMR spectrum exhibits a doublet centred at 4.1 ppm, with the chemical shift and coupling constant being fully consistent with a fluoride anion (^{19}F: I = ½) directly bound to the boron atom. The ^{19}F NMR spectrum exhibits a partially collapsed quartet, which is consistent with a fluoride anion bound directly to boron (^{11}B: I = 3/2). The ^{1}H and ^{13}C spectra are consistent with a fluoride adduct, with two sets of signals for the methyl groups of the pinacol.

Unlike the reaction of [**3**]I with fluoride, which gives rise to no observable change in colour on binding fluoride, treatment of [**4**]I with fluoride gave rise to a dramatic colour change from yellow to colourless (Figure 4.9).

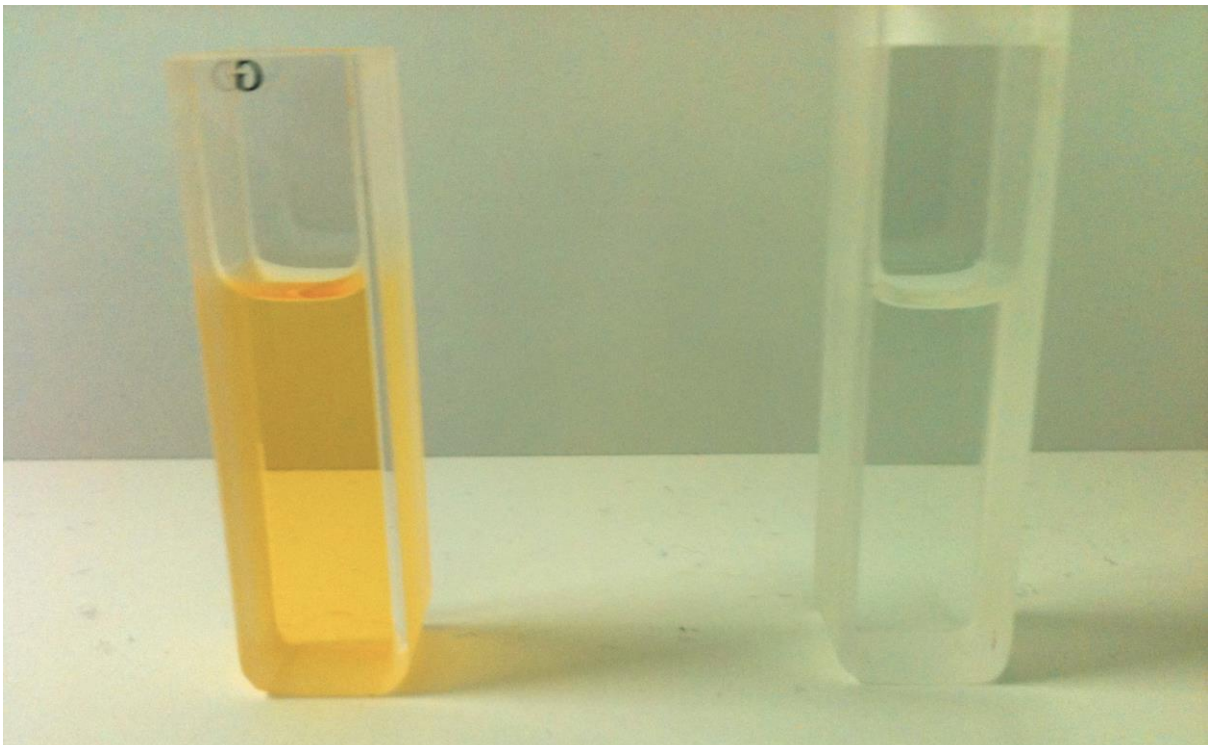

Figure 4.9. A dichloromethane solution of the "free" receptor [**4**]I (left) and its fluoride adduct **[4**·F] (right).

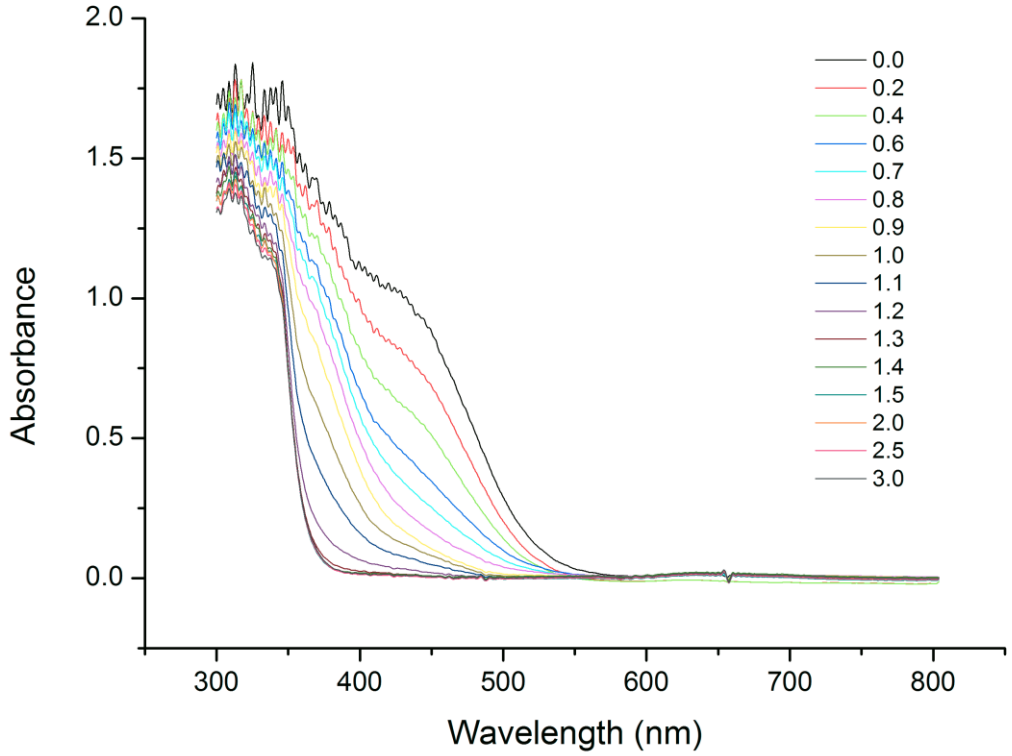

Figure 4.10. The UV-Vis trace of [**4**]I on the gradual addition of [^{n}Bu$_4$N]F·3(H$_2$O). The key to the colour of the line is given in the top right corner.

The changes in the UV-Vis spectrum on the addition of fluoride were investigated by Stuart Cornes (M.Chem student under my supervision). The UV-Vis spectroscopy shows a decrease in intensity on addition of fluoride (as the tetrabutylammonium tetrahydrate salt). The plot of the normalized intensity of the band at 420 nm, against the volume of fluoride-anion-containing solution added, is shown in Figure 4.10. The fluoride binding constant of [**4**]I was determined using this UV-Vis data at using the ReactLab software, to give a binding constant K_F of approximately 10^4 M^{-1} in dichloromethane solution (Figure 4.11). This K_F value is of the same order of magnitude as that calculated for [**3**]I as expected, given the structural similarities of the receptors.

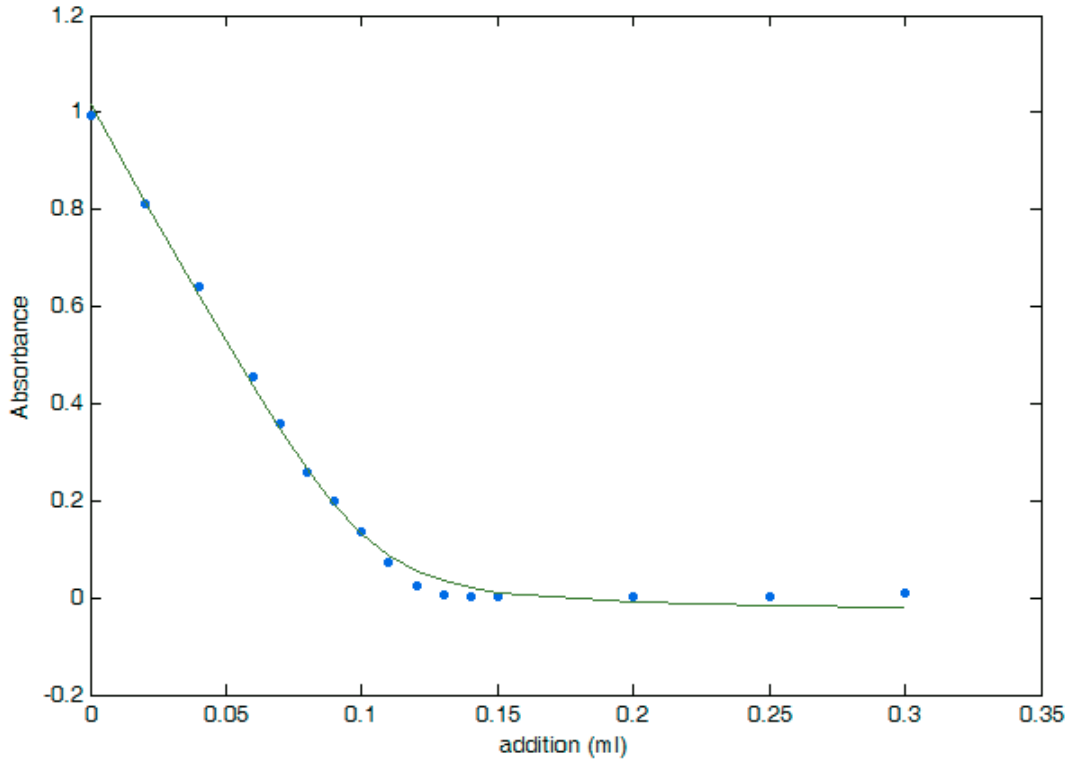

Figure 4.11. Plot of normalized absorbance intensity against the amount of fluoride anion containing solution added. The blue dots are the actual data obtained and the green line is the fitted line determined using ReactLab software.

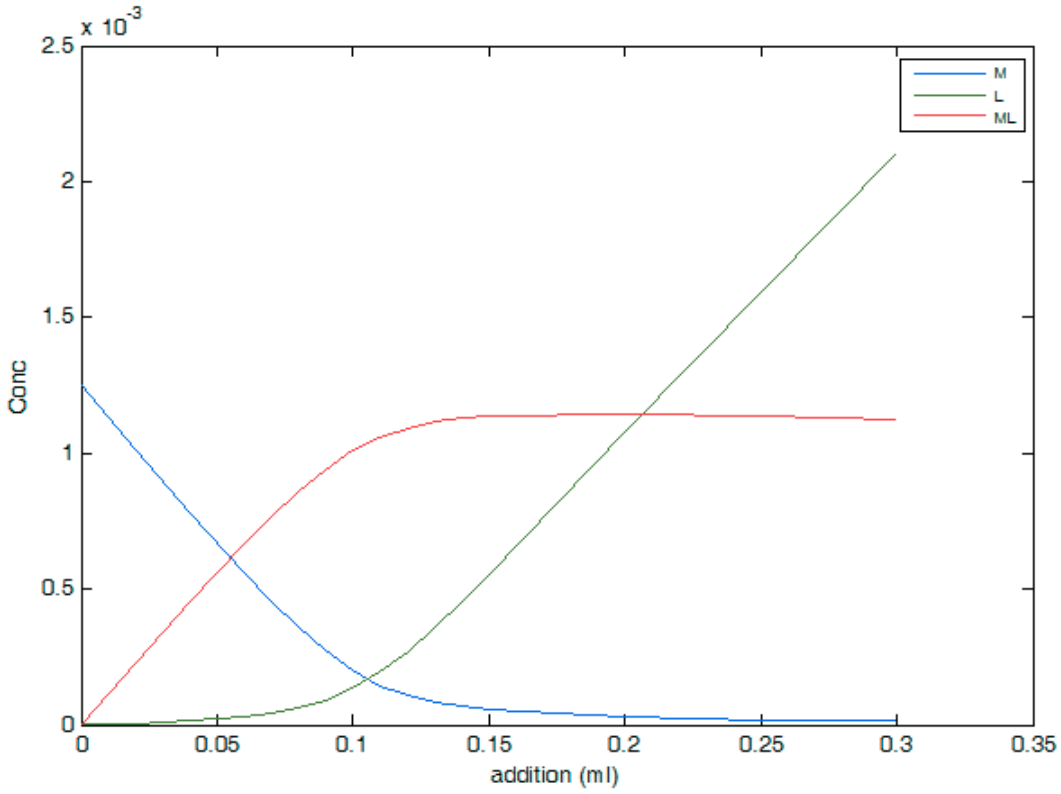

Figure 4.12. The plot of concentrations of receptor [**4**]I (blue), fluoride anion (green) and fluoride adduct [**4**·F] (red) calculated by the ReactLab software during the determination of the fluoride binding constant.

The reaction of [**4**]I with fluoride anions to give [**4**·F] also resulted in a "switching-on" fluorescence response. A dichloromethane solution of [**4**]I was titrated with solutions of [^{n}Bu$_4$N]F·3(H$_2$O) and the fluorescence properties of these mixtures analyzed by Stuart Cornes. A plot of the fluorescence intensity against wavelength for mixtures containing various equivalents of fluoride is shown in Figure 4.13. The fluorescence intensity increases approximately four-fold on adding five equivalents of this anion. Quaternized quinoline groups have been used as fluorescent sensors for the heavier halides, such as iodide; an increase in the concentration of iodide results in lower fluorescence intensity, which has been attributed to dynamic quenching by heavier

halides.[16] It is possible that the iodide anion of [**4**]I remains in proximity to the charged quinoline unit in solution due to Coulombic forces. If this is the case, then the reaction with fluoride to form [**4**·F] should result in a lowering of the Coulombic attraction (due to the formation of the zwitterionic – overall neutral – quinolium fluoroborate) and, hence, a reduction in the average proximity of the iodide, which should consequently result in fewer collisions between the iodide anion and the quinoline system and so, in turn, less dynamic quenching of fluorescence. Hence, a higher fluorescence intensity should be observed.

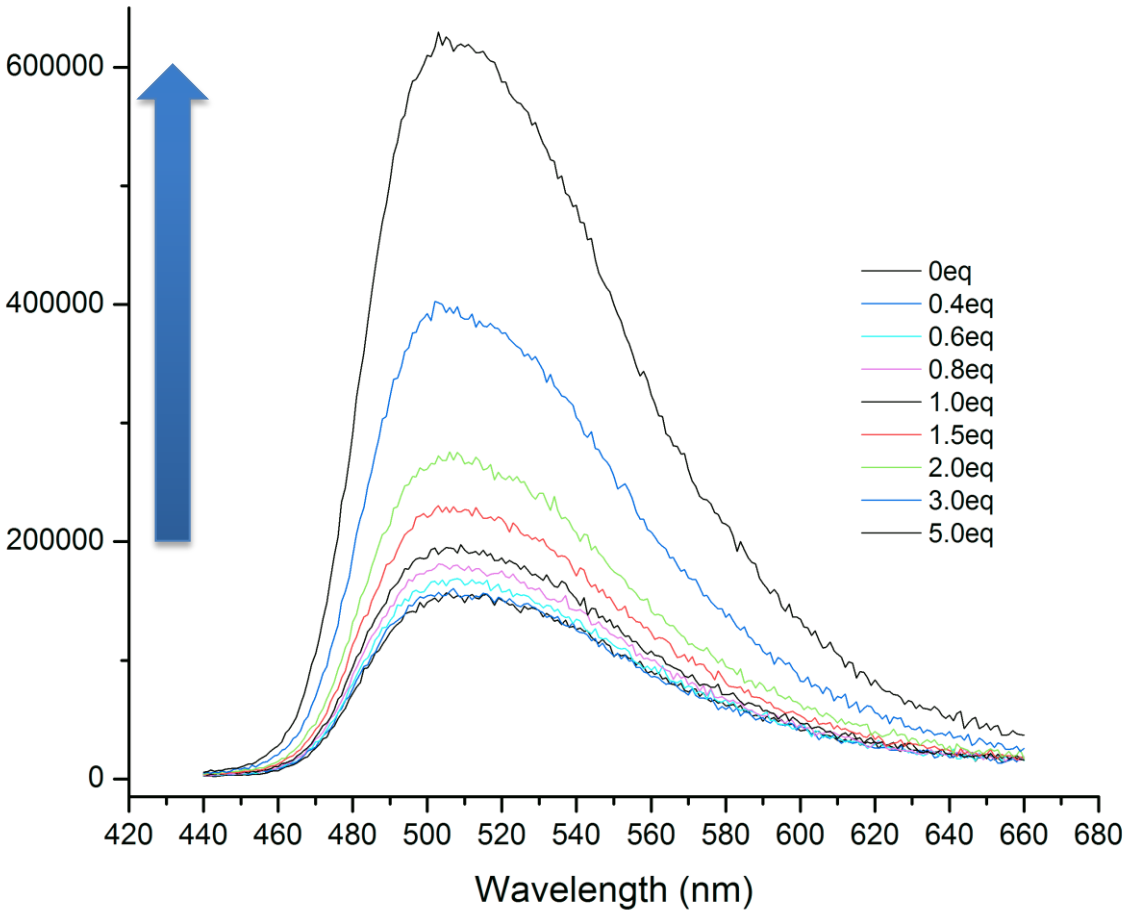

Figure 4.13. The plot of fluorescence intensity of a solution of [**3**]I as a function of the number of equivalents of fluoride added.

Interestingly, treating [**3**]I with one equivalent of the cyanide anion gives rise to the cyanide adduct [**3**·CN] (Scheme 4.14). The ^{11}B NMR spectrum exhibits a single resonance at 5 ppm, which is consistent with such an adduct. The ^{1}H and ^{13}C NMR spectra are fully consistent with a cyanide adduct and are similar to those of **3**, with two sets of peaks for the methyl groups of the pinacolate arising from different alignments with respect to the boron bound cyanide.

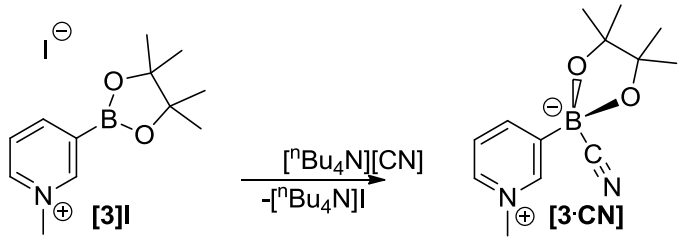

Scheme 4.14. The reaction of [**3**]I with [^{n}Bu$_4$N][CN]·2(H_2O) to give **[3**·CN].

4.4.2. Mixed Alkenyl/Aryl Boranes

A difficulty encountered with the pinacolate ester system was that none were capable of binding either cyanide or fluoride anions in solutions containing more than 10% of water, due to hydrolysis of the B-O bonds in the receptor complex. It was, therefore, of interest to synthesize a receptor employing a more chemically robust borane system. Given that the $BMes_2$ unit exhibits greater resistance to hydrolysis than $B(OR)_2$, it was decided to target a $BMes_2$-functionalized pyridine unit.

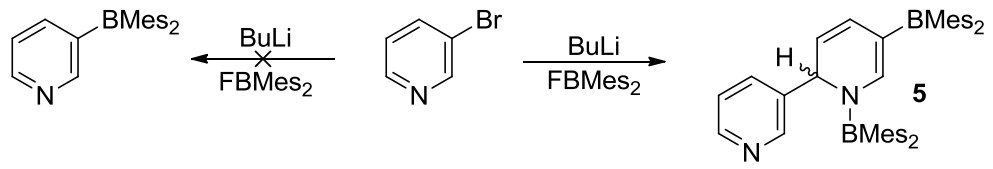

Scheme 4.12. The attempted synthesis of $BMes_2(C_5NH_4)$ [left] and the actual product isolated **5**.

Attempts to synthesize $BMes_2(C_5NH_4)$ directly from 3-bromopyridine *via* lithiation, followed by quenching with $FBMes_2$, were not successful under any of the conditions attempted (Scheme 4.12, Table 4.3.). The products of this reaction appear to result instead from nucleophilic attack at the 6 position of 3-bromopyridine. Amongst the mixture of compounds generated under the various reaction conditions, compound **5** proved to be of the greatest interest. **5** appears to have arisen from a combination of unwanted nucleophilic attack at the 6-position of the pyridine ring and the desired *trans*-metallation and salt-elimination reaction at the 3-position. No attempt was made to determine the order in which these two reactions occur.

The identity of **5** was initially established using analysis by mass spectrometry, with a large peak corresponding to almost exactly twice that expected for the molecular mass peak $BMes_2(C_5NH_4)$, which corresponds exactly that of **5**. **5** exhibits two peaks in the ^{11}B NMR spectra, with one peak at 73 ppm corresponding to typical three-coordinate tri-aryl and related boranes. The second peak in the ^{11}B NMR spectrum at 49 ppm, corresponds to a three-coordinate borane featuring a π donor substituent such as an amido group. Thus the chemical shift is similar to that of 44.5 ppm observed for Me_2NBMes_2 reported by Wilson and coworkers.[17] The ^{1}H, ^{13}C, g-COSY, HSQC and HMBC NMR spectra are fully consistent with the suggested chemical structure. Confidence in the identification of **5** was further bolstered by elemental microanalyses.

Reagent	**Temperature of reagent addition (ºC)**	**Temperature and time of stirring (ºC, hours)**	**Temperature of quench with $FBMes_2$ (ºC)**	**Could 11 be isolated?**
1 eq. ^{n}BuLi	-78	-78, 1	-78	No
1 eq. ^{n}BuLi	-78	-78, 1/12	-78	No
1 eq. ^{n}BuLi	-78	-78, 1/4	-78	No
1 eq. ^{n}BuLi	-78	-40, 1	-78	No
1 eq. ^{n}BuLi	-78	-40, 5	-78	No
1 eq. ^{n}BuLi	-78	-78, 12	-78	No
1 eq. ^{n}BuLi	-78	20, 12	-78	No
1 eq. ^{n}BuLi	-40	-40,1	-40	No
1 eq. ^{n}BuLi	-40	0, 1	-40	No
2 eq. ^{t}BuLi	-78	-40, 1	-78	No
PhMgBr	-78	-78, 5	-78	No

Table 4.3. General reaction conditions for the attempted syntheses of $BMes_2(C_5NH_4)$, with success defined as being able to isolate $BMes_2(C_5NH_4)$ in any quantity.

Crystals that were suitable for single crystal X-ray diffraction studies were grown from a chloroform solution of **5**, and the results of these studies confirm the identity of **5** (Figure 4.16). The crystal structure obtained is not of sufficient quality so as to discuss the bond lengths or angles with any confidence, but is included so that the connectivity can be confirmed.

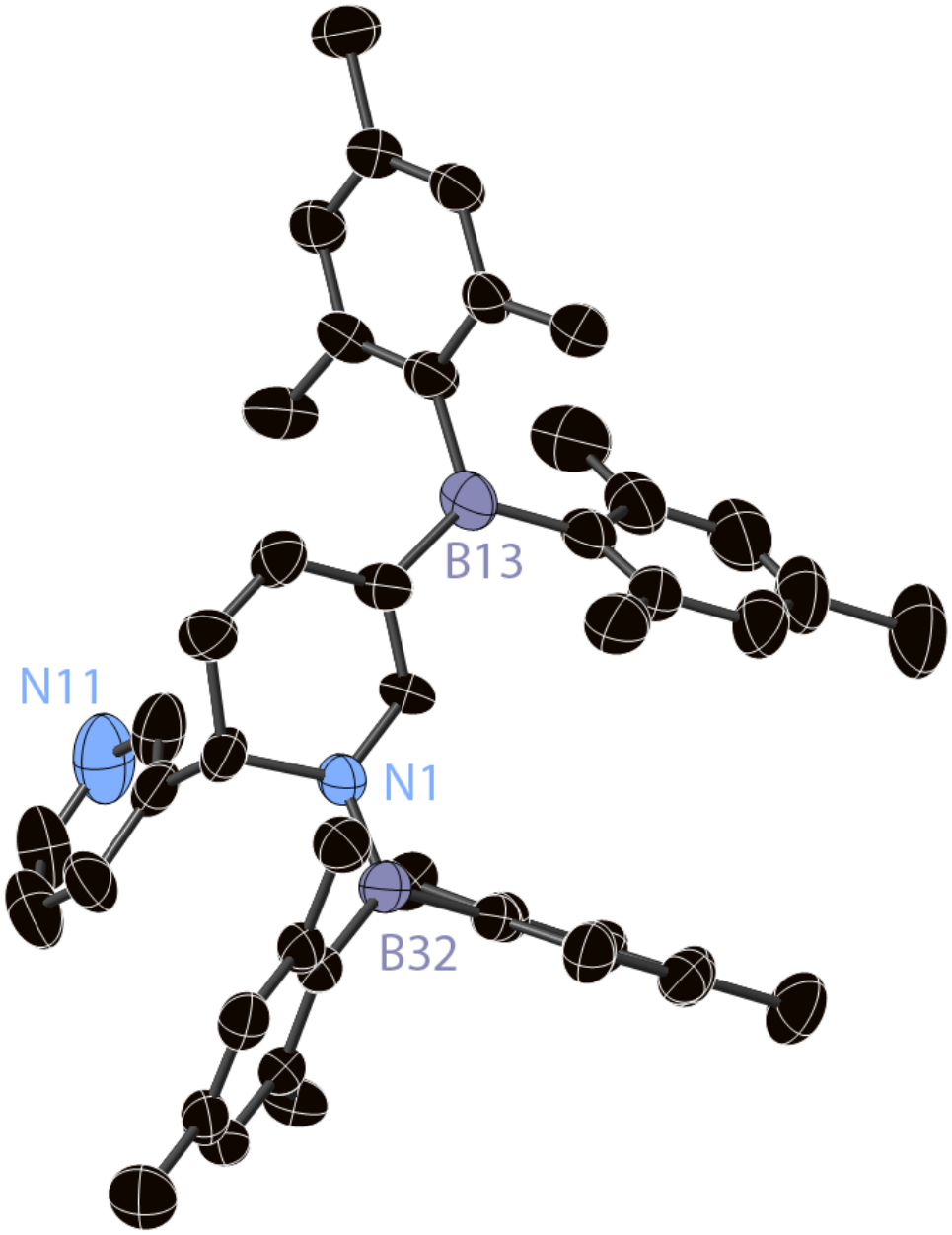

Figure 4.16. The molecular structure of **5** with hydrogen atoms omitted for clarity and ellipsoids drawn at the 50% probability level.

Attack at the two position of pyridine in the presence of $FBMes_2$ is not without precedent, as demonstrated by the work of Okada *et al.*[18] These authors report that a one-to-one mixture of pyridine and $FBMes_2$ yields the adduct, $C_5NH_5{\cdot}BFMes_2$, which was

treated at -30 ºC with organo-lithium reagents, such as *n*-BuLi, PhLi or 3-lithiopyridine; and nucleophilic attack at the 2-position was observed to occur in each case (Scheme 4.17.). The identity of the product of the reaction of $C_5NH_5{\cdot}BFMes_2$ with PhLi was established using single crystal X-ray diffraction. No ^{11}B NMR spectral data was presented by Okada *et al* for this product, but the ^{1}H NMR spectral data for this compound are fully consistent with the crystal structure and exhibits a pattern of resonances that is remarkably similar to that of **5**. No comment on the colour, or any fluorescence properties, of the products of nucleophilic attack on $C_5NH_5{\cdot}BFMes_2$ was made by Okada *et al*.[18]

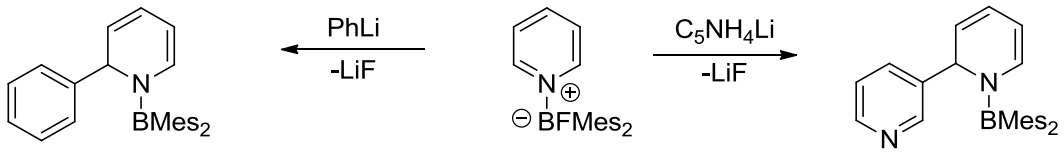

Scheme 4.17. The reaction of the $C_5NH_5{\bullet}BFMes_2$ adduct PhLi or *3*-lithio-pyridine as reported by Okada *et al*.[18]

Attempts were made to minimize the propensity for attack at the 2-position of pyridine fragments by reacting the 3,5-dibromopyridine with bulky *tert*-butyl lithium and subsequently treating this reaction mixture with $FBMes_2$ (Scheme 4.18). A complex mixture of compounds was generated, from which some single crystals were obtained. One of these was studied by single crystal X-ray diffraction, and the structure obtained (**6**) is reminiscent of that of **5** in that a similar bis(borylated) dearomatized N-heterocyclic core is obtained (Figure 4.19). The attack of the *tert*-butyl group at the two position suggested that our attempt to use steric protection of the 2-position was not viable. No further investigation of these reactions was undertaken.

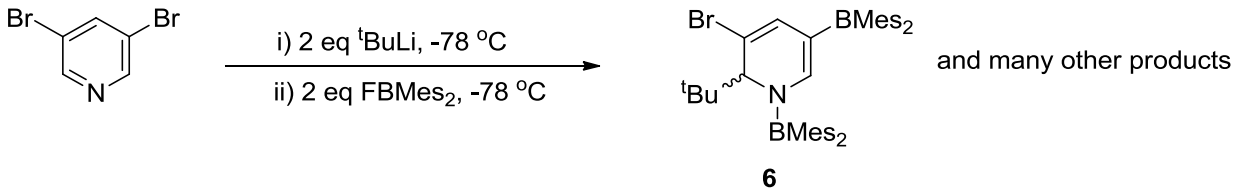

6

Scheme 4.18. The reaction 3,5-dibromopyridine with ^{t}BuLi and $FBMes_2$ to give a mixture of compounds including compound **6**.

Compound **5** is highly fluorescent in both the solid state and in solution. This observation is consistent with the proposed structural connectivity, which contains a B-C=C-N moiety, and should therefore exhibit fluorescence, according to the hypothesis of Kaufmann and coworkers.[19] Compounds featuring partial B=N double bond character have also been reported to exhibit fluorescence, such as for **6**, in the work of Wang and coworkers (Scheme 4.20.).[20]

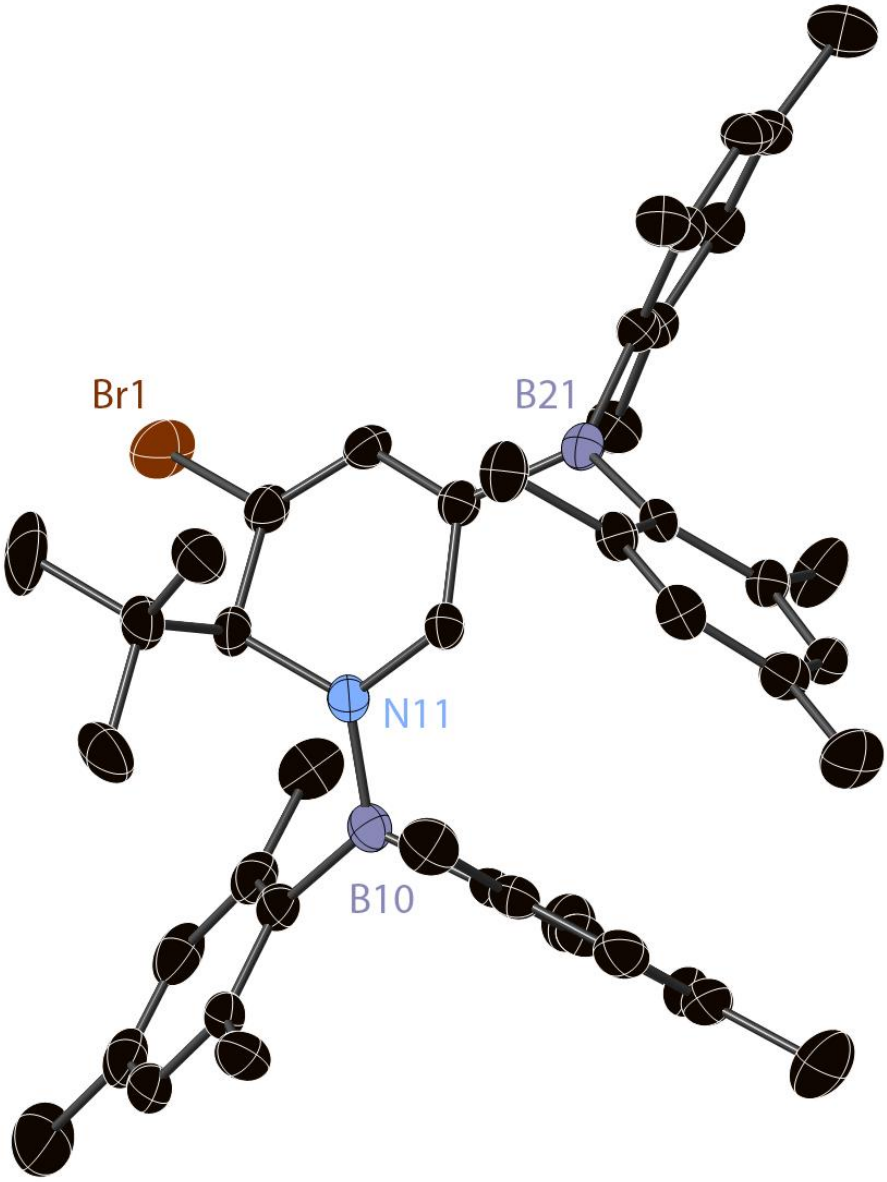

Figure 4.19. The molecular structure of **6** with hydrogen atoms omitted for clarity and ellipsoids drawn at the 50% probability level.

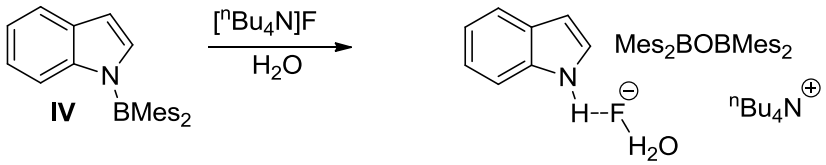

Scheme 4.20. The reaction of **IV** with $[^{n}Bu_4N]F{\cdot}3(H_2O)$.

A solution of **5**, when treated with one equivalent of either fluoride or cyanide, changes colour from a fluorescent yellow to a pale, straw coloured solution. The changes in the UV-Vis absorption properties of a tetrahydrofuran solution were measured as a function of added fluoride or cyanide. The results of these UV-Vis titrations show that only one equivalent of fluoride or cyanide is bound, even with a ten-fold excess of the anion present. The binding constant for fluoride (K_F) in tetrahydrofuran is high (2×10^7 M^{-1}). The bonding constant for cyanide (K_{CN}) in tetrahydrofuran (3×10^8 M^{-1}) is higher than that of fluoride, confirmed by two cross-over binding experiments (Scheme 4.21). The fluoride adduct $[\mathbf{5}{\cdot}F]^-$ reacted, although slowly, with one equivalent of cyanide to give the cyanide adduct $[\mathbf{5}{\cdot}CN]^-$, whereas the cyanide adduct $[\mathbf{5}{\cdot}CN]^-$ did not react with one equivalent of fluoride to give $[\mathbf{5}{\cdot}F]^-$, confirming that **5** binds a cyanide anion more strongly than a fluoride anion.

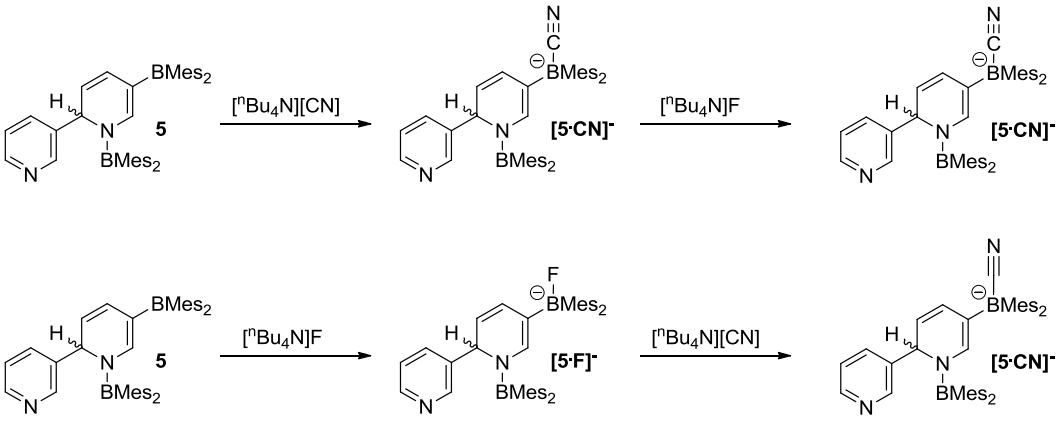

Scheme 4.21 The reaction of **5** to sequential reaction with one equivalent of cyanide then fluoride (top) and the converse order (bottom).

Given that **5** binds only one equivalent of cyanide or fluoride, as established by ^{1}H, ^{11}B and ^{19}F NMR data as well as by UV-vis titration, the question as to where the anion binds is raised. The ^{11}B NMR spectra of the fluoride adduct [**5**·F]$^{-}$ shows two peaks, the first at 4 ppm, corresponding to a four-coordinate borane, and the second at 28 ppm, corresponding to the N-$BMes_2$ unit. A similar ^{11}B NMR spectrum was observed for [**5**·CN]$^{-}$, with peaks at -16 ppm, corresponding to a four-coordinate borane, and at 49 ppm corresponding to the N-$BMes_2$ unit. The $^{`1}$H, ^{13}C and ^{19}F NMR spectra for [**5**·F]$^{-}$ and the ^{1}H and ^{13}C NMR spectrum for [**5**·CN]$^{-}$ are fully consistent with this interpretation.

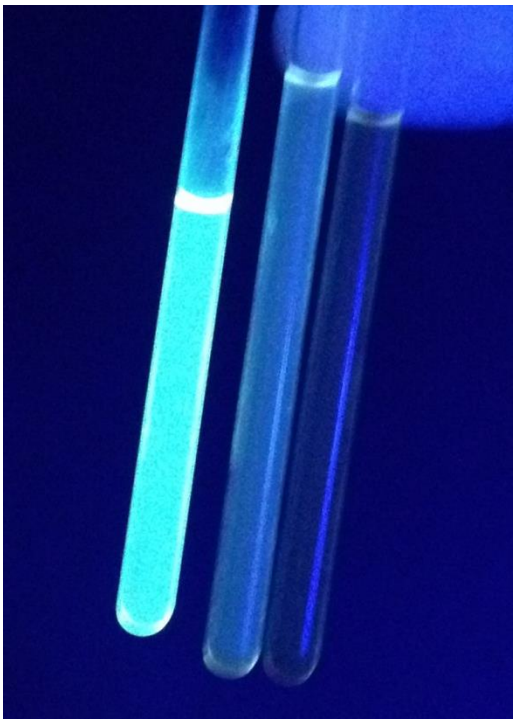

Figure 4.22. A picture of UV-irradiated (254 nm) THF solutions of receptor **5** (left), a one-to-one mixture of **5** and $[^{n}Bu_4N]^{+}[F]^{-}\cdot 3(H_2O)$ (middle) and a one-to-one mixture of **5** and $[^{n}Bu_4N]^{+}[CN]^{-}\cdot 2(H_2O)$ (right).

The fluorescence of solutions of **5** is dramatically reduced on the addition of one equivalent of cyanide or fluoride anions as the tetrabutyl ammonium salt (Figure 4.22). This observation is in sharp contrast to the "switch-on" fluorescence of **4**. Given that the anions bind to the C-$BMes_2$ unit, in preference to the N-$BMes_2$ unit, this strongly suggests that the fluorescence arises from the N-C=C-B unit. That this fluorescence is quenched suggests that transitions to molecular orbitals bearing a major contribution from the formally vacant p-orbital of boron are key to the high fluorescence of **5**. A rigorous investigation of the fluorochemical properties of **5** was not undertaken as this was not an intended product and its isolation as a pure compound was protracted.

4.5. Conclusions

A range of novel cationic boronic esters were synthesised and shown to be competent at binding both fluoride and cyanide anions. Interestingly, one of these cationic boronic esters was capable of reporting the binding of fluoride colourimetrically through the loss of colour. The propensity of these boranes to degrade in the presence of water was established.

Novel synthetic routes have also been developed to a range of mixed alkenyl/aryl boranes, albeit from an unexpected synthetic route. These mixed alkenyl/aryl boranes were shown to be competent at binding both fluoride and cyanide anions, and to report the presence of either anion both colorimetricaly and by quenched fluorescence. This allowed for the anion binding strength of the novel alkenyl/aryl boranes to be determined.

4.6. References

(1) Yamamoto, H.; Ori, A.; Ueda, K.; Dusemund, C.; Shinkai, S. *Chemical Communiations (Cambridge)* **1996**, 407.

(2) Bresner, C.; Day, J. K.; Coombs, N. D.; Fallis, I. A.; Aldridge, S.; Coles, S. J.; Hursthouse, M. B. *Dalton Transactions* **2006**, 3660.

(3) Arimori, S.; Davidson, M. G.; Fyles, T. M.; Hibbert, T. G.; James, T. D.; Kociok-Kohn, G. I. *Chemical Communications (Cambridge)* **2004**, 1640.

(4) Galbraith, E.; Fyles, T. M.; Marken, F.; Davidson, M. G.; James, T. D. *Inorganic Chemistry* **2008**, *47*, 6236.

(5) Bresner, C.; Haynes, C. J. E.; Addy, D. A.; Broomsgrove, A. E. J.; Fitzpatrick, P.; Vidovic, D.; Thompson, A. L.; Fallis, I. A.; Aldridge, S. *New Journal of Chemistry* **2010**, *34*, 1652.

(6) Sole, S.; Gabbaï, F. P. *Chemical Communications (Cambridge)* **2004**, 1284.

(7) Yamaguchi, S.; Akiyama, S.; Tamao, K. *Journal of the American Chemical Society* **2001**, *123*, 11372.

(8) Hudnall, T. W.; Gabbaie, F. P. *Journal of the American Chemical Society* **2007**, *129*, 11978.

(9) Lee, M. H.; Agou, T.; Kobayashi, J.; Kawashima, T.; Gabbaï, F. P. *Chemical Communications (Cambridge)* **2007**, 1133.

(10) Li, W.; Nelson, D. P.; Jensen, M. S.; Hoerrner, R. S.; Cai, D.; Larsen, R. D.; Reider, P. J. *The Journal of Organic Chemistry* **2002**, *67*, 5394.

(11) Bresner, C.; Aldridge, S.; Fallis, I. A.; Jones, C.; Ooi, L.-L. *Angewandte Chemie International Edition* **2005**, *44*, 3606.

(12) Aldridge, S.; Bresner, C.; Fallis, I. A.; Coles, S. J.; Hursthouse, M. B. *Chemical Communications (Cambridge)* **2002**, 740.

(13) Oehlke, A.; Auer, A. A.; Jahre, I.; Walfort, B.; Rüffer, T.; Zoufalá, P.; Lang, H.; Spange, S. *The Journal of Organic Chemistry* **2007**, *72*, 4328.

(14) Reetz, M. T.; Niemeyer, C. M.; Harms, K. *Angewandte Chemie International Edition in English* **1991**, *30*, 1472.

(15) Hynes, M. J. *Journal of the Chemical Society, Dalton Transactions* **1993**, 311.

(16) Badugu, R.; Lakowicz, J. R.; Geddes, C. D. *Sensors and Actuators B: Chemical* **2005**, *104*, 103.

(17) Davidson, F.; Wilson, J. W. *Organic Mass Spectrometry* **1981**, *16*, 467.

(18) Okada, K.; Suzuki, R.; Oda, M. *Journal of the Chemical Society, Chemical Communications* **1995**, 2069.

(19) Albrecht, K.; Kaiser, V.; Boese, R.; Adams, J.; Kaufmann, D. E. *Journal of the Chemical Society, Perkin Transactions 2* **2000**, 2153.

(20) Cui, Y.; Li, F.; Lu, Z.-H.; Wang, S. *Dalton Transactions* **2007**, 2634.

Chapter Five: Frustrated Lewis Pairs in Molecular Detection

5.1. Introduction - Frustrated Lewis Pairs (FLPs)

The publication of Gilbert N. Lewis on the nature of acids and bases has served as a foundation of our understanding of acid/base chemistry for the greater part of a century.[1] By Lewis' definition: acids are electron-pair acceptors and bases are electron-pair donors. The two form dative covalent bonds when mixed together to give an acid-base adduct, thereby quenching the reactivity of both the acid and the base. Within the context of Molecular Orbital Theory, the lowest unoccupied molecular orbital (LUMO) of the acid interacts with the highest occupied molecular orbital (HOMO) of the base to form the adduct. An example would be the classical Lewis adduct that forms on mixing 2,6-dimethyl pyridine with boron trifluoride (Scheme 5.1). [2,3] That a dative covalent bond does not always form on mixing a Lewis acid and a Lewis base was noted by H. C. Brown, whilst working under the direction of H. Schlessinger, as early as 1942.[3] He noted that a mixture of 2,6-dimethyl pyridine and trimethyl borane do not form a Lewis adduct, due to the high steric crowding such an adduct would have to accommodate (Scheme 5.1). These combinations of Lewis acid and base that are too sterically hindered to form a classical Lewis adduct have recently been termed "frustrated Lewis pairs" (FLPs).[4]

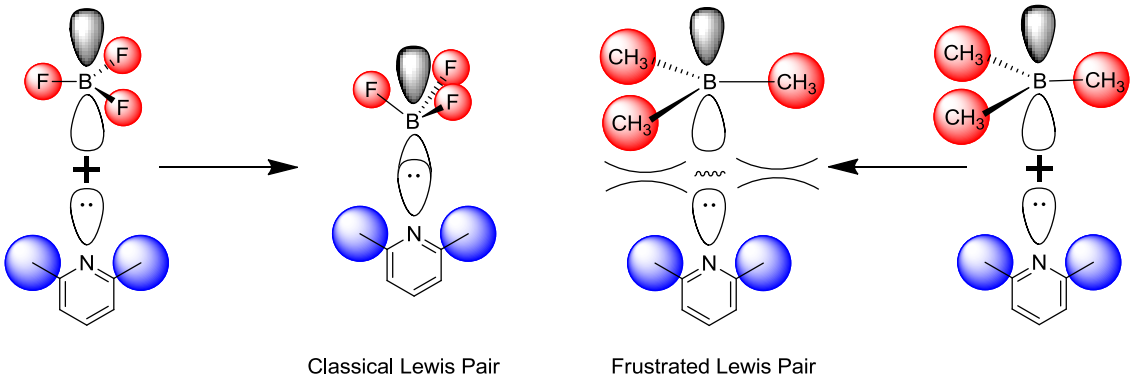

Scheme 5.1. A pictorial representation of the Lewis adduct formation of 2,6-dimethyl pyridine and BF_3 (left) and the frustrated Lewis pair, 2,6-dimethyl pyridine and $(CH_3)_3B$ that do not form a Lewis adduct due to steric strain (right).

Early examples of chemists exploiting the reactivity of frustrated Lewis pairs include the use of BPh_3 and PPh_3 by Witting *et al.* (Scheme 5.2.a) and $NaCPh_3$ and BPh_3 by Tochtermann *et al.* (Scheme 5.2.b) to trap reactive intermediates.[5,6] Despite these early applications, no systematic investigation of the unique reactivity of FLPs for the activation of otherwise unreactive molecules was published until the 2000's.[7]

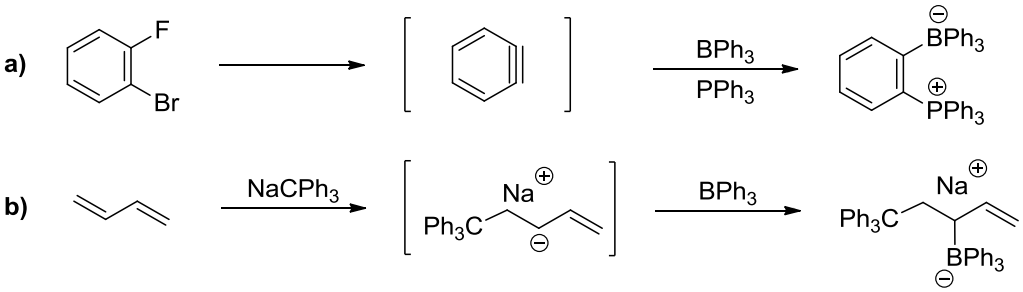

Scheme 5.2. The trapping of a reactive intermediates utilizing frustrated Lewis Pairs.

Widespread interest in the chemistry of FLPs was kindled by the seminal work of Stephan and coworkers, on the first transition-metal free, reversible activation of dihydrogen by $Mes_2P(C_6H_4)B(C_6F_5)_2$ (Scheme 5.3.a).[8] In subsequent investigations by

Spiess *et al.*[8] the aryl linker unit was replaced with an alkyl chain (Scheme 5.3.b), which led to a lack of reversibility for hydrogen activation. Further work by Sumerin *et al.* on an intramolecular nitrogen/boron FLP (Scheme 5.3.c) demonstrated that the basic component could also be an amine in the reversible activation of hydrogen.[9,10]

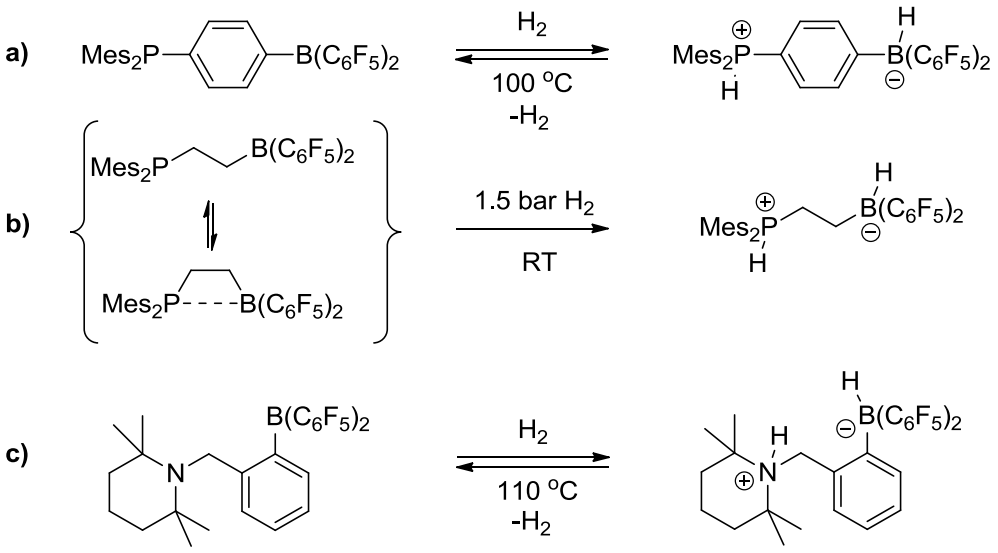

Scheme 5.3. Reversible activation of hydrogen by $Mes_2P(C_6H_4)BMes_2$ (top), $Mes_2P(CH_2)_2B(C_6F_5)_2$ (middle) and an intra-molecular N/B FLP (bottom).

Welch *et al.*,[11] in a quest to simplify the FLP systems capable of heterolytically cleaving hydrogen, placed the acidic and basic components of the FLP on different molecules, with steric congestion alone precluding adduct formation. Stoichiometric mixtures of these unlinked FLPs were found to activate hydrogen at 25 ºC and 1 atmosphere pressure (Scheme 5.4.a). This kind of FLP chemistry has subsequently been extended to several other small molecules that are gaseous at standard temperatures

and pressures, such as carbon dioxide, sulfur dioxide, carbon monoxide and NO (Scheme 5.4.a-e.).[12-20]

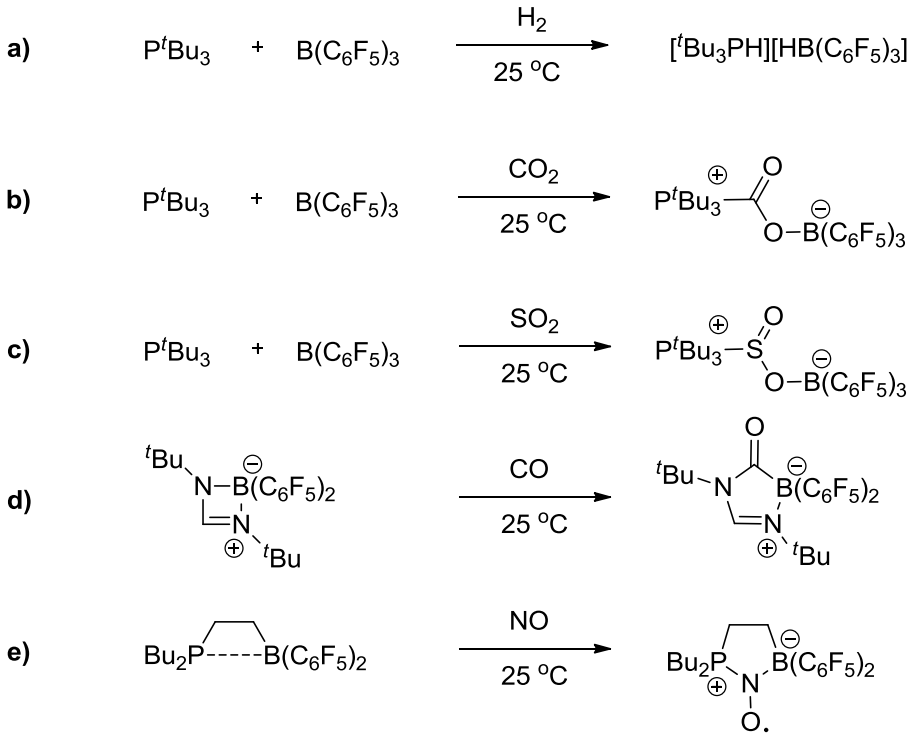

Scheme 5.4. Reactions of FLP systems with H_2 (a), CO_2 (b), SO_2 (c), CO (d) and NO (e).

5.1.1. Nitrous Oxide (N_2O) and its medicinal and environmental aspects / "dephlogisticated nitrous air"

Nitrous oxide first generated by Joseph Priestly in 1772 from the reaction of nitric oxide and iron fillings, is a colourless gas at room temperature and atmospheric pressure.[21] Early research by Humphry Davy on the properties of nitrous oxide, published in 1800, first speculated on its potential medical uses: "As nitrous oxide appears capable of destroying physical pain, it may probably be used with advantage during surgical

operations in which no great effusion of blood takes place".[22] The first documented use in general anesthesia was reported by the dentist Horace Wells in 1844 with widespread use from approximately 1870 through to the 1960s, as a principal agent for pain relief during child-birth.[21,23]

Concerns over accidental and occupational exposure to nitrous oxide are not limited to comedies such as *Laughing Gas* and *Carry on Nurse*, but have also featured extensively in the serious medical literature since the 1970s.[24-31] Long-term occupational exposure to nitrous oxide leads to markedly decreased fertility rates in women.[32-35] Chronic exposure to nitrous oxide has also been linked to liver and kidney damage.[27,36] There are also links between long-term exposure and neurological disorders as well as bone marrow abnormalities linked to continued exposure to nitrous oxide. [37-42]

In addition to worries over some aspects of the medicinal applications of nitrous oxide, concerns have been raised over its environmental impact. Nitrous oxide is a major greenhouse gas, cited as being approximately 300 times more efficient in absorbing IR radiation than carbon dioxide.[43] As such, nitrous oxide emissions are amongst the six greenhouse gasses regulated by the Kyoto protocol.[44] The role of this molecule in the atmosphere is not limited to a global warming effect, but it is also deemed to be the dominant ozone depleting substance emitted in the 21st century.[45] Due to its potency in depleting ozone and the prediction that emissions will double by 2050, if emissions remain unchecked, the regulation and reduction in the emissions of nitrous oxide is of considerable interest for the United Nations.[46]

As a consequence of these environmental and biomedical roles for nitrous oxide, several methods have been developed for detecting and reporting its presence in air. The capacity for N_2O to absorb IR radiation, which makes it such a potent greenhouse gas, has been extensively exploited in the selective gas-phase detection of the molecule, and is exploited in the commercially available Ribble Geotechnical G200 Nitrous Oxide Monitor.[47-64] The photoacoustic effect, where the effect of absorbed radiation on matter is determined by acoustic detection, has also been widely utilized in the detection of gaseous N_2O. [65-73] The effect of the presence of nitrous oxide on the electrochemistry of nano-materials has also shown promise for the detection of gas-phase nitrous oxide.[74,75] Mass spectrometry has also been used to detect the presence of N_2O, usually in combination with gas chromatography. [76-78]

5.1.2. The chemistry of nitrous oxide (N_2O)

Nitrous oxide is stable and generally unreactive at room temperature and atmospheric pressure.[79] Thus, for instance, it does not react with hydrogen, ozone, the halogens or alkali metals.[79] It will decompose upon heating into oxygen and nitrogen at temperatures exceeding 520 ºC, with an enthalpy of decomposition calculated at -82.05 kJ mol^{-1} (Scheme 5.5).[80,81] This property has led to its investigation as a less-toxic rocket fuel, *viz* hydrazine.[82] The combination of an exothermic decomposition and the production of oxygen have led to its use as an oxidizer in rocket fuel, such as NOFBX™ of Firestar technologies, which enabled the flight of SpaceShipOne. The use of nitrous oxide in traditional combustion engines as an oxidizer is well established, dating from its use in

World War Two as Göring-Mischung-I for fighter planes through to modern day motor vehicle racing.[83]

Scheme 5.5. The thermal decomposition of nitrous oxide.

Although nitrous oxide is a thermodynamically competent oxidant, it is typically kinetically inert under standard temperatures and pressures, with notable exceptions in the oxidation of main group elements. Nitrous oxide can oxidize substrates, with an early example from 1951 by Bridson-Jones *et al*. involving the oxidation of cyclohexene to form cyclohexanone under forcing conditions (Scheme 5.6.a).[84] Later work from Parmon and coworkers, showed that these forcing conditions are not always necessary, with room temperature and 10 atmospheres pressure of nitrous oxide sufficient to affect the same types of conversion (Scheme 5.6.b-c.).[85,86] Its use as a mild oxidizing agent has also been exploited in the chemistry of silicon, for example, in the synthesis of an NHC-stabilized silanone by Driess and coworkers (Scheme 5.6.d.); tertiary phosphines have also been oxidized to phosphine oxides using nitrous oxide (Scheme 5.6.e). [87,88]

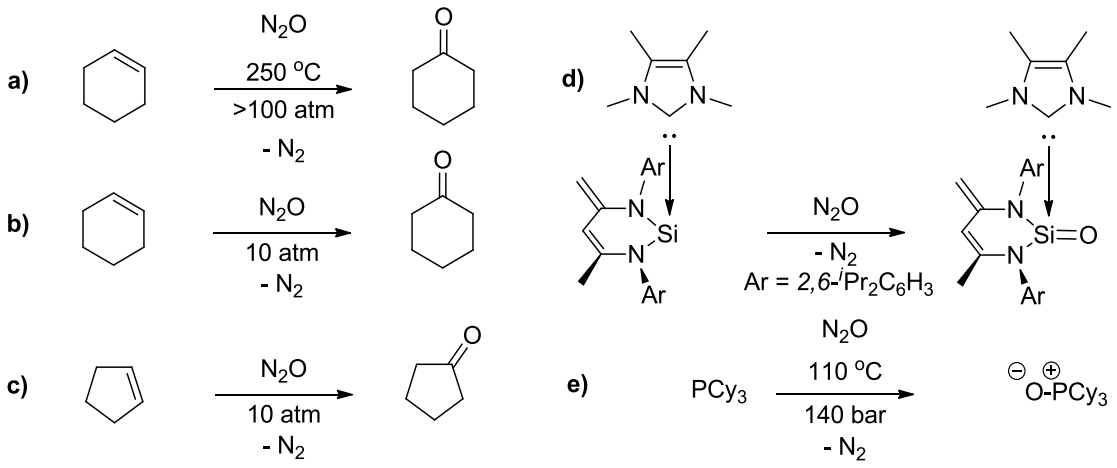

Scheme 5.6. Oxidation of small organic molecules using N_2O as the oxidizing agent.

5.1.3. Binding of nitrous oxide (N_2O) by early transition metal centres

The capacity of nitrous oxide to act as a "mild" oxidant is not limited to the main group elements such as carbon, silicon and phosphorus, but has been extended to include aspects of transition metal chemistry. The oxidation of a metal centre is usually mediated by initial coordination followed by N-O bond cleavage and subsequent loss of N_2.[89,90] Examples of this mode of oxidation to give new M=O bonds, comparable to reactions to give new Si=O or P=O bonds, include the work of Perutz and coworkers on the reaction of $W(CO)_6$ with N_2O to give $W(CO)_4O_2$ (Scheme 5.7.a.).[87,88,91] The capacity to oxidize organometallic compounds was exploited by Lin and coworkers in the reaction of Cp^*_2Ti with N_2O to give $Cp^*_2Ti{=}O$.[92] Further examples include the oxidation of $(silox)_3V$, $(silox)_3WCl$, $Mo(PMe_3)_4Cl_2$ and $W(PMe_3)_4Cl_2$. [93,94] The oxidation of transition metal centres can also give rise to M-O-M linkages. Thus, for example, Bottomley *et al* reported that the reaction of Cp^*_2Cr with N_2O gives rise to a μ_3-O-bridged Cr_4O_4 cuboid (Scheme

5.7.b.).[95] Other examples of oxidation by N_2O that give rise to M-O-M bonding motifs include the oxidation of $(Cp_2TiCl)_2$ and Cp_2V/Cp^*_2V[96-99].

A less common, result of the interaction of N_2O with transition metal centres is N-N bond cleavage. A representative example from the work of Cummins and coworkers is the reaction of $Mo(NRAr)_3$ (R = ^{t}Bu, Ar = 3,5-$C_6H_3Me_2$) with N_2O to give a one-to-one mixture of $Mo(NRAr)_3N$ and $Mo(NRAr)_3(NO)$ (Scheme 5.7.c.).[100-102] A further example from Reed and coworkers is the reaction of $Cp^*Mo[N(^iPr)C(Me)N(^iPr)](CO)_2$ with N_2O to give $Cp^*Mo[N(^iPr)C(Me)N(^iPr)](O)$ and $Cp^*Mo[N(^iPr)C(Me)N(^iPr)](NO)(NCO)$.[103] Further examples of N-N cleavage of N_2O by three coordinate molybdenum systems are found in the work of Nolan *et al*. and Morokuma *et al*. [100,104]

The first examples of metal complexes that bind and preserve an intact N_2O fragment were prepared by Rheingold and coworkers, who exploited ring opening of metallocyclopropene systems to trap the N_2O unit within a five-membered ring (Scheme 5.7.d.).[105] Further examples include complexes of the early transition metal, yttrium, and the lanthanides; lanthanum and samarium, prepared by Magull and Evans, and their respective coworkers (Scheme 5.7.e.).[106,107] In these systems, the N_2O fragment inserts into one or more metal-ligand bond(s).

The N_2O molecule possesses a small dipole moment and weak σ-donor and π-acceptor properties, and is therefore considered a poor ligand.[89] Consequently, there are exceedingly few examples of this small molecule bound intact at metal centres, without insertion into a metal-ligand bond. The first example was prepared by Armor and Taube

in 1969, with $[Ru(NH_3)_5(N_2O)]^{2+}$ exhibiting all the spectroscopic features consistent with an intact N_2O fragment. The next example of a discrete metal N_2O complex was that reported by James and coworkers in 2001, who developed a a low temperature (-78 ºC) synthesis of $RuCl_2(\eta^1\text{-}N_2O)(P\text{-}N)(PPh_3)$ (P-N = [*o*-(*N*,*N*-dimethylamino)phenyl]diphenylphosphine).[108] A dramatic advance in the understanding of these metal-N_2O adducts came in 2011 when Chang and coworkers presented a tpa^{MES}-ligated vanadium system (tpa^{MES} = Tris(2-methyl-5-mesityl-pyrole)amine)), which was the first structurally characterized metal N_2O complex (Scheme 5.7.f.).[109] The N_2O molecule is found within the apical pocket of the crystal structure, bound to the vanadium through the terminal nitrogen. The V-N_2O fragment adopts an approximately linear geometry, with a V-N-N angle of 176.7º.

A further development came with the publication of Einsle and coworkers on the bonding of N_2O at a [4Cu:2S] copper-sulphur cluster in nitrous oxide reductase.[110] In this work, the authors structurally characterized a cluster containing a N_2O molecule within the active site. In contrast to the previously structurally characterized metal N_2O complex, the N_2O fragment here does not adopt an approximately linear geometry with any of the copper centres.

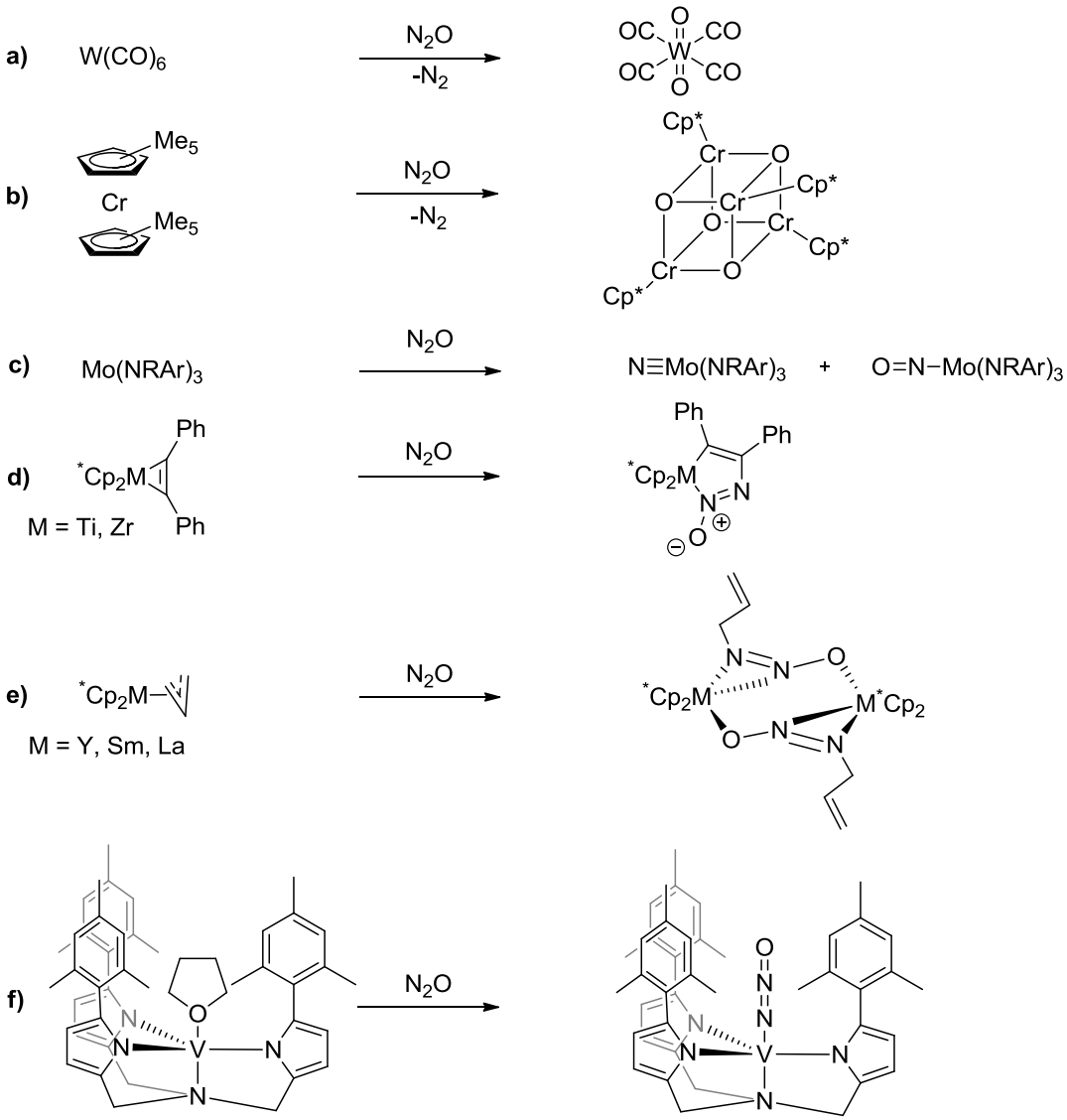

Scheme 5.7. Transition metal capture/activation of N_2O. (a) The ring expansion of titanium and zirconium organometallic compounds by N_2O. (b) Insertion of a complete N_2O fragment into metal-carbon bonds of organometallic compounds of yttrium, samarium and lanthanum.

5.1.4. Nitrogen-Heterocyclic Carbenes (NHCs)

A carbene is an charge-neutral species of the general formula, R_2C: (although historically referring to the central carbon of R=C=R), in which the carbon atom is covalently bonded to two univalent, or one divalent, group and bears two electrons which can be either spin-paired (denoted by the term singlet) or spin-non-paired (denoted by the term triplet).[111] These carbenes are typically very reactive and the parent carbene (H_2C:), for example, will insert into carbon-hydrogen single bonds.[112] The isolation of a stable, liquid dicarbene was reported by Bertrand and coworkers in 1988.[113] The isolation of a stable, solid carbene by Arduengo *et al* was reported in 1991 (Scheme 5.8.a.) and has become the corner-stone of an extensive area of chemistry.[114] These carbenes are still relatively reactive, must generally be handled under inert atmospheres and some may dimerize in solution (Scheme 5.8.b).[115] Nitrogen-heterocyclic carbenes can be designed, so that dimerization is minimized by tuning the nature of the substituents attached to the nitrogen atoms of the central heterocycle, typically favoring sterically demanding groups such as mesityl (Mes, 2,4,6-$Me_3C_6H_2$) or diisopropylphenyl (Dipp, 2,6-$^{i}Pr_2C_6H_3$). By considering the dimerization of singlet NHCs, where an electron-pair from one carbene in a σ-orbital donates to the vacant π-orbital of a second carbene, NHCs may be considered to be a subset of FLPs. This or a "one atom stereo-electronically frustrated Lewis pair" as the carbon atom of the nitrogen-heterocyclic carbene acts both as electron-pair donor and acceptor.

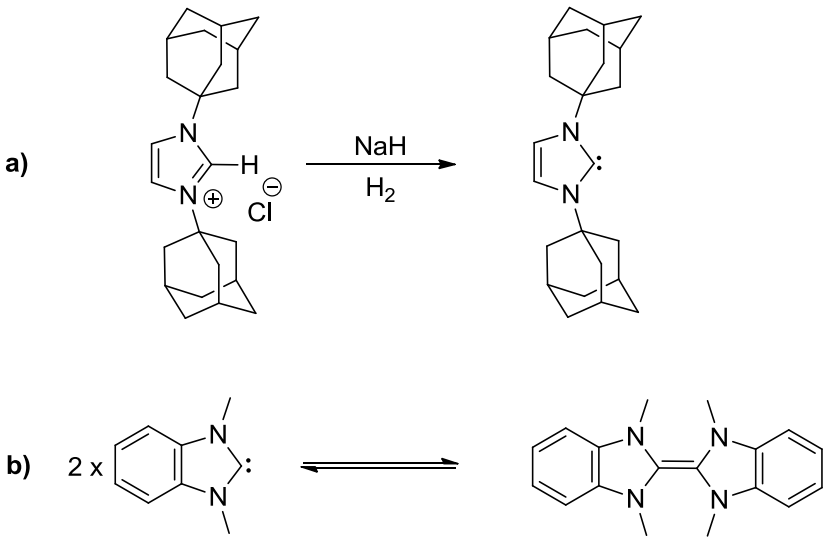

Scheme 5.8. (a) The first synthesis of a stable, nitrogen-heterocyclic carbene that is also isolable as a crystalline solid. (b) The dimerization of a nitrogen-heterocyclic carbene.

5.1.5. The chemical reactivity of IMes-N_2O

In 2011, Severin and coworkers demonstrated that NHCs were capable of capturing N_2O intact, with the formation of a bond between the formerly carbenic carbon and the terminal nitrogen of the N_2O molecule (Scheme 5.9.a.).[116] This chemistry is reminiscent of the vanadium system of Chang and coworkers (Scheme 5.7.f).[109] In contrast to the linear geometry exhibited by the V-N=N=O fragment in Changs vandium-N_2O complex, Severin's mesityl-functionalized NHC-N_2O complex adopts a kinked *trans*, *trans*-geometry for the C=N-N=O fragment, with C-N-N and N-N-O angles of 109.6^o and 113.1^o, respectively.[116] The N-N distance of this NHC-N_2O complex is significantly longer than that of the vanadium complex (1.333(3) Å compared to 1.119(2) Å). The N-O distance is also greater for the carbene-N_2O adduct (1.250(2) Å compared to 1.119(2) Å for the vanadium-N_2O complex). These bond distances illustrate the key difference in the

mode of interaction between these two systems: in the case of the vanadium system the N_2O molecule primarily acts as an electron donor (Lewis base), whereas, in the case of NHCs, N_2O acts primarily as an electron acceptor (Lewis acid).

Systematic investigations of the reactivity of these NHC-N_2O adducts has revealed a range of interesting further chemistry (Scheme 5.9.b-f.).[117,118] Upon heating, chemistry closely resembling that of metal N_2O reactions is observed, in that the N-O bond is cleaved, dinitrogen evolved and the NHC formally oxidized (Scheme 5.8.b.). N-N bond rupture can also be effected by treating the NHC-N_2O adduct with either a Brønsted acid or an acyl chloride (Scheme 5.9.c-d.). The cleavage of the N-N bond strongly suggests that the charge distribution in the N_2O fragment has changed upon binding to the NHC. This purported change in charge distribution is supported by DFT calculations, which indicate that the nitrogen atoms bear a greater Hirshfeld negative charge than the oxygen atom in the NHC adduct.[117] The capacity of the terminal oxygen to act as a Lewis base and coordinate to a carbon-centred Lewis acid was also explored, revealing that NHC-N_2O forms a bond to a CPh_3 cation (Scheme 5.9.d.). The reaction of a NHC-N_2O adduct with $SOCl_2$ on the other hand, proceeds with N-O bond cleavage, loss of dinitrogen and transfer of the oxygen atom to sulfur resulting in the evolution of SO_2 and the formation of a $[(NHC)Cl]^+Cl^-$ salt (Scheme 5.9.f.).

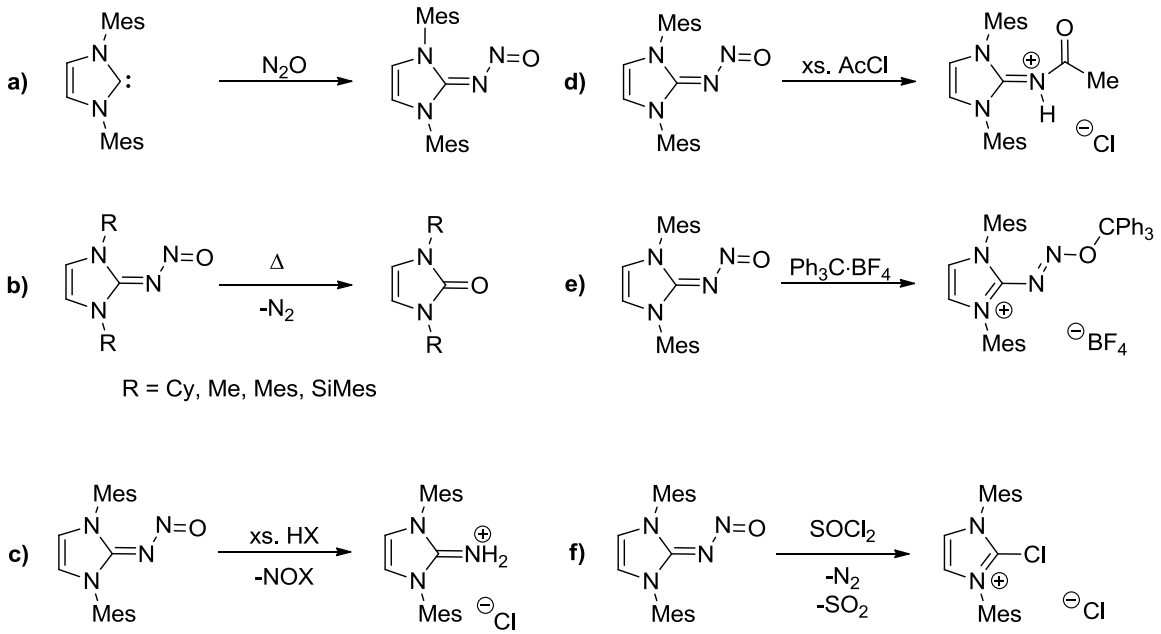

Scheme 5.9. (a) The binding of N_2O by the IMes carbene. (b) The loss of N_2 on heating NHC-N_2O adducts. (c) The reaction of IMes-N_2O with Brønsted acids. (d) The reaction of IMes-N_2O with acyl chloride. (e) The reaction of IMes-N_2O with a source of trityl cation. (f) The reaction of IMes-N_2O with thionyl chloride.

Research by Severin and coworkers into the capacity of NHC-N_2O adducts to act as electron donors to Lewis acids other than the CPh_3 cation centred on transition metals.[118-120] As was seen with the reactions of the N_2O molecule with transition metal centres, a range of reactivity was observed. As with the reaction of N_2O with $W(CO)_6$ to give $W(CO)_4O_2$ as described by Perutz and coworkers[91], Severin and coworkers observed the oxidation of $VMes_3(THF)$, when treated with NHC-N_2O (Scheme 5.10.a.). The reaction also proceeds *via* insertion into the mesityl V-C bond by the NHC-N_2 fragment.

The reaction of IMes-N_2O with $Ni(COD)_2$ gives a nitrosyl complex (Scheme 5.10.b.).[83] This reaction proceeds *via* relatively rare N-N bond cleavage, similar to that seen in the reaction of N_2O and $Mo(NRAr)_3$ (R = ^{t}Bu, Ar = 3,5-$C_6H_3Me_2$) by Cummins. The end-products are markedly dissimilar however, with the $Mo(NRAr)_3$ system giving rise to separate nitrosyl and nitride compounds, whereas the NHC-N_2O system gives rise to a bimolecular, nitride-bridged, nitrosyl compound.[119]

Reaction of IMes-N_2O with half an equivalent of CuOTf led to the formation of $[(\eta^1\text{-NHC-}N_2O)_2Cu]^+[OTf]^-$ (Scheme 5.10.c.).[118] Binding through the carbene-bound nitrogen in an η^1-fashion to the metal centre is reminiscent of Armor and Taube's $[Ru(NH_3)_5(N_2O)]^{2+}$ cation.[121] The IMes-N_2O adduct can also coordinate to Lewis-acidic metal centres (Fe, Cu, Zn and Sn) in a chelating η^2-fashion through the terminal oxygen atom and the carbene-bound nitrogen atom (Scheme 5.10.d.).[118] Furthermore, it can also act as a Lewis base towards a Lewis-acidic chromium atom through the terminal oxygen atom, in the same manner as seen for the CPh_3 cation (Scheme 5.10.e.).[118]

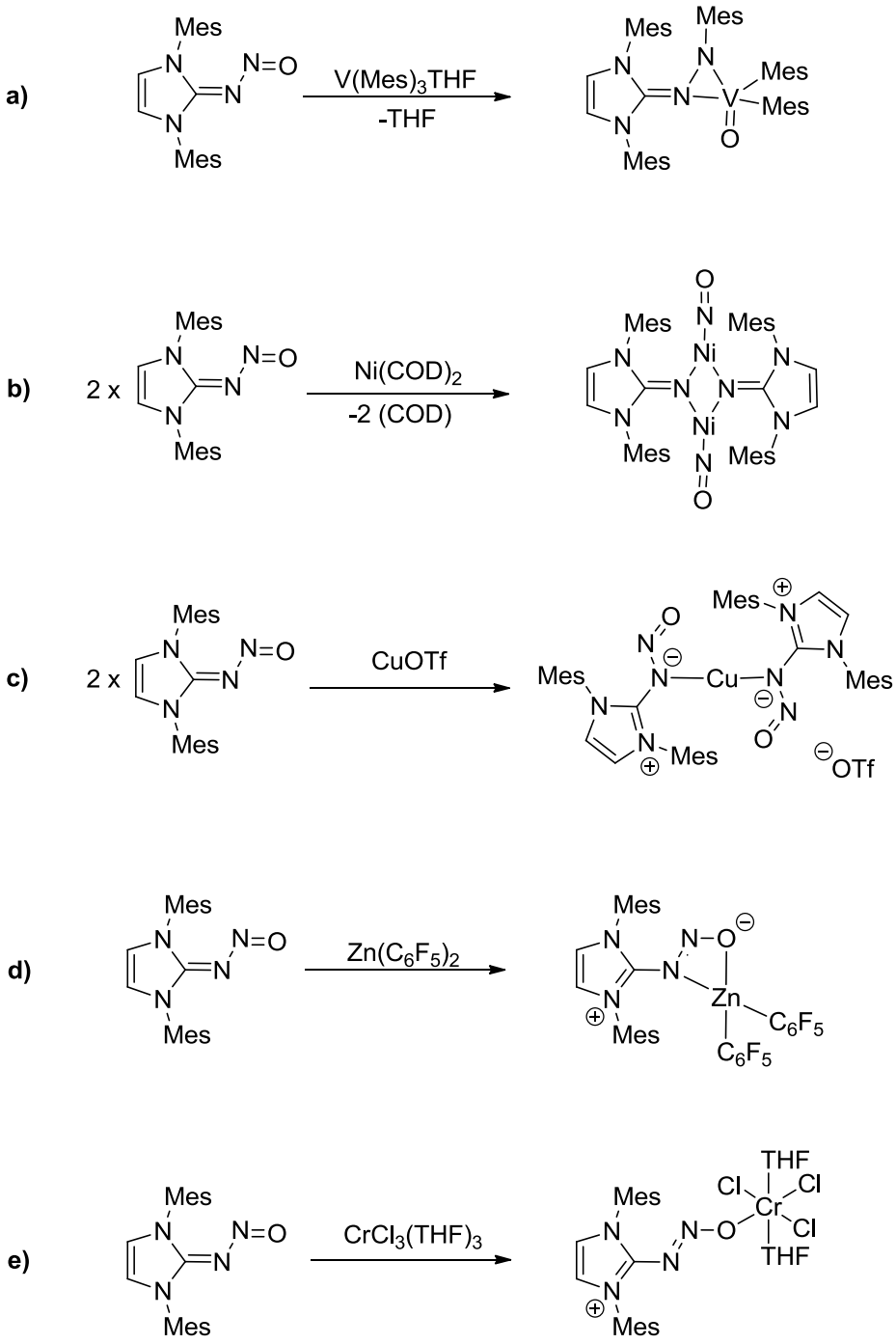

Scheme 5.10. The key modes of ligation by the IMesN$_2$O unit toward Lewis-acidic metal centres.

5.1.6. Reactions of Frustrated Lewis Pairs with Nitrous Oxide

The activation of nitrous oxide is not limited to NHCs, as was shown by the work of Stephan and coworkers. [122-124] They showed that, in the absence of a strong Lewis acid, N_2O will gradually oxidize tri-*tert*-butyl phosphine or tri-cyclohexyl phosphine without the forcing conditions that Jessop and coworkers used to convert PCy_3 to $O{=}PCy_3$ (Scheme 5.11.a.). [88,122] However, if a strong Lewis acid is present, they obtain the formally zwitterionic compound $^{t}Bu_3P{\cdot}NNO{\cdot}B(C_6F_5)_3$, which features an intact N_2O fragment, with the phosphine bound at one end and the borane at the other, to give a gull-wing, or *trans*, *trans*-, shaped molecule (Scheme 5.11.b.). A similar binding motif is obtained from sequentially treating IMes-N_2O with $[CPh_3][BF_4]$ or $CrCl_3(THF)_3$.[118] Computational studies on the binding motif suggest that the *trans*, *trans*- binding motif observed in the crystal structure of $^{t}Bu_3P{\cdot}NNO{\cdot}B(C_6F_5)_3$ is energetically optimal.[125] Similar binding of N_2O occurs for a range of FLPs, including various strong Lewis acids such as $B(C_6F_5)$, $B(C_6F_5)_2Mes$ and $B(C_6F_5)_2(OC_6F_5)$.[122] If compound $^{t}Bu_3P{\cdot}NNO{\cdot}B(C_6F_5)_3$ is heated to 135 ºC for 44 h or photolysed for 5 minutes, loss of N_2 occurs, to give compound $^{t}Bu_3PO{\cdot}B(C_6F_5)_3$, in which the phosphorus and boron atoms are bridged by an oxygen atom (Scheme 5.11.b).[124] Similar adducts would be expected from the reaction of $O{=}PCy_3$ with the corresponding Lewis acid.

This research from Stephan and coworkers further indicated that below a threshold level of Lewis acidity, for instance with the weaker Lewis acid $B(C_6H_4\text{-}p\text{-}F)_3$, compounds such as compound $Cy_3PO{\cdot}B(C_6H_4\text{-}p\text{-}F)_3$ form instead of analogues of compound $^{t}Bu_3P{\cdot}NNO{\cdot}B(C_6F_5)_3$ (Scheme 5.11.C).[122] This is ascribed to the weaker acid not binding

irreversibly to the terminal oxygen atom so as to preclude the loss of N_2 to give a tertiary phosphine, as indeed occurs in the absence of a Lewis acid (Scheme 5.11.a). The resulting phosphine oxide binds to the Lewis acid. It would be expected that a stoichiometric reaction of $O{=}PCy_3$ and $(4\text{-}F^{-}C_6H_4)_3B$ would give rise to compound $Cy_3PO{\cdot}B(C_6H_4\text{-}p\text{-}F)_3$.

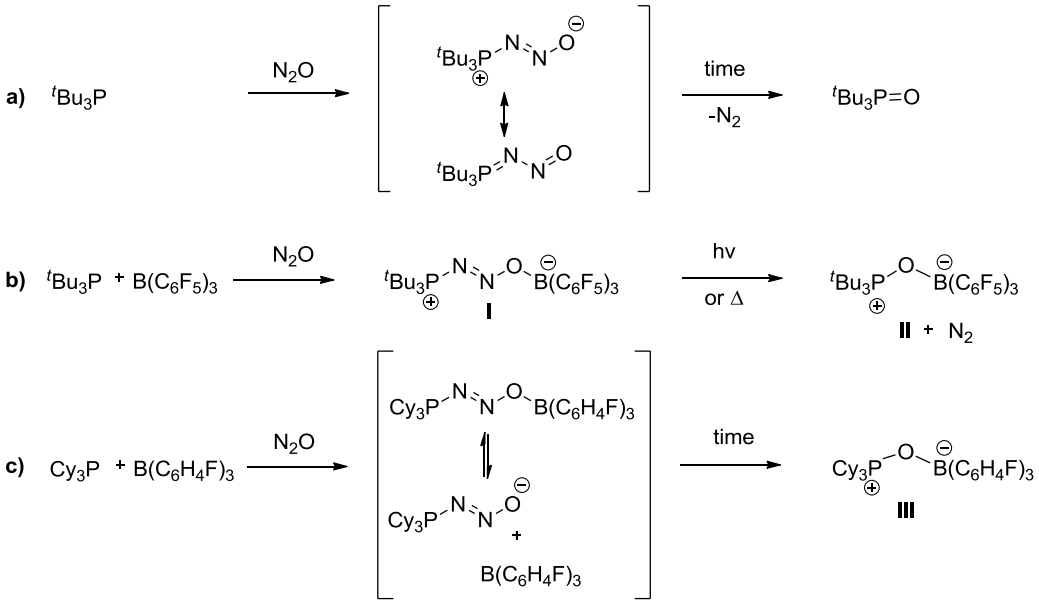

Scheme 5.11. (a) The oxidation of tertiary phosphine to phosphine oxide, (b) the trapping of an intact N_2O fragment by a FLP to give compound **I** and subsequent degradation to give the oxo-bridged compound **II** and (c) the reaction of a FLP, comprised of a relatively weaker Lewis acid, with N_2O to give the oxo-bridged compound **III**.

5.1.7. Highly Lewis-Acidic Ferrocenyl Boranes

Given the propensity for Lewis-acidic ferrocenyl boranes such as $FcBMes_2$ to bind anions such as fluoride and cyanide,[126-128] it is to be expected that a more highly Lewis-acidic borane would form acid-base complexes with an expanded sub-set of molecules. This is clearly established in the work of Piers and coworkers in their

evaluation of $FcB(C_6F_5)_2$, which is capable of complexing PMe_3 and FcOAc (Scheme 5.12.).[129] As in the case of $FcBMes_2$, the ferrocenyl borane is electrochemically active, with an oxidation potential of +450 mV with respect to ferrocene. This oxidation potential shifts dramatically (-550mV) on complexation with the Lewis base, PMe_3, to a new value of -100 mV. This result parallels the effect of complexation of the Lewis base CN^- to $FcBMes_2$, which causes a shift in the oxidation potential (-560 mV) from +181 mV to -383 mV, with respect to ferrocene. Moreover, in both the cases the complexation of a Lewis base (PMe_3 and CN^- respectively) to the borane induces an instantaneous colour change from maroon to yellow.

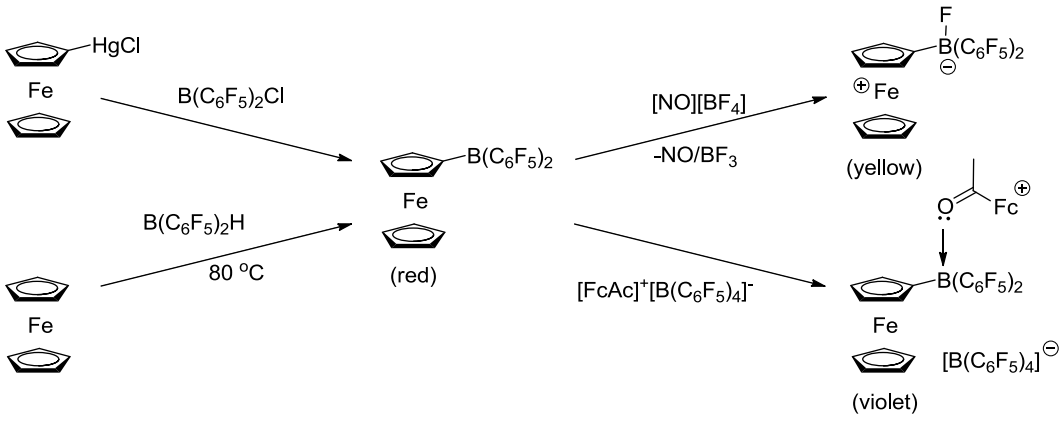

Scheme 5.12. The syntheses of $FcB(C_6F_5)_2$ and its reaction with various Lewis bases.

5.2. Initial Research Goals

The overarching goal of the body of work described in this chapter was to create a chemical detector for nitrous oxide in solution, utilising either a photo-physical or electrochemical response to the presence of N_2O. We sought to utilise a Lewis base to initially trap an intact N_2O molecule. This decision was taken due to the preponderance of Lewis-basic phosphines and carbenes that were capable of capturing an intact N_2O fragment and the paucity of Lewis-acidic metal centres capable of doing the same. The capacity of the phosphine and carbene adducts of N_2O to form dative, covalent bonds to Lewis-acidic centres, such as CPh_3^+ and $B(C_6F_5)_3$, indicated that we could utilise our knowledge of Lewis-acidic ferrocenyl boranes in designing an efficient, selective N_2O detection system. The self-evident complication inherent in this approach to fabricating an N_2O detection system is that both Lewis-acidic and basic components would have to be mixed together, which requires a system with sufficient steric bulk to preclude adduct formation, i.e., a frustrated Lewis pair system. The work of Stephan, Severin and Piers gave us confidence that such a system could be devised, that would meet all of the requirements of this detection system.[14,118,124,129]

5.3. Experimental

FcLi: In a modified procedure based on that of Bildstein *et al.*,[130] *t*-BuLi (45 mL of a 1.6 M solution in hexanes, 72 mmol) was added over 15 min to a suspension of ferrocene (16.0 g, 86 mmol) in THF (80 mL) at 0 ºC. Immediately after the addition, hexane (150 mL) was added and the suspension cooled to -78 ºC. The resulting pyrophoric orange precipitate was separated by filtration at -78 ºC, washed with pre-cooled hexanes (4 x 50 mL) at -78 ºC and volatiles removed *in vacuo* to afford an orange powder (approximately 15 g). This powder was continuously washed with hexane (200 mL) using a Soxhlet apparatus over a period of 12 h, until the extracts were colourless. The remaining solid was dried *in vacuo* to afford the target material as a highly pyrophoric orange powder. This material was used without additional characterisation. Yield 8.17 g, 59%.

$FcB(C_6F_5)_2$ [1]: In a modified procedure to that reported by Piers and coworkers,[129] *n*-BuLi (17.5 mL of a 1.6 M solution in hexanes, 28 mmol) was added dropwise to a solution of 1-bromo-2,3,4,5,6-pentafluorobenzene (3.47 mL, 28 mmol) in hexane (30 mL) at -78˚C. The resulting mixture was stirred at -78˚C for a further 45 min. A solution of $FcBBr_2$ (5.00 g, 14 mmol) in hexane (150 mL) was then added dropwise at -78 ˚C. After warming to room temperature over a period of 12 h, volatiles were removed *in vacuo* and the residue was extracted with hexane (3 x 50 mL). The combined organic extracts were concentrated *in vacuo* and the residue cooled to -20 ˚C to produce maroon crystals, which were separated by filtration at -20 ºC and dried *in vacuo*. Yield 4.80 g, 65%. ^{1}H, ^{11}B and ^{19}F NMR spectra were in agreement with literature data.[129]

Synthesis of IMes·N_2O·$BFc(C_6F_5)_2$ [2]: $B(C_6F_5)_2Fc$ (0.57 g, 1.06 mmol) and IMes·N_2O (0.35 g, 1.00 mmol) were suspended in chloroform (20 mL) and the resulting solution stirred for 2 d at room temperature. Pentane (70 mL) was added to the reaction mixture and the resulting precipitate separated by filtration, taken up in a minimal amount of chloroform and layered with pentane to yield purple crystals, which were separated by filtration and dried *in vacuo* (0.215 g, 42 %). Single crystals of **2** (as the chloroform solvate) suitable for X-ray crystallography were grown from a chloroform solution.

^{1}H NMR (300 MHz, THF-d_8, 20 ºC): δ_H 7.75 (s, 2H, $C_3N_2H_2$), 7.02 (s, 4H, CH of Mes), 3.86 (t, 2H, $^3J_{HH}$ = 1.5 Hz, C_5H_4B), 3.27 (t, 2H, $^3J_{HH}$ = 1.5 Hz, C_5H_4B), 2.32 (s, 6H, *para*-CH_3 of Mes), 2.04 (s, 12H, *ortho*-CH_3 of Mes).

^{11}B[^{1}H] NMR (96 MHz, THF-d_8, 20 ºC): δ_B 3 (br).

^{13}C [^{1}H] NMR (125 MHz, THF-d_8, 20 ºC): δ_C 149.0 (C_6F_5), 147.1 (C_6F_5), 147.0, 141.8 (Mes), 138.3, 136.1 (C_6F_5), 135.0, 131.4, 130.2, 123.5 (Mes), 72.9, 69.4 (C_4H_4B), 68.0 (C_5H_5), 20.9 (*para*-CH_3 of Mes), 17.3 (*ortho*-CH_3 of Mes). B-bound carbon of C_5H_4B not observed.

^{19}F NMR (282 MHz, THF-d_8, 20 ºC): δ_F -129.4 (d, 4F, $^3J_{FF}$ = 15.8 Hz, ortho-CF of C_6F_5), -161.8 (d, 2F, $^3J_{FF}$ = 20.4 Hz, para-CF of C_6F_5), -167.4 (dd, 4F, $^3J_{FF}$ = 15.8 Hz, $^3J_{FF}$ = 20.4 Hz, meta-CF of C_6F_5).

UV-vis (C_6H_5F) λ_{max}, nm (ε): 475 (353 L mol^{-1} cm^{-1}).

MS(HNESP) *m/z* (%): 320.2 (43) $[IMesO]^+$, 349.2 (100) $[IMesN_2OH]^+$, 530.0 (53) $[FcB(C_6F_5)_2]^+$, 668.4 (10) $[IMesBFc(C_6F_5)]^+$, 697.4 (21) $[IMesBFc(C_6F_5)F]^+$, 878.2 (2) $[IMes.N_2O.BFc(C_6F_5)_2]^+$. HRMS(HNESP) (*m*/*z*): calc. for [M+] (^{10}B, ^{54}Fe isotopomer), $C_{43}H_{33}BF_{10}FeN_4O$ 878.1940; meas. 878.1924.

Elemental microanalysis: calc. for $C_{43}H_{33}BF_{10}FeN_4O$, C 58.80%, H 3.79%, N 6.38%, meas. C 58.86, 58.78%, H 3.52, 3.52%, N 6.62, 6.67%.

Crystallographic data: $IMes{\cdot}N_2O{\cdot}BFc(C_6F_5)_2{\cdot}(CHCl_3)$ [**2**·$(CHCl_3)$], $C_{44}H_{34}BCl_3F_{10}FeN_4O$, M_r = 997.78, monoclinic, *P* 21/n, *a* = 18.7399(2), *b* = 20.5214(2), *c* = 24.5916(2) Å, β = 112.1709(4)º, *V* = 8757.9(2) $Å^3$, *Z* = 8, ρc = 1.513 Mg m^{-3}, *T* = 150 K, λ = 0.71073 Å. 19005 independent reflns [R(int) = 0.000] used in all calcns. R_1 = 0.0690, wR_2 = 0.1299 for observed unique reflns [I>2σ(I)] and R_1 = 0.0840, wR_2 = 0.1366 for all unique reflns. Max./min. residual electron densities 0.89 and -0.79 e $Å^3$.

Synthesis of IMes·BFc(C_6F_5)$_2$ [3]: $FcB(C_6F_5)_2$ (0.200 g, 0.38 mmol) and IMes (0.115 g, 0.38 mmol) were dissolved in a minimal amount of benzene (*ca*. 10 mL). The resulting solution was cooled to 6 ºC to yield orange crystals which were separated by filtration and dried *in vacuo*. (0.095 g, 30%). Single crystals suitable for X-ray crystallography were grown from a benzene solution.

^1H NMR (500 MHz, benzene-d_6, 20 ºC): δ_H 6.55, 6.52, 6.32, 6.10 (s, each 1H, CH of Mes) 5.73-5.72 (AB multiplet, 2H, $C_3N_2H_2$), 4.04 (br s, 1H, C_5H_4B), 3.84 (s, 5H Cp), 3.70 (br s, 1H, C_5H_4B), 3.29 (s, 1H, C_5H_4B), 3.19 (s, 1H, C_5H_4B), 2.06 (s, 3H, *ortho*-CH_3

of Mes), 2.04 (s, 3H, *ortho*-CH_3 of Mes), 1.90 (s, 3H, *ortho*-CH_3 of Mes), 1.80 (s, 6H, *para*-CH_3), 1.56 (s, 3H, *ortho*-CH_3 of Mes).

^{11}B [^1H] NMR (96 MHz, benzene-d_6, 20 ºC): δ_B -14 (s).

^{13}C [^1H] NMR (125 MHz, benzene-d_6, 20 ºC): δ_C 140.1, 139.1 (*ipso*-C of Mes), 137.6, 135.0 (*para*-C of Mes), 135.5, 135.4, 135.4, 134.5 (*ortho*-C of Mes), 131.3, 130.4, 129.6, 128.9 (*meta*-CH of Mes), 125.7, 124.4 ($C_3N_2H_2$ backbone), 68.9 (Cp), 76.0, 66.9, 68.2, 76.2 (CH of C_5H_4B), 21.0, 20.7, 19.1, 18.6, 17.6, 17.9 (CH_3 of Mes); carbene and boron-bound carbons not observed.

^{19}F NMR (282 MHz, benzene-d_6, 20 ºC): δ_F -117.1 (d, $^3J_{FF}$ = 25.2 Hz, *ortho*-F of C_6F_5), -120.8 (d, $^3J_{FF}$ = 25.2 Hz, *ortho*-F of C_6F_5), -122.7 (d, $^3J_{FF}$ = 25.2 Hz, *ortho*-F of C_6F_5), -128.5 (d, $^3J_{FF}$ = 25.2 Hz, *ortho*-F of C_6F_5), -159.9 (t, $^3J_{FF}$ = 21.0 Hz, *para*-F of C_6F_5), -161.6 (t, $^3J_{FF}$ = 21.0 Hz, *para*-F of C_6F_5), -164.4 (m, *meta*-F of C_6F_5), -165.0 (m, *meta*-F of C_6F_5), -166.5 (m, *meta*-F of C_6F_5), -167.2 (m, meta-of C_6F_5).

MS(ESI) *m*/*z* (%): 530.0 (100) $[FcB(C_6F_5)_2]^+$, 834.3 (10) $[IMes.BFc(C_6F_5)_2]^+$.

Elemental microanalysis: calc. for $C_{43}H_{33}BF_{10}FeN_2$, C 61.90%, H 3.99%, N 3.36%, meas. C 61.77%, H 4.34%, N 3.26%.

Crystallographic data: IMes·$FcB(C_6F_5)_2$·2(C_6H_6) [**3**·2(C_6H_6)], $C_{55}H_{45}BF_{10}FeN_2$, M_r = 990.61, monoclinic, *P* 21/*n*, *a* = 10.2813(1), *b* = 18.3834(2), *c* = 27.6025(3) Å, β =

90.743(1) º, V = 5216.6(1) Å^3, Z = 4, ρc = 1.261 Mg m^{-3}, T = 150 K, λ = 0.71073 Å. 10130 independent reflections [R(int) = 0.026] used in all calculations. R_1 = 0.0724, wR_2 = 0.1763 for observed s4 unique reflections [I>2σ(I)] and R_1 = 0.0851, wR_2 = 0.1821 for all unique reflections. Max. and min. residual electron densities 0.53 and -0.81 e Å^3.

Synthesis of IDipp·FcB(C$_6$F$_5$)$_2$ [4]: FcB(C$_6$F$_5$)$_2$ (0.196 g, 0.37 mmol) and IDipp (0.144 g, 0.37 mmol) were dissolved in a minimal amount of benzene (*ca*. 10 mL) and the resulting solution cooled to 6 ºC to yield orange crystals, which were separated by filtration and dried *in vacuo* (0.08 g, 22%). Single crystals suitable for X-ray crystallography were grown from a benzene solution.

^{1}H NMR (500 MHz, benzene-d_6, 20 ºC): δ_H 7.06 (t, $^3J_{HH}$ = 8.0 Hz, 1H, CH of Dipp), 6.92, (m, 3H, CH of Dipp), 6.74 (dd, $^3J_{HH}$ = 8.0 Hz, $^4J_{HH}$ = 1.3 Hz, 1H, CH of Dipp), 6.46 (dd, $^3J_{HH}$ = 7.1 Hz, $^4J_{HH}$ = 2.2 Hz, 1H, CH of Dipp), 6.33 (d, $^3J_{HH}$ = 1.9 Hz, 1H, C$_3$N$_2$H$_2$), 6.30 (d, $^3J_{HH}$ = 1.9 Hz, 1H, C$_3$N$_2$H$_2$), 4.08 (br s, 1H, C$_5$H$_4$B) 3.76 (s, 5H, Cp), 3.59 (br s, 1H, C$_5$H$_4$B), 3.29 (br s, 1H, C$_5$H$_4$B), 3.12 (sept , $^3J_{HH}$ = 6.8 Hz, 1H, ^{i}Pr CH of Dipp), 2.97 (br s, 1H, C$_5$H$_4$B), 2.73, 2.49, 2.09 (3 x sept, $^3J_{HH}$ = 6.8 Hz, 1H, ^{i}Pr CH of Dipp), 1.44, 1.13, 0.97, 0.93, 0.85, 0.84, 0.83, 0.57 (8 x d, $^3J_{HH}$ = 6.8 Hz, 3H, ^{i}Pr CH$_3$ of Dipp).

^{11}B [^{1}H] NMR (96 MHz, benzene-d_6, 20 ºC): δ_B -13 (sharp s).

^{13}C [^{1}H] NMR (125 MHz, benzene-d_6, 20 ºC): δ_C 147.0, 146.3, 146.2, 144.7 (*ortho*-C of C6F5), 138.2, 134.7 (*para*-F of C$_6$F$_5$), 128.9, 128.7, 128.5, 128.3 (*meta*-F of

C_6F_5), 131.2, 130.4 (Dipp aromatic), 127.5, 125.4 ($C_3N_2H_2$), 125.3, 125.0, 124.4, 122.3 (Dipp aromatic), 77.5, 77.3 (C_5H_4B), 68.6 (Cp), 68.1, 67.1 (C_5H_4B), 28.7, 28.6 (^{i}Pr CH of Dipp), 28.0, 27.9 (^{i}Pr CH_3 of Dipp), 27.9, 27.8 (^{i}Pr CH of Dipp), 27.6, 26.5, 27.7, 21.5, 21.3, 21.3 (^{i}Pr CH_3 of Dipp); carbene carbon not observed.

^{19}F NMR (282 MHz, benzene-d_6, 20 ºC): δ_F -116.7 (d, $^3J_{FF}$ = 25.2 Hz, *ortho*-F of C_6F_5), -119.8 (d, $^3J_{FF}$ = 24.6 Hz, *ortho*-F of C_6F_5), -120.1 (d, $^3J_{FF}$ = 26.2 Hz, *ortho*-F of C_6F_5), -131.4 (t, $^3J_{FF}$ = 25.8 Hz, *ortho*-F of C_6F_5), -160.5 (t, $^3J_{FF}$ = 21.0 Hz, *para*-F of C_6F_5), -160.9 (t, $^3J_{FF}$ = 21.0 Hz, *para*-F of C_6F_5), -163.3 (m, *meta*-F of C_6F_5), -164.6 (m, *meta*-F of C_6F_5), -165.2 (m, *meta*-F of C_6F_5), -166.6 (m, *meta*-F of C_6F_5).

MS (ESI): 530.0 (100) $[FcB(C_6F_5)_2]^+$, 918.4 (2) $[IDipp{\cdot}BFc(C_6F_5)_2]^+$.

Crystallographic data: IDipp·$FcB(C_6F_5)_2$·3/2(C_6H_6) [**4**·3/2(C_6H_6)], $C_{58}H_{54}BF_{10}FeN_2$, M_r = 1035.72, triclinic, P-1, *a* = 10.4222(1), *b* = 11.9277(1), *c* = 20.8136(3) Å, α = 84.885(1), β = 78.407(1), γ = 77.096(1)º, V = 2468.0(1) Å^3, Z = 3, ρc = 1.394 Mg m^{-3}, T = 150 K, λ = 0.71073 Å. 68319 reflections collected, 11201 independent [R(int) = 0.036] used in all calculations. R_1 = 0.0471, wR_2 = 0.0935 for observed unique reflections [I>2σ(I)] and R_1 = 0.0759, wR_2 = 0.1174 for all unique reflections. Max. and min. residual electron densities 0.56 and -0.60 e Å^3.

Synthesis of $IMesCl_2{\cdot}BFc(C_6F_5)_2$ [5]: $FcB(C_6F_5)_2$ (0.209 g, 0.39 mmol) and Cl_2IMes (0.148 g, 0.39 mmol) were dissolved in a minimal amount of benzene (*ca*. 10 mL). The resulting solution was cooled to 6 ºC to yield orange crystals, which were

separated by filtration and dried *in vacuo*. (0.050 g, 14%). Single crystals suitable for X-ray crystallography were grown from a benzene solution.

^{1}H NMR (500 MHz, benzene-d_6, 20 ºC): δ_H 6.54, 6.51, 6.30, 6.06 (s, each 1H, CH of Mes), 4.05 (br s, 1H, C_5H_4B), 3.81 (s, 5H, Cp), 3.68, 3.26, 3.15 (s, each 1H, C_5H_4B), 2.03, 1.99, 1.90, 1.85, 1.79, 1.63 (s, each 3H, CH_3 of Mes).

^{11}B [^{1}H] NMR (96 MHz, benzene-d_6, 20 ºC): δ_B -13 (sharp s).

^{13}C [^{1}H] NMR (125 MHz, benzene-d_6, 20 ºC): δ_C 151.5, 150.8, 150.4, 149.6, 148.9, 148.5, 147.7, 145.9 (CF of C_6F_5), 141.4 (*ipso*-C of Mes), 140.6 (CF of C_6F_5), 140.3 (*ipso*-C of Mes), 136.9 (*para*-C of Mes), 138.5 (CF of C_6F_5), 135.7, 135.7, 135.6 (*ortho*-C of Mes), 134.2 (*para*-C of Mes), 131.8 (*ortho*-C of Mes), 131.7, 130.7, 130.1, 128.9 (*meta*-CH of Mes), 121.8, 121.4 ($C_3N_2Cl_2$ backbone), 69.1 (Cp), 76.2, 75.9, 68.4, 67.1 (C_5H_4B), 21.0, 20.8 (*para*-CH_3 of Mes), 19.1, 18.8, 18.1, 17.6 (*ortho*-CH_3 of Mes), carbene and boron-bound carbons not observed.

^{19}F NMR (282 MHz, benzene-d_6, 20 ºC): δ_F –116.4 (d, $^{3}J_{FF}$ = 24.8 Hz, *ortho*-F of C_6F_5), -120.5 (d, $^{3}J_{FF}$ = 26.2 Hz, *ortho*-F of C_6F_5), -122.1 (d, $^{3}J_{FF}$ = 24.8 Hz, *ortho*-F of C_6F_5), -128.4 (d, $^{3}J_{FF}$ = 26.2 Hz, *ortho*-F of C_6F_5), -159.0 (t, $^{3}J_{FF}$ = 20.0 Hz, *para*-F of C_6F_5), -160.8 (t, $^{3}J_{FF}$ = 20.0 Hz, *para*-F of C_6F_5), -163.7 (apparent t, *meta*-F of C_6F_5), -164.4 (apparent t, *meta*-F of C_6F_5), -165.5 (apparent t, *meta*-F of C_6F_5), -166.6 (apparent t, *meta*-F of C_6F_5).

MS(ESI) *m*/*z* (%): 530.0 (100) $[FcB(C_6F_5)_2]^+$, 902.2 (0.5) $[IMesCl_2.BFc(C_6F_5)_2]^+$.

Elemental microanalysis: calc. for $C_{43}H_{31}BCl_2F_{10}FeN_2$ C 57.18% H 3.46% N 3.19%, meas. C 57.18 % H 3.16% N 3.05%.

Crystallographic data: $IMesCl_2{\cdot}BFc(C_6F_5)_2{\cdot}(C_6H_6)$ [**5**·(C_6H_6)], $C_{49}H_{37}BCl_2F_{10}FeN_2$, M_r = 981.39, triclinic, *P*-1, *a* = 11.3273(1), *b* = 17.7715(2), *c* = 21.5287(2) Å, α = 97.155(1), β = 96.389(1), γ = 90.053(1)º, *V* = 4272.9(1) $Å^3$, *Z* = 4, *ρ*c = 1.525 Mg m^{-3}, *T* = 150 K, λ = 0.71073 Å. 128324 reflections collected, 19377 independent [R(int) = 0.044] used in all calculations. R_1 = 0.0489, wR_2 = 0.1050 for observed unique reflections [$I>2\sigma(I)$] and R_1 = 0.0918, wR_2 = 0.1461 for all unique reflections. Max. and min. residual electron densities 0.74 and -0.84 e $Å^3$.

$Cy_3PO{\cdot}BFc(C_6F_5)_2$ [6]: $FcB(C_6F_5)_2$ (0.50 g, 0.94 mmol) and Cy_3P (0.26 g, 0.94 mmol) were dissolved in benzene (20 mL) and the resulting solution was subjected to three freeze-pump-thaw cycles and ultimately backfilled with N_2O (*ca*. 4 atm.). The resulting solution was then allowed to stand at room temperature for 24 h to yield orange crystals, which were separated by filtration, washed with pentane (3 x 10 mL) and dried *in vacuo* to afford $Cy_3PO{\cdot}BFc(C_6F_5)_2$ as an orange powder (0.34 g, 0.40 mmol, 43%) in >95% purity. Single crystals of $Cy_3PO{\cdot}BFc(C_6F_5)_2{\cdot}½(C_6H_6)$ suitable for X-ray crystallography were grown from a solution in benzene; after exposure of the crystalline samples to continuous vacuum, 0.33 equivalents of benzene solvate remained, as judged by ^{1}H NMR spectroscopy.

^{1}H NMR (300 MHz, THF-d_8, 20^{o}C): δ_H 7.30 (s, 2H, C_6H_6), 4.26, 4.00 (s, each 2H, C_5H_4B), 3.91 (s, 5H, C_5H_5), 2.11 (br m, 3H, Cy), 1.94 (br m, 6H, Cy), 1.77 (br m, 12H, Cy), 1.26 (br m, 12H, Cy).

^{11}B[^{1}H] NMR (96 MHz, THF-d_8, 20^{o}C): δ_B 6 (br).

^{13}C[^{1}H] NMR (75 MHz, THF-d_8, 20^{o}C): δ_C 149.8 (C_6F_5), 146.5 (C_6F_5), 139.4 (C_6F_5), 136.1 (C_6F_5), 128.8 (C_6H_6), 110.8 (C_5H_4B), 74.8 (C_5H_4B), 70.0 (C_5H_4B), 68.8 (C_5H_5), 35.2 (d, $^{1}J_{PC}$ = 58.7 Hz, Cy), 27.1 (d, $^{3}J_{PC}$ = 12.7 Hz, Cy), 26.6 (d, $^{2}J_{PC}$ = 17.8 Hz, Cy).

^{19}F NMR (282 MHz, THF-d_8, 20^{o}C): δ_F -127.9 (4F, *ortho*-CF of C_6F_5), -160.1 (2F, *para*-CF of C_6F_5), -164.5 (4F, *meta*-CF of C_6F_5).

^{31}P[^{1}H] NMR (121 MHz, THF-d_8, 20^{o}C): δ_P 68.3.

MS (EI) 530.0 (100%, $FcB(C_6F_5)_2$)

Elemental microanalysis: calc. for $C_{42}H_{44}BF_{10}FeOP$, C 59.18%, H 5.20%; meas. C 58.97, 58.82%, H 5.38, 5.47%.

UV-vis (fluorobenzene) λ_{max}, nm (ε): 450 (60 L mol^{-1} cm^{-1}).

$E_{1/2}$ (0.05 M [^{n}Bu$_4$N][B(C$_6$F$_5$)$_4$] electrolyte in fluorobenzene) = +0.01 mV, relative to FcH/FcH$^+$.

Crystallographic data: Cy$_3$PO·BFc(C$_6$F$_5$)$_2$·½(C$_6$H$_6$) [**6**·½(C$_6$H$_6$)], C$_{43}$H$_{45}$BF$_{10}$FeOP, M_r = 865.44, triclinic, *P*-1, *a* = 9.8771(1), *b* = 12.501(1), *c* = 17.2452(3) Å, α = 72.9492(6), β = 79.1339(6), γ = 75.3271(8)º, *V* = 1954.20(5) Å^3, *Z* = 2, ρ_c = 1.471 Mg m^{-3}, *T* = 150 K, λ = 0.71073 Å. 15375 reflections collected, 8842 independent [R(int) = 0.000] used in all calculations. R_1 = 0.0348, wR_2 = 0.0738 for observed unique reflections [I>2σ(I)] and R_1 = 0.0515, wR_2 = 0.0900 for all unique reflections. Maximal and minimal residual electron densities are 0.49 and -0.50 e Å^3. Note: a highly disordered C$_6$D$_6$ molecule with approximately 1/3 occupancy was removed from the model utilising the PLATON SQUEEZE program (details in the CIF).

FcB(F)(C$_6$F$_5$)(C$_6$F$_4$-*p*-PCy$_3$) [7]: FcB(C$_6$F$_5$)$_2$ (0.100 g, 0.19 mmol) and Cy$_3$P (0.053 g, 0.19 mmol) were dissolved in d_6-benzene (2 mL) and the resulting solution stirred for 10 d, during which time a brown oil formed. Volatiles were removed *in vacuo*, the resulting residue taken up in *d*-chloroform (5 mL) and layered with hexane. A very small quantity of orange crystals formed, which was isolated by filtration and dried *in vacuo*. Yield <5%.

^{1}H NMR (300 MHz, CDCl$_3$, 20^{o}C): δ_H 4.42 (br s, 2H, C$_5$H$_4$B), 4.18 (br s, 5H, C$_5$H$_5$), 3.35 (br s, 2H, C$_5$H$_4$B), 2.90 (q, $^4J_{H\text{-}H}$ = 10 Hz, 3H, Cy), 2.13-1.27 (overlapping m, 30 H, Cy).

$^{11}B[^{1}H]$ NMR (96 MHz, $CDCl_3$, 20°C): δ_B 2 (br).

^{19}F NMR (282 MHz, $CDCl_3$, 20°C): δ_F -124.7 (2F, m, C_6F_4), -132.0 (2F, m, C_6F_4), -133.3 (2H, d, $^3J_{H-H}$ = 20.9 Hz, *ortho*-F of C_6F_5), -162.2 (1H, t, $^3J_{H-H}$ = 20.9 Hz, *para*-F of C_6F_5), -165.8 (2F, m, *meta*-F of C_6F_5), -193.7 (1F, br. s, boron-bound F).

$^{31}P[^{1}H]$ NMR (121 MHz, $CDCl_3$, 20°C): δ_P 39.9.

Crystallographic data: FcB(F)(C_6F_5)(C_6F_4-*p*-PCy_3) [**7**], $C_{41}H_{43}BCl_3F_{20}FeP$, M_r = 929.76, triclinic, *P*-1, *a* = 11.7155(3), *b* = 12.6410(4), *c* = 15.6649(3) Å, α = 83.830(2), β = 79.824(2), γ = 66.833(3)º, *V* = 2097.4(1) $Å^3$, *Z* = 2, ρ_c = 1.472 Mg m^{-3}, *T* = 150 K, λ = 1.54180 Å. 8635 reflections collected, 8635 independent [R(int) = 0.019] used in all calculations. R_1 = 0.0357, wR_2 = 0.0824 for observed unique reflections [$I>2\sigma(I)$] and R_1 = 0.0374, wR_2 = 0.0838 for all unique reflections. Maximal and minimal residual electron densities are 0.54 and -0.51 e $Å^3$.

$FcB(C_6Cl_5)_2$ [8]: FcLi (0.33 g, 1.7 mmol) was added slowly at 6 ºC to a suspension of $ClB(C_6Cl_5)_2$ (0.95 g, 1.7 mmol) in benzene (100 mL). The resulting purple suspension was allowed to warm to room temperature over 15 min, and then stirred for 15 h. The precipitate was separated by filtration and then extracted with benzene (2 x 50 mL). The filtrate and extracts were combined and dried *in vacuo* to afford a purple solid (0.49 g), which was analysed by ^1H NMR and found to consist of a mixture ferrocene and the target material. The ferrocene impurity was removed from the desired product by sublimation (2 h at 70 ºC at 10^{-2} mbar) to afford $FcB(C_6Cl_5)_2$ as a purple solid. Yield 0.33

g, 27%. Crystals suitable for X-ray diffraction were obtained by cooling a saturated solution in benzene.

^{1}H NMR (300 MHz, $CDCl_3$, 20^{o}C): δ_H 5.00 (t, 2H, $^{3}J_{H\text{-}H}$ = 1.8 Hz, C_5H_4B), 4.71 (t, 2H, $^{3}J_{H\text{-}H}$ = 1.8 Hz, C_5H_4B), 4.32 (s, 5H, C_5H_5).

^{1}H NMR (300 MHz, C_6D_6, 20^{o}C): δ_H 4.52 (t, 2H $^{3}J_{H\text{-}H}$ = 1.8 Hz, C_5H_4B), 4.49 (t, 2H $^{3}J_{H\text{-}H}$ = 1.8 Hz, C_5H_4B), 3.95 (s, 5H, C_5H_5).

^{11}B[^{1}H] NMR (96 MHz, $CDCl_3$, 20^{o}C): δ_B 62.

^{13}C[^{1}H] NMR (75 MHz, THF-d_8, 20^{o}C): δ_C 139.9 (C_6Cl_5), 132.4 (C_6Cl_5), 129.6 (C_6Cl_5), 124.2 (C_6Cl_5), 77.9 (C_5H_4B), 74.2 (C_5H_4B), 67.8 (C_5H_5). No signal was observed for the boron bound carbon of C_5H_4B.

MS (CI –ve NH_3) 249.8 (43%) $[C_6Cl_5]^-$, 537.7 (39%) $[C_5H_4B(C_6Cl_5)(C_6Cl_4)]^-$, 628.6 (100%) $[Fe(C_5H_4B(C_6Cl_5)_2)]^-$, 693.6 (16%) $[FcB(C_6Cl_5)_2]^-$. Exact mass (EI) (calculated for M^+, ^{10}B, ^{35}Cl, ^{56}Fe, isotopomer) 688.7081, (measured) 688.7066.

Elemental microanalysis: calc. for $C_{22}H_9BCl_{10}Fe$, C 38.05%, H 1.31%; meas. C 37.85, 37.92%, H 1.20, 1.21%.

UV-vis (fluorobenzene) λ_{max}, nm (ε): 546 (358 L mol^{-1} cm^{-1}).

$E_{1/2}$ (0.05 M [^{n}Bu$_4$N][B(C$_6$F$_5$)$_4$] electrolyte in α,α,α-trifluorotoluene) = +550 mV, relative to FcH/FcH$^+$.

Crystallographic data: FcB(C$_6$Cl$_5$)$_2$·C$_6$D$_6$ [**8**·C$_6$D$_6$], C$_{28}$H$_9$D$_6$BCl$_{10}$Fe, M_r = 778.65, monoclinic, P 2$_1$/c, a = 9.20040(10), b = 22.2839(2), c = 14.74670(10) Å, β = 101.7501(4)º, V = 2960.03(5) Å^3, Z = 2, ρ_c = 1.747 Mg m^{-3}, T = 150 K, λ = 0.71073 Å. 12403 reflections collected, 6721 independent [R(int) = 0.000] used in all calculations. R_1 = 0.0381, wR_2 = 0.0987 for observed unique reflections [I>2σ(I)] and R_1 = 0.0506, wR_2 = 0.1067 for all unique reflections. Max. and min. residual electron densities 0.52 and -0.56 e Å^3.

^{t}Bu$_3$P=O·BFc(C$_6$Cl$_5$)$_2$ [^{t}Bu$_3$P=O·8]: FcB(C$_6$Cl$_5$)$_2$ (0.020 g, 0.29 μmol) and ^{t}Bu$_3$P (0.006 g, 0.31 μmol) were dissolved in benzene (2 mL) and the resulting solution subjected to three freeze-pump-thaw cycles before backfilling with N$_2$O (ca. 4 atm). The solution was allowed to stand at room temperature for 12 h to yield an orange solution. Slow diffusion of pentane into a saturated benzene solution gave an orange precipitate that was isolated by filtration and dried *in vacuo*. Yield not determined.

^{1}H NMR (300 MHz, benzene-d_6, 20 ºC): δ_H 4.73 (m, 4H, C$_5$H$_4$B), 3.99 (s, 5H, C$_5$H$_5$), 1.26 (d, $^2J_{H\text{-}P}$ = 9.6 Hz, 27H, P^{t}Bu$_3$).

^{13}C[^{1}H] NMR (75 MHz, benzene-d_6, 20^{o}C): δ_C 142.3 (C$_6$Cl$_5$), 138.7 (C$_6$Cl$_5$), 129.5 (C$_6$Cl$_5$), 75.6 (C$_5$H$_4$B), 73.2 (C$_5$H$_4$B), 67.0 (C$_5$H$_5$), 38.9 (d, $^2J_{C\text{-}P}$ = 49.8 Hz, CH$_3$ of ^{t}Bu). No signal was observed for the boron bound carbons of C$_5$H$_4$B or C$_6$Cl$_5$.

$^{11}B[^{1}H]$ NMR (96 MHz, benzene-d_6, 20 ºC): δ_B 29 (br).

$^{31}P[^{1}H]$ NMR (121 MHz, benzene-d_6, 20^{o}C): δ_P 64.0 (s).

UV-vis (fluorobenzene) λ_{max}, nm (ε): 376 (374 L mol^{-1} cm^{-1}).

FcB(C_6Cl_5)Br [9]: *n*-BuLi (88 mL of a 1.6 M solution in hexanes, 14 mmol) was added dropwise to a suspension of hexachlorobenzene (4.01 g, 14 mmol) in a 1:1 hexane/diethyl ether mixture (200 mL) at -78 ºC. The resulting suspension was allowed to warm to approximately -40 ºC, until the white insoluble material was consumed, yielding a yellow solution, which was quickly transferred to a suspension of $FcBBr_2$ (5.01 g, 14 mmol) in hexane (100 mL) at -78 ºC. The resulting red suspension was allowed to warm to room temperature over 2 h, darkening noticeably around -30 ºC, and was then stirred at room temperature for a further 12 h. Volatiles were removed *in vacuo* to afford a dark maroon tar, which was extracted with dichloromethane (40 mL). The volatiles were removed *in vacuo* from the maroon solution to afford a maroon tar. Condensing argon unto the tar (*ca*. 20mL), subsequent mechanical manipulation of the solid to give a fine suspension in argon and then evacuation for a period of 1 h gave rise to a maroon powder. Yield 6.92 g, 93%.

^{1}H NMR (300 MHz, $CDCl_3$, 20^{o}C): δ_H 4.87 (t, 2H, $^{3}J_{H-H}$ = 1.8 Hz, C_5H_4B), 4.47 (t, 2H, $^{3}J_{H-H}$ = 1.8 Hz, C_5H_4B), 4.32 (s, 5H, C_5H_5).

$^{11}B[^{1}H]$ NMR (96 MHz, $CDCl_3$, 20^{o}C): δ_B 61.

$^{13}C[^{1}H]$ NMR (75 MHz, THF-d_8, 20^{o}C): δ_C 70.8 (C_5H_5), 73.0 (C_5H_4B), 76.4 (C_5H_4B), 76.6 (C_5H_4B), 134.1 (C_6Cl_5B), 132.0 (C_6Cl_5B). The peak corresponding to boron-bound, quaternary carbons of C_6Cl_5 was not observed.

MS (ESI^+) 185.9 (100%) $[FcH]^+$, 249.8 (34%) $[C_6Cl_5H]^+$, 461.8 (59%) $[FcB(C_6Cl_5)(OH)]^+$, 523.8 (16%) $[FcB(C_6Cl_5)Br]^+$, exact mass (calculated for M^+, ^{10}B, ^{35}Cl, ^{54}Fe, ^{79}Br isotopomer) 518.7850, (measured) 518.8750.

Elemental microanalysis: calc. for $C_{16}H_9BBrCl_5Fe$, C 36.60%, H 1.73%; meas. C 36.13, 36.21%, H 1.32, 1.37%.

$E_{1/2}$ (0.05 M $[^{n}Bu_4N][B(C_6F_5)_4]$ electrolyte in fluorobenzene) = -382 mV, relative to FcH/FcH^+.

$FcB(C_6Cl_5)Mes$ [10]: A suspension of $FcB(C_6Cl_5)Br$ (0.858 g, 1.6 mmol) and MesLi (0.205 g, 1.6 mmol) in benzene (50 mL) was heated under reflux for 2 h. The resulting suspension was cooled to room temperature, volatiles removed *in vacuo* and transferred as a suspension in a minimal amount of hexane onto a silica/hexane column. Elution with hexane gave rise to three bands which were isolated, the volatiles removed *in vacuo* from each and their composition analysed by ^{1}H NMR spectroscopy. The first, yellow band (0.030 g) was found to be ferrocene, the second, maroon band (0.390 g, 42%) was found to be the target material and the last, red band (0.080 g) was found to be unreacted starting material.

^{1}H NMR (500 MHz, C_6D_6, 20^{o}C): δ_H 6.79 (s, 2H, CH of Mes), 4.49 (t, 2H, $^{3}J_{H\text{-}H}$ = 2.0 Hz, C_5H_4B), 4.42 (t, 2H, $^{3}J_{H\text{-}H}$ = 2.0 Hz, C_5H_4B), 3.95 (s, 5H, C_5H_5), 2.52 (s, 6H, *ortho*-CH_3 of Mes), 2.15 (s, 3H, *para*-CH_3 of Mes).

^{11}B[^{1}H] NMR (96 MHz, C_6D_6, 20^{o}C): δ_B 72 (br s).

^{13}C[^{1}H] NMR (125 MHz, C_6D_6, 20^{o}C): δ_C 140.4 (*para*-C of Mes), 139.5 (Ar-C), 138.2 (*ortho*-C of Mes), 133.6 (Ar-C), 133.4 (Ar-C), 132.2 (Ar-C), 129.6 (Ar-C), 129.1 (*meta*-C of Mes), 80.2 (C_5H_4B), 75.1 (C_5H_4B), 70.3 (C_5H_5), 25.3 (*ortho*-CH_3 of Mes), 21.1 (*para*-CH_3 of Mes). The boron bound carbon of C_5H_4B could not be observed.

MS (ESI^{+}) 185.9 (31%) $[FcH]^{+}$, 249.8 (16%) $[C_6Cl_5H]^{+}$, 563.9 (100%) $[FcB(C_6Cl_5)Mes]^{+}$. Exact mass (calculated for M^{+}, ^{10}B, ^{35}Cl, ^{54}Fe isotopomer) 558.9529, (measured) 558.9525.

UV-vis (fluorobenzene) λ_{max}, nm (ε): 529 (364 L mol^{-1} cm^{-1}).

^{t}Bu$_3$P·N$_2$O·BFc(C$_6$F$_5$)$_2$ [12]: $FcB(C_6F_5)_2$ (0.220 g, 0.42 mmol) and $^{t}Bu_3P$ (0.081 g, 0.40 mmol) were dissolved in benzene (6 mL) and the resulting solution subjected to three freeze-pump-thaw cycles before backfilling with N_2O (ca. 4 atm). The solution was allowed to stand at room temperature for 12 h to yield orange crystals, which were separated by filtration, washed with pentane (3 x 10 mL) and dried *in vacuo* to afford $^{t}Bu_3P{\cdot}N_2O{\cdot}BFc(C_6F_5)_2$ as an orange powder (0.27 g, 0.34 mmol, 86%, contaminated with trace $^{t}Bu_3PO$). The reaction proceeds to completion significantly more quickly (within 1

h), if stirred, although it does not yield single crystals. Single crystals suitable for X-ray crystallography were grown from a solution in benzene. After exposure of the crystalline samples to continuous vacuum, 0.67 equivalents of benzene solvate remained, as judged by ^{1}H NMR spectroscopy.

^{1}H NMR (300 MHz, THF-d_8, 20^{o}C): δ_H 7.29 (s, 4H, C_6H_6), 4.10 (s, 2H, C_5H_4B), 4.01 (s, 2H, C_5H_4B), 3.86 (s, 5H, C_5H_5), 1.53 (d, 27H, $^{3}J_{PH}$ = 14.7 Hz, $P(CMe_3)_3$).

^{11}B[^{1}H] NMR (96 MHz, THF-d_8, 20^{o}C): δ_B 3 (br).

^{13}C[^{1}H] NMR (125 MHz, THF-d_8, 20^{o}C): δ_C 149.2 (C_6F_5), 147.3 (C_6F_5), 138.3 (C_6F_5), 136.4 (C_6F_5), 128.8 (C_6H_6), 73.8 (C_5H_4B), 69.4 (C_5H_4B), 68.4 (C_5H_5), 41.7 (d, $^{1}J_{PC}$ = 30.0 Hz, quaternary C of $P(CMe_3)_3$), 29.3 (Me of $P(CMe_3)_3$). The signal for the boron bound carbon of C_5H_4B was not observed.

^{19}F NMR (282 MHz, THF-d_8, 20^{o}C): δ_F -131.0 (d, 4F, $^{3}J_{FF}$ = 14.9 Hz, *ortho*-CF of C_6F_5), -163.4 (d, 2F, $^{3}J_{FF}$ = 19.7 Hz, *para*-CF of C_6F_5), -167.4 (dd, 4F, $^{3}J_{FF}$ = 14.9 Hz, $^{3}J_{FF}$ = 19.7 Hz, *meta*-CF of C_6F_5).

^{31}P[^{1}H] NMR (121 MHz, THF-d_8, 20^{o}C): δ_P 65.3 (s).

MS(EI) *m*/*z* (%): 530.0 (11) $[FcB(C_6F_5)_2]^+$, 776.2 (100) $[^{t}Bu_3P{\cdot}N_2O{\cdot}BFc(C_6F_5)_2]^+$. HRMS(EI) (*m*/*z*): calc. for [M^+], $C_{34}H_{36}BF_{10}Fe_1N_2O_1P_1$ (^{10}B, ^{54}Fe isotopomer) 774.1895; meas. 774.1887.

UV-vis (fluorobenzene) λ_{max}, nm (ε): 434 (120 L mol^{-1} cm^{-1}).

$E_{1/2}$ (0.05 M [$^{n}Bu_4N$][$B(C_6F_5)_4$] electrolyte in fluorobenzene) = -0.31 mV, relative to FcH/FcH^{+}.

Crystallographic data: $^{t}Bu_3P{\cdot}N_2O{\cdot}BFc(C_6F_5)_2{\cdot}C_6H_6$ [**12**$\cdot C_6H_6$], $C_{40}H_{42}BF_{10}FeN_2OP$, M_r = 854.40, monoclinic, P 2_1, a = 11.0548(4), b = 15.1745(7), c = 11.6859(5) Å, β = 92.794(2)º, V = 1957.99(14) $Å^3$, Z = 2, ρ_c = 1.449 Mg m^{-3}, T = 150 K, λ = 0.71073 Å. 6191 reflections collected, 6191 independent [R(int) = 0.000] used in all calculations. R_1 = 0.0452, wR_2 = 0.1059 for observed unique reflections [I>2σ(I)] and R_1 = 0.0488, wR_2 = 0.1093 for all unique reflections. Max. and min. residual electron densities 0.25 and -0.48 e $Å^3$.

Binding Study of $B(C_6F_5)_2Fc$ and $^{t}Bu_3PO$: Multinuclear NMR studies carried out on an equimolar mixture of $FcB(C_6F_5)_2$ and $^{t}Bu_3PO$ (such as might be formed from the $^{t}Bu_3P/FcB(C_6F_5)_2$ FLP in the presence of a compatible O-atom transfer agent) at *ca*. 10 mM concentrations reveal a ca. 4:1 mixture of the free acid/base and adduct.

5.4. Discussion of Results

5.4.1. The Reactions of Carbenes, Lewis acids and N_2O

The initial focus of the research was to assess whether or not a Lewis base/nitrous oxide adduct would be capable of binding to a ferrocenyl borane. The N_2O adduct of the IMes carbene and the Lewis acid $FcB(C_6F_5)_2$ (**1**) were made according to slightly modified literature procedures for reasons of synthetic ease.[116,118,129,131] $FcB(C_6F_5)_2$ was synthesised in two steps from ferrocene. The first step was the synthesis of $FcBBr_2$, with moderate yields (ranging from 30-55%), from ferrocene using BBr_3 following a literature procedure [Scheme 5.4.1.].[131] $FcB(C_6F_5)_2$ was then synthesised in good yield (65%) by treatment of $FcBBr_2$ with two equivalents LiC_6F_5 generated *in situ* from either C_6F_6 or C_6F_5Br treated with n-BuLi at -78 ºC. [*N.B.* Care must be taken not to allow the solution of LiC_6F_5 to rise above -30 ºC, as literature and private communications attest to detonation of the reaction mixture at temperatures exceeding this temperature]. This new synthetic route is easier to carry out than those *via* $ClB(C_6F_5)_2$, which itself is made *via* the toxic organotin reagent $Me_2Sn(C_6F_5)_2$.

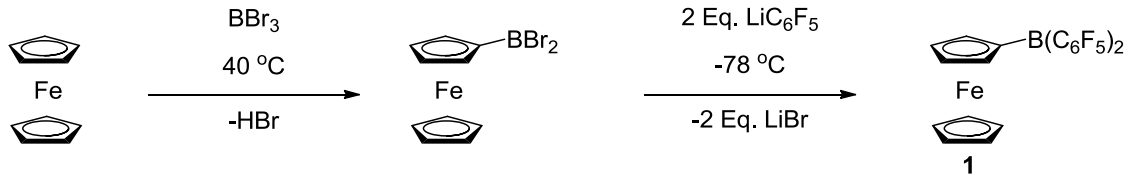

Scheme 5.4.1. The synthesis of $FcB(C_6F_5)_2$.

Mixing together IMes·N_2O and $FcB(C_6F_5)_2$ in a one-to-one stoichiometric ratio led to the formation of the simple 1:1 complex IMes·N_2O·$BFc(C_6F_5)_2$ (**2**) [Scheme 5.4.2.]. The adduct is isolable as an analytically pure solid in moderate yield (42%). The binding event is accompanied by a darkening in colour to a very deep purple, which is somewhat unusual in that four-coordinate, ferrocenyl boranes are typically yellow in colour.[126-129] Evidence for the four-coordinate nature of the adduct **2** includes a change in the ^{11}B NMR chemical shift from 53 ppm for **1** to 3 ppm for **2**, the latter being consistent with neutral, four-coordinate boron centre.[132] The ^{19}F NMR spectrum is also a measure of the degree of coordination at the boron centre, with a reduction in the chemical shift difference, $\Delta_{m,p}$, between the *meta* and *para* fluorines, of C_6F_5 rings, reflecting higher electron density at the boron centre.[133,134] The $\Delta_{m,p}$ value decreases from a value of 9.2 ppm for **1** to a value of 5.6 ppm for **2**.[129] The latter value is the same as that of the $FcB(C_6F_5)_2$·PMe_3 adduct. The ^{11}B and $\Delta_{m,p}$ data for all new compounds and selected values from the literature are presented in Table 5.4.1.

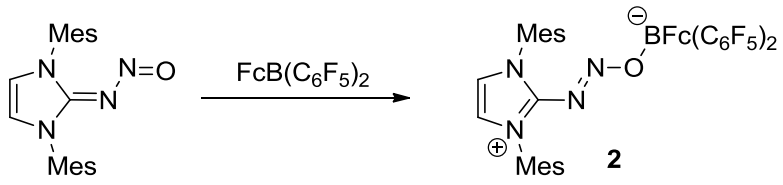

Scheme 5.4.2. The reaction of IMes•N_2O with $FcB(C_6F_5)_2$ **1**.

The IMes·N_2O adduct of $FcB(C_6F_5)_2$ (**2**) was characterized by single-crystal X-ray crystallography as the 1:1 chloroform solvate, and the structure is shown in Figure 5.4.1. Analysis of the structure **2** so determined confirms that the boron centre is

indeed four-coordinate in the solid state with oxygen binding directly to the boron atom (Figure 5.4.1). The bound N_2O molecule adopts a gullwing, or "*trans-trans*", geometry, which has also been seen by Severin and coworkers in $[IMes{\cdot}N_2O{\cdot}CPh_3]^+$ and by Stephan and coworkers in $R_3P{\cdot}N_2O{\cdot}BAr_3$.[118,122-124]

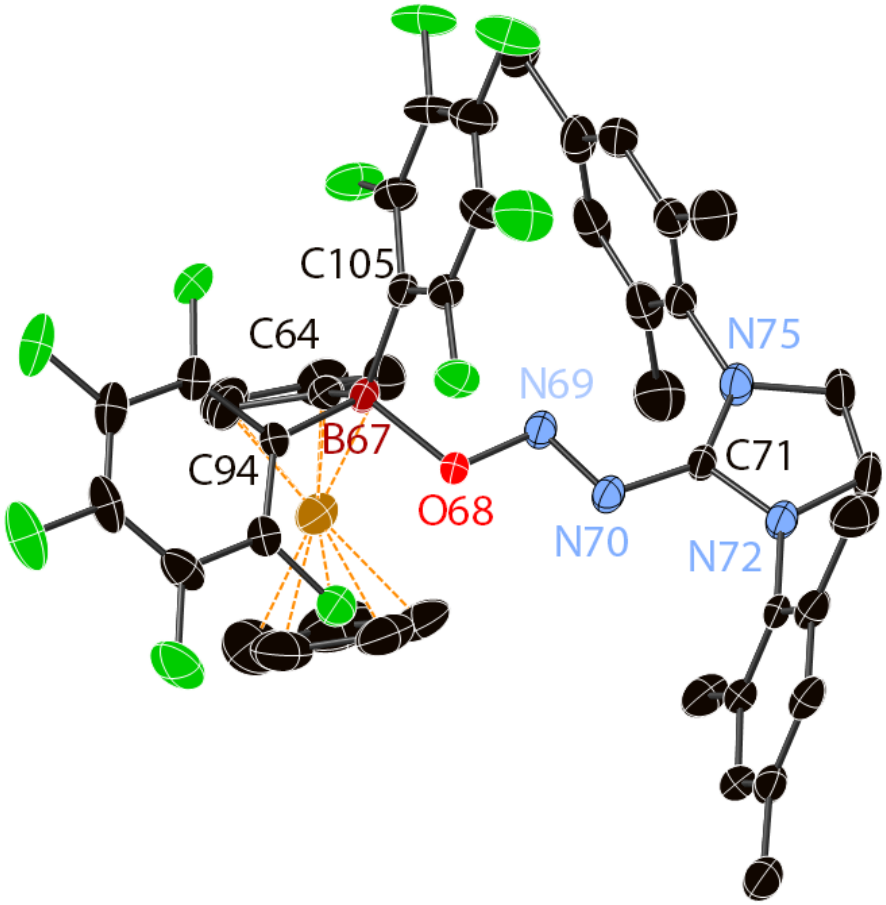

Figure 5.4.1. The molecular structure of $IMes{\bullet}N_2O{\bullet}BFc(C_6F_5)_2$ (**2**). Chloroform solvate molecules and hydrogen atoms omitted for clarity. Ellipsoids drawn at the 50% probability level, with boron in red, carbon in black, nitrogen in blue, fluorine in green and iron in orange.

A list of pertinent bond lengths for IMes•N_2O•BFc$(C_6F_5)_2$ (**2**), as well as some for IMes·N_2O and $[IMes·N_2O·CPh_3]^+[BF_4]^-$, is given in Table 5.4.1. Binding of IMes·N_2O to a Lewis acid results in the elongation of the carbenic carbon-nitrogen and the N-O bond lengths and a shortening of the N-N bond length, as is seen in $[IMes·N_2O·CPh_3]^+[BF_4]^-$ (Table 5.4.1.).[118] The carbenic carbon-nitrogen bond lenths for the two crystallographically unique components in the crystal structure of **2** are 1.376(5) and 1.383(6) Å, which are longer than the corresponding bond in IMes·N_2O [1.360(2) Å].[117] The N-O bonds of **2** are also longer than those of IMes·N_2O [1.319(4) and 1.318(5) Å] compared with a value of 1.250(3) for IMes·N_2O.[117] A shortening of the N-N bond is also exhibited in **2** [1.268(4) and 1.279(4) Å] compared to a value of 1.333(2) Å for IMes·N_2O.[117]

Bond	**Bond length (Å)**		
	IMes·N_2O[117]	$[IMes·N_2O·CPh_3][BF_4]$ [118]	**2**
$C_{carbene}$-$N_{termnial}$	1.360(2)	1.392(2)	1.376(5), 1.383(6)
$N_{terminal}$-$N_{central}$	1.333(2)	1.257(2)	1.268(4), 1.279(4)
$N_{central}$-$O_{terminal}$	1.250(2)	1.365(2)	1.319(4), 1.318(5)
$O_{terminal}$-B	n/a	n/a	1.559(5), 1.572(5)

Table 5.4.1. Key bond lengths for **2**, with the nitrogen atoms and oxygens of the N_2O fragment are labelled according to their position in the free N_2O molecule (terminal/central).

Pertinent bond angles of **2**, IMes·N_2O and $^tBu_3P$•N_2O•$B(C_6F_5)_3$ are compared in Table 5.4.2. The C-N-N-O-B fragment of **2** is almost planar exhibiting torsion angles of

180.0(3) and 179.1(3)º for C-N-N-O and 179.8(3) and 178.5(3)º for N-N-O-B, figures which are remarkably similar to both IMes·N_2O and $^{t}Bu_3P{\cdot}N_2O{\cdot}B(C_6F_5)_3$ [Table 5.4.2.]. The C-N-N, N-N-O and N-O-B angles are also similar to those of both IMes·N_2O and $^{t}Bu_3P{\cdot}N_2O{\cdot}B(C_6F_5)_3$ (Table 5.4.2.).

Bond Angle	**IMes·N_2O (º)[117]**	**IMes·N_2O•$BFc(C_6F_5)_2$ (º) 2**	**$^{t}Bu_3P{\cdot}N_2O{\cdot}B(C_6F_5)_3$ (º)[124]**
$C_{carbene}$-N-N	109.8(2)	113.5(3), 114.2(3)	n/a
P-N-N	n/a	n/a	117.0(1)
N-N-O	107.3(1)	108.8(3), 108.8(3)	109.1(1)
N-O-B	n/a	113.9(3), 114.2(3)	114.4(1)
C-N-N-O (torsion)	175.4(1)	180.0(3), 179.1(3)	n/a
P-N-N-O (torsion)	n/a	n/a	176.72(8)
N-N-O-B (torsion)	n/a	179.8(3), 178.5(3)	176.0(1)

Table 5.4.2. Key bond angles of IMes·N_2O, IMes·N_2O·$BFc(C_6F_5)_2$ (**2**) and $^{t}Bu_3P{\cdot}N_2O{\cdot}B(C_6F_5)_3$..

Given that the N_2O-adduct of IMes is capable of binding to $FcB(C_6F_5)_2$ (**1**), it was of interest to see whether the combination of $FcB(C_6F_5)_2$ and IMes would bind in the absence of N_2O, or if they would constitute a frustrated Lewis pair. Therefore, a one-to-one stoichiometric mixture of IMes and $FcB(C_6F_5)_2$ was examined to provide an answer to this question. The reaction mixture changed colour rapidly from a deep maroon to orange, a change which is often representative of the formation of a four-coordinate, neutral, ferrocenyl borane. Moreover, the fact that the ^{11}B NMR chemical shift moves upfield from +53 ppm to -14 ppm is also highly suggestive of the formation of IMes·$BFc(C_6F_5)_2$

(**3**) (Scheme 5.4.2.). This resonance is markedly further upfield than that **2**, (δ = 3 ppm), which suggests that the boron bears greater electron density in **3** than in **2**, and in turn suggests (not surprisingly) that IMes·N_2O is a weaker electron donor than IMes carbene. De-convoluting the ^{19}F NMR spectrum proved non-trivial, with the signals for all four *ortho*, four *meta* and both *para* fluorines being inequivalent. This is consistent with a marked increase in the steric congestion at the boron centre compared with that present for **2**, for which equivalence in the ^{19}F NMR is ascribed to rapid, free rotation around the B-C_{Ar} and B-C_{Fc} bonds on the NMR time-scale. F-F COSY ^{19}F NMR was not available. The $\Delta_{m,p}$ value ranges from 2.8 to 7.3 ppm. It is clear therefore that the $\Delta_{m,p}$ values are lower than that of $FcB(C_6F_5)_2$ (**1**), which again supports the supposition of greater electron density at the boron centre for **3** than for **1**. The key conclusion to be drawn from this chemistry is that the steric bulk of IMes is insufficient to preclude bond formation to the boron of $FcB(C_6F_5)_2$ and therefore that Imes and $FcB(C_6F_5)_2$ do not comprise an FLP system.

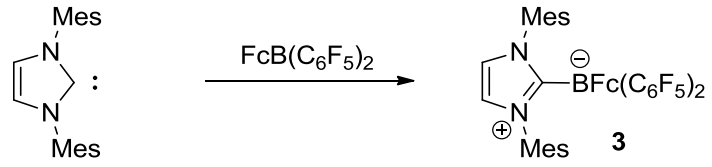

Scheme 5.4.2. The reaction of Imes and $FcB(C_6F_5)_2$ (**1**) to give rise to Imes·$BFc(C_6F_5)_2$ (**3**).

Subsequent research centred on altering the nature of the carbene in an attempt to find a combination of a carbene and **1** that *would* comprise a FLP. The IDipp carbene (also called IPr in some publications) is generally considered a sterically more demanding ligand than IMes, due to the greater volume swept out by the *iso*-propyl groups at the 2- and 6-postions of the aryl group of Dipp, compared to that of the corresponding methyl groups of the IMes. However, the steric pressure imposed by these NHC ligands is not isotropic, and is generally best described in terms of the percentage buried volume,[135,136] which is defined as the percentage of the total volume of a sphere occupied by a ligand, with the "metal" to which the NHC is bound to set as the origin and the radius fixed. The percent buried volume of IMes at a radius of 2 Å is 36.1% and that of IDipp is 46.5% (for the same radius).[135] It is to be expected then, that it is more probable that IDipp would be more likely than IMes to form a FLP system with **1**, purely on steric grounds.

Compound	^{11}B NMR shift [δ_B (ppm)]	^{19}F $\Delta_{m,p}$ [ppm]	Reference
$B(C_6F_5)_3$	80	16.3	[137]
$B(C_6F_5)_2Ph$	73	12.6	[138]
$HB(C_6F_5)_2$	60	18.3	[139]
$FcB(C_6F_5)_2$ (1)	53	9.2	[129]
$FcBBr_2$	47	-	[131]
$Cy_3P{=}O{\cdot}B(C_6H_4\text{-}p\text{-}F)_3$	26	-	[122]
$^tBu_3P{\cdot}N_2O{\cdot}B(C_6H_4\text{-}p\text{-}F)_3$	7	-	[122]
$^tBu_3P{\cdot}N_2O{\cdot}B(C_6F_5)_2(OC_6F_5)$	6	-	[122]
$Cy_3P{=}O{\cdot}BFc(C_6F_5)_2$	6	4.4	n/a
$^tBu_3P{\cdot}N_2O{\cdot}B(C_6F_5)_2Mes$	4	4.6	[122]
$IMes{\cdot}N_2O{\cdot}BFc(C_6F_5)_2$	3	5.6	n/a
$Cy_3P{\cdot}N_2O{\cdot}B(C_6F_4\text{-}p\text{-}H)_3$	1	-	[122]
$^tBu_3P{\cdot}N_2O{\cdot}B(C_6F_5)_3$	0	5.7	[122]
$[FcB(C_6F_5)_2][OTf]$	-5	6.2	[129]
$[FcB(C_6F_5)_3]^{-}{\cdot}[Cp_2Co]^{+}$	-13	3.7	[129]
$IDipp{\cdot}BFc(C_6F_5)_2$	-13	(2.4-6.1)	n/a
$IMesCl_2{\cdot}BFc(C_6F_5)_2$	-13	(2.9-7.6)	n/a
$FcB(C_6F_5)_2{\cdot}PMe_3$	-14	5.6	[129]
$IMes{\cdot}BFc(C_6F_5)_2$	-14	(2.8-7.3)	n/a
$Li[B(C_6F_5)_4]$	-17	3.7	[138]
$[FcB(C_6F_5)_3]^{-}$	-24	6.8	[129]

Table 5.4.3. ^{11}B and ^{19}F $\Delta_{m,p}$ values for various perfluorophenyl-substituted boranes.

Unfortunately, the increased steric bulk of IDipp is insufficient to prevent complex formation. Thus, a one-to-one stoichiometric mixture with **1**, gives rise to IDipp·$BFc(C_6F_5)_2$ (**4**) [Scheme 5.4.3.]. This binding event was accompanied by a colour change from maroon to orange, as with IMes, which is consistent with formation of a four-coordinate boron complex. The ^{11}B NMR chemical shift of the IDipp adduct **4** (-13 ppm), is comparable to that of the IMes adduct **3** (-14 ppm), and is significantly upfield shifted compared to **1**. This fact suggests that there is a comparable electron density at the boron atom of both complexes, which further suggests that the increase in steric loading

of IDipp is insufficient to prevent coordinate bond formation between the carbenic carbon and the boron centre. De-convoluting the ^{19}F NMR again proved non-trivial, with the signals for all four *ortho*, all four *meta* and both *para* fluorines being inequivalent. This is comparable to the situation observed for **3**, and is indicative of high steric congestion at the boron atom. The $\Delta_{m,p}$ value ranges from 2.4 to 6.1 ppm, again supporting a supposition of greater electron density at the boron centre of **4** than that observed for **1**. Here too, the key conclusion to be drawn is that the steric bulk of IDipp is insufficient to preclude bond formation to the boron centre of **1** and, therefore, that IDipp and **1** also do not comprise a FLP system.

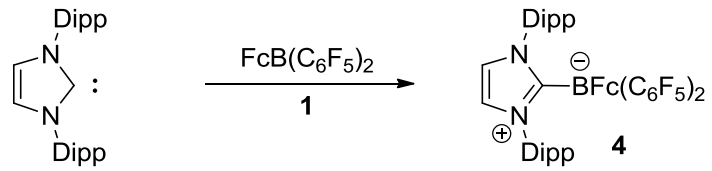

Scheme 5.4.3. The reaction of IDipp and **1** to give rise to IDipp•$BFc(C_6F_5)_2$ (**4**).

Since increasing the steric demands of the carbene did not lead to a FLP system, we sought to modify the electronic component of bonding. This was achieved by chlorinating the backbone of the IMes carbene following the route of Arduengo and co-workers, to give $IMesCl_2$ [Scheme 5.4.4.].[140] This carbene displays remarkable stability to both air and moisture, which has been ascribed to the concerted action of mesomeric induction of electron density to the carbenic carbon, reducing the π-acidity of the carbene, and the sigma-electron withdrawing effect attributable to the significant electronegativity of chlorine, reducing the σ-basicity of the carbene.[140]

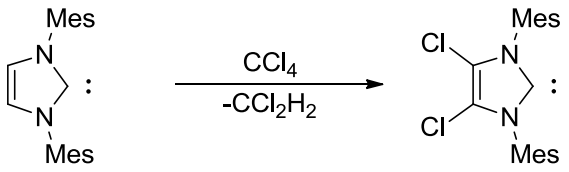

Scheme **5.4.4.** The synthesis of $IMesCl_2$ from IMes according to the method of Arduengo *et al.*[141]

Unfortunately, when this carbene was mixed with **1** in a one-to-one stoichiometry, the analagous 1:1 complex $IMesCl_2 \cdot BFc(C_6F_5)_2$ (**5**) was formed [Scheme 5.4.5.]. As with the reaction of **1** with IMes and IDipp, the reaction proceeds with a colour change from maroon to orange. The four-coordinate nature of complex **5** in solution is further substantiated by the ^{11}B NMR shift (-13 ppm), which is significantly lower than that of **2** and comparable to that of both **3** and **4** (-14 ppm and -13 ppm, respectively). This observation suggests that the carbenic carbon-boron interaction is similar for the chlorinated carbene and that the effect of the decrease in the σ-donor strength of the carbene is insufficient to prevent coordination. De-convoluting the ^{19}F NMR again proved non-trivial, with the signals for all four *ortho*, all four *meta* and both *para* fluorines being inequivalent, which is comparable to the situation determined for **3** and **4**, and is similarly indicative of high steric congestion at the boron atom. The maximum possible $\Delta_{m,p}$ value is 7.6 ppm and the minimum possible $\Delta_{m,p}$ value is 2.9 ppm, which again supports a claim of greater electron density at the boron centre for **5** than for **1**.

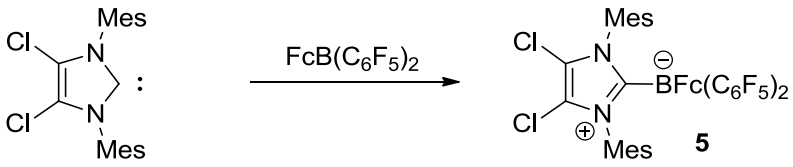

Scheme 5.4.5. The reaction of $IMesCl_2$ and $FcB(C_6F_5)_2$ (**1**) to give rise to $IMesCl_2$•$BFc(C_6F_5)_2$ (**5**).

That $IMesCl_2$ and $FcB(C_6F_5)_2$ do not form a FLP system is not the only limitation to this choice of carbene. The $IMesCl_2$ carbene was also observed not to activate N_2O at all on the same time-scale (24 h) (Scheme 5.4.6), which is further support for the hypothesis that highly σ-donating, and therefore Lewis-basic, ligands are required to activate the N_2O molecule.

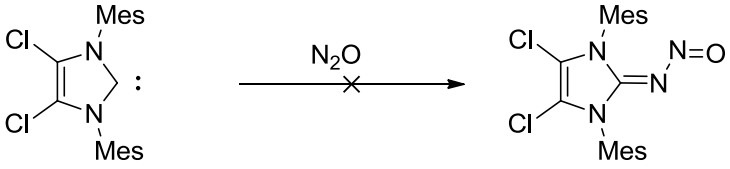

Scheme 5.4.6. The attempted reaction of $IMesCl_2$ and N_2O, that does not give rise to $IMesCl_2 \cdot N_2O$.

All three carbene adducts of $FcB(C_6F_5)_2$, i.e. **3**, **4** and **5**, were also characterized by single-crystal X-ray crystallography as benzene solvates and their structures are shown in Figures 5.4.2 - 5.4.4. A summary of key bond angles (º) and lengths (Å) is included in Table 5.4.4.

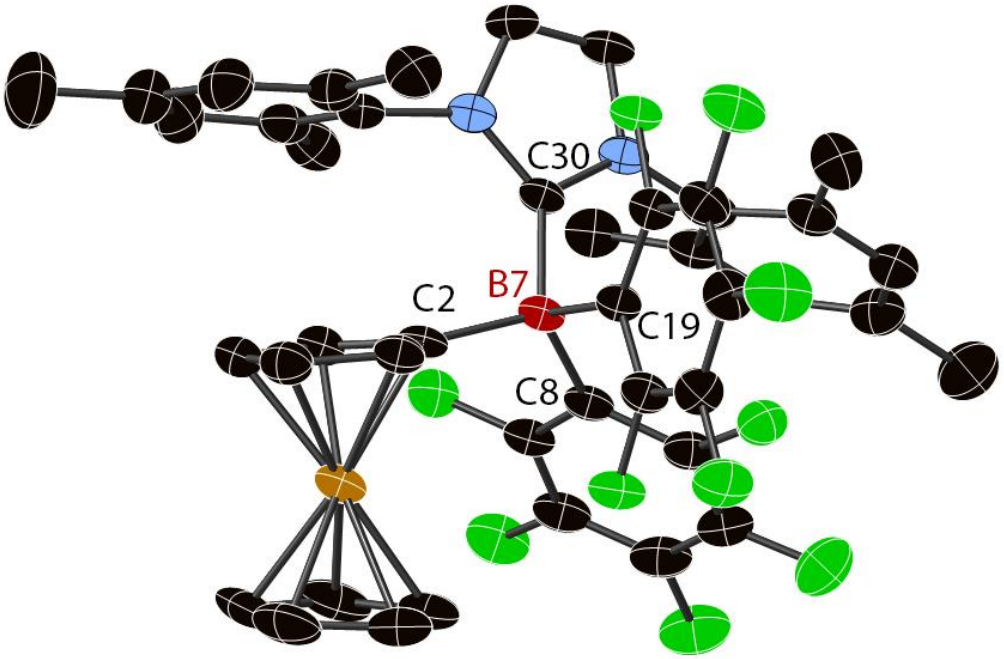

Figure 5.4.2. The molecular structure of IMes·BFc$(C_6F_5)_2$ (**3**). Benzene solvate molecules and hydrogen atoms omitted for clarity. Ellipsoids drawn at the 50% probability level, with boron drawn in maroon, carbon in black, nitrogen in blue, fluorine in green and iron in orange.

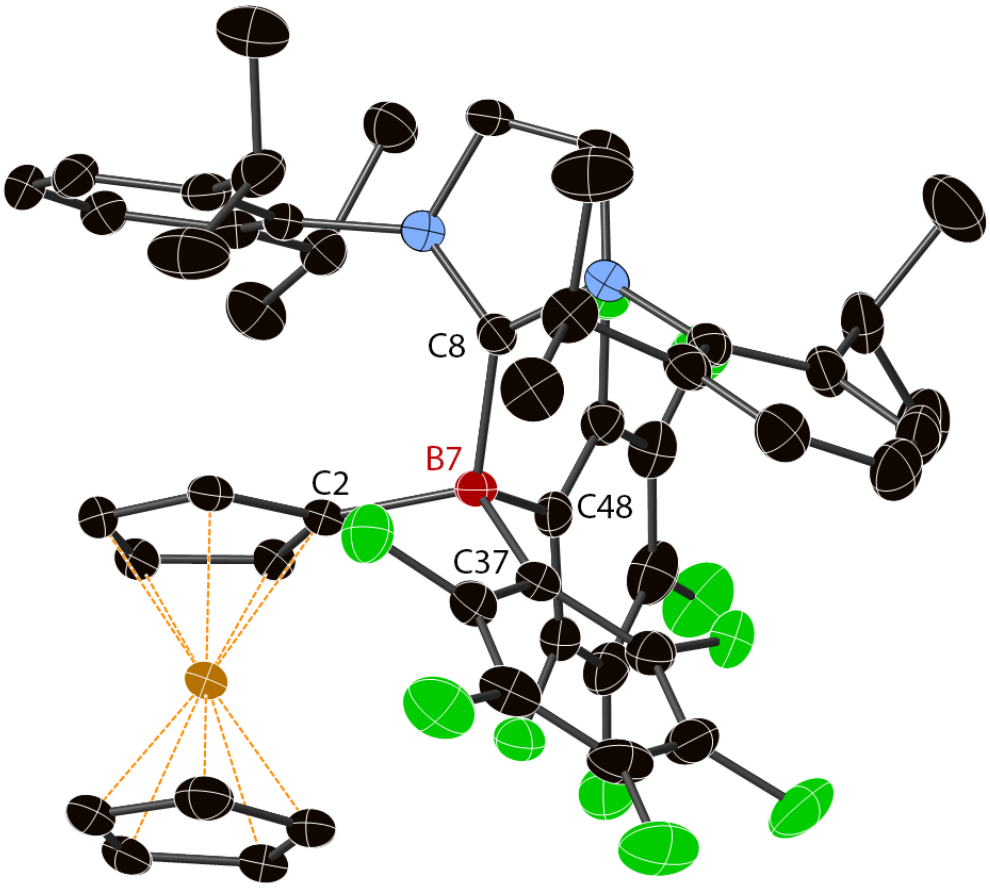

Figure 5.4.3. The molecular structure of IDipp·BFc(C_6F_5)$_2$ (**4**). Benzene solvate molecules and hydrogen atoms omitted for clarity. Ellipsoids drawn at the 50% probability level, with boron drawn in maroon, carbon in black, nitrogen in blue, fluorine in green and iron in orange.

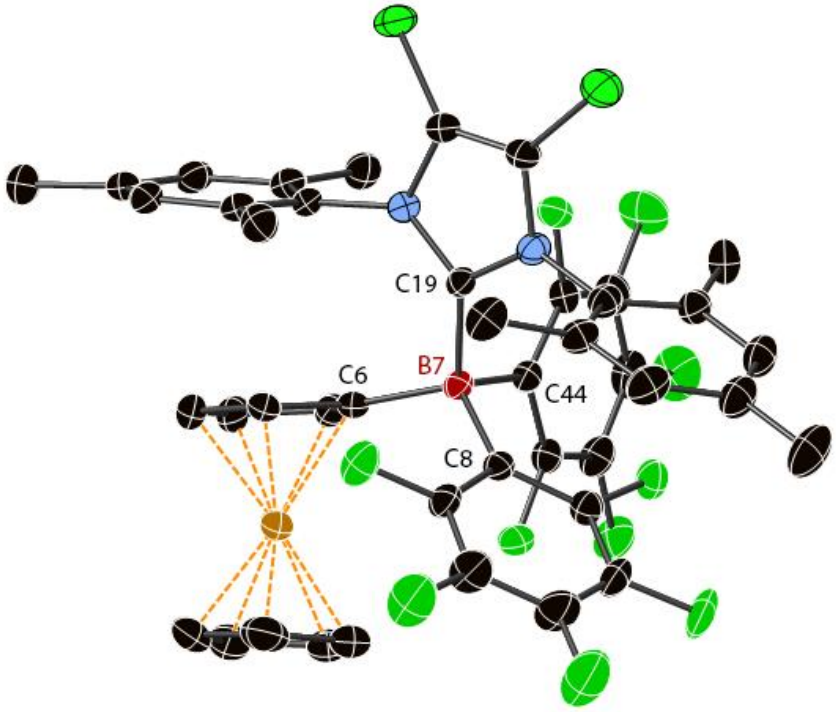

Figure 5.4.4. The molecular structure of IDipp·BFc(C_6F_5)$_2$ (**4**). Benzene solvate molecules and hydrogen atoms omitted for clarity. Ellipsoids drawn at the 50% probability level, with boron drawn in maroon, carbon in black, nitrogen in blue, fluorine in green, chlorine in lime-green and iron in orange.

Compound	B-$C_{Carbene}$ (Å)	B-C_{Aryl}(Å)	B-$C_{Ferrocene}$
FcB(C_6F_5)$_2$ (1) [129]	n/a	1.604(4), 1.584(4)	1.501(4)
FcB(C_6F_5)$_2$·PMe_3 [129]	[B-P: 1.992(9) Å]	1.66(1), 1.64(1)	1.61(1)
IMes·BFc(C_6F_5)$_2$ (3)	1.667(4)	1.668(4), 1.666(4)	1.641(4)
IDipp·BFc(C_6F_5)$_2$ (4)	1.669(3)	1.680(3), 1.672(3)	1.650(3)
IMesCl_2·BFc(C_6F_5)$_2$ (5)	1.679(5)	1.671(5), 1.669(5)	1.647(5)

Table 5.4.4. Key bond lengths of **1** and its adducts.

Analysis of the structures of the three adducts confirms that the boron centres are indeed four coordinate in the solid state with the carbene binding directly to B7 (Figures 5.4.2-5.4.4). The distance from the boron atom to the carbon atom of the carbene in each case is similar, with values of 1.667(4), 1.669(3) and 1.679(5) Å, respectively, which is somewhat surprising given the differences in steric and electronic factors that exist between these NHCs. The boron-carbon bond length to the ferrocenyl substituent is similar for all three adducts **[**1.641(4), 1.650(3) and 1.647(5) Å, respectively] and the boron-carbon bond distances to the perfluoroaryl ligands are also similar (mean values of 1.667, 1.676 and 1.670, respectively) (Table 5.4.2.). The boron-carbon bond lengths determined for **1**, [i.e. 1.501(4) Å to the ferrocenyl substituent and 1.604(4) and 1.584(4) Å to the perfluoroaryl groups, respectively] are shorter than those of the corresponding carbene adducts (**3**, **4** and **5**). This increase in the B-C bond lengths on complexation is ascribed to the greater steric loading and increased coordination number at the boron centre for the adducts. A similar effect is observed on binding of PMe_3 give

$FcB(C_6F_5)_2{\cdot}PMe_3$, which has similar boron-carbon bond distances to those determined for **3** - **5** (Table 5.4.4.). Consistently, the sum of the C_{Aryl}-B-C_{Aryl} and the two C_{Aryl}-B-$C_{Ferrocene}$ angles, Σ(C-B-C), for the carbene adducts **3**, **4** and **5**, as well as for $FcB(C_6F_5)_2{\cdot}PMe_3$ are similar (331, 329, 331 and 330 º, respectively) compared to 359 º for **2** (Table 5.4.5.).

Compound	**C_{Aryl}-B-C_{Aryl} (º)**	**$C_{Ferrocene}$-B-C_{Aryl} (º)**	**Σ(C-B-C) (º)**
$FcB(C_6F_5)_2$ (1) [129]	122.4(2)	118.4(2), 118.0(2)	358.9
$FcB(C_6F_5)_2{\cdot}PMe_3$ [129]	109.8(6)	110.6(6), 109.0(6)	330.0
IMes·$BFc(C_6F_5)_2$ (3)	111.6(2)	114.5(2), 104.7(2)	330.8
IDipp·$BFc(C_6F_5)_2$ (4)	110.1(2)	114.0(2), 105.1(2)	329.1
IMesCl_2·$BFc(C_6F_5)_2$ (5)	112.4(2)	114.7(2), 103.9(3)	331.0
IMes·N_2O·$BFc(C_6F_5)_2$ (2)	108.6(3), 108.0(3)	117.7(4), 108.4(3), 117.6(4), 108.6(3)	334.7, 334.2

Table 5.4.5. Pertinent bond angles of $FcB(C_6F_5)_2$ (**1**) and its adducts. Σ(C-B-C) is the sum of the angles C_{Aryl}-B-C_{Aryl} and C_{Aryl}-B-$C_{Ferrocene}$ and excludes angles to the carbene, where present.

5.4.2. The Reactions of Phosphines, Lewis acids and N_2O

Given that all of the NHCs investigated react with the Lewis acid in the absence of N_2O, we sought to exploit alternative donors such as phosphines as the basic component *in lieu* of the carbene. Given that Piers and coworkers showed that mixing **1** and PMe_3 results in adduct formation,[129] initial work focused on choosing a phosphine with sufficient steric bulk to prevent adduct formation. Guided by the work of Otten and Neu,[122,124] we explored the capacity of PCy_3 and P^tBu_3 to form FLPs with **1**. A one-to-one stoichiometric mixture of the basic and acidic component was made up and analyzed by

NMR spectroscopy. In the case of both the phosphines, no evidence for adduct formation was observed in the ^{1}H, ^{11}B, ^{19}F or ^{31}P NMR spectra.

Having established that these two phosphines do not form adducts with $FcB(C_6F_5)_2$, we sought to explore the capacity of FLP systems comprised of a one-to-one stoichiometric mix of **1** and the corresponding phosphine base to bind and report N_2O. A one-to-one mixture of **1** and PCy_3 in d_6-benzene solution was placed under approximately four atmospheres of N_2O at room temperature. After a period of 24 hours, orange crystals of $Cy_3PO{\cdot}BFc(C_6F_5)_2$ (**6**) had formed in the reaction vessel. These crystals were isolated and analyzed by NMR spectroscopy. The ^{11}B NMR spectrum in d_8-THF exhibits a single broad peak centred at 6 ppm that is indicative of a neutral, four coordinate boron environment. A value of 6 ppm suggests that the moiety bound to boron donates slightly less electron density to the boron centre than does $IMes{\cdot}N_2O$ in $IMes{\cdot}N_2O{\cdot}BFc(C_6F_5)_2$ (Table 5.4.3). The ^{19}F NMR spectrum of the orange crystals further supports the existence of a four-coordinate, neutral borane, with the chemical shift difference between the *meta* and *para* fluorines, $\Delta_{m,p}$ of the C_6F_5 rings, exhibiting a value of 5.7 ppm. The orange colour of the crystalline material, and of solutions of this adduct in C_6H_5F solution (λ_{max} = 450 nm, ε = 60 L mol^{-1} cm^{-1}) also supports the existence of a four coordinate boron centre in both the solid and solution states.

The ^{31}P NMR spectrum in d_8-THF exhibited a single peak at 68.3 ppm. This chemical shift in the ^{31}P spectrum suggests that the phosphorus-containing moiety of this new product is most likely a phosphine oxide, especially when compared to $Cy_3PO{\cdot}B(C_6H_4$-*p*-$F)_3$ (62.6 ppm) and $Cy_3P{\cdot}N_2O{\cdot}B(C_6F_4$-*p*-$H)_3$ (54.4 ppm) (Table 5.4.5.).[122]

Compound	**^{31}P NMR [δ_B (ppm)]**	**^{19}F $\Delta_{m,p}$ [ppm]**	**Reference**
$Cy_3P{\cdot}N_2O{\cdot}B(C_6F_4$-*p*-$H)_3$	54.4	-	[122]
$Cy_3P{=}O{\cdot}B(C_6H_4$-*p*-$F)_3$	62.6	-	[122]
$^t Bu_3P{\cdot}N_2O{\cdot}B(C_6H_4$-*p*-$F)_3$	64.3	-	[122]
$^t Bu_3P{\cdot}N_2O{\cdot}B(C_6F_5)_2Mes$	67.1	4.6	[122]
$Cy_3P{=}O{\cdot}BFc(C_6F_5)_2$	68.3	4.4	n/a
$^t Bu_3P{\cdot}N_2O{\cdot}BFc(C_6F_5)_2$	68.5	5.7	[124]
$^t Bu_3P{\cdot}N_2O{\cdot}B(C_6F_5)_3$	68.5	5.7	[122]
$^t Bu_3P{\cdot}N_2O{\cdot}B(C_6F_5)_2(OC_6F_5)$	69.0	-	[122]

Table 5.4.6. ^{31}P and ^{19}F $\Delta_{m,p}$ values for various perfluorophenyl-substituted boranes.

The hypothesis that the molecule contains the phosphine oxide moiety, Cy_3PO, rather than the $Cy_3P{\cdot}N_2O$ fragment was confirmed by single crystal diffraction studies that were performed on the orange crystals (Figure 5.4.5.). The crystal structure substantiates the supposition that the boron centre is four coordinate in the solid state.

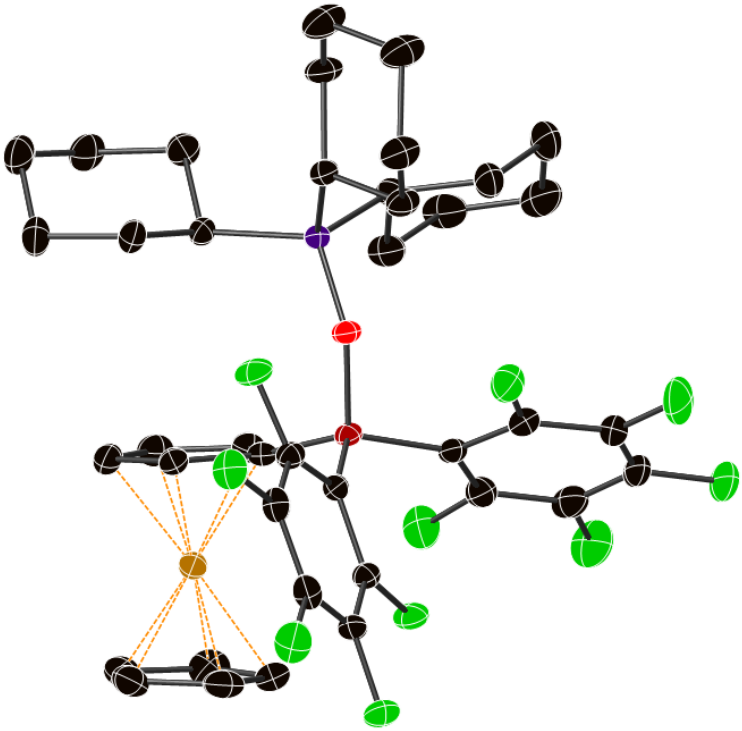

Figure 5.4.5. The molecular structure of $Cy_3PO{\cdot}BFc(C_6F_5)_2$ (**6**). Benzene solvate molecule and hydrogen atoms omitted for clarity. Ellipsoids drawn at the 50% probability level, with boron drawn in maroon, carbon in black, nitrogen in blue, oxygen in red, fluorine in green and iron in orange.

The crystal structure of $Cy_3PO{\cdot}BFc(C_6F_5)_2$ (**6**), as a benzene solvate, allows for the comparison the bond metrics of this system to the related adducts, $Cy_3PO{\cdot}B(C_6H_4\text{-}p\text{-}F)_3$ and $Cy_3P{\cdot}N_2O{\cdot}B(C_6F_4\text{-}p\text{-}H)_3$.[122] The B-O bond length of **6** [1.555(3) Å] is significantly shorter than that of $Cy_3PO{\cdot}B(C_6H_4\text{-}p\text{-}F)_3$ [1.585(2) Å]. This could be interpreted in terms of the decreased steric congestion of **6** allowing for closer approach of the Lewis acid and base moieties. The sum of the C-B-C angles around the boron centre is 339.4 º for **6**,

slightly lower than the value of 333.6 º for $Cy_3PO{\cdot}B(C_6H_4$-*p*-$F)_3$, which suggests that compound **6** bears slightly less steric congestion around the boron centre.

Bond/Angle	**$Cy_3PO{\cdot}BFc(C_6F_5)_2$**	**$Cy_3PO{\cdot}B(C_6H_4$-*p*-$F)_3$**	**$Cy_3P{\cdot}N_2O{\cdot}B(C_6F_4$-*p*-$H)_3$**
B-$C_{aryl/alkyl}$	1.651(3), 1.659(3)	1.626(2), 1.626(2), 1.631(2)	1.645(3), 1.644(3), 1.633(3)
B-C_{Fc}	1.607(3)	-	-
B-O	1.555(3)	1.585(2)	1.551(1)
P-O	1.523(2)	1.5251(8)	-
P-N	-	-	1.715(2)
P-C	1.817(2), 1.828(2), 1.815(2)	1.815(1), 1.820(1), 1.832(1)	1.803(2), 1.815(2), 1.825(2)
N-N	-	-	1.260(2)
N-O	-	-	1.335(2)
B-O-P	149.1(1)	147.26(8)	-
Σ(C-B-C)	339.4	333.6	336.1
Σ(C-P-C)	328.0	325.5	336.6
P-N-N	-	-	111.1(1)
N-N-O	-	-	111.1(1)
N-O-B	-	-	110.3(1)

Table 5.4.6. Pertinent bond lengths (Å) and angles (º) of $Cy_3PO{\cdot}BFc(C_6F_5)_2$, $Cy_3P{=}O{\cdot}B(C_6H_4$-*p*-$F)_3$[122] and $Cy_3P{\cdot}N_2O{\cdot}B(C_6F_4$-*p*-$H)$[122].

The proposed mechanism by which $Cy_3PO{\cdot}BFc(C_6F_5)_2$ (**6**) forms is the same as that proposed by Stephan and coworkers in the reaction of Cy_3P and $B(C_6H_4$-*p*-$F)_3$ with N_2O. Cy_3P slowly reacts with N_2O to form the short-lived adduct $Cy_3P{\cdot}N_2O$. Unlike with the more Lewis acidic boranes, such as $B(C_6F_4$-*p*-$H)_3$, the $Cy_3P{\cdot}N_2O$ adduct is not irreversibly trapped at this stage. Instead, loss of N_2 occurs to give Cy_3PO. This new

Lewis base, Cy_3PO, is not sufficiently sterically demanding to preclude adduct formation, and forms a bond to the boron atom of **1**.

In theory, the FLP system comprising **1** and Cy_3P is capable of colorimetrically reporting the presence of N_2O, as the adduct formed is orange and **1** itself is red. The limitations of using this FLP mixture as a detection protocol for N_2O include the fact that the oxidation of Cy_3P to Cy_3PO by N_2O is slow (90 % complete in 24 h),[122] and that the oxidation of Cy_3P to Cy_3PO can be afforded by several other oxidants. A further complication is the long term stability of the FLP mixture in solution (*vide infra*).

When a one-to-one stoichiometric solution of Cy_3P and **1** in d_6-benzene was left to stir for 10 d, a brown oil was seen to form. This was isolated, taken up in d_1-chloroform and layered with hexanes. The resulting orange crystals were analyzed by single crystal X-ray diffraction in the solid state and by ^{1}H, ^{11}B, ^{19}F and ^{31}P NMR spectroscopy in *d*-chloroform solution. The crystal structure shows that the orange crystals were a chloroform solvate of the zwitterionic species $FcB(F)(C_6F_5)(C_6F_4$-*p*-$PCy_3)$ (**7**) (Figure 5.4.5.). That this structure is retained in solution is supported by the ^{1}H, ^{11}B, ^{19}F and ^{31}P NMR spectra. The ^{11}B NMR spectrum exhibits a broad signal centred at 2 ppm, which is typical of a four coordinate boron centre, especially for a compound containing a fragment such as $[FcB(F)Ar_2]^-$. The coupling to the boron-bound fluorine could not be unambiguously resolved in the ^{11}B NMR spectrum, however the signal did sharpen noticeably on ^{19}F decoupling. The resonances seen in the ^{19}F NMR spectrum are also consistent with the crystal structure, with the resonance at -193.7 ppm, a partially collapsed quartet, strongly suggesting that the fluoride remains bound to the boron centre

on dissolving the crystals in *d*-chloroform. The peak at +39.9 ppm in the ^{31}P NMR spectrum is fully consistent with a positively charged, four coordinate phosphonium centre.

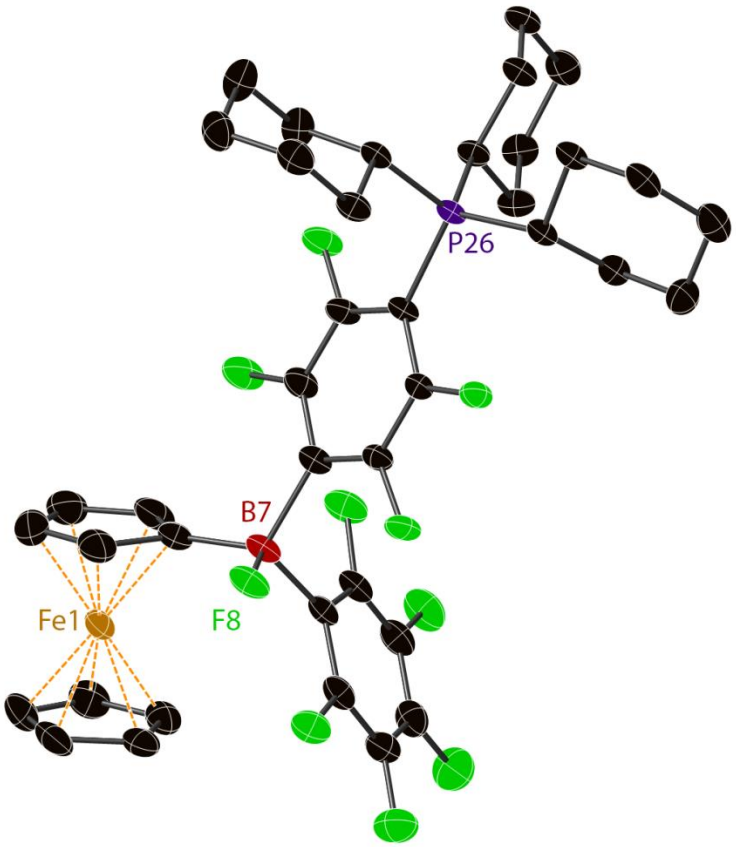

Figure 5.4.5. The molecular structure of FcB(F)(C_6F_5)(C_6F_4-*p*-PCy_3) (**7**). Chloroform solvate molecule and hydrogen atoms omitted for clarity. Ellipsoids drawn at the 50% probability level, with boron drawn in maroon, carbon in black, phosphorus in purple, fluorine in green and iron in orange.

Bond/Angle	**$Cy_3PO{\cdot}BFc(C_6F_5)_2$ (6)**	**$FcB(F)(C_6F_5)(C_6F_4$-*p*-$PCy_3)$ (7)**
B-F	-	1.426(2)
B-O	1.555(3)	-
B-C_{aryl}	1.651(3), 1.659(3)	1.660(3), 1.682(3)
B-C_{Fc}	1.607(3)	1.613(3)
P-C_{alkyl}	1.815(2), 1.817(2), 1.828(2)	1.829(2), 1.829(2), 1.831(2)
P-C_{aryl}	-	1.824(2)
Σ(C-B-C)	339	332
Σ(C_{alkyl}-P-C_{alkyl})	328	331

Table 5.4.9. Pertinent bond lengths (Å) and angles (º) of $Cy_3PO{\cdot}BFc(C_6F_5)_2$ (**6**) and $FcB(F)(C_6F_5)(C_6F_4$-*p*-$PCy_3)$ (**7**).

The B-F bond distance from the crystal structure **7** [1.426(2) Å], is shorter than that of the related complex [(18-crown-6)K][$FcB(F)(Tol)_2$] [1.481(3) Å].[127] This can be attributed to the increased Lewis acidity of the putative free Lewis acid $[FcB(C_6F_5)(C_6F_4$-*p*-$PCy_3)]^+$ compared to $FcB(Tol)_2$, which should therefore result in a stronger B-F bond. The degree of pyramidalization around the boron atom of **7** is slightly greater than that of the Cy_3PO adduct **6**, with the sums of C-B-C angles being 332 and 339 º respectively. If steric factors alone were considered this might be a surprising result, as F^- is a much smaller donor. When the electronic factors are considered it should be evident that the anionic F^- is a stronger electron donor than the neutral Cy_3PO, and so should drive a greater degree of pyramidalization.

The mechanism by which FcB(F)(C_6F_5)(C_6F_4-*p*-PCy_3) (**7**) is formed was not systematically investigated. It is conceivable that the reaction proceeds *via* a nucleophilic, aromatic substitution reaction (S_NAr). In a S_NAr type mechanism, the phosphine would nucleophilically attack at the *para* position of one of the two C_6F_5 rings, forming a Wheland intermediate (stabilized by the electron withdrawing fluorines), followed by ejection of a fluoride anion, which would be taken up at boron to give FcB(F)(C_6F_5)(C_6F_4-*p*-PCy_3) (**7**).

5.4.3. The Effect of Increased Lewis Acidity

The inability of a system comprised of **1** and Cy_3P to trap an intact N_2O fragment quickly limited its utility as a selective N_2O detector. Further, the reaction of **1** with Cy_3PO limits the selectivity of this N_2O detection system over other oxidizing agents. It was therefore of interest to explore ferrocenyl apinged boranes that were both a stronger Lewis acid than **1**, so as to trap an intact N_2O moiety, and also more sterically demanding, so as to preclude adduct formation with phosphine oxides. Given the work of Ashley *et al.* exploring the reactivity of $B(C_6F_5)_x(C_6Cl_5)_y$ ($x + y = 3$), , we sought to synthesize the related system, $FcB(C_6Cl_5)_2$.[142]

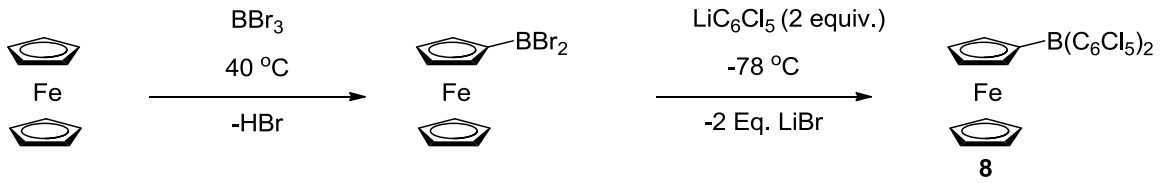

Scheme 5.4.7. Proposed synthetic route to $FcB(C_6Cl_5)_2$ (**8**).

Early attempts to synthesis the novel borane $FcB(C_6Cl_5)_2$ (**8**) sought to treat $FcBBr_2$ with two equivalents the C_6Cl_5Li in an analogous fashion to our synthesis of $FcB(C_6F_5)_2$ as outlined in Scheme 5.4.7. As with the reaction of $FcBBr_2$ with C_6F_5Li, we sought to find conditions that maximized the rate of salt elimination to give our target material over the rate of decomposition of the lithiated species. The lithiated perchloroaryl species, LiC_6Cl_5, starts to decompose at temperature exceeding -30 ºC in hexane solution, which is accompanied by a darkening of the colour of the solution. Under all reaction conditions screened, a mixture of $FcBBr_2$, $FcB(C_6Cl_5)Br$ (**9**) and $FcB(C_6Cl_5)_2$ (**8**) was obtained as is shown in Scheme 5.4.8 (if diethyl ether was used as a solvent, the diethyl ether adducts of **8** and **9** were also observed). That the reaction of $FcBBr_2$ with LiC_6F_5 proceeds without issue, but the reaction with LiC_6Cl_5 does not, is ascribed to steric effects. All attempts to separate **8** from **9** proved fruitless. Attempts to selectively recrystallize one product resulted in co-precipitation. Air-sensitive column chromatography could not adequately separate the two compounds **8** and **9**.

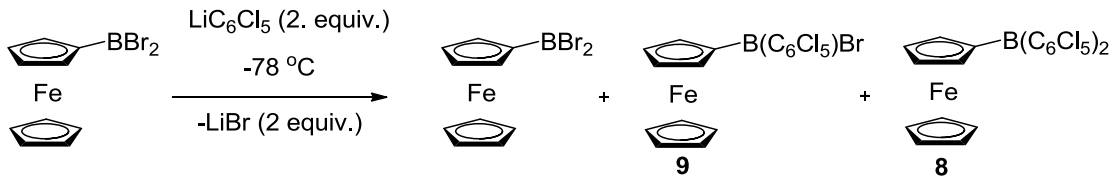

Scheme 5.4.8. Reaction of $FcBBr_2$ with LiC_6Cl_5 to give $FcB(C_6Cl_5)_2$ (**8**) and $FcB(C_6Cl_5)Br$ (**9**).

An early hypothesis was that the target material **8** had decomposed thermally. The basis for this hypothesis was that addition of LiC_6Cl_5 to a suspension of $FcBBr_2$ at -78 ºC did not immediately lead to a colour change from red; on warming a change to a deep

maroon colour was observed at approximately -40 ºC, and a final colour change to a deep purple material at approximately -10 ºC. It was assumed that the target material **8** was maroon in colour, and decomposition was occurring at -10 ºC. Therefore, the reaction mixture was brought to -40 ºC, held there for one hour, cooled to -78 ºC and a maroon solid isolated by filtration. This solid was dried under a flow of argon. The material exploded violently when evacuated. The conclusion was made that unreacted LiC_6Cl_5 had been isolated, along with $FcBBr_2$ and **9**, and that LiC_6Cl_5 had detonated upon being placed under reduced pressure.

Reaction of $FcBBr_2$ with only one equivalent of LiC_6Cl_5, followed by work up, gave $FcB(C_6Cl_5)Br$ (**9**) selectively as a maroon solid in good yield (90-95%). The ^{1}H, ^{11}B and ^{13}C NMR spectra are fully consistent with this formulation. Mass spectrometry and elemental analysis confirmed the identity and purity of this compound. Moreover, refluxing **9** with one equivalent of LiMes gave the product $FcB(C_6Cl_5)Mes$ (**10**), as shown in Scheme 5.4.9. After work-up, compound **10** was isolated in moderate yield (35-45%) as a maroon solid. The ^{11}B NMR spectrum exhibits a broad peak at 72 ppm, upfield of $FcBMes_2$ as would be expected for the more electron deficient boron centre in **10**. The ^{1}H and ^{13}C NMR spectra are fully consistent with this structure. The identity of **10** was further confirmed by mass spectrometry.

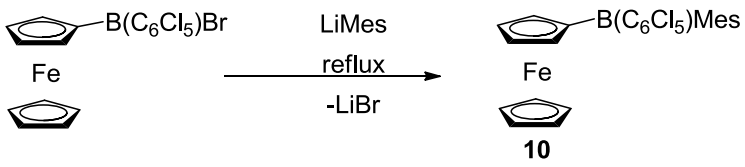

Scheme 5.4.9. Synthetic route to $FcB(C_6Cl_5)Mes$ (**10**).

An alternative pathway to the target compound **8** was therefore sought, as shown in scheme 5.4.10. This pathway required the synthesis of $ClB(C_6Cl_5)_2$ following the work of Ashley *et al*[142] and the synthesis of FcLi by a modified procedure described by Bildstein and coworkers[130]. A difficulty encountered in the reaction of FcLi and $ClB(C_6Cl_5)_2$ was the reaction of the lithiate with a C-Cl bond rather than with the B-Cl bond. This unwanted side reaction was encountered when both compounds were mixed as solutions at -78 ºC and warmed to room temperature slowly. This side reaction could be minimized however by adding FcLi as a powder to a benzene solution of $ClB(C_6Cl_5)_2$ at 6 ºC. After work up, $FcB(C_6Cl_5)_2$ (**8**) could be isolated as a purple solid in low yields (25-30%).

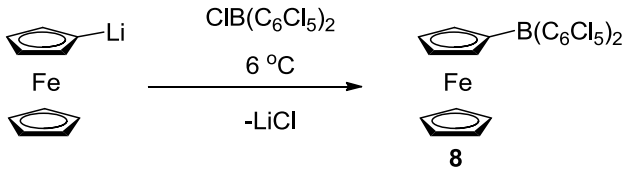

Scheme 5.4.10. Synthetic route to $FcB(C_6Cl_5)_2$ (**8**).

The ^{11}B NMR spectrum of FcB(C_6Cl_5) (**8**) in d_6-benzene exhibited a broad peak at 60 ppm, significantly upfield of FcB(C_6Cl_5)Mes (**10**) (72 ppm). It is of note that the ^{11}B NMR shift is *downfield* of FcB(C_6F_5)$_2$ (**1**) (53 ppm), suggesting that **1** is more electron deficient than **8**. The ^{1}H and ^{13}C NMR spectra are fully consistent with the structure of **8**, with further confirmation of identity and purity being obatained from mass spectrometry and elemental analysis, respectively. The structure in the solid state was determined by single crystal X-ray crystallography as shown in Figure 5.4.7.

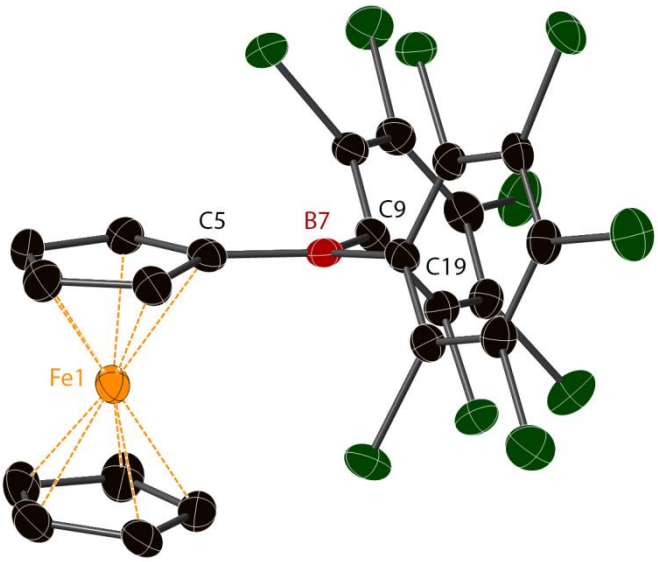

Figure 5.4.7. The molecular structure of FcB(C_6Cl_5)$_2$ (**8**); the hydrogen atoms omitted for clarity. Ellipsoids drawn at the 50% probability level, with boron drawn in maroon, carbon in black, chlorine in dark green and iron in orange.

The crystal structure of **8** is similar to that of **1**. Both systems are essentially planar around the boron atom, with the sum of the angles around boron (C-B-C) being 358.9 º for

1 and 359.8 º for **8**. The B-C bonds to the aryl groups are not significantly different between **1** and **8**. The molecular structure of **1**, however, exhibits a noticeable dip of the boron toward the iron, which Piers and coworkers ascribe to partial electron donation from the iron to the highly electron deficient boron centre.[129] This is manifested in the short Fe-B bond distance of 2.924 for **1**; by contrast that in **8** is much longer at 3.191(3). Thus, there is no evidence for a Fe→B donor/acceptor formulation for **8** as has been suggested for **1**. These differences can be ascribed primarily to steric factors, with the bulkier pentachlorophenyl substituents of **8** preventing any structurally significant interaction between the Fe(II) and the boron centre.

Bond/Angle	**$FcB(C_6F_5)_2$ (1)**	**$FcB(C_6Cl_5)_2$ (8)**
$B\text{-}C_{aryl}$	1.604(4), 1.584(4)	1.610(4), 1.610(4)
$B\text{-}C_{Fc}$	1.501(4)	1.517(5)
B-Fe	2.924	3.191(3)
$C_{aryl}\text{-}B\text{-}C_{aryl}$	118.4(2)	118.5(2)
$C_{aryl}\text{-}B\text{-}C_{Fc}$	118.0(2), 122.5(2)	120.0(3), 121.3(3)
Σ(C-B-C)	358.9	359.8

Table 5.4.10. Key bond lengths (Å) and angles (º) of $FcB(C_6F_5)_2$ (**1**)[129] and $FcB(C_6Cl_5)_2$ (**8**).

5.4.4. Probes of the Relative Electron Deficiency and Lewis Acidity of $FcB(C_6Cl_5)_2$

The electrochemistry of **8** was investigated and compared to that of **1**. Due to the air and moisture sensitive nature of both **1** and **8**, the cyclic voltammetry measurements had to be carried out in a glove box under inert atmosphere. The standard $[^nBu_4N][PF_6]$ electrolyte had already been shown by Piers *et al.* to react with **1**,[129] so dry $[^nBu_4N][B(C_6F_5)_4]$ was employed as the electrolyte. Reproducible results could be obtained in fluorobenzene solution, although voltammograms were clearer for the same concentration in *α,α,α*-trifluoro-toluene. Consistent with the findings of Ashley and coworkers for $B(C_6X_5)_3$ (X = F, Cl), the C_6Cl_5 substituent was found to be more electron withdrawing than its perfluorophenyl analogue.[142] Accordingly, the oxidation potential of the pendant ferrocenyl groupin **1** is +450 mV (*cf.* FcH/FcH^+), whereas that in **8** is +550 mV (*cf* . FcH/FcH^+). The borane **8** is therefore shown to be intrinsically more electron deficient than **1**.

A quantitative empirical parameter for comparing the electrophilic properties of Lewis acids is the acceptor number (A.N.) as outlined by Gutmann and co-workers.[143] This method, subsequently modified by Adamczyk-Wozniak and co-workers,[144] involves adding 0.33 equivalents of Et_3PO to the Lewis acid and analying the resulting ^{31}P NMR spectrum. The ^{31}P chemical shift is dependent on the position of equilibrium between the complex and the uncomplexed phosphine [Lewis Acid + Et_3PO $\rightleftharpoons$ Adduct] (Scheme 5.4.11). The acceptor number is calculated using the chemical shift of complex ($\delta_{complex}$) using the following formula:

$$A.N. = [(\delta_{complex} - \delta_1) / (\delta_2 - \delta_1)] \times 100$$

where δ(1) and δ(2) are the ^{31}P NMR chemical shifts of Et_3PO in hexane (41.0 ppm) and with $SbCl_5$ (86.1 ppm). Assuming no steric effects, the more electrophilic a Lewis acid, the higher the A.N. value should be.

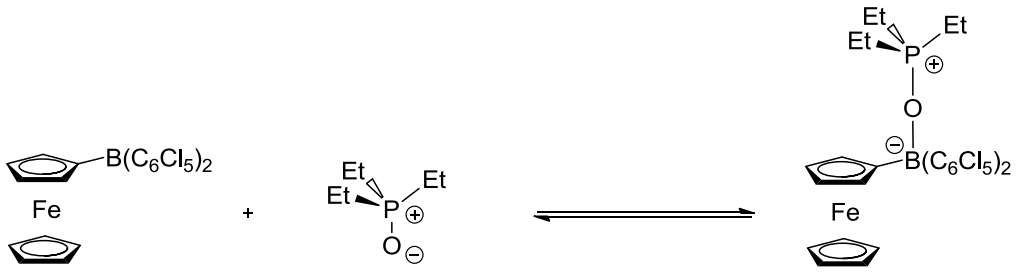

Scheme 5.4.11. Equilibrium that underpins the Gumann method for determining the acceptor number (A.N.). The further the equilibrium lies to the right, the higher the A.N.

In addition to the electrochemical quantification of the electron deficiency of the boranes **1** and **8**, the Adamczyk-Wozniak modified Gutmann-Beckett method was used to determine the relative Lewis acidity of these two boranes[144] The resultant acceptor numbers for the boranes **1** and **8** were 71.9 and 81.0 respectively. Comparing the acceptor number of the borane **1** (A.N. = 71.9) to that of the related borane $B(C_6F_5)_3$ (78.2), suggests that the more electron rich nature of the ferrocenyl group lowers the Lewis acidity of the borane relative to a C_6F_5 substituent, and could be considered addtional proof of Piers postulated Fe→B interaction being retained in solution.[129] The more strongly electron withdrawing perchloroaryl substituents of **8**, in combination with the absence of an observable Fe→B interaction, would be expected to render **8** more Lewis

acidic then **1**, which is borne out by the acceptor numbers obtained with our particular probe (Et_3PO).

The related boranes $B(C_6F_5)_3$ and $B(C_6Cl_5)_3$ exhibit the same trend in their reduction potentials as **1** and **8**, however it was shown that only $B(C_6F_5)_3$ was capable of binding Et_3PO in d_2-dichloromethane.[142] This was ascribed to the greater steric demands of the perchlorinated borane dominating over electronic factors.[142] It is therefore presumed that the reduced steric demands of the ferrocenyl substituent (*cf.* C_6Cl_5) allow for complexation of Et_3PO by **8**, and highlight the complexity of disambiguation between steric and electronic factors on Lewis acidity and the importance of the steric demands of the probe molecule (crotonaldehyde/Et_3PO/$^tBu_3PO$).

5.4.5. The Capacity of Novel Ferrocenyl Boranes to form FLPs

Having synthesised a range of Lewis acidic boranes, $FcBMes_2$ (**11**), $FcB(C_6Cl_5)Mes$ (**10**) and $FcB(C_6Cl_5)_2$ (**8**), we sought to explore their chemistry and their capacity to form FLP systems with phosphines. On replacing mesityl (Mes) groups with perchlorophenyl (C_6Cl_5) substituents the Lewis acidity would be expected to increase. That borane does indeed become more electron deficient as the number of perchlorophenyl groups increases is borne out in the ^{11}B NMR spectra, with the signals shifting from 82 ppm for **11**, to 72 ppm for **10**, and 60 ppm for **8**. On increasing the number of perchlorophenyl groups the wavelength corresponding to the maximum absorption intensity in the UV-vis spectrum (λ_{max}) undergoes a red shift, with values of 507 nm, 529 nm and 545 nm for **11**, **10** and **8** respectively (Figure 5.4.8.). This shift to

lower wavelength would correspond to a smaller transition energy. For $FcBMes_2$, this absorption band has been ascribed to excitation of electrons to a molecular orbital bearing a large contribution from the formally vacant p orbital at boron.[145,146] The more electron-withdrawing are the groups attached to boron, the lower in energy this orbital would be expected to be. Thus the LUMO would be expected to be at a sequentially lower energy for **10** and **8**, and hence a longer wavelength (lower energy) would be associated with this transition.

The acceptor numbers for compounds **11**, **10** and **8** are 11.5, 12.0 and 81.0 respectively. As the number of perchlorophenyl groups increases there is a corresponding increase in the A.N., however the increase is not gradual and the value for **10** seems abnormally low. This is ascribed to steric factors dominating over electonic factors. As mesityl groups are replaced with perchlorophenyl groups, the Lewis acidity increases, but the steric crowding falls. We hypothesise that mesityl-containing Lewis acids are too sterically demanding for facile adduct formation with Et_3PO.

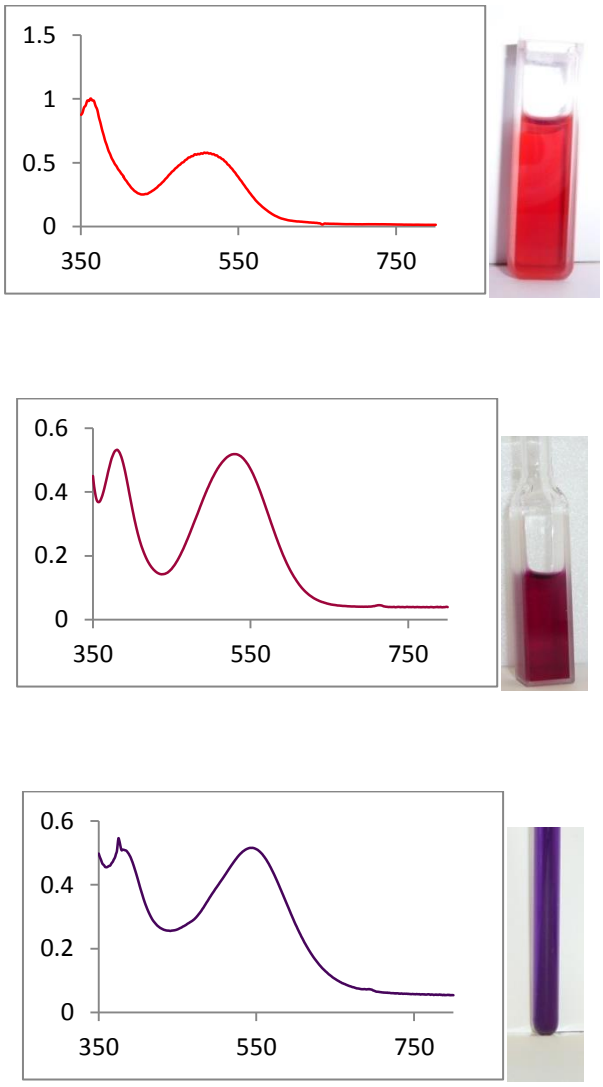

Figure 5.4.8. UV-Vis Spectra of $FcBMes_2$ (top left), $FcB(C_6Cl_5)Mes$ (**10**) (top right) and $FcB(C_6Cl_5)_2$ (**8**) in fluorobenzene solution. Vertical scale corresponds to absorbance (a.u.) and the horizontal scale corresponds to wavelength (nm). Photographs of the three compounds in fluorobenzene solution (*ca.* 1.3 mM) in the bottom right, from left to right: $FcBMes_2$, $FcB(C_6Cl_5)Mes$ (**8**) and $FcB(C_6Cl_5)_2$ (**10**).

$FcBMes_2$ (**11**), $FcB(C_6Cl_5)Mes$ (**10**) and $FcB(C_6Cl_5)_2$ (**8**) were also screened for their ability to form FLPs with $^tBu_3P$ by adding one equivalent of $^tBu_3P$ to the Lewis acid and analysing the mixture by ^1H, ^{11}B and ^{31}P NMR spectroscopy (Scheme 5.4.12.). All three Lewis acids formed an FLP with $^tBu_3P$, as evidenced by unchanged ^1H, ^{11}B and ^{31}P NMR spectra.

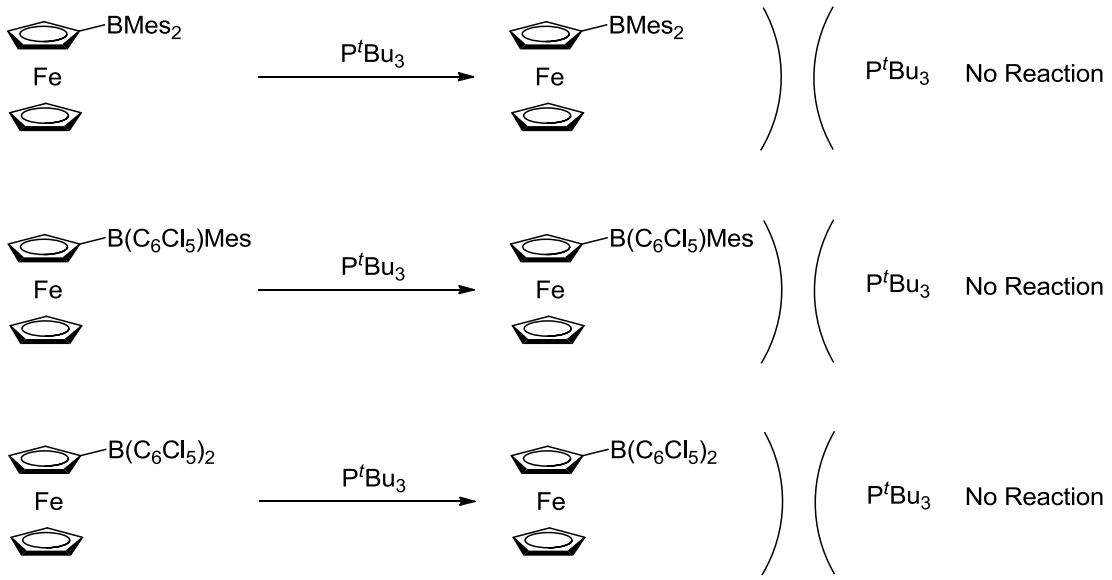

Scheme 5.4.12. Behaviour of the Lewis acids $FcBMes_2$ (**11**), $FcB(C_6Cl_5)Mes$ (**10**) or $FcB(C_6Cl_5)_2$ (**8**) in the presence of P^tBu_3.

5.4.6. Reactions of N_2O and the Novel FLP Mixtures

Given that all three Lewis acids form FLPs with $^{t}Bu_3P$, we then treated a one-to-one stoichiometric mixture of each Lewis acid and $^{t}Bu_3P$ with N_2O (Scheme 5.4.13.). In all three cases, the phosphine was slowly oxidized by the N_2O to phosphine oxide over a period of approximately 12 h. As might be expected from the acceptor number determination [in which the interplay of steric and electronic effects resulted in only $FcB(C_6Cl_5)_2$ forming a strong adduct with Et_3PO], only $FcB(C_6Cl_5)_2$ formed an adduct with $^{t}Bu_3PO$. This was evidenced by new signals in the ^{1}H, ^{11}B and ^{31}P NMR spectra, with a peak (δ_B = 24 ppm) indicative of a neutral, four coordinate borane with one weakly bound substituent. No single crystals could be grown of this material, nor could the adduct be observed by mass spectroscopy. Its identity as $^{t}Bu_3PO{\cdot}BFc(C_6Cl_5)_2$ was, however, inferred by reacting **8** with one equivalent of independently synthesised $^{t}Bu_3PO$ to give an identical product by ^{1}H, ^{11}B and ^{31}P NMR spectroscopy.

The reaction of $FcB(C_6Cl_5)_2$ (**8**) and $^{t}Bu_3P$ with N_2O proceeds with a gradual lightening in colour from a dark purple to a light yellow solution (Figure 5.4.9-10). The colour of **8** is thought to primarily arise from absorption involving a boron centred LUMO. On accepting a pair of electrons from a donor, such as that from $^{t}Bu_3PO$, the former LUMO is now filled; it is therefore no longer possible to excite electrons to this orbital, resulting in the quenching of the colour. The colour change is however too slow for practical use as a N_2O detector (4 hours).

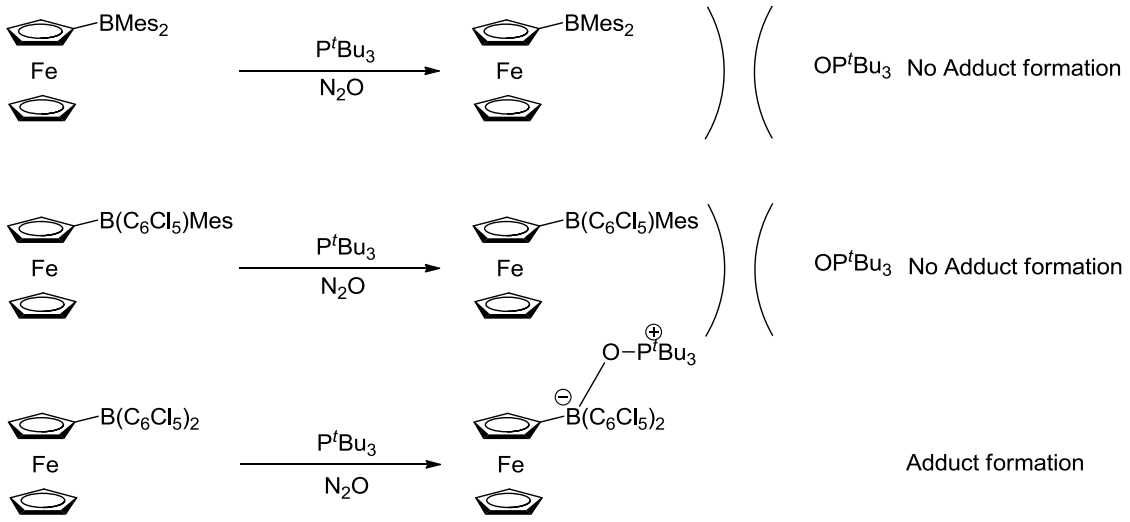

Scheme 5.4.13. Reactions to test if FLP systems comprised of the Lewis acids $FcBMes_2$ (**11**), $FcB(C_6Cl_5)Mes$ (**10**) or $FcB(C_6Cl_5)_2$ (**8**) and $^tBu_3P$ could report the presence of N_2O.

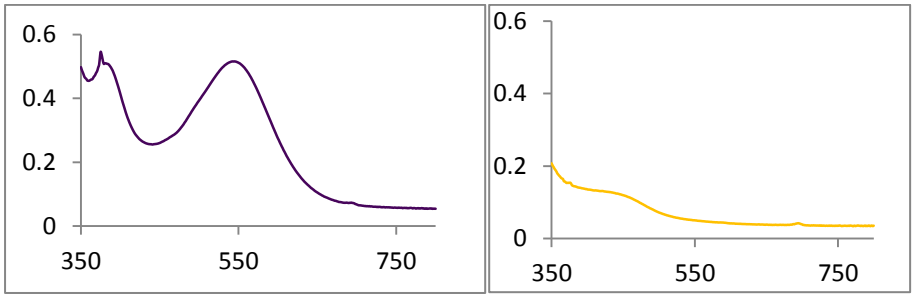

Figure 5.4.9. UV-Vis spctra of $FcB(C_6Cl_5)_2$ (**8**) (left) and $^tBu_3PO{\cdot}BFc(C_6Cl_5)Mes$ (**12**) (right). Vertical scale corresponds to absorbance (a.u.) and the horizontal scale corresponds to wavelength (nm).

The FLP system comprised of $FcB(C_6Cl_5)_2$ (**8**) and $^tBu_3P$ is therefore able to report the presence of N_2O, but it does so only slowly, and cannot discriminate from other oxidants capable of oxidizing $^tBu_3P$ to $^tBu_3PO$. $FcB(C_6Cl_5)_2$ (**8**) was originally synthesised as it was thought that it might be a more electrophilic, and hence stronger, Lewis acid than $FcB(C_6F_5)_2$ (**1**). The ^{11}B NMR spectra and the single crystal X-ray diffraction data suggested that the reverse was in fact true. As the work of Neu *et al* suggested that the higher the Lewis acid strength is, the more likely an intact N_2O fragment is to be trapped, the Lewis acid $FcB(C_6F_5)_2$ (**1**) was re-explored with $^tBu_3P$ as the base in a FLP system.

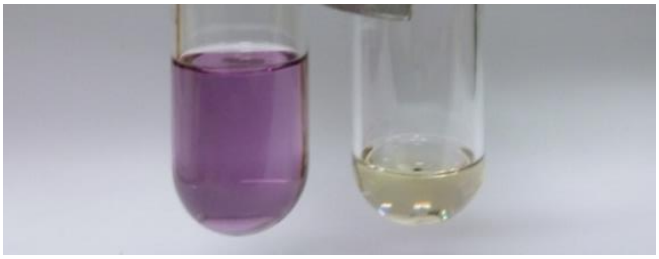

Figure 5.4.10. A 1 mMol solution of $FcB(C_6Cl_5)_2$ (**8**) and $^tBu_3P$ before treatment with N_2O (left) and after (right).

5.4.7. $FcB(C_6F_5)_2$ and $^tBu_3P$ as a Competent N_2O Reporter System

A stoichiometric combination of $FcB(C_6F_5)_2$ (**1**) and $^tBu_3P$ in fluorobenzene was treated with approximately 4 atmospheres of N_2O and stirred for 12 h (Scheme 5.4.14.). The solution changed colour from a dark maroon to orange. The resulting ^{11}B NMR spectrum exhibits a broad peak at 3 ppm typical of a four coordinate borane. The ^{19}F NMR spectrum is also consistent with a four coordinate borane, with a $\Delta_{m,p}$ value of 4.0 ppm. Thus the ^1H, ^{13}C and ^{31}P NMR spectra are fully consistent with the formation of an

adduct containing $^{t}Bu_3P$ and $FcB(C_6F_5)_2$ fragments. Moreover mass spectroscopy and single crystal X-ray crystallography reveal that N_2O has been trapped intact within the adduct $^{t}Bu_3P{\cdot}N_2O{\cdot}BFc(C_6F_5)_2$ (**12**). (Figure 5.4.11.).

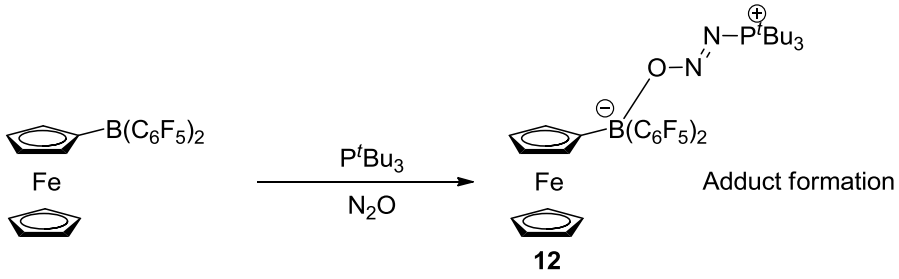

Scheme 5.4.14. Reaction of $FcB(C_6F_5)_2$ and $^{t}Bu_3P$ with N_2O to give the adduct $^{t}Bu_3P{\cdot}N_2O{\cdot}BFc(C_6F_5)_2$.

The crystal structure of $^{t}Bu_3P{\cdot}N_2O{\cdot}BFc(C_6F_5)_2$ (**12**) clearly exhibits the gullwing, or *trans-trans* coordination motif of the PNNOB moiety (Figure 5.4.11.), closely matching the related $^{t}Bu_3P{\cdot}N_2O{\cdot}B(C_6F_5)$ adduct of Stephan and co-workers.[124] The bond distances for the P-N, N-N, N-O and N-B bonds of **12** [1.692(3), 1.251(3), 1.329(3) and 1.543(4) Å respectively] are similar to those of $^{t}Bu_3P{\cdot}N_2O{\cdot}B(C_6F_5)$, which has corresponding values of 1.7087(12), 1.2573(15), 1.3362(15) and 1.5428(18) Å. The bond angles of **12** for the P-N-N, N-N-O and N-O-B units are 118.1(2), 110.5(2) and 112.7(2) º respectively and are also similar to those of $^{t}Bu_3P{\cdot}N_2O{\cdot}B(C_6F_5)$ (117.04(10), 109.11(11) and 114.43(10) º respectively). This suggests that the dominant resonance contribution is that featuring a double bond between the two nitrogen atoms as shown in Scheme 5.4.14.

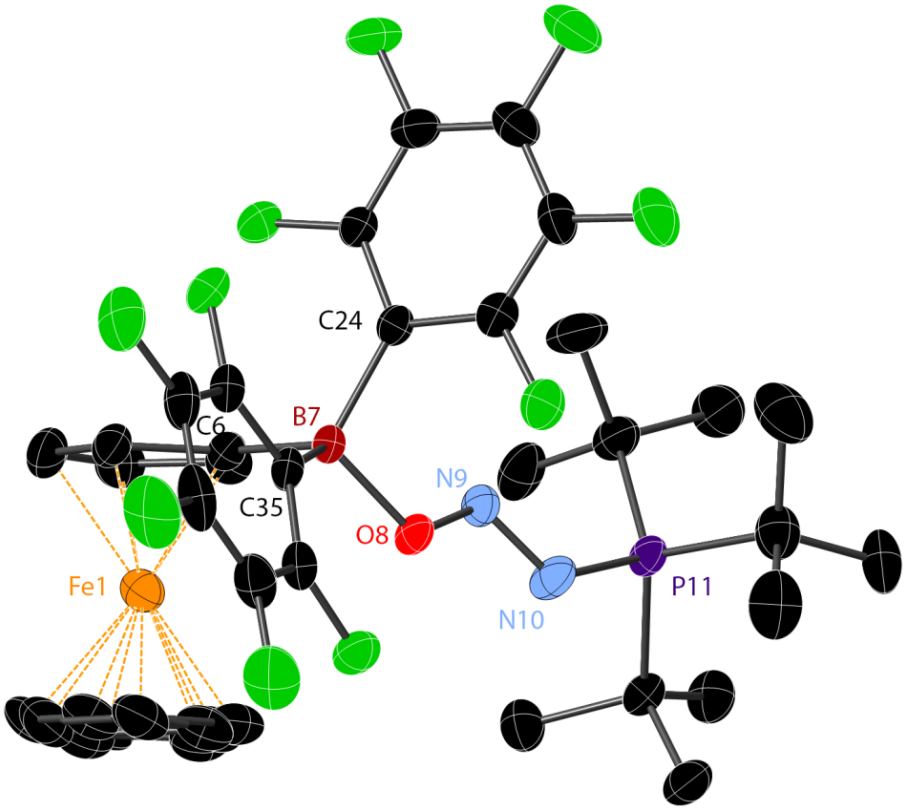

Figure 5.4.15. The molecular structure of $^{t}Bu_3P{\cdot}N_2O{\cdot}BFc(C_6F_5)_2$ (**12**); the hydrogen atoms omitted for clarity. Ellipsoids drawn at the 50% probability level, with boron drawn in maroon, carbon in black, nitrogen in blue, oxygen in red, fluorine in green, phosphorus in purple and iron in orange.

Bond/Angle	**$^{t}Bu_3P{\cdot}N_2O{\cdot}BFc(C_6F_5)_2$ (12)**	**$^{t}Bu_3P{\cdot}N_2O{\cdot}B(C_6F_5)$**
P-N	1.692(3)	1.7087(12)
N-N	1.251(3)	1.2573(15)
N-O	1.329(3)	1.3362(15)
O-B	1.543(4)	1.5428(18)
B-C_{Fc}	1.596(6)	-
P-C_{alkyl}	1.881(5), 1.873(4), 1.889(4)	-
Fe-B	3.301(4)	-
P-N-N	118.1(2)	117.04(10)
N-N-O	110.5(2)	109.11(11)
N-O-B	112.7(2)	114.43(10)
$Cp_{centroid}$-C_{ipso}-B	179	-

Table 5.4.8. Pertinent bond lengths (Å) and angles (º) of $^{t}Bu_3P{\cdot}N_2O{\cdot}BFc(C_6F_5)_2$ (**12**) and $^{t}Bu_3P{\cdot}N_2O{\cdot}B(C_6F_5)$ (**13**).

The exposure of a one-to-one mixture of **1** and $P^{t}Bu_3$ in fluorobenzene solution to N_2O to yield **12** proceeds with a dramatic colour change from dark maroon to orange (Figure 5.4.12). This colour change is attributed to complexation at the boron centre, which is consistent with the behaviour observed by Piers and coworkers occuring on reaction of maroon solutions of **1** with PMe_3 to give the yellow adduct $Me_3P{\cdot}BFc(C_6F_5)_2$. Although $P^{t}Bu_3$ is known to react with oxygen to yield $^{t}Bu_3PO$, the low affinity of the Lewis acid **1** for this phosphine oxide means that no significant quenching of the UV signal (or indeed a visible colour change) is observed for the $^{t}Bu_3P$/**1** FLP in tetrahydrofuran on exposure to dry O_2 over a period of 6 h.

Alternatively, the formation of **12**, and hence the presence of N_2O, can be signaled electronically, through a cathodic shift of greater than 300 mV (from +450 mV, with respect to FcH/FcH^+ to + 150 mV) accompanying the formation of the adduct in α,α,α-trifluorotoluene. Essentially no shift is observed in the presence of O_2 under analogous conditions. For detection applications, electrochemical rather than colorimetric reporting represents a more viable protocol: the large binding induced shift in $E_{1/2}$ enables detection of small quantities of **12** (in the <100 μM concentration range) even in the presence of a large excess of unreacted **1** (Figure 5.4.12). Conversely, the much larger extinction coefficient of **1** compared to **12** means that visible detection of N_2O can only really be achieved once near quantitative consumption of **1** has occured.

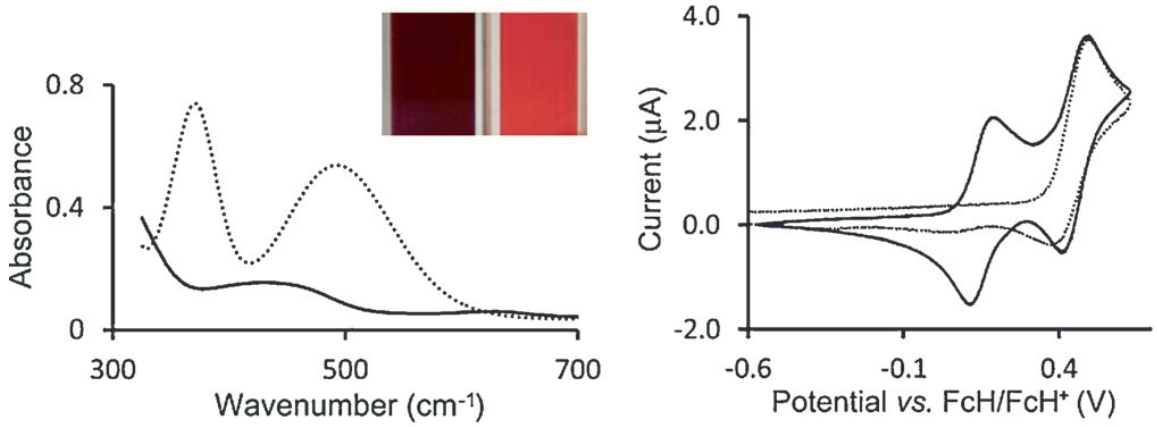

Figure 5.4.12. The effects of exposure of the $^tBu_3P$/**1** FLP system to N_2O, monitored by UV/Vis spectroscopy (left) [dashed line $^tBu_3P$/**1**, solid line **12**] and cyclic voltametry (left) [dashed line $^tBu_3P$/**1**, solid line equimolar mixture of $^tBu_3P$/**1** and **12**]. Insert photograph: benzene solutions of $^tBu_3P$/**1** (left) and **12** (right) [ca. 70 mM concentration, housed in UV curvettes].

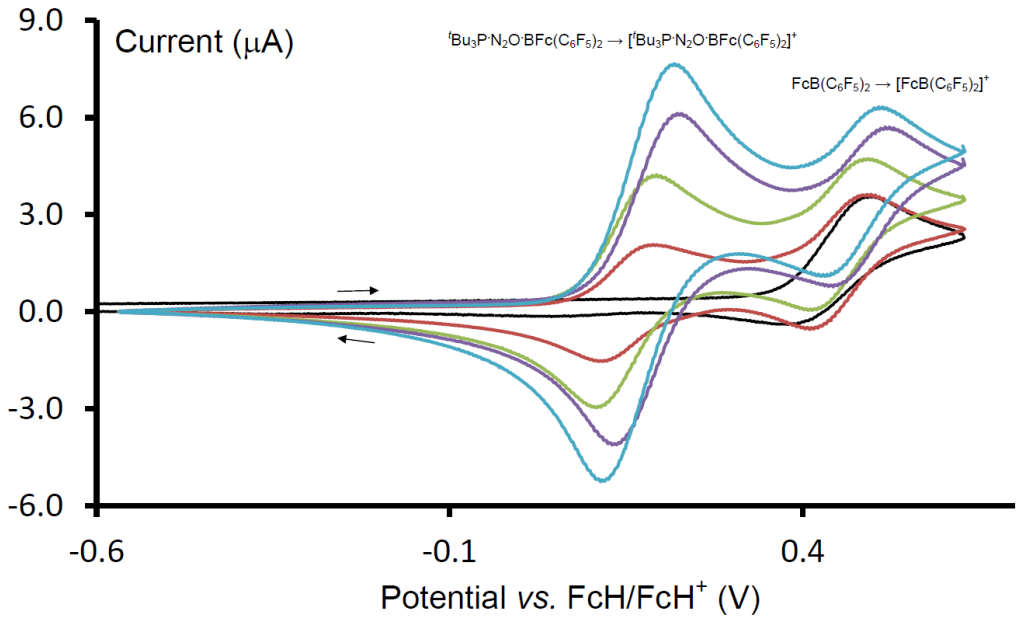

Figure 5.4.13. Probing the potential for detecting N_2O using cyclic voltametry using the ^{t}Bu$_3$P/**1** FLP system. The black trace is the cyclic voltammogram of a 100 μM solution of ^{t}Bu$_3$P/**1** FLP system in α,α,α-trifluorotoluene in the abscence of N_2O. The red/green/purple/blue trace are of a 100 μM solution of ^{t}Bu$_3$P/**1** FLP system in addition to 100/200/300/400 μM solutions of **12** in α,α,α-trifluorotoluene.

In conclusion, the ^{t}Bu$_3$P/**1** FLP mixture is able to report the presence of N_2O both colorimetrically and electrochemically over competing O_2, thereby establishing proof-of-principle for the use of FLP systems in the selective detection of small molecules. This opens a potentially rich and as yet greatly unexplored area of FLP chemistry.

Figure 5.4.12. Fluorobenzene solutions of a one-to-one mixture of $FcB(C_6F_5)_2$ and P^tBu_3 before reaction with N_2O (left), after reaction with N_2O (middle) and the result of exposing the one-to-one mixture to oxygen for 24 hours (right).

5.5. Conclusions

The capacity of $FcB(C_6F_5)_2$ (**1**) to form frustrated Lewis pairs with a range of carbenes and phosphines was explored and range of adducts investigated by a combination of structural, spectroscopic and reactivity studies. Subsequently, two approaches to synthesise the related system $FcB(C_6Cl_5)_2$ (**8**) were explored. The first approach involving treatment of $FcBBr_2$ with LiC_6Cl_5 proved less selective than the analogous synthesis of $FcB(C_6F_5)_2$ (**1**), however it did allow for a viable route to unsymmetrical mono(pentachlorophenyl) derivatives of the type $FcB(C_6Cl_5)X$ (X = Br, Mes). $FcB(C_6Cl_5)_2$ (**8**) is best synthesized from ferrocenyllithum and $ClB(C_6Cl_5)_2$ and is a violet-blue species characterized by an extremely electron deficient Fe(II) centre ($E_{1/2}$ = +550 mV cf FcH/FcH^+). A host of of structural, spectroscopic and reactivity studies of the related ferrocenyl boranes allow some trends to be elucidated about the role of the aryl groups on the ferrocenyl boranes: in terms of steric properties the substituents can be ranked Mes > C_6Cl_5 > C_6F_5, while their capabilities as electron-withdrawing groups are ordered C_6Cl_5 > C_6F_5 > Mes. The combination of $FcB(C_6Cl_5)_2$ (**8**) and $^tBu_3P$ was shown to be capable of activating and reporting the presence of N_2O colorimetrically due to oxidation of the phosphine to $^tBu_3PO$ that was capable of paying the steric cost of complexing the borane. In the search for greater selectivity for N_2O over alternate oxidants, the FLP system comprised of $FcB(C_6F_5)_2$ (**1**) and $^tBu_3P$ was shown to bind an intact N_2O unit. The low affinity for borane **1** for $^tBu_3PO$ provides selectivity for N_2O. Moreover, this binding event was reported both colorimetrically and electrochemically, resulting in the first small molecule reporter based on FLPs, and the first specifically designed colorimetric and electrochemical detector for N_2O.

(1) Lewis, G. N. *Valence and the structure of atoms and molecules*; Chemical Catalogue Company: New Yorl, 1923.

(2) Lennard-Jones, J. E. *Transactions of the Faraday Society* **1929**, *25*, 668.

(3) Brown, H. C.; Schlesinger, H. I.; Cardon, S. Z. *Journal of the American Chemical Society* **1942**, *64*, 325.

(4) Welch, G. C.; Cabrera, L.; Chase, P. A.; Hollink, E.; Masuda, J. D.; Wei, P.; Stephan, D. W. *Dalton Transactions* **2007**, 3407.

(5) Wittig, G.; Benz, E. *Chemische Berichte* **1959**, *92*, 1999.

(6) Tochtermann, W.; Trautwein, H.-D. *Justus Liebigs Annalen der Chemie* **1970**, *735*, 189.

(7) Stephan, D. W.; Erker, G. *Angewandte Chemie International Edition* **2010**, *49*, 46.

(8) Welch, G. C.; Juan, R. R. S.; Masuda, J. D.; Stephan, D. W. *Science* **2006**, *314*, 1124.

(9) Sumerin, V.; Schulz, F.; Atsumi, M.; Wang, C.; Nieger, M.; Leskelä, M.; Repo, T.; Pyykkö, P.; Rieger, B. *Journal of the American Chemical Society* **2008**, *130*, 14117.

(10) Sumerin, V.; Schulz, F.; Nieger, M.; Atsumi, M.; Wang, C.; Leskelä, M.; Pyykkö, P.; Repo, T.; Rieger, B. *Journal of Organometallic Chemistry* **2009**, *694*, 2654.

(11) Welch, G. C.; Stephan, D. W. *Journal of the American Chemical Society* **2007**, *129*, 1880.

(12) Geier, S. J.; Stephan, D. W. *Journal of the American Chemical Society* **2009**, *131*, 3476.

(13) Ashley, A. E.; Thompson, A. L.; O'Hare, D. *Angewandte Chemie International Edition* **2009**, *48*, 9839.

(14) Chase, P. A.; Gille, A. L.; Gilbert, T. M.; Stephan, D. W. *Dalton Transactions* **2009**, 7179.

(15) Ménard, G.; Stephan, D. W. *Journal of the American Chemical Society* **2010**, *132*, 1796.

(16) Berkefeld, A.; Piers, W. E.; Parvez, M. *Journal of the American Chemical Society* **2010**, *132*, 10660.

(17) Mömming, C. M.; Otten, E.; Kehr, G.; Fröhlich, R.; Grimme, S.; Stephan, D. W.; Erker, G. *Angewandte Chemie International Edition* **2009**, *48*, 6643.

(18) Dureen, M. A.; Stephan, D. W. *Journal of the American Chemical Society* **2010**, *132*, 13559.

(19) Sajid, M.; Klose, A.; Birkmann, B.; Liang, L.; Schirmer, B.; Wiegand, T.; Eckert, H.; Lough, A. J.; Frohlich, R.; Daniliuc, C. G.; Grimme, S.; Stephan, D. W.; Kehr, G.; Erker, G. *Chemical Science* **2013**, *4*, 213.

(20) Cardenas, A. J. P.; Culotta, B. J.; Warren, T. H.; Grimme, S.; Stute, A.; Fröhlich, R.; Kehr, G.; Erker, G. *Angewandte Chemie International Edition* **2011**, *50*, 7567.

(21) Zuck, D. E., Peter; Dronsfield, Alan *Education in Chemisrty* **2012**.

(22) Davy, H. *Researches chemical and philosophical; chiefly concerning nitrous oxide, or dephlogisticated nitrous air, and its respiration*; J Johnson: London, UK, 1800.

(23) Newman, M. G. C., Fermin A. Takei, Henry *Carranza's Clinical Periodontology*; 9th ed.; W. B. Saunders Company, 2002.

(24) Chaplin, C.; Keystone Film: 1914, p 12.55.

(25) Thomas, G.; Anglo-Amalgamated Film Distributors 1959, p 86 minutes.

(26) Yagiela, J. A. *Anesthesia Progress* **1991**, *38*, 1.

(27) Whitcher, C. E.; Zimmerman, D. C.; Piziali, R. L. *DHEW (NIOSH) Publ. (U. S.)* **1977**, *77-171*, 42 pp.

(28) Starek, A.; Strucinski, P.; Dobrzanska-Tatarczuch, L. *Rocz. Panstw. Zakl. Hig.* **2004**, *55*, 207.

(29) Baird, P. A. *New England Journal of Medicine* **1992**, *327*, 1026.

(30) Szymanska, J. *Annals of Agricultural and Environmental Medicine* **2001**, *8*, 119.

(31) *Journal of Midwifery and Women's Health* **2013**, *11*, 12103.

(32) Rowland, A. S.; Baird, D. D.; Weinberg, C. R.; Shore, D. L.; Shy, C. M.; Wilcox, A. J. *New England Journal of Medicine* **1992**, *327*, 993.

(33) Ahlborg, G., Jr.; Axelsson, G.; Bodin, L. *International Journal of Epidemiology* **1996**, *25*, 783.

(34) Olfert, S. M. *Journal of the Canadian Dental Association* **2006**, *72*, 821.

(35) Donaldson, D.; Meechan, J. G. British Dental Journal **1995**, *178*, 95.

(36) Gratton, T. B. *Journal of Environmental Health* **1982**, *45*, 24.

(37) Levine, J.; Chengappa, K. N. *Journal of Clinical Psychopharmacology* **2007**, *27*, 238.

(38) Heyer, E. J.; Simpson, D. M.; Bodis-Wollner, I.; Diamond, S. P. *Neurology* **1986**, *36*, 1618.

(39) Iwata, K.; O'Keefe, G. B.; Karanas, A. *American Journal of the Medical Sciences* **2001**, *322*, 173.

(40) Brodsky, J. B.; Cohen, E. N.; Brown, B. W., Jr.; Wu, M. L.; Whitcher, C. E. *Anesthesia & Analgesia (Cleveland)* **1981**, *60*, 297.

(41) Cullen, M. H.; Rees, G. M.; Nancekievill, D. G.; Amess, J. A. *Br J Haematol* **1979**, *42*, 527.

(42) O'Sullivan, H.; Jennings, F.; Ward, K.; McCann, S.; Scott, J. M.; Weir, D. G. *Anesthesiology* **1981**, *55*, 645.

(43) Solomon, S. Q., D.; Manning, M.; Chen, Z.; Marquis, M; Averyt, K.; Tignor, M. M. B.; Miller, H. L.; Cambridge University Press: Cambridge, UK, 2007.

(44) Kyoto Protocols, UNFCCC, Ed. 2011.

(45) Ravishankara, A. R.; Daniel, J. S.; Portmann, R. W. *Science* **2009**, *326*, 123.

(46) Environment, U. N., (UNEP), P., Eds.; United Nations Environment Programme (UNEP): Nairobi, Kenya, 2013.

(47) Zheng, S.; Li, M.; Shi, H.; Zeng, X.; Zhang, J.; Hu, Z.; Ren, Y.; Zhu, Z.; Hefei Institutes of Physical Science, Chinese Academy of Sciences, Peop. Rep. China . 2011, p 6pp.

(48) Macleod, N. A.; Rose, R.; Weidmann, D. *Opt. Lett.* **2013**, *38*, 3708.

(49) van, H. J. H.; Lang, N.; Macherius, U.; Zimmermann, H.; Roepcke, J. *Applied Physics Letters* **2013**, *103*, 131114/1.

(50) Castillo, P. C.; Sydoryk, I.; Gross, B.; Moshary, F. *Proc. SPIE* **2013**, *8718*, 87180J/1.

(51) Tokura, A.; Asobe, M.; Enbutsu, K.; Yoshihara, T.; Hashida, S.-N.; Takenouchi, H. *Sensors* **2013**, *13*, 9999.

(52) Li, J.; Parchatka, U.; Fischer, H. *Sensors and Actuators B: Chemical* **2013**, *182*, 659.

(53) Morris, J. M.; Xin, Y. *IEEE Sensors Journa* **2012**, *12*, 2347.

(54) Rotman, D. N.; Rotman, S. R.; Blumberg, D. G.; Ontiveros, E.; Messinger, D. *Proc. SPIE* **2011**, *8186*, 81860Q/1.

(55) Angelbratt, J.; Mellqvist, J.; Blumenstock, T.; Borsdorff, T.; Brohede, S.; Duchatelet, P.; Forster, F.; Hase, F.; Mahieu, E.; Murtagh, D.; Petersen, A. K.; Schneider, M.; Sussmann, R.; Urban, J. *Atmospheric Chemistry and Physics* **2011**, *11*, 6167.

(56) Sakamoto, Y.; Tanaka, K.; Asakawa, T.; Tonokura, K. *Japanese Journal of Applied Physics* **2011**, *50*, 062401/1.

(57) Khan, A.; Sun, K.; Miller, D. J.; Zondlo, M. A. *Proc. SPIE* **2011**, *8029*, 80291H/1.

(58) Asakawa, T.; Kanno, N.; Tonokura, K. *Sensors* **2010**, *10*, 4686.

(59) Duxbury, G.; Langford, N.; Hay, K.; Tasinato, N. *Journal of Modern Optics* **2009**, *56*, 2034.

(60) Kasyutich, V. L.; Holdsworth, R. J.; Martin, P. A. *Applied Physics B: Lasers and Optics* **2008**, *92*, 271.

(61) Cao, Z.; Gao, X.; Deng, L.; Chen, W. D.; Yuan, Y.; Zhang, W.; Gong, Z. *Spectrochimica Acta Part A: Molecular and Biomolecular Spectroscopy* **2007**, *68A*, 74.

(62) Waechter, H.; Sigrist, M. W. *Applied Physics B: Lasers and Optics* **2007**, *87*, 539.

(63) Susi, R.; Weeks, A. R.; Hefele, D.; Moore, J.; Invivo Research, Inc., USA . 2000, p 32 pp.

(64) Nanami, M.; Suzuki, T.; Tsukamoto, T.; Anritsu Corporation, Japan . 2000, p 14 pp.

(65) Mitsui, T.; Miyamura, M.; Matsunami, A.; Kitagawa, K.; Arai, N. *Clinical Chemistry (Washington, D. C.)* **1997**, *43*, 1993.

(66) Zeninari, V.; Grossel, A.; Joly, L.; Decarpenterie, T.; Grouiez, B.; Bonno, B.; Parvitte, B. Central European Journal of Physics. **2010**, *8*, 194.

(67) Zeninari, V.; Parvitte, B.; Joly, L.; Durry, G.; Le, L. R.; Garcia, J. C.; Hamelin, R.; Universite de Reims Champagne Ardenne, Fr.; Aerovia; C.N.R.S. - Mission des Relations avec les Entreprises . 2012, p 30pp.; Chemical Indexing Equivalent to 156:193592 (WO).

(68) Bartlome, R.; Kaucikas, M.; Sigrist, M. W. *Applied Physics B: Lasers and Optics* **2009**, *96*, 561.

(69) Grossel, A.; Zeninari, V.; Joly, L.; Parvitte, B.; Durry, G.; Courtois, D. *Infrared Physics & Technology* **2007**, *51*, 95.

(70) Grossel, A.; Zeninari, V.; Parvitte, B.; Joly, L.; Courtois, D. *Applied Physics B: Lasers and Optics* **2007**, *88*, 483.

(71) Lima, J. P.; Vargas, H.; Miklos, A.; Angelmahr, M.; Hess, P. *Applied Physics B: Lasers and Optics* **2006**, *85*, 279.

(72) Gomes, d. S. M.; Miklos, A.; Falkenroth, A.; Hess, P. *Applied Physics B: Lasers and Optics* **2006**, *82*, 329.

(73) Miklos, A.; da, S. M. G.; Hess, P. *Journal de Physique IV* **2005**, *125*, 3.

(74) Mattmann, M.; Roman, C.; Helbling, T.; Bechstein, D.; Durrer, L.; Pohle, R.; Fleischer, M.; Hierold, C. *Nanotechnology* **2010**, *21*, 185501/1.

(75) Bradley, K.; Chang, Y.-L.; Gabriel, J.-C. P.; Passmore, J. L.; Skarupo, S.; Tu, E.; Valcke, C.; Nanomix, Inc., USA . 2007, p 43 pp.

(76) Ishimura, Y.; Gao, Y. T.; Panda, S. P.; Roman, L. J.; Masters, B. S. S.; Weintraub, S. T. Biochemical and Biophysical Research Communications **2005**, *338*, 543.

(77) Schoentube, E.; Popp, P.; Oppermann, G.; Dornberger, I.; Faust, H. *Anaesthesiologie und Reanimation* -**1979**, *4*, 3.

(78) Gassmann, G.; Dahlke, S. *Journal of Chromatography* **1992**, *598*, 313.

(79) Braker, W.; Mossman, A. L. *Matheson Gas Data Book*; 6th ed.; Matheson, 1980.

(80) Daintith, J.; 3rd ed.; Oxford University Press, 1996.

(81) *NIST-JANAF Thermochemical Tables*; 4th ed. Journal of Physical and Chemical Reference Data, 1998.

(82) Zakirov, V.; Sweeting, M.; Lawrence, T.; Sellers, J. *Acta Astronautica* **2001**, *48*, 353.

(83) McClurg, B. *How to Install and Tune Nitrous Oxide Systems*; Amazon Kindle.

(84) Bridson-Jones, F. S.; Buckley, G. D.; Cross, L. H.; Driver, A. P. *Journal of the Chemical Society (Resumed)* **1951**, 2999.

(85) Dubkov, K.; Panov, G.; Starokon, E.; Parmon, V. *Reaction Kinetics and Catalysis Letters* **2002**, *77*, 197.

(86) Panov, G.; Dubkov, K.; Starokon, E.; Parmon, V. *Reaction Kinetics and Catalysis Letters* **2002**, *76*, 401.

(87) Yao, S.; Xiong, Y.; Driess, M. *Chemistry – A European Journal* **2010**, *16*, 1281.

(88) Poh, S.; Hernandez, R.; Inagaki, M.; Jessop, P. G. *Organic Letters* **1999**, *1*, 583.

(89) Tolman, W. B. *Angewandte Chemie International Edition* **2010**, *49*, 1018.

(90) Bottomley, F.; Brooks, W. V. F. *Inorganic Chemistry* **1977**, *16*, 501.

(91) Almond, M. J.; Downs, A. J.; Perutz, R. N. *Inorganic Chemistry* **1985**, *24*, 275.

(92) Yu, H.; Jia, G.; Lin, Z. *Organometallics* **2009**, *28*, 1158.

(93) Veige, A. S.; Slaughter, L. M.; Lobkovsky, E. B.; Wolczanski, P. T.; Matsunaga, N.; Decker, S. A.; Cundari, T. R. *Inorganic Chemistry* **2003**, *42*, 6204.

(94) Hall, K. A.; Mayer, J. M. *Journal of the American Chemical Society* **1992**, *114*, 10402.

(95) Bottomley, F.; Chen, J.; MacIntosh, S. M.; Thompson, R. C. *Organometallics* **1991**, *10*, 906.

(96) Bottomley, F.; Lin, I. J. B.; Mukaida, M. *Journal of the American Chemical Society* **1980**, *102*, 5238.

(97) Smith, M. R.; Matsunaga, P. T.; Andersen, R. A. *Journal of the American Chemical Society* **1993**, *115*, 7049.

(98) Bottomley, F.; Magill, C. P.; Zhao, B. *Organometallics* **1991**, *10*, 1946.

(99) Bottomley, F.; Paez, D. E.; White, P. S. *Journal of the American Chemical Society* **1982**, *104*, 5651.

(100) Johnson, A. R.; Davis, W. M.; Cummins, C. C.; Serron, S.; Nolan, S. P.; Musaev, D. G.; Morokuma, K. *Journal of the American Chemical Society* **1998**, *120*, 2071.

(101) Laplaza, C. E.; Odom, A. L.; Davis, W. M.; Cummins, C. C.; Protasiewicz, J. D. *Journal of the American Chemical Society* **1995**, *117*, 4999.

(102) Laplaza, C. E.; Johnson, M. J. A.; Peters, J. C.; Odom, A. L.; Kim, E.; Cummins, C. C.; George, G. N.; Pickering, I. J. *Journal of the American Chemical Society* **1996**, *118*, 8623.

(103) Reeds, J. P.; Yonke, B. L.; Zavalij, P. Y.; Sita, L. R. *Journal of the American Chemical Society* **2011**, *133*, 18602.

(104) Cherry, J.-P. F.; Johnson, A. R.; Baraldo, L. M.; Tsai, Y.-C.; Cummins, C. C.; Kryatov, S. V.; Rybak-Akimova, E. V.; Capps, K. B.; Hoff, C. D.; Haar, C. M.; Nolan, S. P. *Journal of the American Chemical Society* **2001**, *123*, 7271.

(105) Vaughan, G. A.; Sofield, C. D.; Hillhouse, G. L.; Rheingold, A. L. *Journal of the American Chemical Society* **1989**, *111*, 5491.

(106) Demir, S.; Montalvo, E.; Ziller, J. W.; Meyer, G.; Evans, W. J. *Organometallics* **2010**, *29*, 6608.

(107) Labahn, T.; Mandel, A.; Magull, J. *Zeitschrift für anorganische und allgemeine Chemie* **1999**, *625*, 1273.

(108) Pamplin, C. B.; Ma, E. S. F.; Safari, N.; Rettig, S. J.; James, B. R. *Journal of the American Chemical Society* **2001**, *123*, 8596.

(109) Piro, N. A.; Lichterman, M. F.; Harman, W. H.; Chang, C. J. *Journal of the American Chemical Society* **2011**, *133*, 2108.

(110) Pomowski, A.; Zumft, W. G.; Kroneck, P. M. H.; Einsle, O. *Nature* **2011**, *477*, 234.

(111) Mcnaught, A. D.; Wilkinson, A. *Compendium of Chemical Terminology-IUPAC Recommendations*; Taylor&Francis Ltd., 2000.

(112) Skell, P. S.; Woodworth, R. C. *Journal of the American Chemical Society* **1956**, *78*, 4496.

(113) Igau, A.; Grutzmacher, H.; Baceiredo, A.; Bertrand, G. *Journal of the American Chemical Society* **1988**, *110*, 6463.

(114) Arduengo, A. J.; Harlow, R. L.; Kline, M. *Journal of the American Chemical Society* **1991**, *113*, 361.

(115) Böhm, V. P. W.; Herrmann, W. A. *Angewandte Chemie International Edition* **2000**, *39*, 4036.

(116) Tskhovrebov, A. G.; Solari, E.; Wodrich, M. D.; Scopelliti, R.; Severin, K. *Angewandte Chemie., International Edition* **2012**, *51*, 232.

(117) Tskhovrebov, A. G.; Solari, E.; Wodrich, M. D.; Scopelliti, R.; Severin, K. *Angewandte Chemie International Edition* **2012**, *51*, 232.

(118) Tskhovrebov, A. G.; Vuichoud, B.; Solari, E.; Scopelliti, R.; Severin, K. *Journal of the American Chemical Society* **2013**, *135*, 9486.

(119) Tskhovrebov, A. G.; Solari, E.; Scopelliti, R.; Severin, K. *Inorganic Chemistry* **2013**.

(120) Tskhovrebov, A. G.; Solari, E.; Wodrich, M. D.; Scopelliti, R.; Severin, K. *Journal of the American Chemical Society* **2012**, *134*, 1471.

(121) Armor, J. N.; Taube, H. *Journal of the American Chemical Society* **1969**, *91*, 6874.

(122) Neu, R. C.; Otten, E.; Lough, A.; Stephan, D. W. *Chemical Science* **2011**, *2*, 170.

(123) Neu, R. C.; Otten, E.; Stephan, D. W. *Angewandte Chemie International Edition* **2009**, *48*, 9709.

(124) Otten, E.; Neu, R. C.; Stephan, D. W. *Journal of the American Chemical Society* **2009**, *131*, 9918.

(125) Gilbert, T. M. *Dalton Transactions* **2012**, *41*, 9046.

(126) Broomsgrove, A. E. J.; A. Addy, D.; Di Paolo, A.; Morgan, I. R.; Bresner, C.; Chislett, V.; Fallis, I. A.; Thompson, A. L.; Vidovic, D.; Aldridge, S. *Inorganic Chemistry* **2009**, *49*, 157.

(127) Siewert, I.; Fitzpatrick, P.; Broomsgrove, A. E. J.; Kelly, M.; Vidovic, D.; Aldridge, S. *Dalton Transactions* **2011**, *40*, 10345.

(128) Broomsgrove, A. E. J.; Addy, D. A.; Bresner, C.; Fallis, I. A.; Thompson, A. L.; Aldridge, S. *Chemistry – A European Journal* **2008**, *14*, 7525.

(129) Carpenter, B. E.; Piers, W. E.; Parvez, M.; Yap, G. P. A.; Rettig, S. J. *Canadian Journal of Chemistry* **2001**, *79*, 857.

(130) Bildstein, B.; Malaun, M.; Kopacka, H.; Wurst, K.; Mitterböck, M.; Ongania, K.-H.; Opromolla, G.; Zanello, P. *Organometallics* **1999**, *18*, 4325.

(131) Renk, T.; Ruf, W.; Siebert, W. *Journal of Organometallic Chemistry* **1976**, *120*, 1.

(132) Laszlo, P.; Editor *NMR of Newly Accessible Nuclei, Vol. 2: Chemically and Biochemically Important Elements*; Academic Press, 1983.

(133) Horton, A. D.; de With, J. *Organometallics* **1997**, *16*, 5424.

(134) Horton, A. D.; de With, J.; van der Linden, A. J.; van de Weg, H. *Organometallics* **1996**, *15*, 2672.

(135) Clavier, H.; Nolan, S. P. *Chemical Communications* **2010**, *46*, 841.

(136) Hillier, A. C.; Sommer, W. J.; Yong, B. S.; Petersen, J. L.; Cavallo, L.; Nolan, S. P. *Organometallics* **2003**, *22*, 4322.

(137) Massey, A. G.; Park, A. J. *Journal of Organometallic Chemistry* **1966**, *5*, 218.

(138) Deck, P. A.; Beswick, C. L.; Marks, T. J. *Journal of the American Chemical Society* **1998**, *120*, 1772.

(139) Parks, D. J.; Piers, W. E.; Yap, G. P. A. *Organometallics* **1998**, *17*, 5492.

(140) Arduengo, A. J.; Davidson, F.; Dias, H. V. R.; Goerlich, J. R.; Khasnis, D.; Marshall, W. J.; Prakasha, T. K. *Journal of the American Chemical Society* **1997**, *119*, 12742.

(141) Arduengo, A. J., III; Davidson, F.; Dias, H. V. R.; Goerlich, J. R.; Khasnis, D.; Marshall, W. J.; Prakasha, T. K. *Journal of the American Chemical Society* **1997**, *119*, 12742.

(142) Ashley, A. E.; Herrington, T. J.; Wildgoose, G. G.; Zaher, H.; Thompson, A. L.; Rees, N. H.; Krämer, T.; O'Hare, D. *Journal of the American Chemical Society* **2011**, *133*, 14727.

(143) Mayer, U.; Gutmann, V.; Gerger, W. *Monatshefte für Chemie* **1975**, *106*, 1235.

(144) Adamczyk-Woźniak, A.; Jakubczyk, M.; Sporzyński, A.; Żukowska, G. *Inorganic Chemistry Communications* **2011**, *14*, 1753.

(145) Yamaguchi, S.; Akiyama, S.; Tamao, K. *Journal of the American Chemical Society* **2001**, *123*, 11372.

(146) Wade, C. R.; Broomsgrove, A. E. J.; Aldridge, S.; Gabbaï, F. P. *Chemical Reviews* **2010**, *110*, 3958.

Appendix I – List of Publications

(16) Protchenko, A. V.; Dange, D.; Harmer, J.; Tang, C. Y.; Schwarz, A. D.; **Kelly, M. J**.; Phillips, N.; Birjkumar, K. H.; Jones, C.; Kaltsoyannis, N.; Mountford, P.; Aldridge, S. *Nature Chemistry*, **2014**, *6*, 315.

(15) **Kelly, M. J**.; Gilbert, J.; Tirfoin, R.; Aldridge, S. *Angew. Chem. Int. Ed. Eng.*, **2013**, *52*, 14094.

(14) Addy, D. A.; Bates, J. I.; **Kelly, M. J.**; Abdalla, J.; Phillips, N.; Riddlestone, I. M.; Aldridge, S. *Aust. J. Chem.*, **2013**, *66*, 1211.

(13) Turner, J.; Abdalla, J. A. B.; Bates, J. I.; Tirfoin, R.; **Kelly, M. J.**; Phillips, N.; Aldridge, S. *Chemical Science* **2013**, ***4***, 4245.

(12) Addy, D. A.; Bates, J. I.; **Kelly, M. J**.; Riddlestone, I. M.; Aldridge, S. *Organometallics* **2013**, *32*, 1583.

(11) **Kelly, M. J**.; Broomsgrove, A. E. J.; Morgan, I. R.; Siewert, I.; Fitzpatrick, P.; Smart, J.; Vidovic, D.; Aldridge, S. *Organometallics* **2013,** *32*, 2674.

(10) Phillips, N.; Rowles, J.; **Kelly, M. J.**; Riddlestone, I.; Rees, N. H.; Dervisi, A.; Fallis, I. A.; Aldridge, S. *Organometallics* **2012**, *31*, 8075.

(9) Riddlestone, I. M.; Edmonds, S.; Kaufman, P. A.; Urbano, J.; Bates, J. I.; **Kelly, M. J.**; Thompson, A. L.; Taylor, R.; Aldridge, S. *J. Am. Chem. Soc.* **2012**, *134*, 2551.

(8) Riddlestone, I. M.; Urbano, J.; Phillips, N.; **Kelly, M. J.**; Vidovic, D.; Bates, J. I.; Taylor, R.; Aldridge, S. *Dalton Trans.* **2013**, *42*, 249.

(7) Siewert, I.; Fitzpatrick, P.; Broomsgrove, A. E. J.; **Kelly, M. J.**; Vidovic, D.; Aldridge, S. *Dalton Trans.* **2011**, *40*, 10345.

(6) Tang, C. Y.; Phillips, N.; **Kelly, M. J**.; Aldridge, S. *Chem. Commun.* **2012**, *48*,11999.

(5) Mansaray, H. B.; **Kelly, M. J.**; Vidovic, D.; Aldridge, S. *Chem. - Eur. J.* **2011**, *17*, 5381. *[University of Oxford, M.Chem.]*

(4) Mansaray, H. B.; Rowe, A. D. L.; Phillips, N.; Niemeyer, J.; **Kelly, M. J.**; Addy, D. A.; Bates, J. I.; Aldridge, S. *Chem. Commun.* **2011**, *47*, 12295. *[University of Oxford, M.Chem.]*

(3) Niemeyer, J.; Addy, D. A.; Riddlestone, I.; **Kelly, M. J.**; Thompson, A. L.; Vidovic, D.; Aldridge, S. *Angew. Chem. Int. Ed. Eng.* **2011**, *50*, 8908.

(2) O'Neill, M.; Addy, D. A.; Riddlestone, I.; **Kelly, M. J.**; Phillips, N.; Aldridge, S. *J. Am. Chem. Soc.* **2011**, *133*, 11500.

(1) Bao, W.; Reddy Billa, M.; Kassireddy, K.; Haro, M.; **Kelly, M. J**.; Kitney, S. P.; Al Kalifah, M. S.; Wei, P.; Dong, D.; O'Neill, M.; Kelly, S. M. *Liq. Cryst.* **2010**, *37*, 1289. *[University of Hull, summer project]*